
THE UNIVERSITY *of* EDINBURGH

# The role of heme arginate in modulation of inflammation and type 2 diabetes

**Abhijeet Kumar Choudhary**

**A thesis submitted for the degree of Doctor of Philosophy**

**The University of Edinburgh**

**2012**

**DECLARATION**

I hereby declare that this thesis has been composed by myself and has not been submitted for any other degree elsewhere. The work presented herein is my own and all referenced work and assistance given to me is duly acknowledged.

Signed ……. Date……

Abhijeet Kumar Choudhary
Student ID: 0895280
MRC/Centre for Inflammation Research, University of Edinburgh.

Certified that the present work entitled *''The role of heme arginate in modulation of inflammation and type 2 diabetes''* submitted to the University of Edinburgh in fulfilment of the requirement for the award of the Doctor of Philosophy, was carried out by Mr. Abhijeet Kumar Choudhary (0895280) under the supervision of Dr. Bryan Conway at Centre for Inflammation Research (CIR), QMRI, University of Edinburgh.

Signed…….. Date…….

Dr. Bryan Conway
BHF Centre for Cardiovascular Science, University of Edinburgh.

**ABSTRACT**

Heme oxygenase (HO) is an enzyme that facilitates the oxidative breakdown of free heme into equi-molar concentrations of carbon monoxide (CO), the bile pigment biliverdin IX and free iron. These products have immuno-modulatory and anti-oxidative properties, which may be useful in the treatment of diseases characterised by low-grade inflammation and oxidative stress, such as insulin resistance and hyperglycaemia in type 2 diabetes. In fact, HO-1 protein levels and carbon monoxide generation are down-regulated in murine models of obesity and type 2 diabetes. Two independent research teams have reported that pharmacological induction of HO activity by protoporphyrin-based compounds, such as hemin and cobalt (III) protoporphyrin IX chloride (CoPP), exerts anti-diabetic effects, including protection from weight gain, systemic inflammation and peripheral insulin resistance, in various experimental models of type 2 diabetes. However, the relative insolubility and instability of hemin in solution and the multiple side-effects of CoPP, including weight loss, preclude their use for the treatment of patients in clinic.

Heme arginate (HA) is a stable and soluble composition of hemin and L-arginine (LA) in a solution containing propylene glycol, ethanol and water. Furthermore, HA is licensed for the treatment of acute porphyria in several European countries. Therefore, HA may potentially be used in clinical trials. The current PhD thesis tests the hypothesis that **the heme component of HA ameliorates hyperglycaemia via induction of HO activity in the leptin receptor deficient db/db (db/db) mouse model of type 2 diabetes.**

A preliminary *in vivo* study demonstrates that the heme but not the LA component of HA exerts an anti-hyperglycaemic effect in db/db mice. In a separate *in vivo* study, concomitant treatment of HA with stannous (IV) mesoporphyrin IX dichloride (SM), an inhibitor of HO activity, further improves the glycaemic control despite complete abrogation of the HA-mediated increase in HO activity in db/db mice. This result is in contrast to the above stated hypothesis, and demonstrates that the anti-hyperglycaemic effect of HA is due to a HO activity independent mechanism. Furthermore, the ameliorative effect of HA and HA+SM treatment on hyperglycaemia in db/db mice coincides with a gain in body and visceral fat weight, a reduction in islet β-cell inflammation and the preservation of islet β-cell function. Subsequent *in vitro* experiments demonstrate that HA exerts anti-inflammatory effects by a HO activity independent mechanism in pro-inflammatory *in vitro* models such as in cytokine mix-stimulated MIN6 β-cells and in classically activated bone marrow derived macrophages (BMDMs).

In conclusion, the current thesis demonstrates the novel finding that the heme component of HA can exert anti-inflammatory and anti-diabetic effects via a HO activity independent mechanism. Future work should focus on studies to test the hypothesis that **the interaction of heme with the nuclear receptor Rev-erb-α is responsible for the anti-inflammatory and anti-diabetic effects of HA.**

**ACKNOWLEDGEMENTS**

First and foremost I would like to express my deepest gratitude to my *Supervisor*, Dr. Bryan Conway for his patient guidance and support whilst encouraging and allowing me to express my views and work with freedom. The completion of this thesis would not have been possible without his guidance and feedback.

Profound thanks to my *second and third Supervisors,* Dr. David Kluth and Dr. Nicholas Morton, for their guidance, suggestions and active involvement in my project despite of their other professional commitments. I take the opportunity to thank Dr. Jeremy Hughes for his valuable suggestions and encouragement.

I am deeply indebted to Jillian Rennie, a skilled researcher and a good friend, for teaching me various techniques, performing *'mouse high molecular weight adiponectin ELISA'* and for her invaluable experienced guidance.

I am thankful to all the members of the Phagocytosis group within the Centre for Inflammation Research and Dr. Morton's group in Centre for Cardiovascular Science for their help and valuable suggestions. I am indebted to Gary Borthwick for his help with the *in vivo* studies and Bob Morris and the histology department for the processing of histological specimens.

I take this opportunity to thank my parents Dr. A.K. Choudhary and Dr. (Mrs.) J. Sinha, my sister Svetleena, brother-in-law Mukul and nephew Suryan, as their love and belief in me have been the source of my inspiration. Sincere thanks to my in-laws Mrs and Dr. Pandey for their encouragement and extended support.

I am thankful to my wife Lucky for her confidence in me. The completion of this project would not have been possible without her patience and unconditional support.

Lastly, I am hugely indebted to MTEM Ltd, a University of Edinburgh spin-out company and to the CIR for their scholarship and studentship respectively which has made this study possible in the first place.

## POSTERS AND PUBLICATION

### Posters

**i.** Choudhary, A.K., Rennie, J., Borthwick, G., Hughes, J., Morton, N.M., Kluth, D., Conway, B.R. (2011) **Novel heme oxygenase (HO) activity-independent amelioration of type 2 diabetes by HO activator/inhibitor combination therapy**. Scottish Society for Experimental Medicine Conference.

**ii.** Choudhary, A.K., Rennie, J., Borthwick, G., Hughes, J., Morton, N.M., Kluth, D., Conway, B.R. (2011) **Amelioration of hyperglycemia and islet inflammation independent of heme oxygenase activity in db/db$^{LRD}$ mice model of type 2 diabetes**. Diabetes UK Annual Professional Conference, Abstract P48. *Diabetic Medicine*, 28 (Suppl 1).

### Publications

**i.** Ferenbach, D.A., Nkejabega, N.C.J., McKay, J., Choudhary, A.K., Vernon, M.A., Beesley, M.F., Clay, S., Conway, B.C., Marson, L.P., Kluth, D.C., Hughes, J. (2011). **The induction of macrophage hemeoxygenase-1 is protective during acute kidney injury in aging mice.** *Kidney International*, 79 (966-976).

**ii.** Choudhary, A.K., Rennie, J., Borthwick, G., Hughes, J., Morton, N.M., Kluth, D., Conway, B.R. **Pharmacological inhibition of heme oxygenase activity accentuates the anti-hyperglycaemic effect of heme arginate in leptin receptor deficient db/db mouse model of type 2 diabetes.** *Manuscript in preparation.*

## TABLE OF CONTENT

## ABBREVIATIONS

| *Abbreviation* | *Full name* |
|---|---|
| AGE | Advanced glycation end product |
| ALAS | 5-aminolevulinate synthase |
| AMPK | 5' adenosine monophosphate-activated protein kinase |
| AP-1 | Activation protein-1 |
| BMDM | Bone marrow derived macrophages |
| c-JUN | c-Jun N-terminal kinase |
| CO | Carbon monoxide |
| CoPP | Cobalt (III) protoporphyrin IX chloride |
| CrMP | Chromium (III) mesoporphyrin IX chloride |
| CVD | Cardiovascular disease |
| DAG | Diacylglycerol |
| DAMPs | Damage associated molecular pattern molecules |
| DM | Diabetes mellitus |
| FoxO1 | Forkhead box O1 |
| G-6-P | Glucose-6-phosphatase |
| GAPDH | Glyceraldehyde 3-phosphate dehydrogenase |
| GK | Goto-Kakizaki |
| HA | Heme arginate |
| HDAC | Histone deacetylase |
| HMW | High molecular weight |
| HO | Heme oxygenase |
| IKK | Inhibitor of kappa B kinase |
| IL-1 | Interleukin-1 |
| IL-1R | Interleukin-1 receptor |
| IL-1Ra | Interleukin-1 receptor antagonist |
| IL-6 | Interleukin-6 |
| IL-10 | Interleukin-10 |
| IRS | Insulin receptor |
| IRS | Insulin receptor substrate |

| | |
|---|---|
| iNOS | Inducible nitric oxide synthase |
| LA | L-arginine |
| μM | Micro molar |
| mM | Milli molar |
| MAPK | Mitogen-activated protein kinases |
| MCP-1 | Monocyte chemo-attractant protein-1 |
| MIP-1 | Macrophage inflammatory protein-1 |
| NADPH | Nicotinamide adenine dinucleotide phosphate |
| NCoR | Nuclear receptor corepressor |
| NF-κB | Nuclear factor kappa-light-chain-enhancer of activated B cells |
| NO | Nitric oxide |
| PARP | Poly (ADP-ribose) polymerase |
| PBS | Phosphate buffered saline |
| PEPCK | Phosphoenolpyruvate carboxykinase |
| PI3K | Phosphatidylinositol 3-kinase |
| PKC | Protein kinase C |
| PPAR-γ | Nuclear receptor peroxisome proliferator-activated receptors-gamma |
| ROS | Reactive oxygen species |
| sGC | Soluble guanylyl cyclase |
| SM (or SnMP) | Stannous (IV) mesoporphyrin IX dichloride |
| SOD | Superoxide dismutase |
| TLR | Toll-like receptor |
| TNF-α | Tumor necrosis factor- α |
| TSA | Trichostatin |
| ZDF | Zucker diabetic fatty |

## LIST OF TABLES

## LIST OF FIGURES

# 1. CHAPTER 1: INTRODUCTION

## 1.1. DIABETES MELLITUS (DM)

Diabetes mellitus (DM) can be described as *''a metabolic disorder of multiple aetiology characterised by chronic hyperglycaemia with disturbances of carbohydrate, fat and protein metabolism resulting from defects in insulin secretion, insulin action, or both''* (Alberti et al., 1999). Insulin, a hormone secreted by pancreatic β-cells plays a vital role in regulating glucose homeostasis (Seino et al., 2011). The development of DM is dependent on pathogenic processes which either cause loss of pancreatic β-cells resulting in consequent insulin deficiency, or promote resistance to insulin action in the insulin responsive organs (Gavin et al., 2002).

### 1.1.1. HISTORICAL PERSPECTIVE OF DM

DM has a remarkable history of discoveries spanning over 3500 years. The ancient Egyptians were the first to acknowledge and document the polyuric state associated with DM around 1550 BC. The term *''Diabetes''* itself was coined by Greek physician Aretaeus in the first century AD to describe a disease state with symptoms of polyuria, polydipsia and weight loss (Sanders, 2002). Later, English neuroanatomists Thomas Willis added the latin term *''mellitus''* to describe the sweet taste of diabetic urine in 1675. The first experimental evidence of the presence of excess glucose in urine of diabetic subjects was presented by Matthew Dobson in 1776 (Sanders, 2002, Molnar, 2004). In 1889, Oskar Minkowski and Joseph von Mering, employed total extirpation of the pancreas in the dog in order to test the hypothesis that free-fatty acids (FFA) were vital for fat absorption, and unexpectedly

found that the pancreas was essential for blood sugar control. This remains one of the most significant discoveries of experimental medicine (Luft, 1989). Over 30 years later, the collective effort of the Canadian research team of J.J.R. Macleod, F.G. Banting, Charles Best, J.B. Collip and Eli Lilly and Company led to the first successful clinical use of pancreatic insulin extract to treat diabetes (Banting et al., 1922, Rosenfeld, 2002). In 1936, the first report distinguishing between the two distinct types of DM i.e. insulin-sensitive and insulin-insensitive was published in the Lancet (Himsworth, 1936) by the British scientist Sir Harold P. Himsworth.

### 1.1.2. CLASSIFICATION SYSTEM FOR DM

The first organised effort to address the chaotic nomenclature and classification of DM was made in 1979 by National Diabetes Data Group (NDDG). Subsequent reviews were made in 1980, 1985 and 1997 (Alberti et al., 1999) by the World Health Organisation (WHO). The current classification system is based on recommendations made by a joint review conducted by the WHO and the International Diabetes Federation (IDF) in 2005. There are three broad etiopathogenetic categories of classification:

i. **Type 1 diabetes (T1D):** Previously known as insulin-dependent DM as the patients required routine insulin replacement therapy for survival (Gavin et al., 2002). Type 1 diabetes arises due to destruction of β-cells or insulin either by auto-antibodies (auto-immune type 1 diabetes) or for other as yet unknown reasons (idiopathic type 1 diabetes), which results in absolute insulin deficiency

and leads to hyperglycaemia and ketoacidosis (Yoon and Jun, 2005, Notkins and Lernmark, 2001). The mechanisms promoting autoimmunity are poorly understood, but it is believed to be triggered by interactions between environmental and genetic susceptibility factors (Alberti et al., 1999).

ii. **Type 2 diabetes:** Previously known as non-insulin dependent DM (NIDDM) as patients survived even without insulin replacement therapy (Gavin et al., 2002). Type 2 diabetes occurs due to the development of resistance to insulin action in peripheral organs and a relatively inadequate insulin secretion by β-cells (Lebovitz, 2002, Kahn et al., 2006). The aetiological factors are not well understood, however, obesity, high calorie diet and lack of physical activity are increasingly associated with the development of type 2 diabetes (Kahn and Flier, 2000). As the focus of the current thesis is on type 2 diabetes, the pathophysiology of type 2 diabetes will be discussed in more detail in section 1.3.

iii. **Other specific type:** DM arising due to specific aetiological causes which result in specific genetic and immunological defects leading to hyperglycaemia is clustered in this group. Cases of hyperglycaemia occurring during pregnancy (gestational DM), due to maturity-onset diabetes of young, damage to the exocrine pancreas, genetic mutations of insulin receptors and infection and chemical induced damage to islet β-cells constitute this group (Alberti et al., 1999, Gavin et al., 2002).

### 1.1.3. PREVALENCE OF DM

The western world, as well as developing countries, faces a paramount challenge posed by an increase in the prevalence of DM, as each year over 10 million new cases of DM are detected worldwide (Wild et al., 2004, Shaw et al., 2009). The percentage of death due to DM associated complications is alarmingly high, 9 to 18 % in persons aged 35-64 years in the U.S.A., Europe and South-east Asia (Roglic et al., 2005). The Scottish diabetic survey conducted by the National Health Service (NHS) Scotland is reflective of the worldwide concern regarding the increase in the incidence of type 2 diabetes. There has been a steady increase in the incidence of type 2 diabetes from 1.5% to 4% of the Scottish population between 2001 and 2010 (Figure 1.1; Source: NHS Scottish Diabetic Survey publications, http://www.diabetesinscotland.org.uk/Publications.aspx?catId=3). In the same period of time, the incidence of type 1 diabetes has remained below 0.5% of the population.

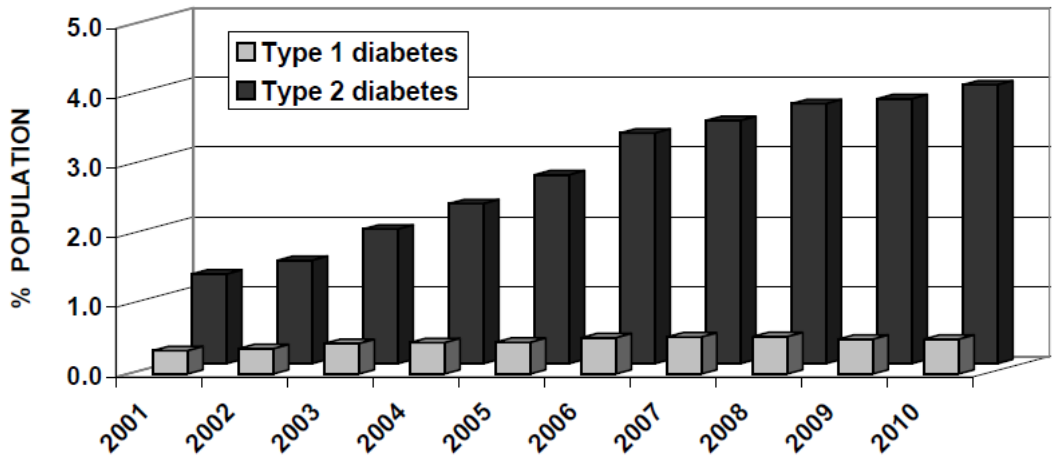


**Figure 1.1 Incidence of type 1 and 2 diabetes in Scotland between 2001 and 2010.** Source: National Health Service (NHS), U.K. Scottish Diabetes Survey (http://www.diabetesinscotland.org.uk/Publications.aspx?catId=3). Data is crude percentage prevalence calculated based on the number of patients with type 1 and type 2 diabetes who are registered on the national diabetes database.

### 1.1.4. COMPLICATIONS OF DM

The onset of DM can lead to the development of long-term vascular complications which contribute to the increased morbidity and mortality associated with DM. The network of arteries and capillaries responsible for constant blood supply to vital organs are severely put under stress by the injurious effects of pathophysiological concentrations of glucose in the blood (Fowler, 2008, Standl et al., 2011). Factors such as obesity, smoking, blood pressure and cholesterol levels increase the risk of vascular complication in DM (Van Gaal et al., 2006, Price et al., 1999, Fowler, 2008, Staessen, 2008). The vascular complications of DM are categorised into macro- and micro-vascular complications.

#### 1.1.4.1. MACRO-VASCULAR COMPLICATIONS

Large population studies have demonstrated a strong correlation between DM and cardiovascular disease (CVD) which remains the primary cause of mortality in people with DM (Ledru et al., 2001). The narrowing of the arterial walls, a pathophysiological feature of atherosclerosis is the hallmark of macrovascular complication that includes coronary and peripheral arterial diseases (Fowler, 2008). Immune cell infiltration, especially macrophages and T-lymphocytes, and their interaction with oxidised lipid molecules to form foam cells is a critical feature in generating atherosclerotic lesions that lead to thrombosis and organ infarction (Hansson, 2005).

The precise mechanisms by which diabetic conditions lead to atherosclerotic plaque formation in CVD are not well understood (Fowler, 2008). One would expect therapeutic interventions targeting hyperglycaemia to improve CVD outcome. However, reports from prospective studies such as the United Kingdom Prospective Diabetes Study (UKPDS) suggests otherwise, as no significant improvement in cardiovascular outcomes was noted in patients with type 2 diabetes on treatment with insulin or sulfonylureas (Turner et al., 1998). Hence, treatments exclusively targeting hyperglycaemia may be inadequate for reducing atherosclerotic plaque formation.

One potential mechanism by which hyperglycaemia may link to endothelial dysfunction is via endothelium-derived nitric oxide (NO). In normoglycaemia NO has vasoprotective properties: it promotes dilatation of blood vessels and inhibits oxidation of low density lipoprotein (LDL) cholesterol, platelet aggregation and proliferation of vascular smooth muscle cells (Forstermann and Munzel, 2006, Forstermann, 2008). However, hyperglycaemia-induced free radical production and reactive oxygen species (ROS) formation may abrogate the vasoprotective actions of NO via oxidative inactivation of NO by superoxide ($O_2^{\cdot}$) and the consequent formation of peroxynitrite (Peluffo and Radi, 2007).

#### 1.1.4.2. MICRO-VASCULAR COMPLICATIONS

Gluco-toxicity mediated damage of small blood vessels lead to microangiopathy-related complications including diabetic retinopathy, diabetic neuropathy and diabetic nephropathy. The duration and severity of gluco-toxicity increases the risk

of diabetic retinopathy and neuropathy (Fowler, 2008). Diabetic patients with micro-albuminuria (defined as excretion of albumin at a rate of 30-299mg/24 hours) are at a greater risk of diabetic nephropathy which is the leading cause of renal failure and associated mortality in United States (Dronavalli et al., 2008).

Gluco-toxicity mediated dysfunctions of the endothelial cell lining of blood capillaries are primarily responsible for micro-vascular complications. Endothelial cell damage in micro-vascular diseases is closely associated with numerous molecular signalling pathways: protein kinase C (PKC) activation, advanced glycation end product (AGE) production, an increase in the sorbitol-aldose reductase (polyol) pathway and hexosamine pathway flux (Vasavada and Agarwal, 2005). Hyperglycaemia stimulated ROS production by the mitochondrial electron chain has been implicated in endothelial cell damage (Reusch, 2003). Elevated ROS production in the endothelial cells mediate DNA strand breaks and subsequent activation of Poly (ADP-ribose) polymerase (PARP) that facilitates inactivation of glyceraldehyde 3-phosphate dehydrogenase (GAPDH), an important enzyme of glycolytic pathway necessary for optimal glucose metabolism. Inhibition of GAPDH activity shunts glucose into the polyol pathway and leads to activation of PKC by diacylglycerol and stimulation of AGE production (Figure 1.2) (Nishikawa et al., 2000, Du et al., 2003).

There is also evidence of a pro-inflammatory response in micro-vascular complication. ROS generation has been reported to increase transcription activity of nuclear factor kappa-light-chain-enhancer of activated B cells (NF-κB) in endothelial

cells (Nishikawa et al., 2000, Reusch, 2003). A recent study in the db/db mouse model of diabetic nephropathy has shown correlation between increased macrophage infiltration in the kidney and hyperglycaemia, albuminuria, glomerular and tubular damage, renal fibrosis and chemokine expression *(Ch*ow et al., 2004).

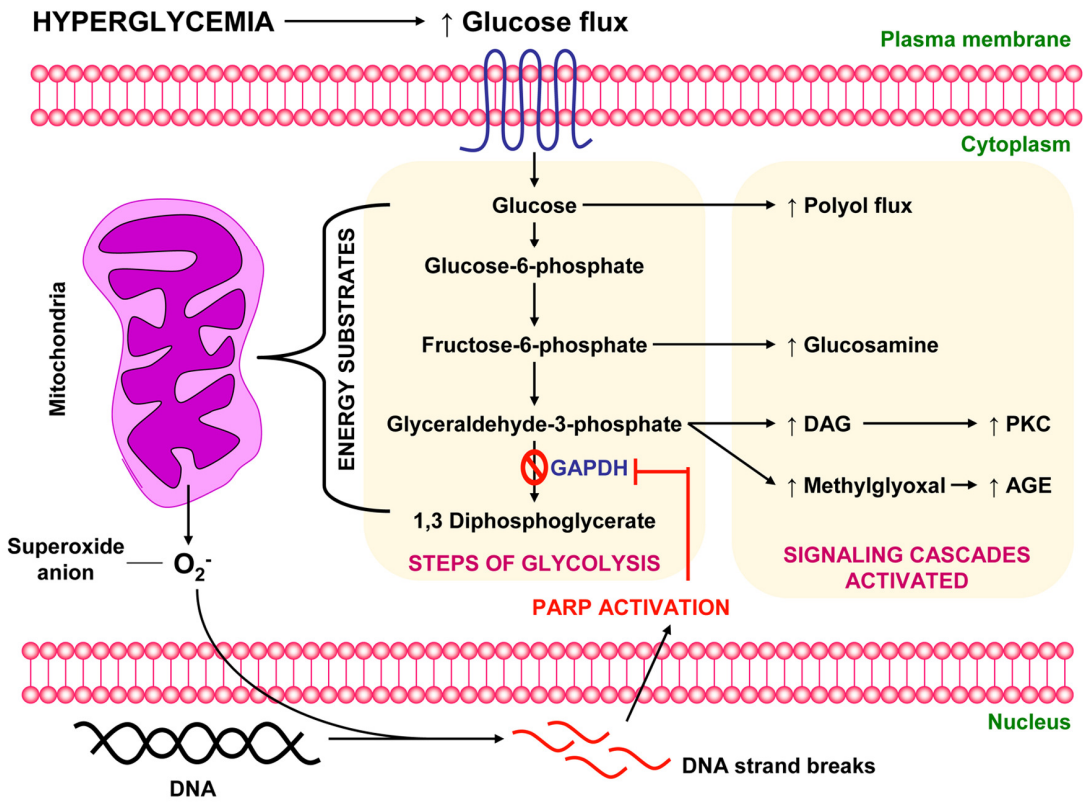


**Figure 1.2 Diagrammatic representation of the gluco-toxicity mediated damage of the endothelial cells in the micro-vascular complications of DM.** Elevated levels of blood glucose (hyperglycemia) increases the glucose and mitochondrial energy substrate flux resulting in an increase in generation of reactive oxygen species (ROS, $O_2^-$) which can cause breakage of DNA strands and activate PARP. PARP inhibits GAPDH activity which activates signalling pathways such as the polyol and glucosamine flux, PKC and AGE that are associated with the pathophysiology of micro-vascular complications of DM. **Abbreviations.** GAPDH: Glyceraldehyde 3-phosphate dehydrogenase, DAG: Diacylglycerol, PKC: Protein kinase C, AGE: Advanced glycation end product, PARP: Poly (ADP-ribose) polymerase. **Picture adapted from** Reusch, J.E.B. 2003. Diabetes, microvascular complications, and cardiovascular complications: what is it about glucose. *The Journal of Clinical Investigation* 112 (7). Pg. 987.

### 1.1.5. CLINICAL MANAGEMENT OF DM

The worldwide increase in the incidence of DM presents a daunting task for health care management. Due to the chronic nature of the disorder, treatment must be targeted at maintaining glycaemic control and also preventing and treating macrovascular and microvascular complications. Insulin replacement therapy remains the mainstay treatment for type 1 diabetes, and this requires regular monitoring of blood glucose levels to ensure efficacy and avoid hypoglycaemic excursion (Gallen, 2004, Owens et al., 2001). Pancreas or islet β-cell transplantation is an alternative for treatment of type 1 diabetes, however, this requires the use of immuno-suppressants which can increase the life-long risk of a plethora of infectious agents and malignancies and there is a possibility of recurrence of the disease particularly with islet transplant (Reach, 2001, Vendrame et al., 2010).

Research spanning decades has increased the present understanding of the molecular and cellular regulation of energy homeostasis but has not translated into therapeutic interventions. The clinical management of type 2 diabetes has been largely restricted to therapies involving insulin analogues and insulin secretagogues, like sulfonylureas, which promote insulin secretion from β-cells (Robertson et al., 2003, Sheehan, 2003). In addition, oral agents such as metformin [modulator of 5' adenosine monophosphate-activated protein kinase (AMPK)] and the thiazolidinedione group of compounds [nuclear receptor peroxisome proliferator-activated receptors-gamma (PPAR-γ) agonist] reduce hepatic glucose production and

promote insulin sensitization in peripheral organs (Figure 1.3) (Zhou et al., 2001, Hawley et al., 2002, Maeda et al., 2001, Day, 1999, Cheng and Fantus, 2005).

Chronic low-grade inflammation is a key component of the pathophysiology of obesity-associated type 2 diabetes (Donath and Shoelson, 2011) and represents an interesting target for therapeutic intervention. Indeed, trials employing interleukin-1β receptor antagonists (IL-1Ra) have already demonstrated the efficacy of this approach in reducing hyperglycemia (Larsen et al., 2007).

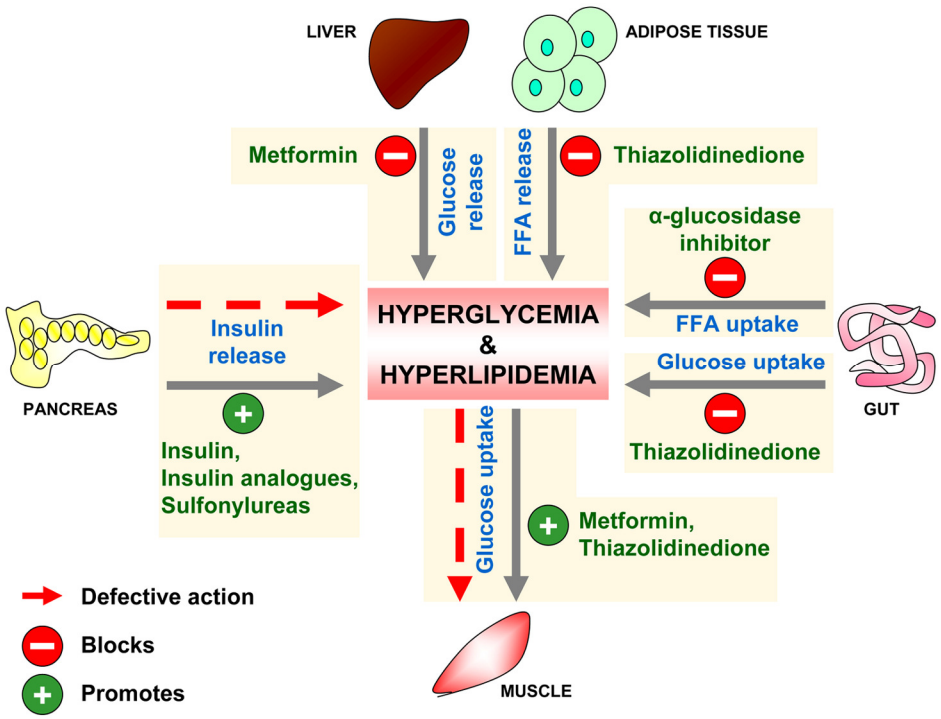


**Figure 1.3 Diagrammatic representation of the target organs and action of anti-hyperglycaemic agents in type 2 diabetes.** Text in blue represents the action, text in green represents the anti-hyperglycemic agents, and green and red circles represent the mode of action of the agents. **Abbreviations.** FFA: Free fatty acid. **Picture adapted from** Cheng, A.Y.Y. and Fantus, I.G. 2005. Oral antihyperglycemic therapy for type 2 diabetes mellitus. *Canadian Medical Association Journal* 172 (2). Pg. 215.

## 1.2. INSULIN: AN OVERVIEW

Insulin, secreted by the β-cells residing in islet of Langerhans in the pancreas, is a key hormone regulating glucose homeostasis. Insulin secretion is tightly regulated by nutrient status and hormonal factors such as incretins secreted from gastrointestinal tract (Seino et al., 2011). Importantly, insulin action in peripheral insulin-sensitive organs, including muscle, liver and adipose tissue is indispensable for maintaining glycaemic control (Ferrannini, 1998).

### 1.2.1. INSULIN BIOSYNTHESIS

The expression of insulin gene is restricted to islet β-cells. A highly conserved insulin promoter region is present ~340 base pair upstream of the transcription initiation start site (Qiu et al., 2002). Transcription of insulin gene is regulated by transcription factors, including pancreatic and duodenal homeobox-1 (PDX-1), β-cell E-box transactivator (BETA)/NeuroD and RIPE3b1/MafA (Kim et al., 2012). Glucose mediates insulin gene expression by promoting PDX-1 and MafA binding to A3 and C1 transcription control elements, respectively (Poitout et al., 2006).

Preproinsulin is the primary translation product of insulin gene. Preproinsulin, a precursor of the functional insulin polypeptide, is synthesised in the cytoplasm. Preproinsulin has a signal peptide, which confers inactivity to the preproinsulin polypeptide (Weiss, 2009). The interaction between the signal peptide of preproinsulin and the signal recognition particle on the endoplasmic reticulum (ER)

membrane facilitates translocation of preproinsulin into the lumen of ER. Proteolytic cleavage of the signal peptide from preproinsulin polypeptide in the lumen of ER produces proinsulin. Proinsulin undergoes post-translational modification to form three disulphide bonds vital for proinsulin stability (Harding and Ron, 2002, Kim et al., 2012). Proinsulin is delivered to the Golgi apparatus and gets packaged into clathrin-coated secretory granules (Orci et al., 1987). Peptidases cleave proinsulin into insulin and C-peptide. Insulin crystals are stored as hexamer molecule and are in inactive state (Orci et al., 1984).

### 1.2.2. INSULIN SECRETION

Glucose-dependent insulin secretion by β-cells is facilitated by presence of channels that allow flow of ions, particularly potassium ($K^+$) and calcium ($Ca^{2+}$) ions, into and out of the cell. Glucose transporter 2 (GLUT2), a transmembrane carrier protein, acts as glucose sensor in islet β-cells and mediates glucose entry into the β-cells (Prentki and Nolan, 2006). Glucose undergoes phosphorylation by the rate-limiting enzyme glucokinase to generate glucose-6-phosphate (G-6-P), which consequently passes through the glycolytic pathway to form pyruvate. Pyruvate dehydrogenase metabolises pyruvate to generate acetyl-CoA which enters the tricarboxylic acid cycle to generate adenosine-5'-triphosphate (ATP). The increase in ATP/ADP (adenosine diphosphate) ratio results in closure of ATP-gated potassium channel (Jones and Persaud, 1998). The closure of potassium channel facilitates depolarisation of the cell due to an increase in positive charge with in the cell. Depolarisation of the cell results in activation of the voltage-gated calcium channel

(MacDonald and Rorsman, 2006, Ashcroft and Rorsman, 1989), leading to an influx of $Ca^{2+}$ ions within the cell which promotes insulin secretory granules to fuse with the membrane and release hexamer insulin molecules by exocytosis (Figure 1.4). On release, inactive hexamer insulin molecule dissociates to produce the active monomeric form of insulin (Renström et al., 2008).

Free fatty acids (FFA) play a key role in amplifying the glucose-stimulated insulin release (GSIS) from islet β-cells (Nolan et al., 2006). Two separate pathways are responsible for the FFA potentiating GSIS (Figure 1.4). The first pathway involves binding of FFA to GPR40, a G protein-coupled receptor present, expressed on the cell membrane of β-cells. The intracellular signalling activated by FFA binding to GPR40 promotes an increase in intracellular $Ca^{2+}$ ions, consequently increasing exocytosis of insulin granules in the membrane (Itoh et al., 2003, Gromada, 2006). The second pathway involves activation of protein kinase C (PKC) due to an increase in long chain acyl-CoA. The increase in malonyl-CoA concentration within the β-cells lead to inhibition of β-oxidation of long chain acyl-CoA (Nolan et al., 2006). As a result, long chain acyl-CoA is shunted into the fatty acid-triglyceride pathway which promotes insulin secretion by directly increasing exocytosis of insulin granules and by activation of PKC (Prentki and Nolan, 2006).

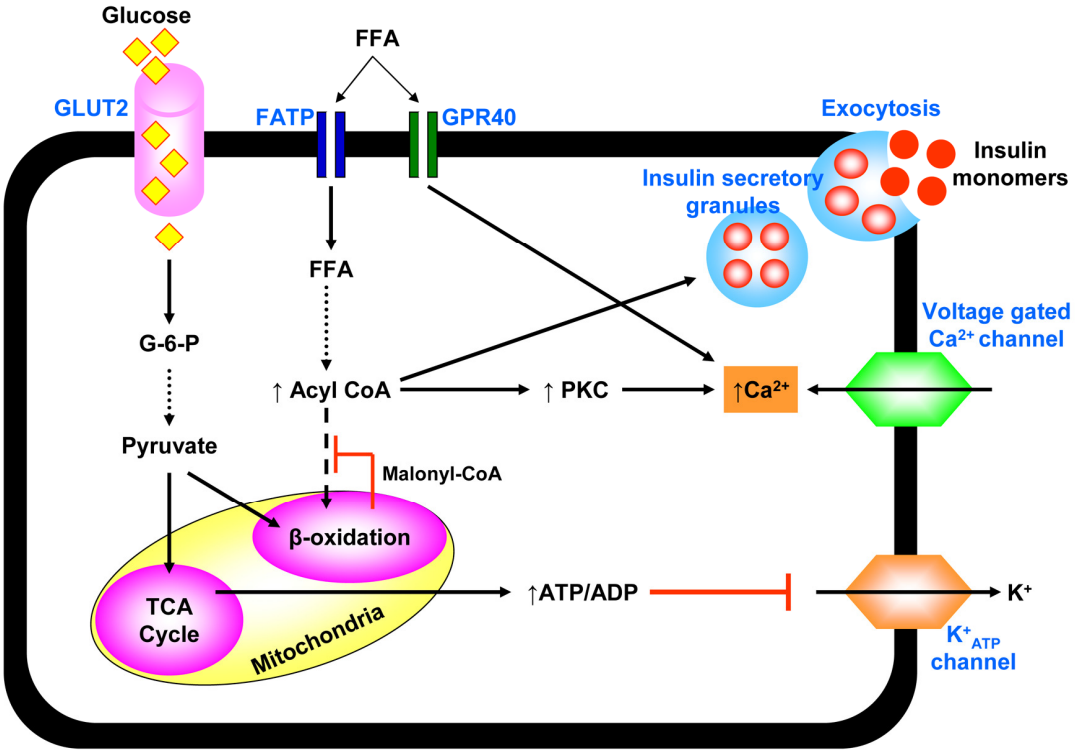


**Figure 1.4 Diagrammatic representation of the insulin secretion by islet β-cells.** GLUT2 facilitates entry for glucose into the cell where glucose is metabolised via glycolysis and the TCA cycle to produce ATP. The increase in the intracellular ATP/ADP ratio causes closure of the $K^+_{ATP}$ channel resulting in depolarisation of the plasma membrane. This allows an influx of $Ca^{2+}$ ions in the cytoplasm through the voltage-gated $Ca^{2+}$ channel, facilitating release of insulin secretory granules by exocytosis. FFAs potentiate insulin release by directly activating GPR40 and through an increase in malonyl-CoA with a consequent increase in long chain acyl CoA which stimulates exocytosis of insulin granules either directly or by activating PKC. **Abbreviations.** FFA: Free fatty acid, FATP: Fatty acid transport protein, $K^+$: Potassium ions, $Ca^{2+}$: Calcium ions, PKC: Protein kinase C, TCA: Tricarboxylic acid, G-6-P: Glucose-6-phosphate. **Picture adapted from** Jones, P.M. and Persaud, S.J. 1998. Protein kinase, protein phosphorylation, and the regulation of insulin secretion from pancreatic β-cells. *Endocrine Reviews* 19 (4). Pg. 429.

### 1.2.3. INSULIN ACTION

The insulin receptor is a tyrosine kinase transmembrane receptor (Pirola et al., 2004) composed of two alpha (α) and two beta (β) subunits, attached by disulfide bonds. Insulin binds to the extracellular α-subunit of the insulin receptor leading to conformational changes, facilitating ATP-binding to the intracellular β-subunits.

ATP-binding to β-subunits results in autophosphorylation of β-subunits which stimulates their kinase activity for intracellular substrates (Saltiel and Kahn, 2001, Kido et al., 2001).

Insulin has pleiotropic effects (Figure 1.5) in the peripheral organs, such as modulating hepatic glucose production, glucose uptake by muscles and lipolysis in adipose tissue and liver (Ferrannini, 1998). Hence, an intact insulin secreting apparatus and physiological action of insulin are essential to maintain energy homeostasis and glycaemic control.

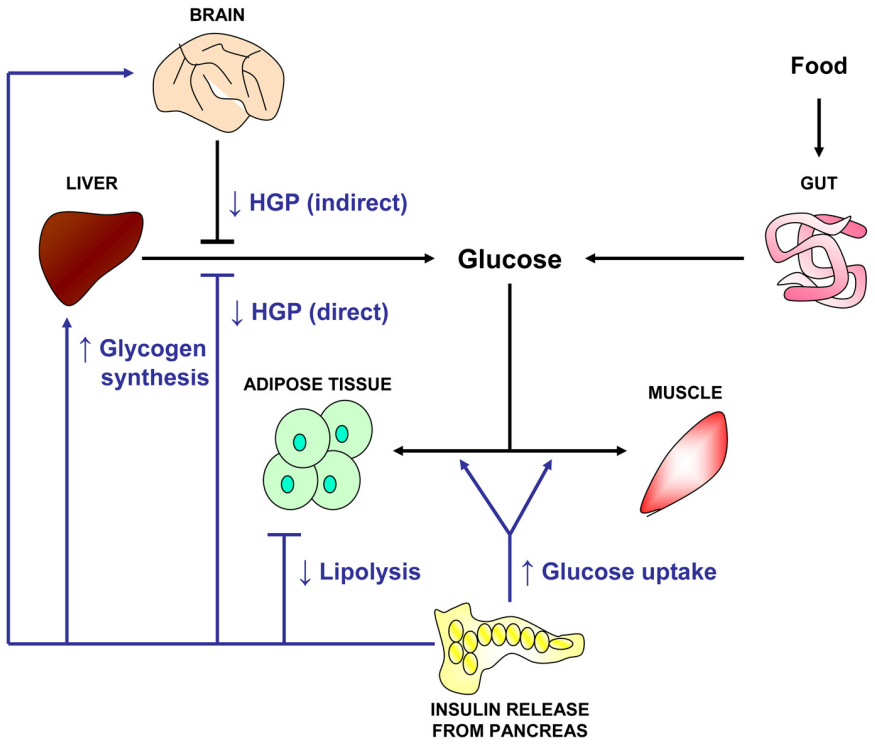


**Figure 1.5 Diagrammatic representation of the pleiotropic effects of insulin that contribute to energy homeostasis.** Elegant studies over the years have established insulin to have multiple functions in various organs such as to stimulate glucose uptake (Herman and Kahn, 2006), synthesize glycogen (Kasuga et al., 2003), inhibit lipolysis (Morimoto et al., 1998) and hepatic glucose production (HGP) (Girard, 2006) which contributes to maintenance of energy homeostasis. **Picture adapted from** Rosen, E.D. and Spiegelman, B.M. 2006. Adipocytes as regulators of energy balance and glucose homeostasis. *Nature* 444. Pg. 849.

## 1.3. PATHOPHYSIOLOGY OF TYPE 2 DIABETES

The common pathophysiological features displayed in type 2 diabetes arise from multiple aetiological factors, including the development of peripheral insulin resistance and relatively insufficient secretion of insulin (Kah*n* et al*.,* 2006).

### 1.3.1. INSULIN RESISTANCE IN TYPE 2 DIABETES

The discrete molecular mechanisms underlying the development of insulin resistance are still elusive. Obesity and a high energy diet are factors promoting insulin resistance (Kahn and Flier, 2000). Extensive research in this field over the last couple of decades has generated two key hypotheses to explain the molecular mechanisms responsible for obesity mediated insulin resistance, as is discussed below.

#### 1.3.1.1. ECTOPIC FAT/LIPID STORAGE PARADIGM

The underlying mechanisms for ectopic deposition of lipids are proposed to be failure of fat cell formation and lipid oxidation (Heilbronn et al., 2004). The failure of adipocyte proliferation and differentiation limits the increase in adipose mass in type 2 diabetes. The finite ability of adipose tissue to expand and take up lipid, coupled with increased lipolysis due to insulin resistance in adipose tissue, leads to ectopic deposition of lipids in liver, skeletal muscle and pancreas (Szendroedi and Roden, 2009). Lipid deposition in the liver and muscle in obese individuals strongly correlates with the degree of insulin resistance (Goodpaster et al., 1997).

Ectopic deposition of lipid in skeletal muscle and liver impairs the efficacy of insulin in stimulating glucose uptake in skeletal muscle (Boden and Shulman, 2002) and suppressing hepatic glucose production (Matsumoto et al., 2006). An increase in glucose metabolism in the muscle and liver elevates the concentration of malonyl-CoA which inhibits transfer of free-fatty acids (FFAs) to the mitochondria for β-oxidation (Winder and Hardie, 1996, Ruderman et al., 1999, Szendroedi and Roden, 2009). The increase in the concentration of FFAs result in shunting of FFAs into the glycerol-lipid pathway to synthesise diacylglycerol (DAG), a lipid metabolite which can activate isoforms of protein kinase C (PKC) (Kelley and Mandarino, 2000, Holland et al., 2007). PKC activation has been implicated in impairment of insulin signalling in the muscle and liver via inhibition of the tyrosine kinase activity of the insulin receptor and inhibition of tyrosine phosphorylation of the insulin receptor substrate (IRS)-1 which are both required for insulin signalling (Figure 1.6) (Donnelly et al., 1994, Unger, 2003). Impaired insulin signalling in the muscle leads to inefficient glucose disposal in the muscle resulting in an increase in blood glucose levels.

In liver, insulin mediates phosphorylation of transcription factor forkhead box O1 (FoxO1) to prevent FoxO1 entry into the nucleus and subsequent expression of gluconeogenic genes, including phosphoenolpyruvate carboxykinase (PEPCK) and glucose-6-phosphatase (G-6-P) (Matsumoto et al., 2006). The FoxO1 pathway becomes resistant to the effects of insulin in the leptin deficient ob/ob and lipodystrophic mouse models of type 2 diabetes (Shimomura et al., 2000). However, in these mouse models, the sterol regulatory element-binding protein 1c (SREBP-1c)

pathway which promotes insulin-dependent fatty acid and triglyceride biosynthesis does not become insensitive to insulin action (Horton et al., 2002). Hence, selective regulation of transcription factors FoxO1 and SREBP-1c by insulin in insulin-resistant mice contributes to the classical triad of hyperglycaemia, hyperlipidaemia and hyperinsulinaemia observed in type 2 diabetes (Brown and Goldstein, 2008).

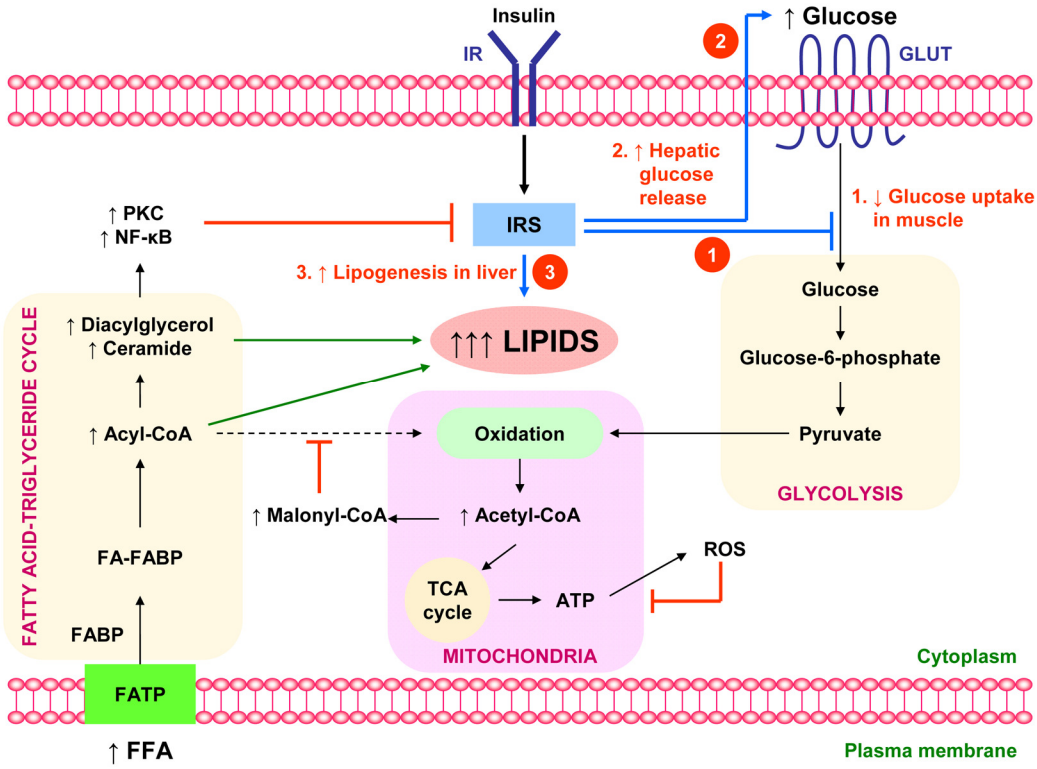


**Figure 1.6 Diagrammatic representation of ectopic deposition of lipid in muscle and liver hypothesis.** The model suggests an increase in oxidation of glucose because of increased glucose flux resulting from hyperglycemia. The increased glucose oxidation yields malonyl-CoA which impairs lipid oxidation and shunts lipid into the free fatty acid-triglyceride cycle. The lipid intermediates activate the PKC and NF-κB pathways which can impair insulin signalling by inhibiting tyrosine activity of the IR and phosphorylation of IRS. Impairment of insulin signalling results in **1.** Reduced glucose uptake by muscle, **2.** Increased hepatic glucose release and **3.** Promote lipogenesis in the liver. Increased mitochondrial oxidation will promote ROS generation which can in turn impair the function of the mitochondria. These processes lead to significant increase in lipid concentration in the muscle and liver. **Abbreviations.** FFA: Free fatty acid, FATP: Fatty acid transporter protein, FABP: Fatty acid binding protein, PKC: Protein kinase C, NF-κB: Nuclear factor kappa-light-chain-enhancer of activated B cells, IRS: Insulin receptor substrate, IR: Insulin receptor. **Picture adapted from** Szendroeidi, J. and Roden, M. 2009. Ectopic lipids and organ function. *Current Opinion in Lipidology* 20. Pg 51.

### 1.3.1.2. ENDOCRINE PARADIGM

This emerged as an alternative hypothesis to explain insulin resistance alongside the ectopic fat deposition paradigm in the mid 1990s with the discovery that adipose tissue had endocrine functions (Friedman and Halaas, 1998). Adipose tissue was no longer viewed solely as an organ for storing energy reserve. The multiple bioactive peptides (popularly known as adipokines), including leptin and adiponectin released by adipose tissue, were demonstrated to have modulatory effects on energy homeostasis (Ronti et al., 2006). Leptin was the first molecule to be characterised extensively and has been shown to regulate satiety and energy expenditure (Barinaga, 1995, Myers et al., 2008). Adiponectin is the most abundant circulating adipokine and has received a great deal of attention because of its ability to promote insulin sensitisation in liver and muscle (Berg et al., 2001, Fruebis et al., 2001). The recognition of the difference in the secretory pattern of leptin and adiponectin in individuals with obesity, insulin resistance or type 2 diabetes, directed research towards translational benefits. The thiazolidinedione group of compounds are PPAR-γ ligands and one of their mechanisms of action is to promote insulin sensitisation by increasing the circulatory levels of adiponectin (Day, 1999, Maeda et al., 2001).

Adipose tissue has been shown to secrete inflammatory molecules, such as interleukin-6 (IL-6) and tumor necrosis factor-α (TNF-α), which are significantly elevated in insulin resistance and type 2 diabetes. This observation has been largely responsible for proposing the existence of low-grade chronic inflammation in type 2 diabetes. (Hotamisligil et al., 1993, Kern et al., 1995, Uysal et al., 1997).

| S.N. | Adipokine | Metabolic effect | References |
|---|---|---|---|
| | | | |
| 01 | Leptin | Promotes satiety, reduces insulin resistance, hepatic steatosis and improves hepatic insulin responsiveness. | (Toyoshima et al., 2005, Petersen et al., 2002, Friedman and Halaas, 1998) |
| 02 | Adiponectin | Promotes insulin sensitivity in liver and muscle through increased lipid oxidation. | (Yamauchi et al., 2001, Yamauchi et al., 2003) |
| 03 | TNF-α | Impairs insulin signalling. Reduces adiponectin synthesis. Promotes lipolysis. | (Hotamisligil et al., 1993, Hotamisligil et al., 1995, Saghizadeh et al., 1996) |

**Table 1.1 Metabolic effects of some of the adipokines secreted by adipose tissue.**

### 1.3.2. β-CELL DYSFUNCTION IN TYPE 2 DIABETES

The pancreatic islet β-cells respond to chronic fuel (glucose and lipid) overflow and insulin resistance by compensatory hypersecretion of insulin to achieve normoglycaemia. Longitudinal studies lend support to this observation as hyperinsulinaemia is often observed in insulin resistant volunteers despite a normal glycaemic level (Prentki and Nolan, 2006). The U.K. Prospective Diabetes Study group reported a progressive increase in hyperglycaemia in newly diagnosed patients with type 2 diabetic, over a period of 6 years which was associated with progressive loss of β-cell function (UKPDS, 1995). Hence, deterioration of islet β-cell function is crucial for the development of type 2 diabetes. However, the molecular determinants responsible for islet β-cell dysfunction are not well understood in type 2 diabetes.

There are several lines of evidence that implicate glucolipotoxicity and inflammatory mediators in promoting islet β-cell dysfunction and damage *in vitro* (Donath et al.,

2005, Donath et al., 2009). However, the underlying mechanisms responsible for islet β-cell dysfunction in animal models or in humans are still elusive. Key molecular determinants that are believed to contribute in islet β-cell dysfunction are discussed below, except for inflammation, which is will be discussed in section 1.4.3.

#### 1.3.2.1. SPECIES AND GENETIC FACTOR

The genetic composition of a particular species is of importance in determining the propensity for islet β-cell dysfunction. For example, leptin receptor deficiency results in severe β-cell dysfunction and profound hyperglycaemia on the C57BL/KsJ, but not on the C57BL/6J background, in which the hyperglycaemia is more modest and insulin levels are robustly preserved (Hummel et al., 1972, Leiter et al., 1981). Other evidence is derived from the *ex vivo* culture of islets from various species under varying concentrations of glucose to determine their susceptibility to glucotoxicity. Islets isolated from human and *Psammomys obesus* (sand rat) are susceptible to apoptosis and exhibit defective insulin release when cultured in a high glucose medium (Federici et al., 2001, Kaiser et al., 2005), whereas, the islets isolated from rodents are found to be resistant (Efanova et al., 1998).

#### 1.3.2.2. GLUCOLIPOTOXICITY

The degree of β-cell susceptibility to glucotoxicity varies between species. Culture of human islets in a high glucose concentration (33mM) resulted in a marked increase in apoptosis. However, β-cells from islets of obese (ob/ob) mice were relatively

resistant to apoptosis at a pathophysiological concentration of 11mM of glucose (Federici et al., 2001, Efanova et al., 1998).

The evidence for an isolated effect of lipotoxicity in promoting β-cell toxicity remains inconclusive. β-cells should be susceptible to an increase in ROS induced by a high mitochondrial lipid flux as they have low levels of ROS-detoxifying enzymes (Laybutt et al., 2002). However, *ex vivo* culture of islets isolated from Zucker fatty rats demonstrated that β-cells were relatively protected from hyperlipidaemia and stimulated insulin secretion (Nolan et al., 2006, Haber et al., 2003).

The evidence for the toxicity of glucose and lipids (glucolipotoxicity) in combination are much stronger. Extensive studies with pharmacological inducers and inhibitors of lipid oxidation demonstrated that lipotoxicity in the insulinoma INS 832/13 β-cell line was due to an increase in glucose oxidation combined with accumulation of complex lipid molecules, some of which are cytotoxic (El-Assaad et al., 2003, Prentki and Nolan, 2006). The presence of islet steatosis (lipid retention) and reduced insulin gene expression in hyperglycaemic Zucker diabetic rats but not in Zucker fatty rats (Lee et al., 1994, Harmon et al., 2001) lends further support to the fact that both hyperglycaemia and hyperlipidaemia are required for β-cell dysfunction.

## 1.4. INFLAMMATION IN TYPE 2 DIABETES

Inflammation is a well orchestrated response of the host to restore homeostasis following injury. Initiation, progression and resolution are key stages of inflammation that are tightly intertwined with the innate immune system (Tracy, 2006, Henson, 2005). The dynamic process of inflammation involves a complex interaction between resident cells and circulatory immune cells mediated by the release of soluble proteins such as damage associated molecular pattern molecules (DAMPs) by resident cells and cytokines by immune cells. The inflammatory response at the site of injury is necessary to orchestrate the wound healing process (Eming et al., 2007). However ongoing inflammation for a prolonged period of time can have deleterious effects on the host tissues or organs due to the cytotoxic effects of substances released from immune cells (Wellen and Hotamisligil, 2005). Low-grade chronic inflammatory processes have been implicated in various disease states, including obesity and type 2 diabetes, where inflammation is believed to be a cause as well as a consequence of the disorder (Hotamisligil, 2006, Kahn et al., 2006).

Anti-inflammatory mediators such as salsalate and anakinra target pro-inflammatory pathways and facilitate NF-κB inhibition and interleukin-1 receptor (IL-1R) blockade, respectively. These compounds have shown encouraging anti-diabetic efficacy in clinical trials (Larsen et al., 2007, Fleischman et al., 2008). This has led to an increase in interest in the scientific community to pursue inflammation as a therapeutic target for type 2 diabetes.

### 1.4.1. OBESITY: AN INFLAMMATORY DISORDER

Obesity is a risk factor for the metabolic syndrome and type 2 diabetes, and the obese state is also recognised as a chronic inflammatory disorder. The link between inflammation and a metabolic disorder is perhaps not surprising from an evolutionary perspective. Metabolic and immune responses are key factors determining survival when species are challenged with nutrient restriction and infective organisms during natural calamities such as famine and epidemic out-breaks (Hotamisligil, 2006). In fact, the Drosophila fat body which is equivalent to human adipose tissue has been reported to incorporate mammalian homologues of both the liver and the immune system which demonstrates the existence of link between the functional units of the metabolic and immune systems (Søndergaard, 1993). The concurrent aberration of metabolic and immune responses in obesity further strengthens the link between these two responses.

The first experimental evidence of the presence of a low-grade chronic inflammation in obesity came with the discovery of increased expression of the pro-inflammatory mediator, TNF-α, in visceral fat of humans and in experimental models of obesity (Hotamisligil et al., 1993, Kern et al., 1995, Hotamisligil et al., 1995). Simultaneously, adipose tissue was discovered to have endocrine functions, as adipocytes were found to secrete a large variety of soluble factors, including cytokines, which may be responsible for eliciting pro-inflammatory responses (Barinaga, 1995, Heilbronn et al., 2004). Notably, adipocytes express toll-like

receptors (TLRs), like macrophages, and are activated by nutrients such as fatty acids, promoting inflammation in adipose tissue (Song et al., 2006, Shi et al., 2006).

The underlying mechanisms responsible for generating inflammation in obesity are not well understood. However, adipocyte hypertrophy is believed to be responsible for the initiation of inflammation (Figure 1.7). The adipocytes are significantly enlarged (hypertrophy), which may promote microhypoxia (Hosogai et al., 2007). Hypoxia in adipocytes has been shown to activate the c-Jun N-terminal kinase (JNK) and NF-κB pathways, which induce chemokine release and recruitment of macrophages to remove the cellular debris resulting from adipocyte death (Ye et al., 2007). However, a prolonged autocrine and paracrine inflammatory engagement between the macrophages and adipocytes is established, which leads to further adipocyte injury (Figure 1.7) (Cinti et al., 2005). Relevant studies have established that the JNK and NF-κB pathways have a direct inhibitory effect on the insulin signaling cascade too (Schenk et al., 2008).

Macrophage accumulation in adipose tissue is a characteristic feature of obesity. Extensive gene profiling in white adipose tissues from various rodent models of obesity and type 2 diabetes demonstrated elevated gene expression of macrophage chemo-attractants including monocyte chemo-attractant protein-1 (MCP-1) and macrophage inflammatory protein-1 (MIP-1) (Xu et al., 2003). Macrophages isolated from the adipose tissue of obese mice demonstrate a phenotypic switch from an alternately activated (anti-inflammatory) to classically activated (pro-inflammatory) phenotype (Lumeng et al., 2007).

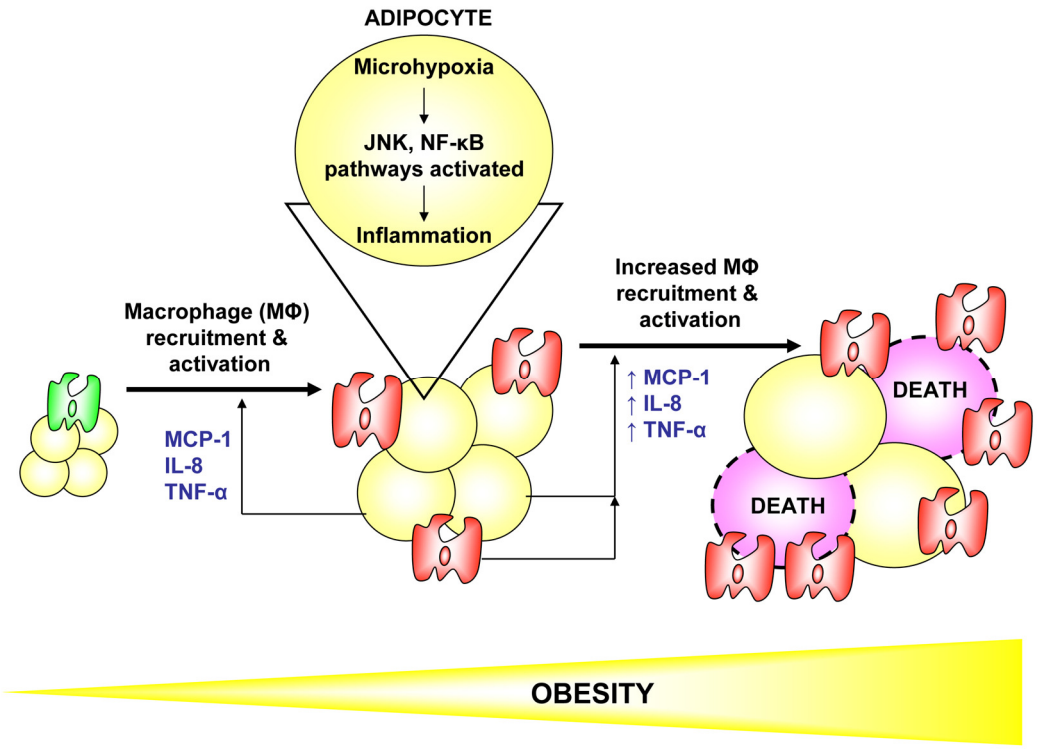


**Figure 1.7 Diagrammatic representation of the initiation of inflammation in the adipose tissue in obesity.** An increase in energy influx due to high intake of energy-rich diet leads to an increase in adipocyte size resulting in microhypoxia. Microhypoxia has been reported to initiate inflammation through activation of the JNK and NF-κB pathways resulting in release of pro-inflammatory cytokines such as MCP-1, IL-8 and TNF-α which promote macrophage recruitment and activation in adipose tissue. The microhypoxia and inflammatory response results in adipocyte death and further recruitment of macrophages, leading to a vicious pro-inflammatory chain reaction. **Abbreviations.** JNK: c-Jun N-terminal kinase, NF-κB: Nuclear factor kappa-light-chain-enhancer of activated B cells, TNF-α: Tumor necrosis factor-α, MCP-1: Monocyte chemo-attractant protein-1, IL-8: Interleukin-8 (chemokine KC). **Picture adapted from** Schenk, S. et al 2008. *Personal perspective.* Insulin sensitivity: modulation by nutrients and inflammation. *The Journal of Clinical Investigation* 118 (9). Pg. 2996.

It is believed that inflammation in adipose tissue impairs insulin signalling and hence promotes lipolysis. The pro-inflammatory response and increase in lipolysis in the adipose tissue leads to the release of pro-inflammatory mediators and free fatty acids into the circulation, resulting in ectopic deposition of lipid in muscle and liver, which promotes insulin resistance (Figure 1.8) (Hotamisligil, 2006, Shoelson et al., 2006, Van Gaal et al., 2006).

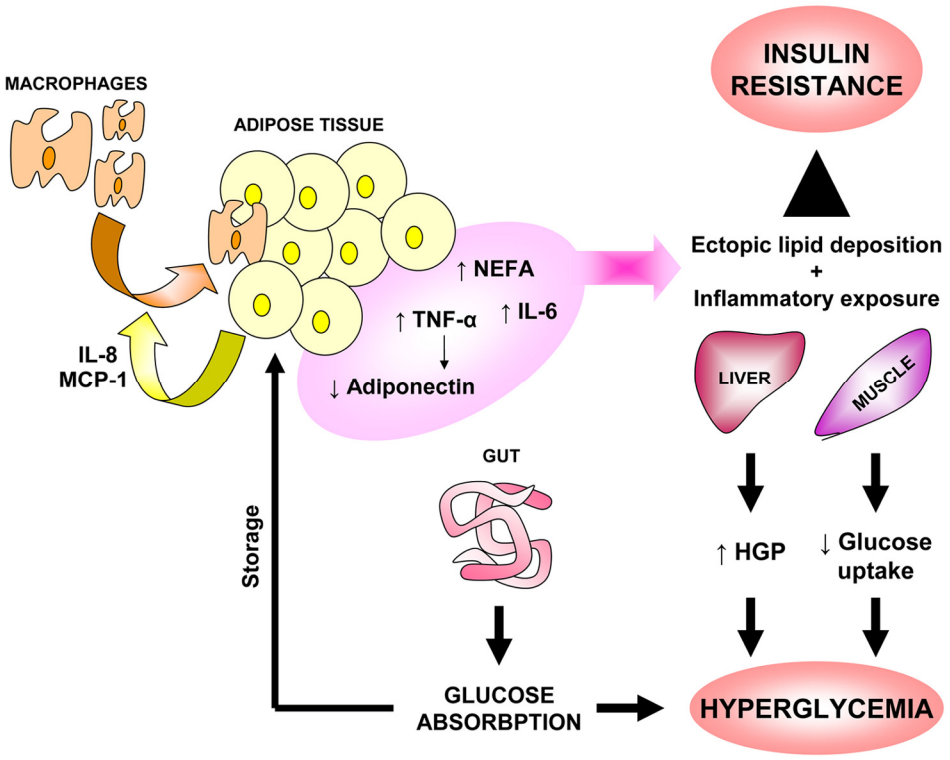


**Figure 1.8 Diagrammatic representation of inflammation promoting insulin resistance and hyperglycaemia.** Obesity associated inflammation in adipose tissue with recruitment of macrophages promote lipolysis (NEFA/FFA secretion) and increased secretion of pro-inflammatory mediators such as TNF-α, IL-6, MCP-1 and IL-8 into the circulation. The ectopic lipid deposition in liver and fat and possible exposure to inflammatory mediators impairs insulin action which leads to development of hyperglycaemia. **Abbreviations.** TNF-α: Tumor necrosis factor-α, MCP-1: Monocyte chemo-attractant protein-1, NEFA: Non-esterified fatty acid (also called FFA; free fatty acid), HGP: Hepatic glucose production. **Picture adapted from** Gaal, L.F.V. et al 2006. Mechanisms linking obesity with cardiovascular disease. *Nature* 444. Pg. 878.

### 1.4.2. ROLE OF INFLAMMATION IN DEVELOPMENT OF PERIPHERAL INSULIN RESISTANCE

Obesity-induced low-grade chronic inflammation in the peripheral organs is associated with the development of insulin resistance. An early study demonstrated that TNF-α neutralization in obese insulin-resistant mice resulted in a profound improvement in glucose uptake into muscle (Hotamisligil et al., 1993). Interleukin-1β (IL-1β) treatment has been reported to increase insulin resistance in human adipocytes by impairing insulin signaling through ERK-dependent transcription and non-ERK dependent port-translational modification of IRS-1 (Jager et al., 2007). The role of IL-6 in insulin resistance is not clear, as IL-6 production in visceral fat is high and is associated with insulin resistance in humans (Fontana et al., 2007). Furthermore, IL-6 knock-out mice have been reported to have improved insulin sensitivity (Tilg and Moschen, 2008). However, IL-6 is a potent inducer of AMPK and lipid oxidation, both of which should have an anti-diabetic effect (Febbraio, 2007).

Strong evidence links the pathways responsible for inflammatory responses and insulin signaling. JNK, which belongs to the serine/threonine kinase family, primarily mediates inflammatory responses by regulating transcriptional control of activation protein-1 (AP-1) (Davis, 2000, Shoelson et al., 2006). JNK is activated in liver, muscle and adipose tissue during obesity, potentially via endoplasmic reticulum (ER) stress, as well as increased levels of cytokines and free fatty acids (Figure 1.9). Interestingly, loss of JNK1 in experimental models of obesity has been

reported to ameliorate insulin resistance (Hirosumi et al., 2002, Wellen and Hotamisligil, 2005, Nakatani et al., 2004). Relevant studies aimed at studying the molecular link between JNK and insulin signaling in different organs have found that JNK activation causes phosphorylation of insulin receptor substrate-1 (IRS-1) at serine 307 residue, which impairs signaling between the insulin receptor (IR) and IRS-1 (Aguirre et al., 2002). Increased levels of lipid intermediates, such as diacylglycerol (DAG) and ceramide, during lipid infusion result in protein kinase C-θ (PKC-θ)-dependent phosphorylation of IRS-1 at Ser307 (Yu et al., 2002). A recent study demonstrated that removal of JNK1 specifically from hematopoietic cells had no impact on obesity, but protected mice from high-fat diet-mediated insulin resistance (Solinas et al., 2007, Solinas and Karin, 2010).

The NF-κB pathway is also implicated in insulin resistance, as salicylates reverse hyperglycaemia and hyperlipidaemia in ob/ob mice via inhibition of the NF-κB pathway (Yuan et al., 2001, Yin et al., 1998). Inhibitor of kappa B kinase (IKK) can impair insulin signalling, either through direct serine 307 phosphorylation of IRS-1, or via transcriptional activation of NF-κB, which results in secretion of cytokines such as TNF-α (Figure 1.9) (Wellen and Hotamisligil, 2005, Schenk et al., 2008). In addition, TNF-α-mediated signaling has been reported to phosphorylate IRS-1 at serine 307 residue (Rui et al., 2001).

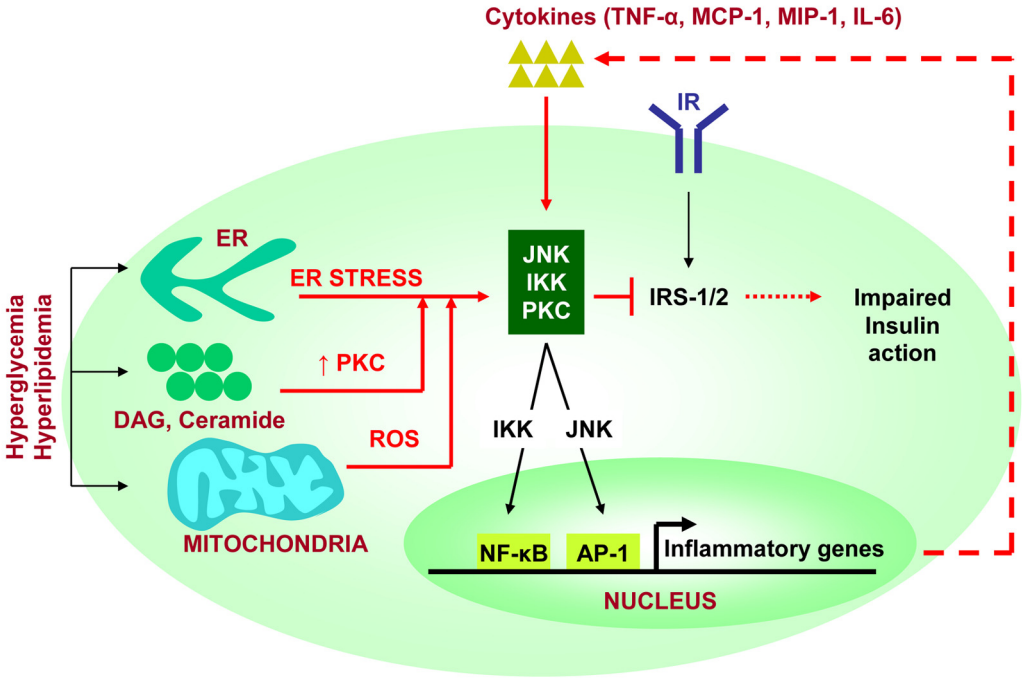


**Figure 1.9 Diagrammatic representation of the molecular signaling pathways orchestrating an inflammatory response and insulin resistance in peripheral organs.** Increased influx of glucose and lipids in type 2 diabetes can initiate inflammatory pathways such as JNK, IKK/NF-Kb, and PKC through increased production of mitochondrial ROS, accumulation of lipid intermediates such as DAG and ceramide or elevated ER stress. These pathways can also inhibit IRS-1/2 and impair insulin signaling. **Abbreviations.** ER: Endoplasmic reticulum, DAG: Diacyl glycerol, ROS: Reactive oxygen species, PKC: Protein kinase C, JNK: c-Jun N-terminal kinase, NF-κB: Nuclear factor kappa-light-chain-enhancer of activated B cells, IRS: Insulin receptor substrate, IR: Insulin receptor, IKK: Inhibitor of kappa B kinase, AP-1: Activator protein-1, TNF-α: Tumor necrosis factor-α, MCP-1: Monocyte chemo-attractant protein-1, MIP-1: Macrophage inflammatory protein-1. **Picture adapted from** Wellen, K.E. and Hostamisligil, G.S. 2005. Inflammation, stress and diabetes. *The Journal of Clinical Investigation* 115 (5). Pg. 1116.

### 1.4.3. INFLAMMATION IN ISLET β-CELL DYSFUNCTION

Glucolipotoxicity, oxidative stress, endoplasmic reticulum stress and mitochondrial dysfunction cause malfunction of islet β-cells in type 2 diabetes. A unifying mechanism to explain islet β-cell dysfunction for each of the above mechanisms may be inflammation because they all elicit a pro-inflammatory response (Donath et al.,

2005). Gene expression profiling of islets from Goto-Kakizaki (GK) rats, which is a model of type 2 diabetes, demonstrated over-expression of >70 genes compared to non-diabetic rats, of which 34% belonged to the immune/inflammatory response families (Homo-Delarche et al., 2006). In another study, increased islet gene expression of pro-inflammatory cytokines (IL-1β, TNF-α, IL-6) and chemokines (Chemokine KC, MCP-1, MIP-1) were reported in GK rats (Ehses et al., 2009). Islet macrophage infiltration has been reported in various experimental models of type 2 diabetes including GK rats, high-fat fed C57BL/6J, leptin deficient ob/ob and leptin receptor deficient db/db mice (Ehses et al., 2007b). Hence, there is increasing evidence linking the existence of islet inflammation in type 2 diabetes.

#### 1.4.3.1. IL-1 PATHWAY AS A SENSOR OF METABOLIC STRESS

Gene profiling studies on islets from human donors with type 2 diabetes has demonstrated increased expression of the IL-1β gene. Ex vivo culture of human islets at high concentration of glucose results in islet β-cell death and the underlying mechanism for β-cell apoptosis was increased expression of the pro-apoptotic receptor FAS on β-cells. This process is further enhanced by glucose-stimulated release of IL-1β (Maedler et al., 2001, Schumann et al., 2007, Donath and Shoelson, 2011). The concept of the IL-1 system as a sensor of metabolic stress in β-cell is based on a model where glucose is believed to activate inflammasomes which cleave the inactive pro-IL-1β produced by the free fatty acid (FFA)-toll-like receptor (TLR)-NF-κB pathway into active IL-1β. Secreted IL-1β further stimulates the NF-κB pathway through IL-1 receptor (IL-1R) signaling to produce chemo-attractants such

as IL-8 and MCP-1 which recruit immune cells such as macrophages into islets (Figure 1.10) (Donath and Shoelson, 2011, Martinon et al., 2002). The model receives support from multiple observations including

- The islet β-cells respond to a transient rise in glucose via activation of the NF-κB pathway to promote insulin release and β-cell proliferation (Maedler et al., 2002, Bernal-Mizrachi et al., 2002).
- FFA increase IL-1β expression in islets via TLR-2/4, a receptor cascade involved in mediating the pro-inflammatory response to lipopolysaccharide (Beutler, 2004, Lee et al., 2001, Haversen et al., 2009, Ehses et al., 2010).
- The combination of glucose and FFA induces higher cytokine production than FFA alone (Boni-Schnetzler et al., 2009).

The interaction of the cytokine IL-1β with the IL-1R receptor is tightly regulated by the presence of another molecule named IL-1 receptor antagonist (IL-1Ra) which binds to the IL-1R receptor and blocks IL-1β interacting with the IL-1R (Donath et al., 2005). In islets cultured from type 2 diabetic GK rats, the addition of IL-1Ra has been reported to suppress the gene expression of chemokines such as chemokine KC, MCP-1 and MIP-1 demonstrating IL-1 activity to be partially responsible for the pro-inflammatory response in islets in type 2 diabetes. Treatment of GK rats with IL-1Ra led to a significant improvement in peripheral insulin sensitivity, a decrease in pro-insulin to insulin ratio, a reduction in islet immune cell infiltration and chemokine gene expression in the pancreatic islets (Ehses et al., 2009). An IL-1R activity

blocker named anakinra has been reported to have anti-diabetic efficacy in patients with type 2 diabetes (Larsen et al., 2007).

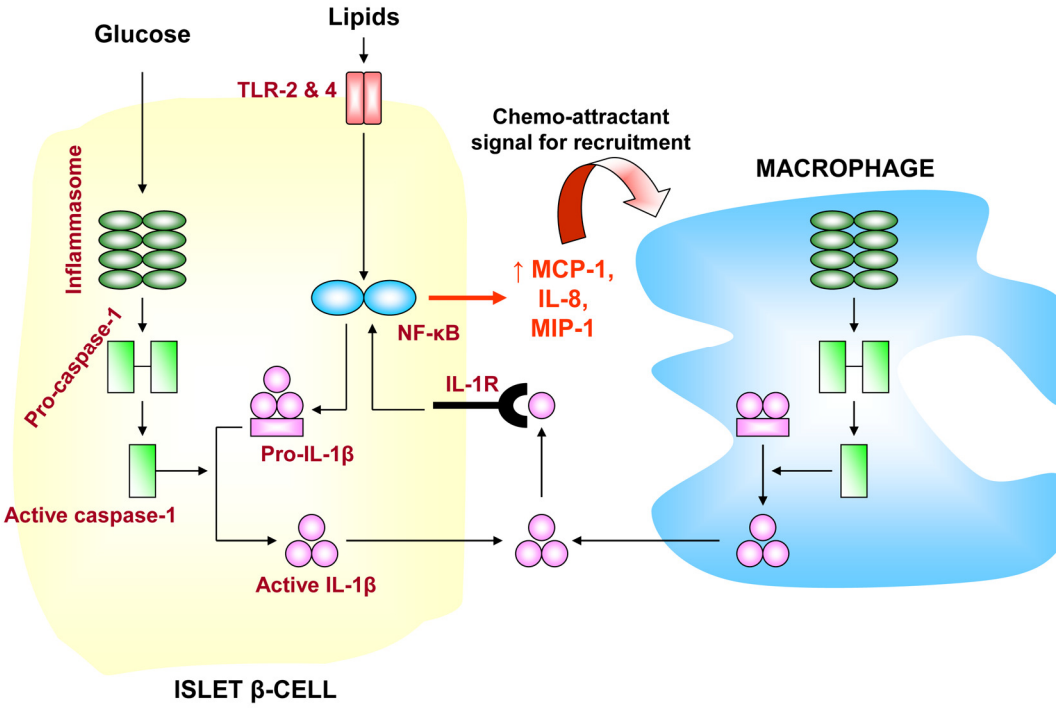


**Figure 1.10 Interleukin-1β induced inflammation and apoptosis in islets of patients with type 2 diabetes.** A model based on *ex vivo* studies involving islets from patients with type 2 diabetes. Glucose can activate pro-apoptotic caspase-1 via the inflammasome. Inactive pro-IL-1β generated by lipids via TLR/NF-κB pathway is then cleaved by activated caspase-1, generating active IL-1β which can stimulate the NF-κB pathway to produce pro-inflammatory chemo-attractants that promote macrophage infiltration. **Abbreviations.** TLR: Toll-like receptors, MCP-1: Monocyte chemo-attractant protein-1, MIP: Macrophage inflammatory protein, IL-1: Interleukin 1, IL-1R: Interleukin-1 receptor. **Picture adapted from** Donath, M.Y. and Shoelson, S.E. 2011. Type 2 diabetes as an inflammatory disease. *Nature Reviews Immunology* 11. Pg. 103.

### 1.4.3.2. THE ROLE OF NITRIC OXIDE IN ISLET INFLAMMATION

Nitric oxide (NO) has been implicated in islet β-cell dysfunction and destruction primarily in type 1 diabetes (Spinas, 1999). *Ex vivo* culture of rodent islets with a cytokine cocktail of IL-1β in presence of either interferon-gamma (IFN-γ) or TNF-α, or both, reduces β-cell secretion of insulin. This can be reversed by treatment with nitric oxide synthase (NOS) inhibitors (Corbett and McDaniel, 1995, Thomas et al., 2002). The role of NO as a pathogenic mediator in human islets is less well established (Spinas, 1999).

In the last decade, an increase in gene and protein expression of inducible isoform of NOS (iNOS) has been reported in islets of rodent models of type 2 diabetes including GK and ZDF rats (Salehi et al., 2008, Chentouf et al., 2011). Treatment with NOS inhibitors has been reported to rescue islet β-cell insulin secretion from the deleterious effects of NO (Kato et al., 2003, Corbett and McDaniel, 1995, Thomas et al., 2002). However, while *ex vivo* culture of islets isolated from diabetic rodents has demonstrated an increase in iNOS expression, a similar effect was not observed in patients with type 2 diabetes (Donath et al., 2009). Hence, there may be different mechanisms responsible for the β-cell dysfunction in humans compared with rodents.

*Ex vivo* culture of rodent islets with either a cytokine mix or lipid increases NO production and iNOS expression (Oprescu et al., 2007, Corbett and McDaniel, 1995). It is widely believed that macrophages and endothelial cells are the primary source of NO in the islets. Culture of both cell-types under different conditions, such as

increased glucose and lipid concentration has resulted in a pro-inflammatory response that includes NO production (Figure 1.11) (Koliwad et al., 2010, Yan et al., 2006). A recent study has reported that an NO donor reduces IRS-2 protein expression via proteosome-dependent degradation of the IRS-2 protein (Tanioka et al., 2011). Thus, there is an acceptance of a role of iNOS and NO in islet β-cell dysfunction in rodents. However, the existence of an interaction between different cell-types within an islet to facilitate NO generation has yet to be established *in vivo*.

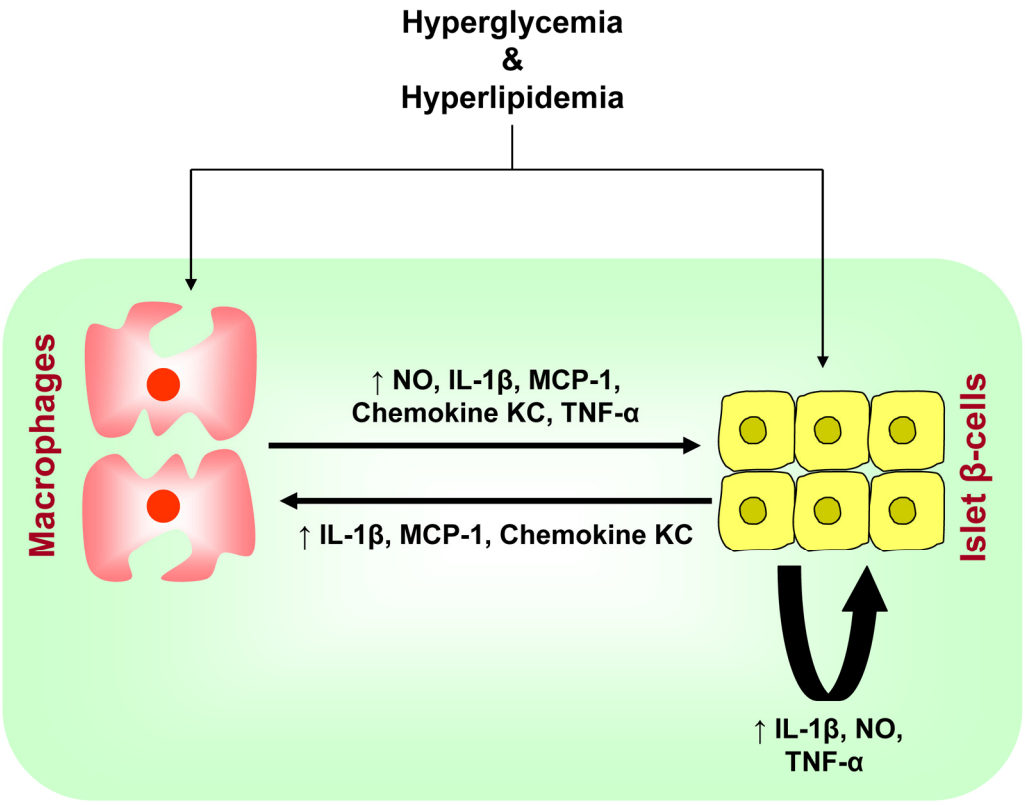


**Figure 1.11 Interaction between β-cells and macrophages within islet to promote inflammation in type 2 diabetes.** Increased glucose and lipid concentration can activate β-cells and macrophages to produce cytokines via the JNK and NF-κB pathways. The cytokines produced by β-cells can further activate adjacent β-cells and immune cells such as macrophages through autocrine and paracrine signaling. The activated macrophages infiltrating the islets can produce pro-inflammatory cytokines (and NO in rodents) to further damage β-cells. **Abbreviations.** NO: Nitric oxide, MCP-1: Monocyte chemo-attractant protein-1, IL-1: Interleukin 1. **Picture adapted from** Donath, M.Y. and Shoelson, S.E. 2011. Type 2 diabetes as an inflammatory disease. *Nature Reviews Immunology* 11. Pg. 100.

## 1.5. HEME OXYGENASE SYSTEM

Heme is a complex of ferrous iron and protoporphyrin IX and is a prosthetic group in several proteins including haemoglobin, myoglobin, nicotinamide adenine dinucleotide phosphate oxidase (NADPH oxidase), microsomal and mitochondrial cytochromes. The heme prosthetic group regulates key biological functions of proteins by facilitating oxygen transport and the electron transfer required for bio-chemical reactions. However, accumulation of free heme has cytotoxic effects on cells and tissues (Furuyama et al., 2007, Tsiftsoglou et al., 2006).

The intracellular level of heme is tightly regulated. The heme biosynthetic pathway is essentially a 7 step process for synthesis of the protoporphyrin structure, followed by a terminal step where ferrous iron is inserted into the protoporphyrin ring to form heme (Figure 1.12). Each step is facilitated by a different enzyme. The first step of heme biosynthesis involves condensation of the amino acid, glycine, with succinyl-coenzyme A (succinyl-CoA), an intermediate in the citric acid cycle. This is catalysed by 5-aminolevulinate synthase (ALAS), which is the rate-limiting enzyme in heme biosynthesis (Furuyama et al., 2007, Ajioka et al., 2006).

The heme oxygenase (HO) system is the most effective mechanism for oxidative catabolism of free heme. Heme breakdown by HO produces equi molar amounts of carbon monoxide (CO), the bile pigment biliverdin IX and free iron (Figure 1.13). Biliverdin reductase immediately converts biliverdin IX into bilirubin IX. The free

iron is readily sequestered by ferritin which is the primary form of iron storage in the body (Abraham and Kappas, 2008, Maines, 2005a).

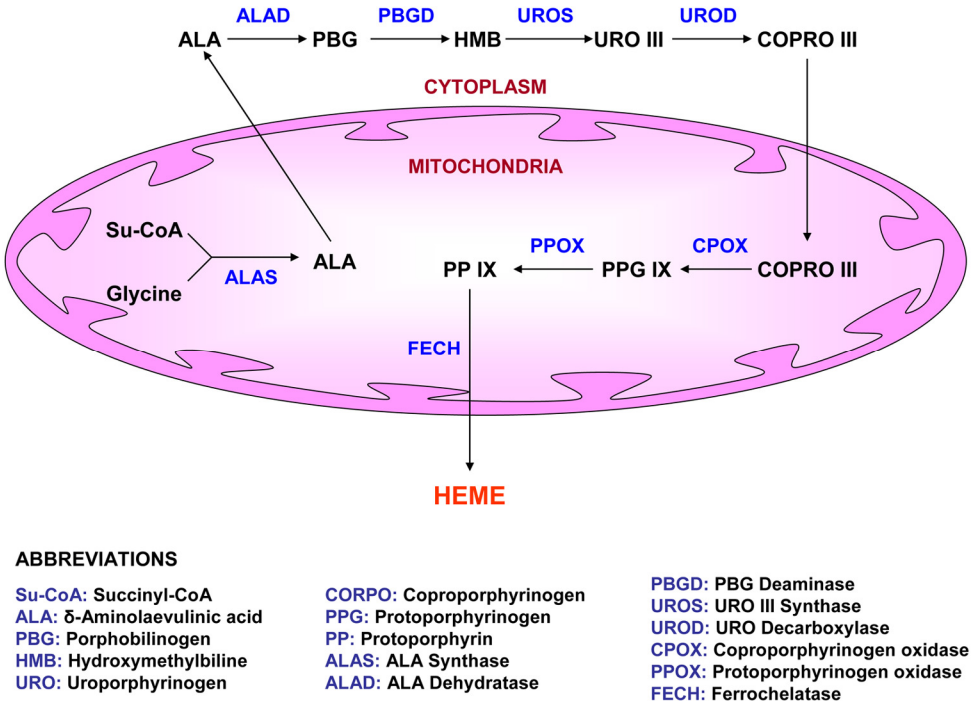


**Figure 1.12 Diagrammatic representation of heme biosynthetic pathway in mammals. Picture adapted from** Furuyama, K., Kaneko, K. and Vargas V., P.D. 2007. Heme as a magnificent molecule with multiple missions: Heme determines its own fate and governs cellular homeostasis. *Tohoku J. Exp. Med.* 213. Pg. 2.

The two major isoforms of HO system are microsomal HO-1, an inducible isoform, and constitutive HO-2 isoform. HO-1 is a 32 kilo dalton (kDa) protein which is induced by a wide range of stimuli, including heme and non-heme based molecules, such as cytokines, endotoxins, ultra-violet radiation, oxidants, and heavy metal compounds (Abraham and Kappas, 2008). The enzymatic process of heme degradation was first reported in the 1960s by the Schmitt group (Tenhunen et al., 1968, Tenhunen et al., 1969). The initial excitement with discovery of HO enzyme was due the belief that HO was a new member of the cytochrome P450 group.

However, subsequent research showed a disparity in the organ distribution of HO and cytochrome P450 (Abraham and Kappas, 2008). A decade later, induction of the HO enzyme in the liver by cobalt in a cytochrome P450 independent fashion conclusively demonstrated that HO was an independent system (Maines and Kappas, 1975).

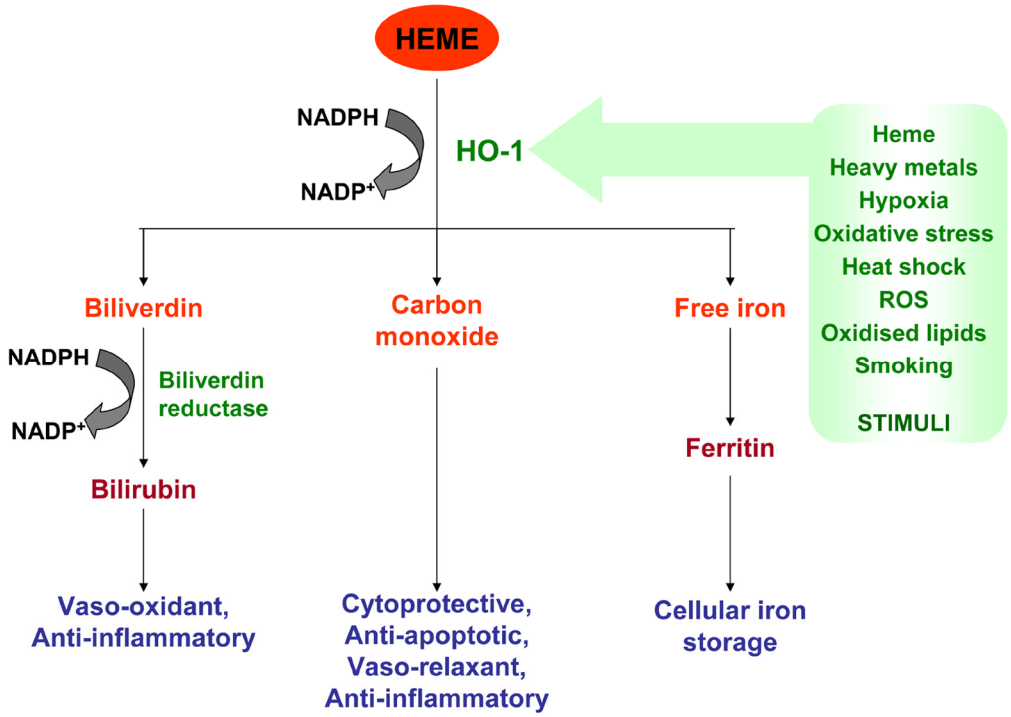


**Figure 1.13 Diagrammatic representation of heme oxygenase-1 (HO-1) in mammals. Picture adapted from** Abraham, N.G. and Kappas, A. 2008. Pharmacological and clinical aspects of heme oxygenase. *Pharmacological Reviews* 60 (1). Pg. 82.

The vitality of HO-1 in tissue homeostasis is best emphasized by the unfortunate case of an individual who had HO-1 deficiency, the only case reported in the literature. The individual suffered from growth failure, leukocytosis, tissue iron deposition and anaemia before dying prematurely at 7 years of age (Morse and Choi, 2002, Yachie and Toma, 1999).

### 1.5.1. PHARMACOLOGICAL INDUCTION OF HEME OXYGENASE

A large proportion of the research in the HO field relies on pharmacological induction and inhibition of HO activity using metallo-porphyrins (Figure 1.14). Hemin (ferrous protoporphyrin IX) and cobalt protoporphyrin IX are routinely used to induce HO activity, whereas chromium and stannous mesoporphyrin IX have been used for competitive inhibition of HO activity (Abraham and Kappas, 2008).

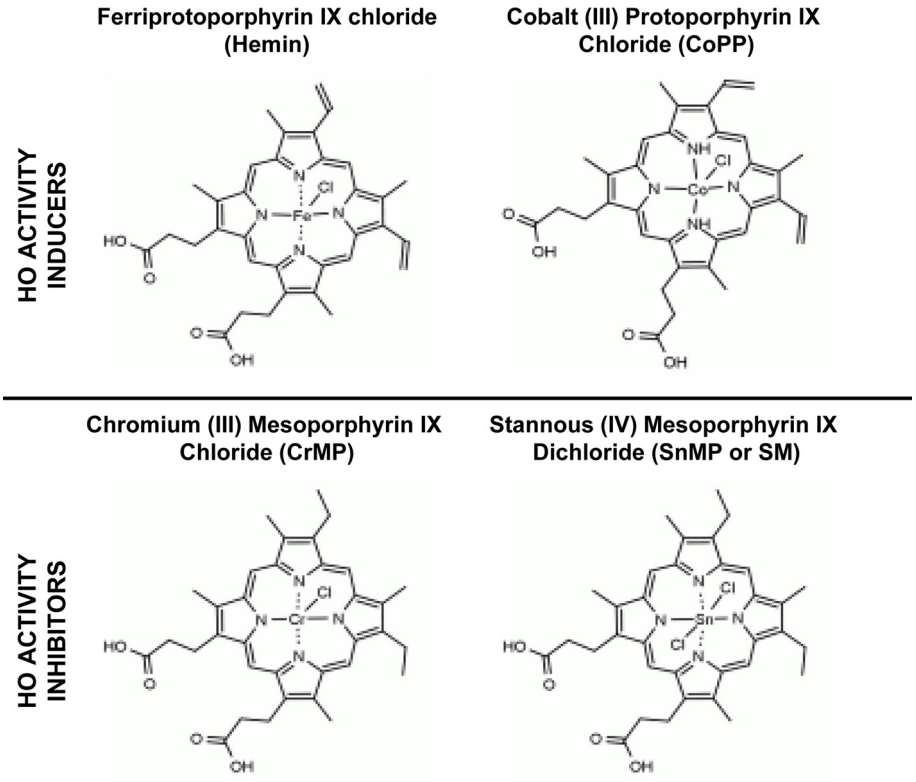


**Figure 1.14 Routinely used metallo-porphyrins for modulating HO activity in experimental and cell culture models of diseases.**
**Pictures taken from** Frontier Scientific, Logan, U.S. website.

However, metallo-porphyrins have been reported to have effects which are independent on HO activity including those listed below:

- **Anti-apoptotic effect:** Cobalt, tin or zinc protoporphyrins have been reported to directly inhibit caspase-3 activity. The porphyrin structure was demonstrated to occupy the active site of caspase-3 through molecular modeling studies (Blumenthal et al., 2005).
- **Inhibition of other enzymatic activity:** Zinc- and tin-based porphyrin compounds inhibit nitric oxide synthase (NOS) and soluble guanylyl cyclase (sGC) activity in cell culture models. Minimum interference in NOS and sGC activity has been reported with chromium mesoporphyrin (Appleton et al., 1999, Grundemar and Ny, 1997).
- **Anti-oxidant potential:** Manganese- and iron-based metallo-porphyrin compounds have been used as mimetics of superoxide dismutase (SOD), a potent anti-oxidative enzyme which protects from the cytotoxic effect of ROS (Patel and Day, 1999).

The metallo-porphyrins remain the most common method of modulating HO activity despite their numerous off-target effects. Homozygous HO-1 knock-out ($HO\text{-}1^{-/-}$) mice are a more incisive tool to demonstrate the effect of HO-1 deficiency. However, given the key role of HO-1 in heme degradation and as an anti-oxidant, it is perhaps not surprising that they have reduced viability and are therefore difficult to breed. Indeed, HO-1 homozygous knock-out mice are infertile and the rate of generation of live $HO\text{-}1^{-/-}$ offspring from breeding $HO\text{-}1^{+/-}$ mice is 1 in 4 (Poss and Tonegawa, 1997), indicating substantial loss of life *in vivo*. Given the difficulties in generating $HO\text{-}1^{-/-}$ mice, it is likely that pharmacological modulators of HO activity will continue to be used, despite their limitations.

### 1.5.2. ANTI-INFLAMMATORY POTENTIAL OF HO-1

Induction of HO activity has cytoprotective effects in various inflammatory animal models. However, the underlying mechanisms are not well understood. Clearance of the pro-oxidant heme and the anti-inflammatory and anti-oxidant properties of the products of heme catabolism are possible reasons for HO-1 being cytoprotective (Nath, 2006).

CO is a diatomic gas molecule best known to operate as a signaling molecule in biological systems. CO signals by either stimulating soluble guanylate cyclase (sGC) (Morita et al., 1995, Morita and Kourembanas, 1995) or activating mitogen-activated protein kinases (MAPK) (Otterbein et al., 2003, Otterbein et al., 2000). *In vivo* and *in vitro* studies have implicated $p38^{MAPK}$ activation to be a key mechanism for the cytoprotective effect achieved with HO-1 induction and CO. Lipopolysaccharide (LPS) treatment in the presence of CO led to elevated interleukin-10 (IL-10) expression and decreased TNF-α (Ryter et al., 2002, Otterbein et al., 2000).

Biliverdin and bilirubin, long considered as waste products have recently been viewed to have potent anti-oxidant properties. Their functional ability to scavenge ROS, thereby reducing the oxidation related stress and cellular damage, is beneficial for tissue homeostasis (Maines and Gibbs, 2005, Maines, 2005). Recently biliverdin reductase has been demonstrated to present on the external plasma membrane of macrophages and other cell-types (Wegiel et al., 2009). Tyrosine phosphorylation of biliverdin reductase, which occurs during conversion of biliverdin to bilirubin has

been implicated in activation of phosphatidylinositol 3-kinase (PI3K) and Akt which may confer an anti-inflammatory effect in LPS activated macrophages (Wegiel et al., 2009). The activation of PI3K and Akt may also be responsible for the protection that HO confers against hypoxia and oxidative stress (Pachori et al., 2007, Worou et al., 2011).

Another heme catabolic product, free iron, is known to generate ROS. However, HO-1 up-regulation also results in ferritin synthesis, which sequesters the free iron released, thereby ensuring cytoprotection from the deleterious effects of free iron (Pae, 2008).

| S.N | Agent | Cell-type | Mechanism | Reference |
|---|---|---|---|---|
| | | | | |
| 01 | Carbon monoxide (CO) | Macrophages | ↑ $p38^{MAPK}$ | (Otterbein et al., 2000) |
| 02 | CO releasing molecules | Macrophages | ↑ CO | (Sawle et al., 2005) |
| 03 | Biliverdin reductase | Macrophages | ↑ PI3K-Akt-IL-10 | (Wegiel et al., 2009) |
| 04 | IL-10 | Macrophages | ↑ $p38^{MAPK}$ | (Lee and Chau, 2002) |
| 05 | 15d-$PGJ_2$ | Macrophages | ↑ $p38^{MAPK}$ | (Lee et al., 2003) |
| 06 | Hemin | Macrophage foam cells | ↑ IL-10 | (Ma et al., 2007) |
| 07 | Apoptotic cell supernatant | Macrophages | ↑ Adenosine receptor $A_{2A}$ | (Weis et al., 2009) |

**Table 1.2 List of molecules which are either derived from (1-3) or induce the heme oxygenase (HO) pathway (4-7) and demonstrate anti-inflammatory effect in classically activated macrophages. Abbreviations**. 15d-$PGJ_2$: 15-Deoxy-12, 14-prostaglandin J2, PI3K: phosphatidylinositol 3-kinase.

### 1.5.3. ANTI-DIABETIC EFFECTS OF HO-1

Systemic administration of HO-1 inducers in rodent models of type 2 diabetes has been shown to ameliorate obesity, peripheral insulin resistance and hyperglycaemia (Li et al., 2008). The anti-diabetic efficacy of various HO activity inducers such as hemin, cobalt (III) protoporphyrin IX chloride (CoPP) and curcumin has been extensively studied in rodent models of insulin resistance including leptin deficient ob/ob mice, high-fed diet fed C57BL/6J mice, non-obese insulin resistant Goto-Kakizaki (GK) rats and Zucker fatty (Zucker fa/fa) rats (Ndisang and Jadhav, 2009, Ndisang et al., 2009b, Weisberg et al., 2008, Kim et al., 2008, Li et al., 2008).

N.G. Abraham's research group based in New York Medical College has specifically studied the effect of the HO activity inducer CoPP in obesity and insulin resistance. They were the first to report that induction of HO activity by CoPP has an anti-inflammatory effect in obese mice which improve insulin sensitivity in peripheral organs. Intraperitoneal administration of CoPP once a week for six weeks in the ob/ob mice increased serum adiponectin, decreased body weight, plasma IL-6 and TNF-α levels and improve glucose and insulin sensitivity (Li et al., 2008). Reduced insulin resistance along with decreased visceral and adipose tissue volume were reported in similar studies with an identical treatment schedule of CoPP in the Zucker diabetic fatty (ZDF) rat and Zucker fa/fa model of type 2 diabetes (Nicolai et al., 2009, Kim et al., 2008). Importantly these studies demonstrated induction of HO activity to be responsible for the beneficial effects of CoPP as co-treatment with the HO activity inhibitor stannous (tin) mesoporphyrin IX (SnMP or, SM) abolished the

beneficial effects of CoPP (Kim et al., 2008, Li et al., 2008). The authors of these reports have proposed induction of a HO/adiponectin axis as the central mechanism for the efficacy of CoPP. The increase in HO activity with CoPP results in weight loss, a decrease in inflammation and remodelling of adipose tissue characterised by smaller adipocytes with less macrophage infiltration and greater adiponectin production. There was also an increase in phosphorylation of AMPK in skeletal muscle (Nicolai et al., 2009, Kim et al., 2008, Li et al., 2008). Adiponectin and AMPK are widely accepted to promote insulin sensitivity through their action in peripheral tissues.

| **Published studies** | **Rodent model** | **HO inducer**<br>**Dose**<br>**Duration** | **HO inhibitor**<br>**Dose**<br>**Duration** |
|---|---|---|---|
| | | | |
| (Li et al., 2008) | ob/ob mouse | CoPP<br>3mg/kg i.p., 1x/week<br>6 weeks | SM<br>20mg/kg i.p., 3x/week<br>6 weeks |
| (Kim et al., 2008) | Zucker obese rat | CoPP<br>2mg/kg i.p., 1x/week<br>6 weeks | SM<br>5mg/kg i.p., 3x/week<br>6 weeks |
| (Nicolai et al., 2009) | Zucker diabetic fatty rat | CoPP<br>2mg/kg i.p., 1x/week<br>6 weeks | Not used |

**Table 1.3 List of studies and dosage of HO activity inducer and inhibitor used in rodent models of type 2 diabetes by Abraham's research group.**
**Abbreviation.** i.p.- intra-peritoneal administration.

In 2009, J.F. Ndisang and co-workers published three research studies in which hemin administration in the ZDF and non-obese GK rat models of type 2 diabetes was demonstrated to efficiently reduce hyperglycaemia by promoting peripheral

insulin sensitivity. The beneficial effects of hemin were reversed by co-treatment with the HO activity inhibitor chromium (III) mesoporphyrin IX chloride (CrMP). Hemin treatment significantly reduced peripheral insulin resistance and improved glucose sensitivity by promoting weight loss and increasing serum adiponectin levels. The extensive characterization of the effect of hemin in soleus muscle demonstrated a reduction in mRNA expression of AP-1, NF-κB and JNK as well as restoration of the protein levels of AMPK and GLUT4. Hence, hemin administration was observed to have pleotropic effects which contributed towards its anti-diabetic efficacy in these studies (Ndisang and Jadhav, 2009, Ndisang et al., 2009b, Ndisang et al., 2009a).

| **Published studies** | **Rodent model** | **HO inducer**<br>**Dose**<br>**Duration** | **HO inhibitor**<br>**Dose**<br>**Duration** |
|---|---|---|---|
| | | | |
| (Ndisang and Jadhav, 2009) | Non-obese Goto-Kakizaki (GK) rat | Hemin<br>30mg/kg i.p., daily<br>6 weeks | CrMP<br>4μmol/kg i.p., daily<br>6 weeks |
| (Ndisang et al., 2009a) | Zucker diabetic fatty rat | Hemin<br>30mg/kg i.p., daily<br>5 weeks | Not used |
| (Ndisang et al., 2009b) | Non-obese Goto-Kakizaki (GK) rat | Hemin<br>30mg/kg i.p., daily<br>4 weeks | CrMP<br>4μmol/kg i.p., daily<br>4 weeks |

**Table 1.4 List of studies and dosage of HO activity inducer and inhibitor used in rodent models of type 2 diabetes by Ndisang's research group.**
**Abbreviation.** i.p.- intra-peritoneal administration.

There have been a few studies reporting an anti-diabetic effect of curcumin, which is an inducer of HO-1 (McNally et al., 2007). Curcumin supplementation for 6 weeks (semi-synthetic diet with 0.2g/kg curcumin) in leptin receptor deficient db/db mice significantly reduced serum lipid levels, normalized hepatic anti-oxidant levels, increased hepatic glycogen storage, decreased hepatic β-oxidation and ameliorated hyperglycaemia (Seo et al., 2008). In another study, curcumin supplementation over a period of 40-60 days reduced hyperglycemia in the ob/ob and diet induced obesity (DIO) murine model of insulin resistance and type 2 diabetes by promoting an increase in serum adiponectin levels, weight loss and reducing macrophage infiltration in the adipose tissue (Weisberg et al., 2008).

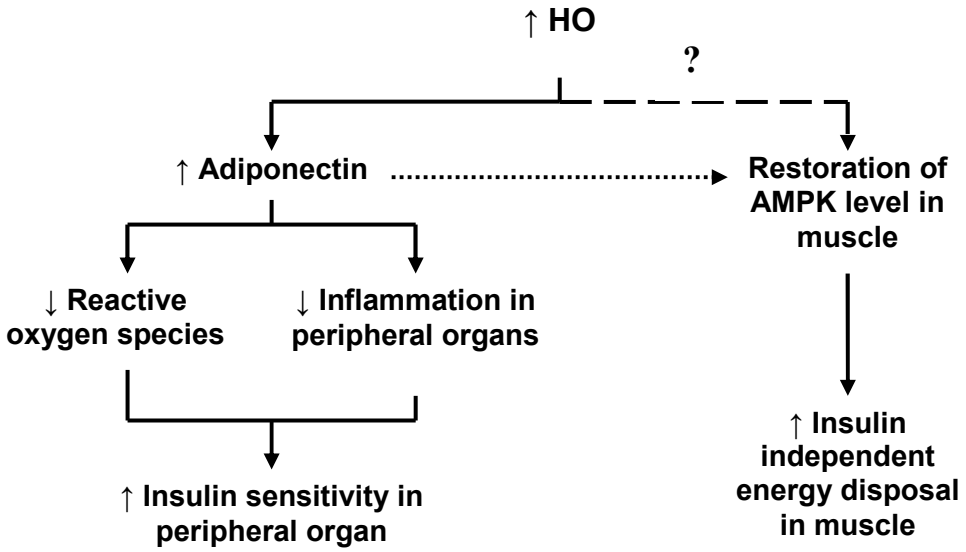


**Figure 1.15 Published anti-diabetic effect of metallo-porphyrin-based inducers of HO activity.** Studies with HO inducers have reported an increase in adiponectin to have an insulin sensitizing effect. The restoration of AMPK levels in muscle may be due to an increase in high molecular weight adiponectin level or an increase in HO activity.

### 1.5.4. HEME: A LIGAND OF REV-ERB AND ROLE IN METABOLIC AND INFLAMMATORY PROCESSES

The nuclear receptor Rev-erb is a potent repressor of gene transcription. Rev-erb mediates repression of gene transcription through its interaction with the nuclear receptor corepressor (NCoR)-histone deacetylase-3 (HDAC3) complex (Yin et al., 2010).

Heme is a ligand for Rev-erb (Yin et al., 2010) and it suppresses the mRNA levels of gluconeogenic genes including phosphoenolpyruvate carboxykinase (PEPCK) and glucose-6-phosphatase (G-6-P) in a hepatic cell line by stabilising binding of the NCoR-HDAC3 co-repressor complex to Rev-erbα (Figure 1.16) (Yin et al., 2007). Furthermore, Rev-erbα potentiates adipogenesis, as both a rise in the intracellular heme concentration and treatment with exogenous Rev-erbα ligands have been reported to induce adipocyte differentiation in 3T3-L1 cells (Kumar et al., 2010).

The NCoR-HDAC3 co-repressor complex has been implicated in repression of some pro-inflammatory genes including iNOS too. LPS stimulation of murine macrophages releases the NCoR-HDAC3 co-repressor complex from the iNOS promoter and induces iNOS gene expression (Pascual et al., 2005). PPAR-γ agonists increase the stability of a PPAR-γ-NCoR-HDAC3 complex on the iNOS promoter, preventing release of the NCoR-HDAC3 co-repressor complex from the iNOS promoter and hence iNOS expression (Pascual et al., 2005). However, whether heme

can act as a Rev-erb ligand to inhibit LPS-induced iNOS expression (Figure 1.16) has not yet been determined.

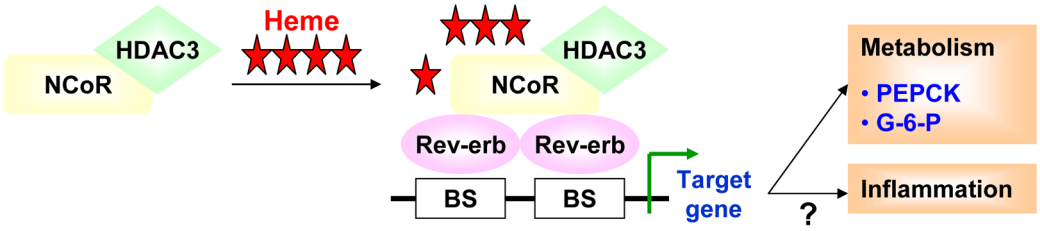


**Figure 1.16 Heme dependent Rev-erb mediated metabolic and inflammatory processes.** Heme binds to Rev-erbα to recruit NCoR-HDAC3 co-repressor complex on the promoter of PEPCK and G-6-P and inhibit the gene expression of PEPCK and G-6-P in hepatocyte cell line. Whether it can also inhibit pro-inflammatory gene expression by a similar mechanism has yet to be explained. **Abbreviations.** BS: Binding site, NCoR: Nuclear receptor corepressor, HDAC3: Histone deacetylases-3, PEPCK: Phosphoenolpyruvate carboxykinase, G-6-P: Glucose-6-phosphatase. **Picture adapted from** Yin, L., Wu, N. and Lazar, M.A. 2010. Nuclear receptor Rev-erbα: a heme receptor that coordinates circadian rhythm and metabolism. *Nuclear Receptor Signaling* 8. Pg.3.

Two recent publications describe the role of Rev-erb in the regulation of circadian behaviour and metabolism (Solt et al., 2012b, Cho et al., 2012b). T.P. Burris and co-workers have shown that two synthetic Rev-erb agonists, named SR9011 and SR9009, modulate the expression of key metabolic genes in the liver, skeletal muscle and adipose tissue, resulting in enhanced energy expenditure, a reduction in body weight and fat mass and a marked improvement in hyperlipidaemia and hyperglycaemia in the high fat diet model of type 2 diabetes. (Solt et al., 2012b). R.M. Evans and co-workers report an increase in circulatory glucose and triglyceride levels in tamoxifen-induced Rev-erb double knockout (Rev-erb $\alpha^{-/-}$ and $\beta^{-/-}$) C57BL/6 mice compared to wild-type mice, suggesting that the presence of functional Rev-erb isoforms is critical for maintenance of energy homeostasis (Cho et al., 2012b).

## 1.6. NITRIC OXIDE: AN OVERVIEW

Nitric oxide synthases (NOS) are flavo-hemoproteins which regulate the synthesis of nitric oxide (NO) (Alderton et al., 2001). NO is a short-lived free radical which can diffuse freely between cells and mediates its action in an autocrine and paracrine fashion (Aktan, 2004, Lowenstein and Padalko, 2004). NO acts as a signalling molecule to facilitate biological functions, such as vasodilatation, neurotransmission but it may also promote cytotoxicity (Hibbs et al., 1987, Palmer et al., 1987).

### 1.6.1. STRUCTURE OF NITRIC OXIDE SYNTHASE

Each monomer of the NOS enzyme constitutes of two major domains, a C-terminal reductase domain and an N-terminal oxygenase domain. The C-terminal reductase domain has a binding site each for cofactors, nicotinamide adenine dinucleotide phosphate (NADPH), flavin adenine dinucleotide (FAD) and flavin mononucleotide (FMN) (Bredt et al., 1991). The N-terminal oxygenase domain possessesbinding sites for cofactors, including, heme and tetrahydrobiopterin ($BH_4$) and also for its substrate, L-arginine. In the reductase domain, the flavin cofactors, FAD and FMN, facilitate electron transfer from NADPH to heme. The oxygenase domain acts as the active site for synthesis of NO (Crane et al., 1998). NOS are activated following homodimer formation, which is facilitated by the oxygenase domain (Figure 1.17) (Andrew and Mayer, 1999, Alderton et al., 2001). In the final step of the dimerisation process, stable incorporation of $BH_4$ facilitates the dimerisation of NOS monomers, which have both a reductase and a heme-binding domain (Baek et al., 1993). The two

domains of the NOS monomer are linked by a calmodulin (CaM) recognition site. Binding of CaM, a calcium-binding messenger protein, to the CaM recognition site in the NOS monomer plays a critical role by potentiating electron transfer from the reductase domain to the heme (Bredt and Snyder, 1990, Stevens-Truss et al., 1997).

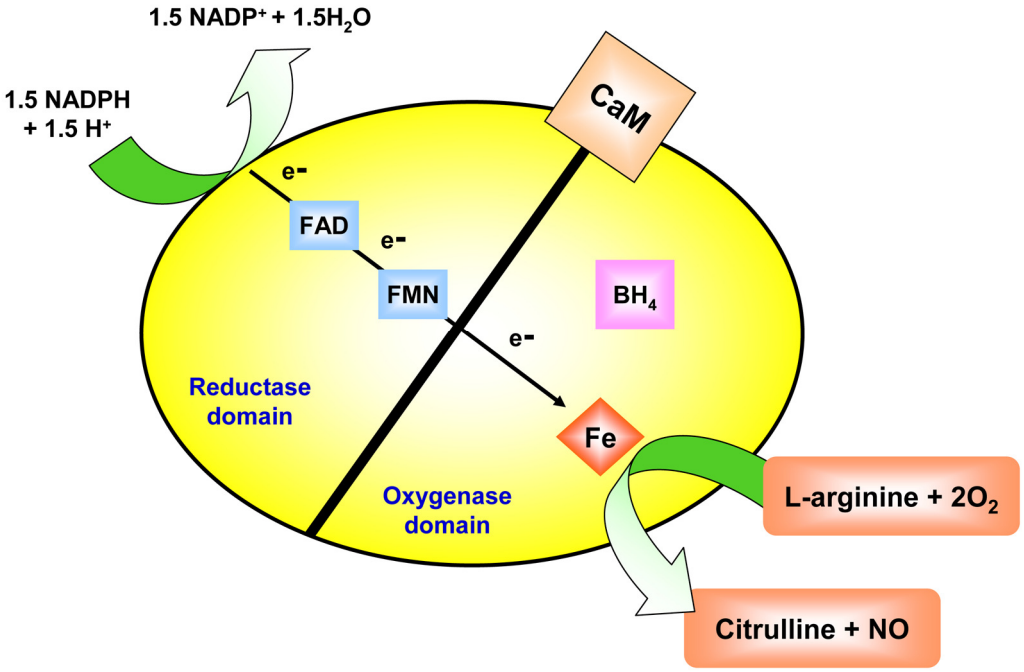


**Figure 1.17 Structure and reaction catalysed by nitric oxide synthase (NOS).** Electrons generated by oxidation of NADPH in the reductase domain, reache heme present in the oxygenase domain, via flavin cofactors including FAD and FMN, to facilitate a reaction between L-arginine and O2 to synthesise citrulline and NO. **Abbreviations.** NADPH, $NADP^+$: Nicotinamide adenine dinucleotide phosphate ± hydrogen ion, FAD: Flavin adenine dinucleotide, FMN: Flavin mononucleotide, $e^-$: Electron, $BH_4$: tetrahydrobiopterin, Fe: Heme, CaM: Calmodulin, $O_2$: Oxygen, NO: Nitric oxide. **Picture adapted from** Alderton, W.K., Cooper, C.E., and Knowles, R.G. 2001. Nitric oxide synthases: structure, function and inhibition. *Biochem J* 357. Pg.594.

### 1.6.2. ISOFORMS OF NITRIC OXIDE SYNTHASE

Three distinct isoforms of NOS have been identified and they differ in their localisation and regulation (Table 1.5). The two constitutive isoforms, endothelial

NOS (eNOS) and neuronal NOS (nNOS), are dependent on calcium ($Ca^{2+}$) for their functionality (Feng, 2012). Both, eNOS and nNOS are expressed as an inactive monomer form. The increase in intracellular $Ca^{2+}$ concentration initiates CaM binding to inactive eNOS and nNOS monomers, potentiating formation of active homodimers (Stuehr, 1999). In contrast, activity of the inducible NOS (iNOS) isoform, is independent of the increase in intracellular $Ca^{2+}$ concentration because CaM binds to iNOS at physiological concentration of $Ca^{2+}$ (Cho et al., 1992). Hence, permanent binding of CaM to iNOS potentiates constant dimerisation and consequently, catalytic activity of iNOS (Andrew and Mayer, 1999).

| **NOS isoforms/ Alternative name** | **Distinctive feature** | **Subcellular localisation** | **Tissue expression** |
|---|---|---|---|
| | | | |
| Neuronal<br>Type 1/nNOS | Constitutively expressed, $Ca^{2+}$ dependent | Binds to specific proteins via N-terminal domain | Neuronal cells,<br>Skeletal muscle |
| Inducible<br>Type II/iNOS | Inducible, $Ca^{2+}$ independent | Soluble | Macrophages, Astrocytes,<br>Hepatocytes and more |
| Endothelial<br>Type III/eNOS | Constitutively expressed, $Ca^{2+}$ dependent | Targets to Golgi via N-terminal domain | Endothelial cells<br>Epithelial cells |

**Table 1.5 List of isoforms of nitric oxide synthase and their distinctive feature, subcellular localisation and tissue expression.**
**Abbreviation.** $Ca^{2+}$- Calcium.

### 1.6.3. REACTIONS CATALYSED BY NITRIC OXIDE SYNTHASE

NOS facilitate synthesis of NO under physiological conditions (Kwon et al., 1990). However, NOS can also cause the synthesis of superoxides in absence of L-arginine (List et al., 1997). Both reactions are discussed below in detail.

#### 1.6.3.1. NITRIC OXIDE SYNTHESIS

The primary function of the NOS homodimer is to synthesise NO. The reaction between the substrates, L-arginine, NADPH and $O_2$ results in formation of L-citrulline and NO (Figure 1.17) (Kwon et al., 1990). NO synthesis is a two-step process. The first step involves the hydroxylation of L-arginine to form an intermediate, NG-hydroxy-L-arginine (NOHLA). In the second step, electron oxidation of NOHLA produces L-citrulline and NO (Stuehr et al., 1991). The complete reaction consumes 1.5 moles of NADPH and 2 moles of $O_2$ (Feng, 2012).

#### 1.6.3.2. SUPEROXIDE SYNTHESIS

NOS are capable of synthesising superoxide ($O_2^-$), particularly in the absence or at low concentrations of L-arginine (List et al., 1997). L-arginine is the only physiological donor of nitrogen for NOS mediated synthesis of NO. In the absence of L-arginine, uncoupled reduction of oxygen leads to the production of superoxide and hydrogen peroxide (Morris and Billiar, 1994). The uncoupled reduction of oxygen is

dependent on the rate of NADPH oxidation achieved by transfer of electrons from NADPH to heme (Andrew and Mayer, 1999).

### 1.6.4. METABOLITES OF NITRIC OXIDE

Nitrite ($NO_2^-$) and nitrate ($NO_3^-$) are metabolites of NO. NO reacts with molecular oxygen to produce nitrite (Kelm, 1999), a stable metabolite that has also been recognised to act as a biological signalling molecule (Bryan et al., 2005). The cytotoxicity of NO is chiefly due to the formation of peroxynitrite ($ONOO^-$), an unstable structural isomer of nitrate, resulting from a reaction between NO and superoxide (Pacher et al., 2007). Peroxynitrite reacts with transition metal centres and amino acids to modify protein structure and function (Boccini and Herold, 2004, Radi et al., 1991b), initiates lipid peroxidation to cause degeneration of lipids in the membrane (Radi et al., 1991a) and mediates oxidative modifications in nucleobases and the sugar-phosphate backbone causing to DNA damage (Burney et al., 1999).

## 1.7. HEME ARGINATE

Heme arginate (HA) is a stable and soluble composition of hemin, isolated from human blood, and L-arginine in a solution containing propylene glycol, ethanol and water (Smirnov et al., 2000). HA was first prepared and tested by Tenhunen and co-workers in Finland, to improve on hematin solutions (Tenhunen et al., 1987), which have a tendency to form heme aggregates and degrade (Goetsch and Bissell, 1986). Hematin infusion inhibits coagulation by inactivating thrombin and forming complexes with coagulation factors (Jones, 1986). HA unlike hematin, is stable for over 2 years if stored at 6$^{o}$C (Tenhunen et al., 1987) and does not cause significant changes in coagulation and fibrinolysis parameters in healthy human volunteers (Volin et al., 1988). Importantly, HA has been reported to act as a substrate for heme oxygenase and displays anti-porphyrogenic properties in experimental porphyria and in humans (Tenhunen et al., 1987, Mustajoki and Nordmann, 1993).

### 1.7.1. PHARMACOKINETICS OF HEME ARGINATE

The pharmacokinetics of HA in human volunteers were reported by Tokolo et al in 1986, where 4 healthy volunteers and 4 asymptomatic patients with porphyria received a single intravenous dose of 3 mg/kg of HA (Tokola et al., 1986). No significant changes in pharmacokinetics were observed between the two groups. Hence, the authors of the research article have presented mean values for pharmacokinetic parameters (Table) from all 8 volunteers (Tokola et al., 1986).

| Parameter | Description | Values |
|---|---|---|
| | | |
| Elimination half-life ($t_{1/2}$) | Represents time required for the drug to reach half of its original concentration. | 10.8 ± 1.6 hours |
| Total plasma clearance (Cl) | Represents volume of plasma cleared of the drug per unit time. | 3.7 ± 1.2 ml/min |
| Volume of distribution ($V_D$) | Represents volume needed for immediate distribution of the drug after intravenous injection. | 3.4 ± 0.9 l |

**Table 1.6 Pharmacokinetic parameters determined for HA in 8 human volunteers.** (Tokola et al., 1986).

### 1.7.2. PORPHYRIAS

Porphyrias are a genetically heterogenous group of diseases resulting from mutations in the genes which encode enzymes that mediate heme biosynthesis (Foran and Ãbel, 2003). These defects lead to accumulation of toxic intermediates from the heme biosynthesis pathway. Porphyrias are clinically classified into acute or non-acute forms based on the occurrence of life-threatening acute neurological attacks (Poblete-Gutiérrez et al., 2006). Acute intermittent porphyria (AIP) is the most common acute porphyria arising due to the autosomal dominant inheritance of a defect in porphobilinogen deaminase (PBGD) enzyme (Kauppinen and von und zu Fraunberg, 2002) which facilitates synthesis of hydroxymethylbiline, the third enzyme in the heme biosynthetic pathway (Figure 1.12) (Furuyama et al., 2007). Symptoms of AIP include abdominal pain, constipation, mental disturbances, convulsions, fever, and respiratory paralysis that may lead to coma and death (Foran and Ãbel, 2003). Biochemical detection of AIP includes identification of the porphyrin precursor porphobilinogen (PBG) in the urine as the PBG level has been

found to be increased by more than 50-fold compared with controls (Kauppinen and von und zu Fraunberg, 2002). Factors including high alcohol consumption, reduced carbohydrate intake, or hormones increase the frequency of acute attacks in AIP (Poblete-Gutiérrez et al., 2006).

### 1.7.3. TREATMENT OF PORPHYRIAS

In United Kingdom, patients with acute symptomatic porphyria receive treatment. Glucose and heme-based infusion therapy are standard therapies for the treatment of porphyrias (Poblete-Gutiérrez et al., 2006), which are discussed below.

#### 1.7.3.1. GLUCOSE ADMINISTRATION

One of the therapies for porphyria is administration of glucose as this can decrease heme biosynthesis (Foran and Ãbel, 2003).. The glucose-dependent decrease in porphyrin synthesis is mediated by the insulin/PGC-1α/ALAS1 axis in liver (Handschin et al., 2005). Proliferator-activated receptor γ coactivator 1α (PGC-1α) is a coactivator of nuclear receptors and transcription factors (Puigserver and Spiegelman, 2003). An increase in gluconeogenesis is mediated by PGC-1α during the fasted state. In addition, PGC-1α induces gene expression of ALAS1 (Handschin et al., 2005), the rate limiting enzyme in heme biosynthesis (Furuyama et al., 2007). Insulin exerts negative control over PGC-1α expression, firstly by reducing glucagon release (Bansal and Wang, 2008), and secondly, by inhibiting PGC-1α via Akt mediated phosphorylation of FoxO1 (Puigserver et al., 2003). Hence, an increase in

insulin secretion following glucose administration can reduce the PGC-1α mediated increase in ALAS1 function, resulting in a decrease in heme synthesis (Handschin et al., 2005).

### 1.7.3.2. HEME ARGINATE INFUSION

The mainstay of treatment for AIP is administration of a heme preparation (Foran and Ãbel, 2003). Heme arginate (HA) is licensed for use in patients with porphyria in several countries of Europe including United Kingdom. The recommended dose for HA is 3 mg/kg, once daily for 4 consecutive days (Poblete-Gutiérrez et al., 2006). The underlying principle for using HA is the ability of the heme component of HA to repress ALAS1 by a number of feed-back mechanisms including a reduction in gene transcription, mRNA stability and transport of pre-ALAS1 into mitochondria (Figure 1.18) (Yamamoto et al., 1988). A study using the avian ALAS1 gene promoter in Leghorn male hepatoma cells in culture showed that the promoter region of the ALAS1 gene had regulatory regions which respond to hemin (Kolluri et al., 2005). Hemin has been shown reduce ALAS1 mRNA stability by decreasing the half-life of ALAS1 mRNA in chick embryo hepatocytes (Hamilton et al., 1991). Furthermore, hemin specifically inhibits transfer of pre-ALAS1 from the cytosol into the mitochondria in chick liver embryos (Srivastava et al., 1983).

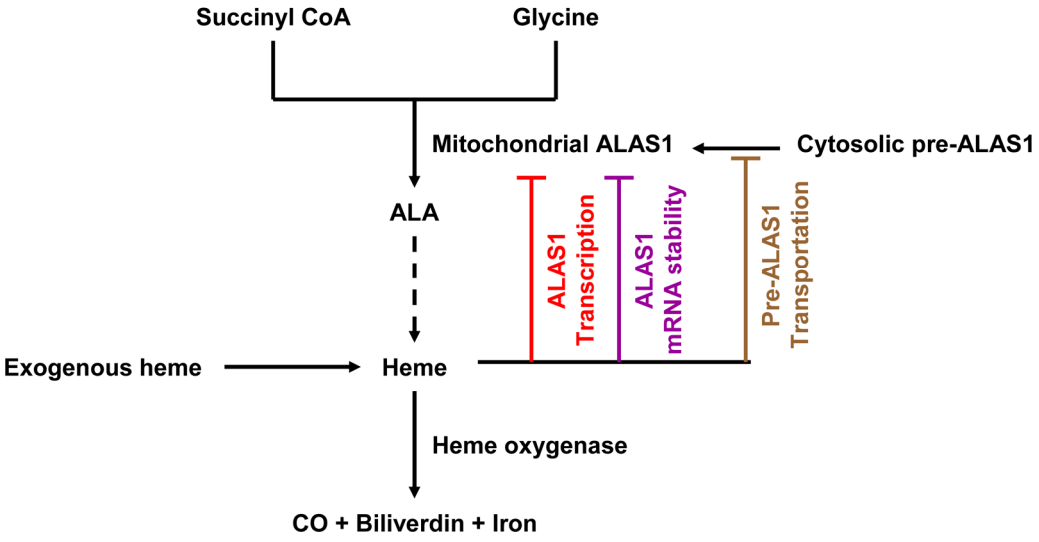


**Figure 1.18 Negative feedback regulation of ALAS1 by heme.** An increase in intracellular heme concentration leads to negative feedback control of ALAS1 gene expression by several mechanisms, including reduction in the transcription, and mRNA stability of ALAS1 and inhibition of transportation of pre-ALAS1 from the cytosol into mitochondria. **Abbreviations.** ALAS1: 5-aminolevulinate synthase, CO: Carbon monoxide. **Picture adapted from** Kolluri, S., Sadlon, T.J., May, B.K. and Bonkovsky, H.L. 2005. Haem repression of the housekeeping 5-aminolevulinic acid synthase gene in the hepatoma cell line LMH. *Biochem J* 392. Pg.178.

## 1.8. AIMS OF THE PROJECT

In the current PhD project entitled *'The role of heme arginate in modulation of inflammation and type 2 diabetes'*, three key hypothesises listed below were tested

**i.** Heme component of heme arginate (HA) has anti-hyperglycaemic effect in the db/db mouse model of type 2 diabetes.

**ii.** HA induced heme oxygenase (HO) activity potentiates anti-hyperglycaemic effect in db/db mouse model of type 2 diabetes.

**iii.** Anti-inflammatory effect of HA in primary macrophages is dependent on HO activity.

# 2. CHAPTER 2: METHODS AND MATERIALS

## 2.1. MATERIALS AND REAGENTS

### 2.1.1. METALLO-PORPHYRIN COMPOUNDS

Heme arginate (HA) was purchased from Orphan Europe (Paris La Défense, France). Other metallo-porphyrin compounds, including the HO activity inducer, cobalt (III) protoporphyrin IX chloride **(CoPP),** and the HO activity inhibitors, stannous (IV) mesoporphyrin IX dichloride **(SM)** and chromium (III) mesoporphyrin IX chloride **(CrMP),** were purchased from Frontier scientific (Logan, U.S.A). For *in vitro* studies, 25mg of amorphous CoPP, SM and CrMP were dissolved in 3ml of 10mmol/l Tris-NaOH solution, pH 14.0. The stock concentration and pH were adjusted to 8-12μM and pH 7.4 respectively using 10mmol/l Tris-HCl solution, pH 7.0 and 0.1N hydrochloric acid (HCl). The aliquots were wrapped in foil and stored at $4^{o}$C and for a month.

The tetrapyrrole structure of porphyrin molecule enables it to absorb light energy in the visible spectrum, particularly in the sorbet (400 nm) band (Poh-Fitzpatrick, 1985, Spikes, 1975). This causes transformation of the stable porphyrin molecule into an excited state molecule, where it can act as electron donor to facilitate several chemical reactions, including formation of reactive oxygen species (Dalton et al., 1972). Hence, to avoid the unwarranted photosensitive chemical reactions, the porphyrin compounds used were prepared under minimal light exposure.

### 2.1.2. TISSUE CULTURE REAGENTS, MATERIALS AND EQUIPMENTS

Tissue culture reagents and materials, including heat-inactivated fetal calf serum (HI-FCS), penicillin streptomycin (PS), Corning tissue culture flasks and plates were from Sigma Aldrich (Dorset, U.K.). GIBCO Dulbecco's modified Eagle medium [DMEM] from Invitrogen (Paisley, U.K.), Dulbecco's phosphate buffered saline [PBS] from PAA laboratories (Somerset, U.K.) and Falcon conical tubes, syringes and needles from Becton, Dickinson (Oxford, U.K.) were also employed. All other chemicals were purchased from Sigma Aldrich (Dorset, U.K.) unless otherwise stated in the text. A IEC Micro CL17R microfuge from Thermo Electron Corp. (Wilmington, U.S.A) and a Rotina 420R from DJB Labcare (Buckinghamshire, U.K.) were used for centrifugation.

## 2.2. *IN VIVO* STUDIES AND FUNCTIONAL TESTS

*In vivo* studies were carried out in diabetic (C57BL/KsOlaHsd-lepr$^{db}$/lepr$^{db}$ or, db/db) mice, a model of type 2 diabetes. The db/db mice are C57BL/KsJ inbred strain of mice with mutation for leptin receptor on chromosome 4. Hence, leptin regulated control over appetite is lost leading to hyperphagia that results in obesity and the development of insulin resistance and type 2 diabetes (Shafrir et al., 1999). Therefore, wild-type C57BL/KsJ mice were used as lean and non-diabetic control for the *in vivo* experiments.

### 2.2.1. COMPOUND PREPARATION FOR *IN VIVO* STUDIES

Dilution of HA and SM was performed in minimal light. HA was available as a solution at concentration of 25mg/ml. It was diluted 1:5 in PBS prior to intravenous (i.v.) injections. Amorphous SM (25mg) was dissolved in 3ml of 10mmol/l Tris-NaOH solution, pH 14.0. The concentration and pH were adjusted to 5mg/ml and pH 7.8 respectively using 10mmol/l Tris-HCl solution, pH 7.0 and 0.1 N HCl.

### 2.2.2. PROTOCOL FOR *IN VIVO* STUDIES

All *in vivo* experiments were carried out in accordance with protocols and guidelines outlined in project and personal license issued by the Home Office, U.K. Ten week old male lean C57BL/KsJ and diabetic db/db (Harlan laboratories, U.K.) mice were housed in groups of four per cage in the animal facility of the College of Medicine and Veterinary Medicine, University of Edinburgh. The mice were provided with water and RM1 feed ad libitum, except when fasted for four hours, to perform functional tests. The mice were weight and blood sugar matched on day 1 of the experiments for allocation to their treatment groups. The mice were anaesthetized using iso-flurane prior to intravenous injections to minimize stress. *In vivo* experiments were carried out for 8 weeks according to the treatment regime outlined in table 2.1.

At the end of the *in vivo* study, mice were anaesthetized to collect blood by cardiac puncture and organs, including pancreas, fat depots (epididymal, sub-cutaneous,

retroperitoneal), liver, spleen and kidneys. Organs were snap-frozen in liquid nitrogen and fixed in methyl-Carnoy's solution (60% methanol, 30% chloroform and 10% acetic acid) for histological examination.

| Study No. | Treatments | Dose | Injection/ week | Administration route |
|---|---|---|---|---|
| | | | | |
| 01 & 02 | PBS | 150µl | 2 | Intravenously via tail vein |
| 01 & 02 | HA | 15 mg/kg | 2 | |
| 01 | L-arginine (LA) | 20 mg/kg | 2 | |
| 02 | SM | 20 mg/kg | 3 | Intraperitoneal |
| 02 | Tris-NaOH pH 7.8 | 150µl | 3 | Intraperitoneal |

**Table 2.1 Treatments, doses, administration and duration of the *in vivo* studies.**

### 2.2.3. FUNCTIONAL TESTS CARRIED OUT DURING *IN VIVO* STUDIES

i. **Fasting blood glucose:** The mice were weighed and fasted for four hours. A small tail vein prick was made using a sterile needle and a drop of blood was applied to the glucose monitor strip attached to the glucometer (Accu-check Aviva glucometer, Roche, U.S.A.) to measure fasting blood glucose concentrations. Tail vein blood from each mouse was collected in a microvette (CB300 Kalium-EDTA blood collecting vials, SARSTEDT, U.K.) for further diagnostic assays to measure insulin, free fatty acids, and triglycerides.

ii. **Glucose tolerance test (GTT):** The mice were fasted for 4 hours, weighed and injected intraperitoneally (i.p.) with glucose solution to achieve a final dose of 2 gram glucose per kilogram body weight (2g/kg). Tail vein prick was performed

to collect blood at 0, 15, 30, 60 and 120 minutes post i.p. glucose injection. Microvettes were centrifuged at 7000*g* for 10 minutes at 4$^{o}$C. Non-haemolysed serum (~20µl) was aspirated and transferred to 0.5ml labelled Eppendorff tubes for storage at -80$^{o}$C. The blood sugar levels were then quantified using a hexokinase glucose assay (see 2.4), as blood glucose concentrations during the GTT frequently exceeded the upper limit of the quantification range of the glucometer.

iii. **Insulin tolerance test (ITT):** The mice were fasted for 4 hours, weighed and injected i.p. with insulin at a concentration of 1 unit insulin per kilogram body weight (1 unit/kg). Tail vein prick was performed and blood glucose readings were obtained at 0, 15, 30, 60 and 120 minutes post insulin injection using a glucometer.

iv. **Food intake:** Food intake was monitored over six days during week 7 and 8 of the *in vivo* study. The db/db mice were housed in individual cages and each cage was provided with 150 grams of RM1 chow. The chow left on each cage was weighed at the end of 6 days and mean daily food intake was determined by the formula *'(150-end chow weight)/6'*.

## 2.3. INSULIN ELISA ASSAY

The kit is based on the sandwich enzyme-linked immuno-sorbent assay (ELISA) technique, where an antigen is immobilized between two antigen specific antibodies

of which one is conjugated to an enzyme that oxidises the chromogenic substrate to produce a blue coloured end-product (Figure 2.1) (Jordan et al., 2005). Absorbance is then quantified in each well of the plate using a plate reader. The absorbance signal is proportionate to the amount of insulin antigen in the sample and is converted to an insulin concentration by reference to a standard curve.

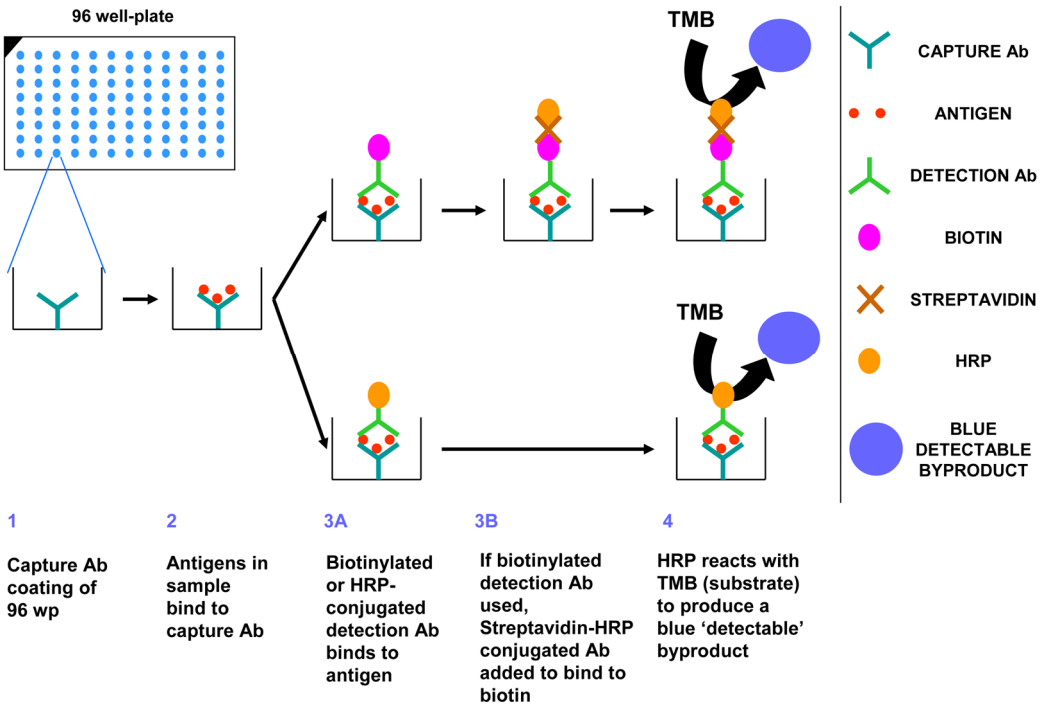


**Figure 2.1 Principle of sandwich enzyme-linked immuno-sorbent assay (ELISA).** The technique utilizes an enzyme-substrate reaction to convert a colourless chromogen into a coloured end product. 96 well-plates (wp) are coated with an antigen specific capture antibody to capture and immobilize antigens present in the sample. A second biotin or horseradish peroxidase (HRP) conjugated antigen specific detection antibody is added to sandwich the antigen between two layers of antibodies for greater specificity. At the end, 3, 3', 5, 5'- tetramethylbenzidine (TMB) which is a substrate for HRP is added to catalyze a reaction that produces a blue detectable byproduct. If a biotin-labeled detection antibody has been used (as in Duoset ELISA kits for cytokine measurements unlike Insulin ELISA kit which uses HRP-conjugated detection antibody), a streptavidin-HRP conjugated secondary detection antibody is applied prior to reaction with TMB. Biotin-streptavidin is often used for to amplify the signal as (strep)avidin has four binding sites for biotin and can therefore conjugate with several molecules of biotin.

**MATERIALS:** Ultra sensitive mouse insulin ELISA kit (Crystal Chem Inc, Downers Grove, U.S.A.), Synergy HT microplate reader (BioTek, Bad, Germany).

**METHOD:** To create a standard curve, an insulin standard (12.8ng/ml) underwent 8 serial 1:2 dilution in reagent diluent. The serum samples were diluted 20x in reagent diluent. The diluted samples and standards were pipetted (100µl/well; in duplicates) into a microplate pre-coated with guinea pig anti-insulin antibody and incubated for 2 hours at 4$^{o}$C The plate was washed 5x with wash buffer (PBS + 0.05% v/v Tween-20) before incubating with 100µl/well of horse radish peroxidase (HRP) conjugated anti-insulin antibody at room temperature for 30 minutes. The plate was washed 7x with wash buffer before adding 100µl/well of 3, 3', 5, 5'- tetramethylbenzidine (TMB) substrate solution to facilitate the reaction with HRP to produce a blue-coloured by-product over a period of 40 minutes at room temperature in the dark. The reaction was stopped by addition of 1N sulphuric acid and absorbance was read at 450nm on the microplate reader. The concentration of insulin in serum samples were determined based on absorbance readings from the insulin standard curve.

## 2.4. MEASUREMENT OF SERUM GLUCOSE LEVELS USING HEXOKINASE 'GLUCOSE' ASSAY

The hexokinase reagent initiate a two-step breakdown of glucose into 6-phosphogluconate with glucose-6-phosphate as an intermediate product. The reaction results in the reduction of nicotine adenine dinucleotide ($NAD^{+}$) into NADH whose absorbance is measured to quantify the amount of glucose in system.

**MATERIALS:** Infinity glucose hexokinase reagent (Thermo Scientific, Wilmington, U.K.), 44.4 mmol/l D-glucose solution, Synergy HT microplate reader.

**METHOD:** Serum samples from the GTT were thawed on ice. A four point standard curve (1:2 serial dilutions) was prepared using a starting concentration of 44.4mmol/l D-glucose. 2µl of standards and samples were pipetted into a flat bottom 96 well-plate kept on ice for 15 minutes. The plate was incubated for 3 minutes at 37$^{o}$C and absorbance was read at 340 nm on a microplate reader set at 37$^{o}$C.

## 2.5. NON-ESTERIFIED FATTY ACIDS (NEFA) ASSAY

The NEFA assay is based on the three-step enzymatic reactions outlined in table 2.2.

| Steps | Reactant | Catalyst | Product |
|---|---|---|---|
| | | | |
| 01 | NEFA | Acyl-CoA synthetase (ACS) | Acyl-CoA |
| 02 | Acyl-CoA | Acyl-CoA oxidase (ACOD) | 2, 3-trans-Enoyl-CoA + $H_20_2$ |
| 03 | $H_20_2$+MEHA+4-AAP | Peroxidase | Purple coloured product |

**Table 2.2 Enzymatic reactions catalysed by NEFA reagents.**
**Abbreviations.** $H_2O_2$- Hydrogen peroxide, MEHA- 3-methyl-N-ethyl-N-(β-hydroxyethyl)-aniline, 4-AAP- 4-aminoantipyrine.

**MATERIALS:** NEFA-HR2 kit (Wako Chemicals, Neuss, Germany), flat bottom 96 well plate, Synergy HT microplate reader.

**METHOD:** 5µl/well of water (blank), standard (1mmol/l) and thawed serum samples were pipetted into a 96 well-plate which was cooled on ice for 15 minutes.

160µl/well of reagent A (0.53U/ml ACS, 0.31mmol/l CoA, 4.3mmol/l ATP, 1.5mmol/l 4-AA) was added and incubated at 37°C for 3 minutes to initiate the first reaction. Immediately, 80µl/well of reagent B (12U/ml ACOD, 14U/ml HRP, 2.4mmol/l MEHA) was added and the plate was incubated at 37°C for 4.5 minutes to produce purple coloured end-product. Absorbance was read at 546 and 660nm at 37°C. The absorbance read at 660nm was deducted from the absorbance reading taken at 546nm for each sample and standard. Serum NEFA concentration was determined based on absorbance reading for the standard.

## 2.6. TRIGLYCERIDE ASSAY

The enzymatic triglyceride conversion assay is based on the method of Wako and modifications by McGowan et al. and Fossati et al. The four-step conversion reaction is outlined in table 2.3.

| Steps | Reactant | Catalyst | Product |
|---|---|---|---|
| | | | |
| 01 | Triglyceride | Lipase | Glycerol +NEFA |
| 02 | Glycerol | Glycerol kinase + ATP | Glycerol-3-phosphate |
| 03 | Glycerol-3-phosphate | Glycerol phosphate oxidase | Di-hydroxyacetone phosphate + $H_20_2$ |
| 04 | $H_20_2$ + 4-AAP + DHBS | Peroxidase | Red coloured dye |

**Table 2.3 Enzymatic reactions catalysed by triglyceride reagent.**
**Abbreviations:** $H_2O_2$- Hydrogen peroxide, 4-AAP- 4-aminoantipyrine, DHBS- 3, 5-dichloro-2-hydroxybenzene sulfonate.

**MATERIALS:** Infinity triglyceride kit (Thermo Scientific, Northumberland, U.K.), Synergy HT microplate reader.

**METHOD:** Liver triglyceride content was determined by performing isopropanol extraction of lipids. Approximately 100mg of frozen liver was homogenised in 1ml of isopropanol. The homogenate was placed on a plate shaker for 45 minutes with a vigorous vortex every 10 minutes. The homogenates were centrifuged at 3000*g* for 10 minutes and the clear supernatant was collected and stored on ice. In the meantime, a 96 well-plate was placed on ice. 2µl of isopropanol (blank), standard (2.5mmol/l) and liver samples were pipetted into 96 well-plates. The plate was incubated at 37$^{o}$C for 5 minutes after 200µl/well of triglyceride reagent was added. Absorbance was read at 500nm at 37$^{o}$C. The triglyceride concentration of samples was determined based on the absorbance reading for standards and was normalized for the mass of liver that was homogenised.

## 2.7. CULTURING AND STIMULATION OF MIN6 β-CELL LINE

MIN6 is a routinely used mouse β-cell line which was established from the insulinoma that developed in a transgenic mouse which had a human insulin promoter connected to SV40 T-antigen gene (Inada et al., 1996). The mouse insulinoma MIN6 β-cell line was kindly provided by Dr. N.M. Morton (University of Edinburgh/Centre for Cardiovascular Science) for the current study.

**MATERIALS:** Insulinoma MIN6 β-cell line cell at passage number 18, cell culture reagents and materials mentioned in section 2.1.2., TNF-α and IL-1β derived from E.coli (R&D system, Abingdon, U.K.), TRIZOL reagent (Invitrogen, Paisley, U.K.).

**METHOD:** The MIN6 β-cell line was serially passaged once or twice a week once a confluency of approximately 80% was achieved. Serial passaging was performed for 2-3 weeks prior to performing experiments in DMEM medium containing 5.5mM D-glucose, 15% heat-inactivated fetal calf serum (HI-FCS), penicillin (100U/ml), streptomycin (100µg/ml) and β-mercaptoethanol (5µl/ml) at 37$^{o}$C, 5% $CO_2$.

The experiments were carried out between cell passage numbers 25-35. MIN6 β-cells was plated at cell density of half a million (0.5 x $10^6$) cells per well in 12 well-plates. The plates were incubated for 48 hours at 37$^{o}$C, 5% $CO_2$. Non-adherent cells were washed off twice with PBS. The cells were pre-treated in fresh medium with either 10µl of PBS (vehicle) or the HO activity inhibitor SM (20µM) for 2 hours before adding the HO activity inducer HA (20µM). The cells with PBS and HA±SM added were either incubated at 37$^{o}$C, 5% $CO_2$ for 24 hours for western blotting or for 4 hours prior to stimulation with cytokine mix. The cytokine mix containing IL-1β, IFN-γ and TNF-α at final concentration of 5ng/ml, 100ng/ml and 10ng/ml respectively was added to the medium and incubated for 20 hours at 37$^{o}$C, 5% $CO_2$.

Following 20 hours stimulation with cytokine mix, supernatant for each treatment was harvested for nitrite determination. The plated cells for each treatment were washed twice with PBS and harvested in 1ml of TRIZOL reagent and stored at -80$^{o}$C for subsequent RNA extraction. In some experiments, plated cells for each treatment were trypsinised to dislodge them from the surface of the plate and collected by centrifugation at 300*g* for 5 minutes at room temperature to perform cytospin preparations (Refer to section-2.20) to determine iNOS expression by immuno-

fluorescence. Please refer to the section 5.2 of chapter 5 for a flow chart representation (Figure 5.1) of the protocol and for the concentration of compounds used (Table 5.1).

## 2.8. PREPARATION AND CULTURING OF BONE MARROW DERIVED MACROPHAGES (BMDMs)

Bone marrow derived macrophages (BMDM) are routinely used to characterize the anti-inflammatory effect of different compounds.

**MATERIALS:** DMEM, cell culture reagents and materials mentioned in section 2.1.2., 70% ethanol, autoclaved teflon pots and forceps, 10ml syringes and 19G and 25G needles.

**METHOD:** DMEM medium with 10% HI FCS and 1% PS (DMEM-PS10F) was made up in a sterile tissue culture hood. BMDMs were prepared from 6-8 week old C57BL/KsJ mice. The mice were sacrificed by cervical dislocation (schedule 1 procedure). The abdomen and lower limbs were wiped and cleaned with 70% ethanol and the lower limbs were exposed by making a midline incision and removing the fur coat. The femur was isolated by cutting the lower limbs at the pelvis level and at the mid-point of the tibia and transferred to ice-cold DMEM-PS10F. Under aseptic conditions in a tissue culture hood, the soft tissues attached to the femur were removed using a sterilised scalpel and thoroughly cleaned with a bacteriological wipe. The cleaned femurs were surface sterilised by dipping in 70% ethanol and

transferred to bijous containing 5ml of DMEM-PS10F. The femur was decapitated at both ends, exposing the marrow cavity. Bone marrow from the femur was isolated by flushing 10ml of DMEM-PS10F using a 25G needle through the marrow cavity into a 60ml teflon pot. Bone marrow cell clumps were broken into a single cell suspension by aspirating through a 19G needle five times in the teflon pot. 30ml of DMEM-PS10F with 20% (v/v) of L929 medium containing macrophage colony stimulating factor (M-CSF) was added to produce a final volume to 40ml in teflon pots. Teflon pots were incubated at 37$^{o}$C, 5% $CO_2$ for 6 days. 10ml of medium from the teflon pot was replaced with fresh L929 containing medium on alternate days. At the end of 6 days, the entire medium containing BMDM was transferred to a 50ml falcon tube and centrifuged at 300*g* for 5 minutes at room temperature. BMDM pellets were re-suspended in DMEM-PS10F containing 20% (v/v) of L929 medium and plated in 6 or 12 well plates for terminal differentiation.

## 2.9. STIMULATION OF BMDMs FOR *IN VITRO* STUDIES

The *in vitro* stimulation of macrophages with either lipopolysaccharide (LPS) or interferon (IFN)-γ or both mimics the activation of macrophage in an inflammatory micro-environment *in vivo.*

**MATERIALS:** LPS (Sigma Aldrich, Dorset, U.K.), DMEM-PS10F, Micro-centrifuge, trichostatin, metallo-porphyrin compounds listed in section 2.1.1. and tissue culture reagents and materials listed in section 2.1.2.

**METHOD:** BMDM were plated in either 6 or 12 well plates at a cell density of 0.5 x $10^6$ cells/well in 1ml of fresh medium (DMEM-PS10F supplemented with 20% (v/v) of L929 medium) and incubated overnight at 37$^oC$, 5% $CO_2$, The medium in each well was aspirated off and 1ml of fresh medium was added. BMDMs were pre-treated with either PBS or HO activity inhibitors or trichostatin (TSA; inhibitor of histone deacetylases) for 2-4 hours prior to addition of PBS or HO activity inducers. Following incubation for 20 hours, the BMDMs in each well were washed twice with warm PBS before being stimulated with LPS for another 24 hours. Each treatment was performed in duplicate.

At the end of experiment, the medium from each well was collected, centrifuged at 10,000*g* for 2 minutes and the supernatants were aliquoted in 0.5ml Eppendorff tubes and stored at -80$^oC$ for ELISA and Griess assay. The cells for each treatment were either lysed in 1ml of TRIZOL or scraped off and harvested for gene and protein expression studies respectively. Refer to section 6.2 of chapter 6 for a flow chart representation (Figure 6.2) of the protocol and the concentration of compounds used (Table 6.1).

## 2.10. ALAMAR BLUE CELL VIABILITY ASSAY

The alamar blue cell viability assay is based on the colorimetric conversion of the cell permeable blue coloured dye *'resazurin'* into the fluorescent red molecule *'resorufin'* in response to cellular metabolic reduction.

**MATERIALS:** Flat bottom 96 well-plates, Multi-channel pipette (Thermo Scientific, Wilmington, U.K.), Alamar blue (AbD Serotec, Kidlington, U.K.), Synergy HT microplate reader.

**METHOD:** A diluted cell suspension stock of MIN6 β-cells and BMDMs was prepared to a density of 25000 cells per 100µl. An automatic multi-tip pipette was used to pipette 100µl of cell suspension per well in a 96 well-plate. The plates were then incubated in the incubator at 37$^{o}$C, 5% $CO_2$ for 24 hours. Post incubation, HA and other metallo-porphyrin compounds were diluted in PBS at the desired concentration (ranged between 1-10µM). The medium in the 96 well-plate was aspirated off and plated cells were washed twice with 100µl/well of warm PBS. 100µl/well of the diluted compounds was added in triplicate to the seeded plates which were incubated for 24 hours at 37$^{o}$C and 5% $CO_2$. After 24 hour, the media containing the treatments were aspirated off and the cells were washed twice with warm PBS. 100µl/well of 10% (v/v) of Alamar Blue diluted in DMEM medium was added and the 96 well-plate was placed back in the incubator for 4 hours. The absorbance was read at excitation 570nm and 600nm.

**ANALYSIS:** The percentage reduction in Alamar blue (AB) was calculated based on the equation provided $[\{(O2 \times A1) - (O1 \times A2)\}\ \{(R1 \times N2) - (R2 \times N1)\}^{-1}] \times 100$ where,

- O1: Molar extinction coefficient (E) of oxidised AB at 570nm (E=80586)
- O2: E of oxidised AB at 600nm (E=117216)
- A1: Absorbance of test wells at 570nm

- A2: Absorbance of test wells at 600nm
- R1: E of reduced AB at 570nm (E=155677)
- R2: E of reduced AB at 600nm (E=14652)
- N1: Absorbance of negative control (medium + Alamar blue - cells) at 570nm
- N2: Absorbance of negative control at 600nm

Once the percentage of reduction in alamar blue was calculated, the values for test samples were normalised to the value of the control (PBS treatment) sample and expressed as *'percentage cell viability'*.

## 2.11. ELISA ASSAY FOR INFLAMMATORY MEDIATORS

Activated macrophages release inflammatory mediators, including cytokines, to orchestrate different stages of inflammation. In the present study, the levels of pro-inflammatory mediators including TNF-α and IL-6 as well as IL-10, a potent anti-inflammatory cytokine release by LPS activated BMDMs with different pre-treatments were determined using detection kits based on the sandwich ELISA methodology (Figure 2.1).

**MATERIALS:** Duoset ELISA kits for TNF-α, IL-6, IL-10 (R&D system, Abingdon, U.K.), RIA flat bottom 96 well-plates, Synergy HT microplate reader.

**METHOD:** Kits based on the sandwich ELISA technique was used for cytokine determination. The cytokine ELISAs were performed according to the

manufacturers' instructions. Briefly, RIA 96 well-plates were coated with 100µl/well of capture antibody and left overnight at room temperature. The plates were blocked with 1% BSA solution in PBS for an hour. Standards were prepared using 1:2 serial dilutions and 100µl/ml of samples (BMDM supernatant) and standards were added (duplicate wells/sample) and incubated for 2 hours at room temperature for antigen capture. The plate was washed 3x with wash buffer (PBS + 0.05% v/v Tween-20) before incubating with 100µl/well of biotin-labeled detection antibody at room temperature for 90 minutes. Post incubation with detection antibody, 100µl/well of 1:200 diluted streptavidin-HRP conjugated secondary detection antibody was added once the plate was washed 3x with wash buffer. The plate was incubated at 30 minutes at room temperature in dark. Post incubation, the plate was washed with 3x with wash buffer before adding 100µl/well of TMB substrate which was converted by HRP into a blue-coloured byproduct over a period of 10 minutes at room temperature in the dark. The reaction was stopped by the addition of 50µl/well of 1N sulphuric acid and the absorbance was read at 450nm on the microplate reader. The concentration of cytokines in the samples was determined by referencing the absorbance of the sample to the absorbance in the standard curve.

## 2.12. GRIESS 'NITRITE' ASSAY

The Griess method of nitrite determination is based on the reaction of nitrite with sulfanilic acid to form a diazonium salt that reacts with *N*-(1-naphthyl) ethylenediamine to produce a coloured azo-dye whose absorbance was read spectrophotometrically.

**MATERIALS:** Griess reagent, Nitrite standard 0.1M (Promega, Southampton, U.K.), flat bottom 96 well-plate, Synergy HT microplate reader.

**METHOD:** 50µl of 1:2 serially diluted standards and samples (BMDM supernatant) and 50µl Griess reagent were pipetted into a 96 well-plate. Each standard and sample was in duplicate wells. The plate was placed on a shaker for 20 minutes at room temperature and the absorbance was read at 540nm. The concentration of nitrite in the samples was determined by referencing the absorbance of the sample to the absorbance in the standard curve.

## 2.13. RNA EXTRACTION FROM CELLS AND TISSUES

An extraction buffer containing high chaotropic ions and RNase inhibitors is used to solubilise macromolecules and prevent RNA degradation respectively during the extraction process.

**MATERIALS**: NucleoSpin RNA II kit (Macherey-Nagel, Düren, Germany).

**METHOD**: Different kits were employed for RNA extractions from cells and tissues, hence they are discussed separately.

i. **RNA extraction from MIN6 β-cells and BMDMs:** RNA extraction from cells was carried out according to manufacturer's guidelines for TRIZOL reagent. TRIZOL reagent contains phenol and guanidine isothiocyanate that inhibit RNase

activity thereby preventing RNA degradation. TRIZOL lysed cells stored at -80$^{o}$C were thawed on the bench for 10 minutes prior to performing a phase separation step using chloroform. 200µl of chloroform per ml of TRIZOL was added to the Eppendorff tubes, vortexed and incubated at room temperature for 5 minutes. The Eppendorff tubes were centrifuged at 13,000*g* for 10 minutes at 4$^{o}$C. The clear phase was pipetted into a new Eppendorff tubes and incubated with an equal volume of isopropanol for 15 minutes at 4$^{o}$C. RNA in samples was precipitated by centrifuging at 13,000*g* for 25 minutes at 4$^{o}$C. The supernatant was aspirated and RNA precipitates in the Eppendorff tubes were washed with ice-cold 75% ethanol. RNA precipitates were dissolved in 20µl RNase free water once ethanol was evaporated and incubated for 10 minutes at 55$^{o}$C on a hot plate.

ii. **RNA extraction from tissues including liver and adipose tissue**: RNA extraction from tissues of C57BL/KsJ and db/db mice was performed using the NucleoSpin RNA II kit. Briefly, tissues were homogenised in 350µl of RA1 buffer which contained 1% (v/v) β-mercaptoethanol and centrifuged for 1 minute at 11,000*g* in a NucleoSpin filter column. Clear filtrate was mixed with equal volume of ice-cold 70% ethanol in RNase free water in a RNA binding column and centrifuged at 11,000*g* for 30 seconds to bind RNA in the filtrate to a silica membrane. Silica membrane bound RNA was washed subsequently with desalting buffer, DNase for DNA removal and wash buffers. Purified RNA was eluted using 30µl of RNase free water and placed on ice.

## 2.14. cDNA SYNTHESIS BY REVERSE TRANSCRIPTION

Prior to performing real time PCR, RNA must be reverse transcribed into complementary DNA (cDNA). RNA-directed DNA polymerase enzyme initiates cDNA synthesis using mRNA as a template in the presence of deoxy-ribonucleotide triphosphates (dNTP) and random primers to produce short pieces of cDNA from different regions of the mRNA template.

**MATERIALS**: High capacity cDNA reverse transcription (RT) kit (Applied Biosystems, Warrington, U.K.), PTC-100 Thermal controller (MJ Research Inc., Reno, U.S.A.), NanoDrop ND-1000 spectrophotometer (Thermo Scientific, Wilmington, U.K.).

| S.No. | Constituent | Volume/Reaction (µl) | Final concentration |
|---|---|---|---|
| | | | |
| 01 | 10x RT Buffer | 2 | 1x |
| 02 | 25x dNTP mix (100mM) | 0.8 | 4mM |
| 03 | 10x RT Random primers | 2 | 1x |
| 04 | Reverse transcriptase (50U/µl) | 1 | 50U |
| 05 | RNase inhibitor | 1 | |
| 06 | Nuclease free water | 3.2 | |

**Table 2.4 Reverse transcription master mix constituent.**
Abbreviations. RT: Reverse transcription, dNTP: Deoxyribonucleotide triphosphate, U: Unit

**METHOD**: RNA was quantified in samples by reading the absorbance at 340nm on a NanoDrop spectrophotometer. The cDNA synthesis from mRNA was performed according to the RT kit instruction manual. Briefly, 1µg of mRNA was adjusted to a volume of 10µl using RNase free water and mixed with 10µl reverse transcription

master mix (table 2.4). Reverse transcription was carried out at 37$^{o}$C for 2 hours and the reaction was terminated by raising the temperature to 85$^{o}$C for 5 minutes on a programmed thermal controller. The cDNA samples were then stored at -80$^{o}$C.

## 2.15. REAL TIME POLYMERASE CHAIN REACTION (RT PCR)

In RT PCR, the amount of cDNA present at the end of each PCR cycle is determined by the use of fluorescent probes. Oligonucleotide probes are designed to be complementary to a short sequence of the target cDNA and primers are complementary to the target cDNA on either side of the probe, thus amplifying the DNA region containing the probe binding site.

The oligonucleotide probes contain a fluorophore at 5'end and a quencher at 3' end. The quencher inhibits the fluorophore activity as long as they are in association by proximity (Figure 2.2). The nuclease activity of DNA polymerase (polymerase isolated from thermophilic bacterium *Thermus aquaticus* also known as Taq polymerase) initiates synthesis of the strand in a 5'→3' direction and cleaves the fluorophore molecule attached to the 5' end of the primer. The level of fluorescence of the cleaved fluorophore is proportional to the amount of target DNA present at end of each PCR cycle.

**MATERIALS**: TaqMan inventoried primers and TaqMan Universal PCR master mix (Applied Biosystems, Warrington, U.K.).

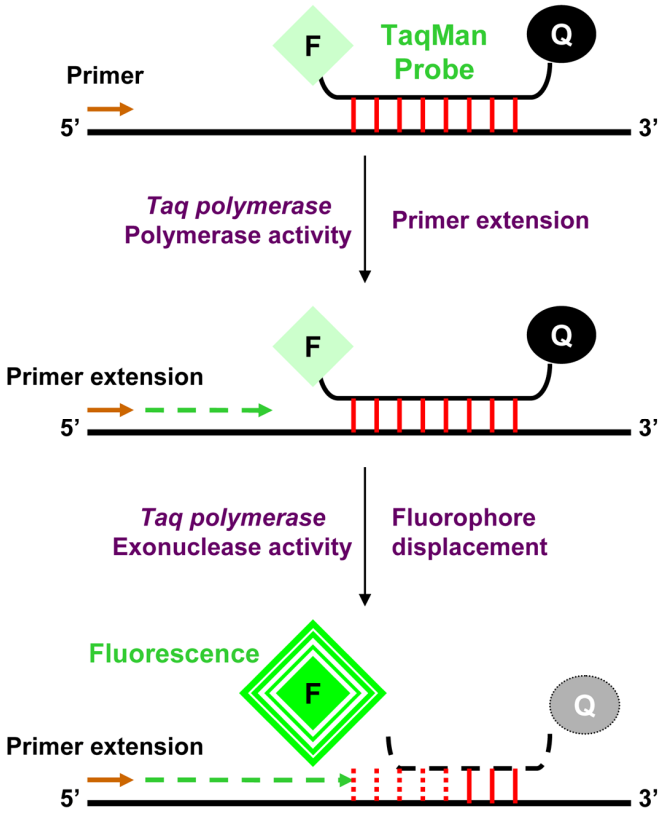


**Figure 2.2 Diagrammatic representation of the Taq polymerase based detection system for quantitative analysis of DNA synthesis.** An oligonucleotide probe complementary to the target cDNA contains a fluorophore at the 5'end and a quencher at the 3' end. The quencher (Q) inhibits the fluorophore (F) activity while they are in close proximity. Once the amplification process i.e. synthesis of the nascent strand from the primers annealed to the cDNA strand by the activity begins, the 5'→3' exonuclease activity of Taq polymerase cleaves the probe from the 5' end releasing the fluorophore from the proximity of quencher to allow the fluorophore to fluorescence. The fluorescence is then proportional to the amount of DNA.

**METHOD**: 1µl of 20x TaqMan inventoried primers and probe of interest and 9µl of 2x PCR master mixes was added to 5ng cDNA in a total volume of 20µl in a fast 96 well reaction plate. Polymerase chain reaction was performed for 40 cycles on an Applied Biosystems Fast Real time 7500 PCR machine using the automated program as outlined in table 2.5.

| S. No | Steps | Duration | Temperature |
|---|---|---|---|
| | | | |
| 01 | DNA polymerase activation | 10 minutes | 95°C |
| 02 | Melting (per cycle) | 15 seconds | 95°C |
| 03 | Annealing & extension (per cycle) | 1 minute | 60°C |

**Table 2.5 Steps of polymerase chain reaction.**

**ANALYSIS:** Analysis was performed on SDS Software 1.3.1. The baseline amplification plot was adjusted such that the threshold was located in the linear phase of the exponential fluorescence curve, above the background noise. The software generated a threshold cycle ($C_T$) value for each sample that represented the cycle number at which the fluorescence passed the threshold.

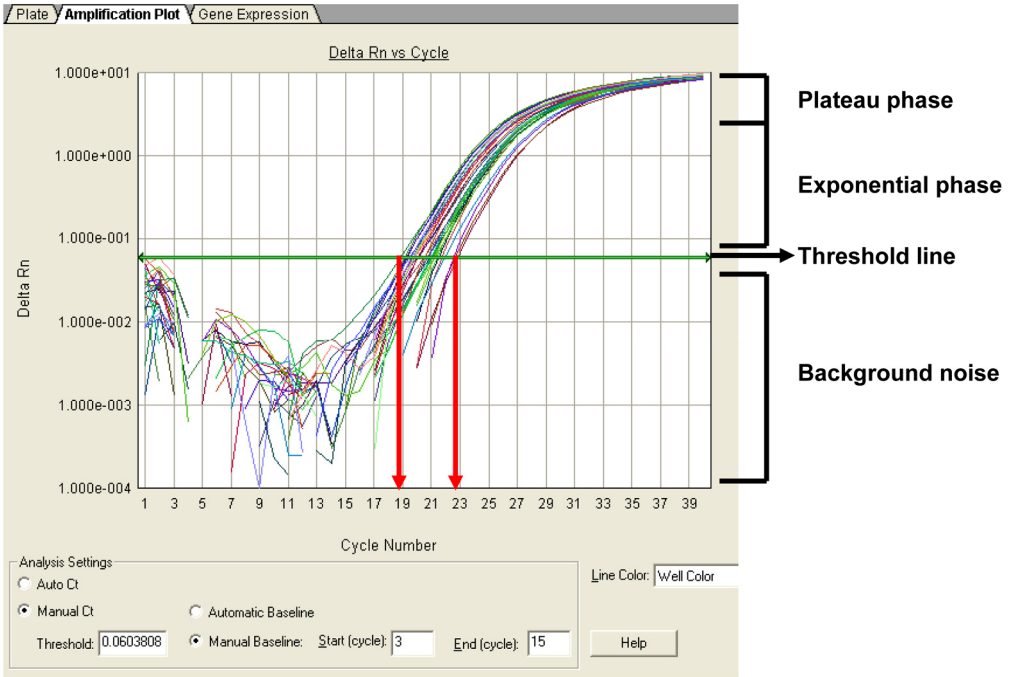


**Figure 2.3 Representative amplification plot for 18S gene in the BMDMs.** The baseline was set to capture the exponential phase of fluorescence and discount the background. The cycle number at which fluorescence level crosses threshold limit represents the threshold cycle ($C_T$) value. In the above representative figure, the red arrows represent the $C_T$ values. The cycle numbers between which the fluorescence for the 18S gene reached threshold.

The gene expression is expressed relative to a house-keeping gene expression. Hence, the $\Delta C_T$ value was calculated based on the difference of the $C_T$ values between the target gene and house-keeping gene such as 18S. The gene expression needs to be normalized to the control group of the experiment too. Thus, calibrator value was calculated by averaging the $\Delta C_T$ value of the control group (Eg: PBS treatment) of the experiment. Then, the $\Delta\Delta C_T$ value for each sample was calculated by subtracting the mean $\Delta C_T$ value of the calibrator from the $\Delta C_T$ value for each sample. Finally, the relative expression was determined by raising 2 to the power of the $\Delta\Delta C_T$ value which is known as the RQ value (see table 2.6).

| S. No. | Determinant | Equation |
|---|---|---|
| | | |
| 01 | $\Delta C_T$ | $C_T$ (Target gene) - $C_T$ (House-keeping gene) |
| 02 | Calibrator | Av ($\Delta C_T$ of control group) |
| 03 | $\Delta\Delta C_T$ | $\Delta C_T$ - Calibrator |
| 04 | RQ | Power (2, $\Delta\Delta C_T^{-1}$) |

**Table 2.6 Equations to determine relative gene expression.**

**VALIDATION OF ENDOGENOUS CONTROL GENE:** Relative gene expression studies require an endogenous control (reference) gene, such as house-keeping genes, to enable normalisation for differences in the amount of total cDNA in each sample. (VanGuilder et al., 2008). It's important to determine that variability in gene expression of reference gene is minimal across different treatment samples, to achieve a robust relative difference in expression of target genes between different treatment regimes.

Two endogenous control genes, 18S and tata-box binding protein (TBP), were used for validating endogenous control gene. The degree of variation between the animals across different treatments groups, as assessed by the standard deviation, was comparable between

18S and TBP. Hence, either of the two was used as the endogenous control gene for further gene expression studies.

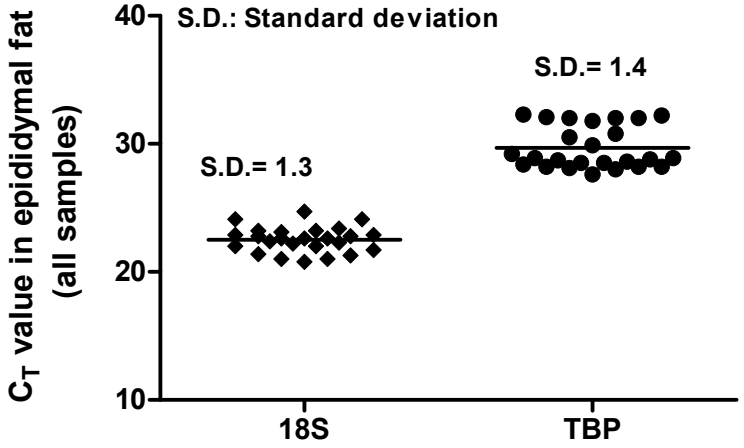


**Figure 2.4 Validation of endogenous control gene in epididymal fat.** 18S and TBP were endogenous control (reference) genes in mice treated with PBS or HA±SM.. Variability in CT values as assessed by standard deviation in sample size (N=25) showed comparable variability between 18S and TBP. **Abbreviations.** TBP: Tata box-binding protein, HO-1: Heme oxygenase-1, S.D.: Standard deviation.

## 2.16. BCA PROTEIN DETERMINATION ASSAY

The peptide bonds present in protein reduce cupric sulphate from the $Cu^{2+}$ to the $Cu^{1+}$ state at 37$^{o}$C. Bicinchoninic acid (BCA) molecules chelate $Cu^{1+}$ to form a purple coloured end-product whose absorbance is measured.

**MATERIALS**: Pierce BCA kit (Thermo scientific, Wilmington, U.K.), flat bottom 96 well-plate, Synergy HT microplate reader.

**METHOD:** Tissue or cell samples were homogenised in a small volume (100-200µl) of homogenisation buffer. Standards using 1:2 serial dilutions of 1.5mg/ml

BSA were made up. 25µl/well of standards and 20x diluted samples were pipetted in flat bottom 96 well-plate. 50 volume of BCA reagent A (bicinchoninic acid, sodium carbonate, sodium bicarbonate, sodium tartate) was mixed with 1 volume of BCA reagent B (4% cupric sulphate) and 250µl/well was added to the 96 well-plate. The plate was incubated at 37$^{o}$C for 30 minutes and absorbance was read at 565nm. Protein concentrations in samples were determined based on the BSA standard curve.

## 2.17. WESTERN BLOTTING FOR PROTEIN EXPRESSION

A gel electrophoresis system was used to separate proteins present in the sample based on the difference in molecular size of proteins under the influence of an electric field. The fractionalised proteins are transferred onto a porous membrane and probed with antibodies conjugated to an enzyme that cleaves a chemoluminescent substrate.

**MATERIALS:** List of antibodies and dilutions in table 2.7, Mini protean tetra gel electrophoresis system and power pac 300 (Bio-Rad, U.K.), Pierce ECL western blotting detection reagent (Thermo scientific, Wilmington, U.K.), Hybond ECL nitrocellulose membrane (Amersham Biosciences, Buckinghamshire, U.K.), CL-Xposure film (Thermo scientific, Wilmington, U.K.), ColorBurst electrophoresis marker (Sigma Aldrich, Dorset, U.K.).

**METHOD:** Tissues including liver and fat were homogenised in ice-cold buffer A (50mM HEPES, pH 7.0, containing 20mM NaCl, 1mM DTT, 10mM sodium

pyrophosphate, 10mM sodium fluoride, 1mM sodium orthovanadate and 1x Complete protease inhibitors cocktail) using a mixer mill MM200 tissue homogeniser. MIN6 β-cells and BMDM plated in 6 well plates were lifted in buffer A and underwent 3 freeze-thaw cycles. Homogenised tissue or cell lysates were left on ice for 30 minutes before being centrifuged at 10,000*g* for 15 minutes at 4$^{o}$C. Supernatant were transferred into pre-chilled Eppendorff tubess and protein quantification was carried out using the BCA assay. Samples of equal protein content were prepared in 5x laemmli sample buffer **(**60mM Tris-HCl pH 6.8, 2% SDS, 10% glycerol, 0.01% bromophenol blue) containing 5% (v/v) β-mercaptoethanol and boiled at 95$^{o}$C for 10 minutes.

10% Tris-acrylamide gels were cast (also known as sodium dodecyl sulphate polyacrylamide gel electrophoresis, SDS-PAGE) and loaded onto a vertical electrophoresis system. The inner chamber of the electrophoresis unit was filled with cathode buffer (50mM Tris, pH 8.6 containing 383.5mM glycine and 0.1% (w/v) SDS) and the tank with anode buffer (50mM Tris, pH 8.6 containing 0.1% (w/v) SDS). Samples containing 30µg protein and protein standard (ColorBurst electrophoresis marker) were resolved by running the gel at 70 volts. The resulting fractionated samples on the gel were transferred onto the nitrocellulose membrane cushioned on both sides with a sheet of wet filter paper and sponge at 90 volts for an hour in transfer buffer (50mM TRIS, 383.5mM glycine, 20% (v/v) methanol). The nitrocellulose membrane containing the transferred proteins was washed twice for 5 minutes each in TBST (50mM TRIS pH 7.5, 150mM NaCl, 0.05% (v/v) Tween-20). The membranes were stained with 0.2% ponceau's solution to check for equal

loading of the samples. The membranes were washed twice in TBST for five minutes before being blocked in 5% (w/v) non-fat milk solution in TBST for an hour. The membranes were incubated with primary antibodies in 3% milk or 5% BSA solution in TBST overnight at 4$^{o}$C. The next morning the membranes were given 3x washes with TBST for 10 minutes each, before being incubated with a species appropriate secondary HRP conjugated antibody diluted in 3% milk in TBST for an hour at room temperature. The membranes were washed 3x for 10 minutes each in TBST. Membranes were drained and placed on saran wrap and 3 ml of freshly prepared ECL western blotting detection reagent was added to the surface of each membrane for three minute. The ECL solution was removed with the tissues and the membranes were wrapped in saran wrap and transferred to a film cassette. The membranes were exposed to x-ray film in the dark for the appropriate time (between 5 seconds and 10 minutes) to develop the film.

| S. No | Primary (1$^{o}$) antibody | Dilution | Secondary (2$^{o}$) antibody | Dilution |
|---|---|---|---|---|
| | (Rabbit anti-mouse) | | | |
| | | | | |
| 01 | HO-1<br>(Stressgen, U.K.) | 1:5000 | Goat anti-rabbit HRP<br>(Dako, U.K.) | 1:5000 |
| 02 | HO-2<br>(Stressgen, U.K.) | 1:1000 | | 1:5000 |
| 03 | β-Actin<br>(Sigma Aldrich, U.K.) | 1:10000 | | 1:10,000 |

**Table 2.7 List of antibodies and dilution used for western blotting.**

## 2.18. HEME OXYGENASE BIOACTIVITY ASSAY

The heme oxygenase (HO) activity assay is a paired enzyme reaction that catalyses the conversion of heme into bilirubin as shown in Figure 2.5. The bilirubin levels are measured spectrophotometrically by determining the difference in absorption at 454 and 530nm. If the heme, NADPH and biliverdin reductase are all present in excess, HO is the rate-limiting enzyme and hence the concentration of bilirubin will be proportional to the HO activity. The method was first described by Tenhunen et al. in 1968 and with minor modifications has been used over the years and found to be robust method for measuring HO activity.

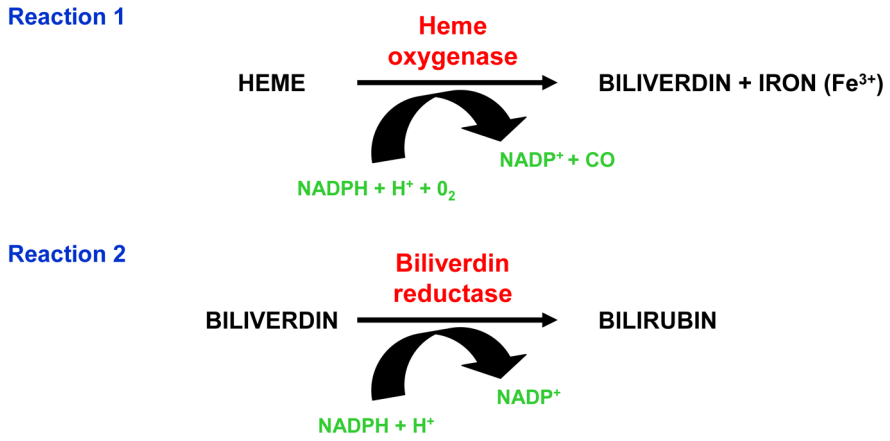


**Figure 2.5 The principle of the paired enzyme assay for determination of heme oxygenase (HO) bioactivity.**

**MATERIALS**: Mixer mill MM200 (Retch, Yorkshire, U.K.), Master mix constituents listed in table 2.7 were from Sigma Aldrich (Dorset, U.K.), HA, Quartz cuvette, Biomate 3 spectrophotometer (Thermo scientific, Wilmington, U.K.).

**METHOD:** Liver lysates were prepared by homogenizing liver samples in 250µl of phosphate buffer (0.1M di-potassium phosphate, 2mM magnesium chloride, pH 7.4) using a mixer mill MM200 tissue homogeniser. For cell culture experiments, MIN6 β-cells were plated in 10mm petri-dishes at a cell density of 5 x $10^6$ cells per plate in 10ml of medium. The BMDMs were plated in 6 well plates at a cell density of 2 x $10^6$ cells per well in 4ml of medium and were pooled later. Following treatment with the compound of interest, the plated MIN6 β-cells and BMDMs were washed twice with 3ml of PBS and scrapped off in 300µl of phosphate buffer. The cell lysates under-went 3 freeze-thaw cycles.

Liver and cell lysates were centrifuged at 10,000*g* for 10 minutes at 4$^o$C and the supernatant was transferred into pre-chilled Eppendorff tubess. Protein concentrations in the lysates were determined by the BCA assay and adjusted to a concentration of 5µg/µl using phosphate buffer. Master mix was prepared as outlined in table 2.8 and 200µl (1mg protein) of lysate was added to an equal volume of master mix in an Eppendorff tubes. Samples were incubated in the dark for an hour at 37$^o$C in a water bath. An additional sample was incubated on ice as a negative control for the experiment.

Chloroform extraction of bilirubin was performed by adding an equal volume (400µl) of chloroform to each sample to terminate the reaction at the end of the one hour incubation. Samples were mixed by vortexing for 30 seconds and centrifuged at 10,000*g* for 2 minutes at room temperature. The clear chloroform fraction (~400µl) at the bottom of the Eppendorff tubes was transferred to a new 1.5ml Eppendorff

tubes. The absorbance at 454 and 530nm (extinction coefficient, $\varepsilon$=40$Mm^{-1}cm^{-1}$) was measured using a quartz curvette in a Biomate 3 spectrophotometer. Result was expressed as 'pmol bilirubin/mg protein/hour' (McNally et al., 2004).

| S.No | Master mix constituents | Function | Stock conc. | Req conc. | Vol/ml (5 tests) |
|---|---|---|---|---|---|
| | | | | | µl |
| 01 | Glucose-6-phosphate dehydrogenase (G-6-P-D) | To maintain NADPH | 200U | 0.2U | 1 |
| 02 | d-glucose-6-phosphate | Substrate for G-6-P-D | 1.13M | 4mM | 3.5 |
| 03 | Heme arginate (HA) | Substrate for HO enzyme | 31.53mM | 100µM | 3.2 |
| 04 | Bilirubin reductase-A Activity: ~700 unit/mg | Rate limiting enzyme | 425µg/ml | 0.4 nmol | 6.5 |
| 05 | NADPH | | 100mM | 2.5mM | 25 |
| 06 | Phosphate buffer | | | | 960.8 |

**Table 2.8 Master mix constituents for heme oxygenase activity assay.**

## 2.19. IMMUNO-HISTOCHEMISTRY (IHC)

IHC is based on the principle that an antibody will bind specifically to a target antigen of interest. In general, the primary antibody will be raised against the antigen of interest in a different species to that of the target species. A secondary antibody that binds to the $F_C$ portion of antibodies from the species that the primary antibody was raised in is then applied. To visualize the bound antibody the avidin and biotin conjugated horseradish peroxidase macro-molecule complex (ABC) is the most widely used enzyme system. It exploits the high affinity binding of strept(avidin) to the biotinylated secondary antibody to form a irreversible complex. Binding of

strept(avidin) to additional biotin molecules result in signal amplification. Colourless chromogen substrate which is a good electron donor is then oxidised by the peroxidase enzyme system which is conjugated to the avidin molecule to produce coloured *'detectable'* end-product (Figure 2.6).

**MATERIALS:** A list of antibodies used and their source is provided in table 2.9. Biotinylated secondary antibodies, Avidin/Biotin blocking kit and RTU (ABC) vectastain (Vector laboratories, Peterborough, U.K.). Serum free protein block, antibody diluent, liquid diaminobenzidine (DAB) and substrate chromogen (Dako, Cambridgeshire, U.K.), HistoGreen substrate kit for peroxidase (Linaris biologische produkte, Germany).

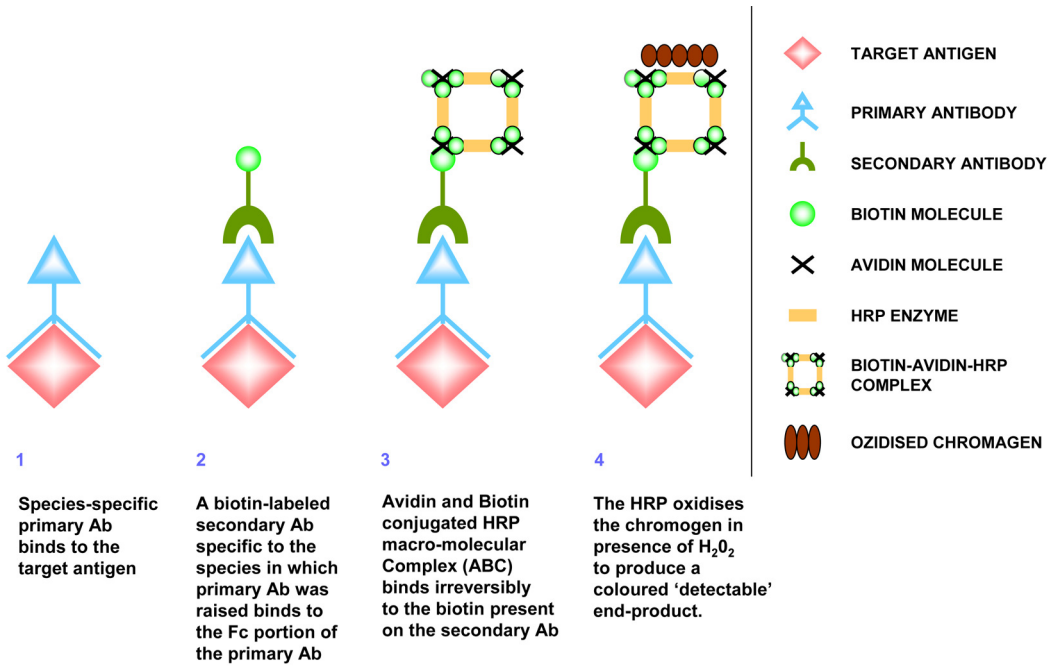


**Figure 2.6 Principle for the detection of antigen by immuno-histochemistry (IHC) staining.** ABC (**A**vidin and **B**iotin conjugated horseradish peroxidase macro-molecular **C**omplex) technology was used for the detection of target antigen where a secondary antibody conjugated to biotin undergoes an irreversible binding to ABC reagent which is later detected by applying a chromogen substrate of horseradish peroxidase.

**METHOD:** 5µm sections/slides of methyl-Carnoy fixed organs embedded in paraffin were employed. For islet studies, sections at least 75µm apart were used. The sections were deparaffinised for 15 minutes in xylene and serially rehydrated through 100, 90, 75 and 50% ethanol. The endogenous tissue peroxidase activity was blocked by incubating sections in 3% hydrogen peroxide on a shaker for 15 minutes at room temperature. Endogenous tissue avidin and biotin were blocked using 100µl/slide of blocking kit for ten minutes each at room temperature with 2x PBS wash in between blocking steps. The slides were then blocked with 3 drops of serum-free protein block for 30 minutes at room temperature before incubating overnight with primary antibodies (F4/80, iNOS, 4-HNE or HO-1) at $4^{o}$C. Antibody treated sections were incubated with a species-specific biotin labeled secondary antibody for 2 hours at room temperature. After 2x PBS washes, sections were incubated for 2 hours at room temperature with 3 drops/slide of ABC reagent. Lastly, sections were stained with 125µl/slide of chromogen DAB for 1-7 minutes to obtain brown staining localized to the region of primary antibody binding. PBS wash x2 was performed between each step to remove unbound material. For double staining, the process was repeated from the endogenous tissue avidin and biotin blocking step to stain for insulin. Lastly, sections were stained for 10 minutes with HistoGreen chromogen for detection of insulin producing islet β-cells. The sections were then counterstained in Meyer's haematoxylin and Scott's tap water for 15 seconds each with washes in tap-water in between before being dehydrated serially in 50, 75, 90, 100% ethanol and then xylene. Coverslips were applied using DPX mounting medium.

| **Host/ Specificity/Antigen Concentration Clonality/Isotype Manufacturer Catalogue number** | **Purpose** | **Dilution** | **$2^{O}$ antibody Concentration Catalogue No** | **Dilution** |
|---|---|---|---|---|
| | | | | |
| **Rabbit anti-mouse iNOS Type II**<br>250 µg/ml<br>Polyclonal / IgG<br>BD Transduction Lab. (U.K)<br>#610333 | Expressed by various cell types during cellular stress | 1:100 | Biotinylated Goat anti-rabbit<br>1.5mg/ml<br>#BA1000 | 1:300 |
| **Rat anti-mouse F4/80**<br>200 µg/ml<br>Monoclonal/ IgG2a<br>Invitrogen (U.K.)<br>#MF48000 | Marker for macrophage | 1:100 | Biotinylated Rabbit anti-rat<br>0.5mg/ml<br>#BA4001 | 1:200 |
| **Guinea pig anti-mouse Insulin**<br>Not determined<br>Polyclonal / IgG<br>Abcam (U.K.)<br>#ab7842 | Identify islet by staining for insulin producing β-cells | 1:100 | Biotinylated Goat anti-guinea pig<br>2.0mg/ml<br>Abcam (U.K.)<br>#ab6907 | 1:500 |

**Table 2.9 List of antibodies and dilutions used for immuno-histochemistry.**

**IMAGING AND ANALYSIS:** The staining on sections was visualised on a Zeiss Axioskop microscope (Zeiss, Germany). Images of pancreatic islets were captured at 200x magnification using QCapture Pro imaging software. Minor adjustment for brightness and contrast were performed on images using Adobe Photoshop. ImageJ is a publically available, Java-based image processing program developed by the U.S. National Institute of Health and was used to count the number of cells which stained positively for a particular antigen using the *'cell counter'* plugin. The islet

area was calculated in pixels by drawing a circle around the periphery of the islet using the *'Free hand selection'* on ImageJ (Figure 2.7). The area in pixels was converted into *'$\mu m^2$'*, based on a measurement taken using a graticule at the same magnification. As the islet area was different between treatments, it was standardized by expressing the number of positive staining cells per $100\mu m^2$ of islet.

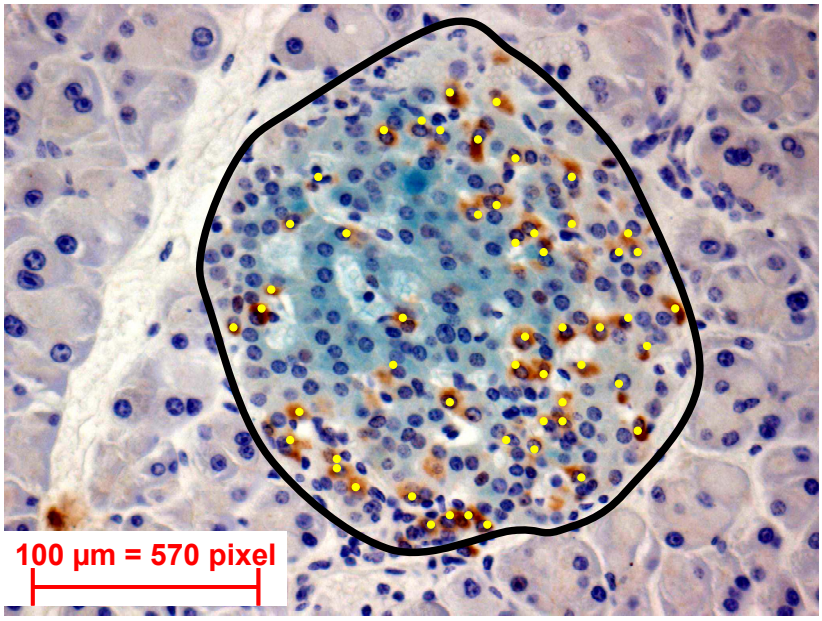


**Figure 2.7 IHC staining specimen.** Pancreatic islet stained for insulin (green) and iNOS (brown). Black boundary shows *'free hand selection'* performed to measure islet area based on the distance measured using a graticule (shown in red). Yellow dots represent manual counting performed using the *'cell counter'* plugin to count the number of positively stained cells.

## 2.20. INDIRECT IMMUNO-FLUORESCENCE (IF)

An indirect method of detection of antigen of interest using fluorescent dye labeled antibodies. The fluorescent dye is excited and the emission spectrum at the wavelength specified for the dye is viewed using a fluorescent microscope.

Availability of fluorescent dyes that are excited and emit light at different wavelengths aid co-localization of two or more markers.

**MATERIALS:** Refer to table 2.10 for antibody list and source. Vectashield mounting medium with DAPI (Vector laboratories, Peterborough, U.K.), Molecular probe tertiary antibody streptavidin conjugated 488 and 555 (Invitrogen, Paisley, U.K.) serum free protein block and antibody diluent (Dako, Cambridgeshire, U.K.).

**METHOD:** Paraffin embedded methyl-Carnoy fixed section, cryostat cut frozen sections or cytospin sections were used for the indirect immuno-fluorescence study. Paraffin embedded sections were deparaffinised and rehydrated (similar to IHC protocol) in graded ethanol. Frozen and cytospin sections were fixed for 3 minutes in 90% acetone+10% methanol solution. The sections were the blocked for endogenous biotin and avidin for ten minutes each with PBS washes in between steps. The sections were treated with 125µl/section of serum-free protein block for 30 minutes before being incubated overnight with 125µl/section of diluted primary antibody at $4^{o}$C. Next morning, sections were treated with biotinylated secondary antibody (125µl/section) and incubated in dark at room temperature for 2 hours. Then, sections were incubated with streptavidin conjugated tertiary antibody attached to a fluorescent dye (125µl/section) for an hour at room temperature in the dark. Unbound materials on sections were washed off with PBS at the end of each incubation step. Sections were mounted with mounting medium containing DAPI and stored in the dark at $4^{o}$C for single label IF. For double-labelling IF, steps from avidin and biotin blocking were repeated for detecting a second antigen on same

section. Ideally, a tertiary antibody conjugated to a fluorochrome with an excitation/emission spectrum that does not overlap that of previous fluorochrome is used to localise the second antigen of interest. The flurochromes were visualised using a Zeiss Axioskop 2 MOT PLUS fluorescent microscope (Zeiss, Germany) and images were captured at 400x magnification using Open Lab software.

| **Host/ Specificity/Antigen**<br>**Dilution**<br>**Manufacturer** | **Biotinylated $2^{O}$ antibody**<br>**Dilution**<br>**Manufacturer** | **Fluorophore $3^{O}$ antibody**<br>**Dilution**<br>**Manufacturer** |
|---|---|---|
| | | |
| **Rabbit anti-mouse iNOS Type II**<br>1:100<br>BD Transduction Lab (U.K.) | Goat anti-rabbit<br>1:300<br>Vector laboratories (U.K.) | Alexa Fluor 595 conjugate<br>1:500<br>Invitrogen (U.K.) |
| **Guinea pig anti-mouse Insulin**<br>1:100<br>Abcam (U.K.) | Biotinylated Goat anti-guinea pig<br>1:500<br>Abcam (U.K.) | Streptavidin Alexa Fluor 488 conjugate<br>1:500<br>Invitrogen (U.K.) |

**Table 2.10 List of antibodies and dilutions used for indirect immuno-fluorescence staining.**

## 2.21. STATISTICAL ANALYSIS

Non-parametric statistical tests were employed to assess for significant differences between different treatment regimes. A Two-tailed Mann-Whitney test, the non-parametric equivalent of the non-paired t-test was employed to compare two treatment groups, whereas the Kruskal-Wallis test, the non-parametric test equivalent to one-way analysis of variance, was used to compare multiple treatment groups. The Friedman test, the non-parametric equivalent of the repeated measures one-way analysis of variance, was used for data analysis where multiple treatment groups

were compared across serial time-points. For data with serial time-points, either the area under the curve using the trapezoid method or, the relative difference to baseline level was calculated and tested for statistical significance using the Kruskal-Wallis test.Dunn's multiple comparison post-test was performed to derive P-values between treatment groups, when $P<0.05$ by either Friedman or Kruskal-Wallis test, with confidence interval set at 95%. All data are expressed as mean ± standard error mean (s.e.m.). All statistical analysis was performed using GraphPad Prism version 4.0 (GraphPad Software, San Diego, CA, www.graphpad.com).

# 3. CHAPTER 3: *IN VIVO* STUDY 1: DETERMINING THE ANTI-DIABETIC EFFECT OF HEME ARGINATE IN LEPTIN RECEPTOR DEFICIENT db/db MOUSE MODEL OF TYPE 2 DIABETES

## 3.1. INTRODUCTION

Inducers of heme oxygenase (HO) activity have been reported to reduce obesity and hyperglycaemia in experimental models of type 2 diabetes. A HO activity-dependent increase in circulatory adiponectin has been postulated to promote a protective phenotype that included weight loss, reduced insulin resistance and suppressed levels of circulatory cytokines and mediators of oxidative stress (Li et al., 2008, Weisberg et al., 2008). In addition, hemin treatment in diabetic rats restores muscle AMPK levels (Ndisang et al., 2009a).

Heme arginate (HA) is a potent inducer of HO activity *in vitro* and *in vivo* (Ferenbach et al., 2011) and is licensed for use in humans to treat acute intermittent porphyria. An *in vivo* experiment was designed to test the hypothesis that **the heme component of HA ameliorates hyperglycaemia in the leptin receptor deficient diabetic (db/db) mouse model of type 2 diabetes**.

## 3.2. AN OVERVIEW OF THE DIABETIC (db/db) MOUSE MODEL OF TYPE 2 DIABETES

The diabetic (db/db) mouse is a genetic model of type 2 diabetes, first discovered at Jackson Laboratory, when an autosomal recessive mutation occurred in the leptin receptor gene ($Lepr^{db}$) on chromosome 4 in the C57BL/KsJ inbred strain of mice (Panchal and Brown, 2010).

Leptin is an adipokine hormone and acts as part of a negative feedback loop to maintain body fat. Circulatory leptin levels increase in adiposity. Leptin interacts with leptin receptors present in hypothalamic nuclei of the brain to suppress appetite (Friedman and Halaas, 1998). Interaction of leptin with its receptor in the hypothalamic nuclei counteracts the effect of feeding stimulants such as neuropeptide Y (Friedman, 1997). Melanocyte-stimulating hormone (MSH) is an appetite suppressant and is required for the biological response of leptin (Erickson et al., 1996).

The $Lepr^{db}$ mutation in the C57BL/KsJ strain of mice (db/db mouse) prevents leptin interacting with leptin receptors in hypothalamic nuclei thereby resulting in loss of control over appetite. This leads to an unregulated increase in food intake (hyperphagia) resulting in obesity and severe hyperglycaemia (Hummel et al., 1966). Profound weight gain can be observed by 6 weeks of age, followed by development of glucose intolerance, hyperinsulinemia and islet hyperplasia and hypertrophy between 8 and 12 weeks of age. A drop in the plasma insulin level coincides with

islet β-cell loss and a further increase in hyperglycaemia between 16 and 24 weeks of age (Coleman and Hummel, 1967, Coleman, 1978). The $Lepr^{db}$ mutation in the C57BL/6J inbred strain of mice also causes hyperphagia and obesity; however hyperglycaemia is transient due to the compensatory effect of hyperinsulinaemia because C57BL/6J mice are resistant to islet atrophy (Davis et al., 2012).

The db/db mouse was used for *in vivo* experiments to test the following hypotheses:

- Chapter 3: Heme component of HA ameliorate hyperglycaemia.
- Chapter 4: Anti-hyperglycaemic effect of HA is dependent on HA's ability to induce HO activity.

Wild-type C57BL/KsJ inbred mice were used as lean, non-diabetic controls for the *in vivo* experiments.

## 3.3. DETERMINATION OF THE OPTIMAL HA DOSE FOR SUSTAINED INDUCTION OF HO ACTIVITY

C57BL/KsJ mice were intravenously administered either PBS or HA at 3 different concentrations, 5, 15, and 30mg/kg. Livers from PBS and HA-treated C57BL/KsJ mice were isolated 24 hours after intravenous administration. Western blotting performed on liver lysates demonstrated that all three concentrations of HA induced HO-1 protein (Figure 3.1A).

As 15mg/kg of HA significantly induced HO-1 protein in the liver of C57BL/KsJ mice, this dose was chosen to assess the time course of HO-1 induction. Western blotting showed that a single dose of 15mg/kg of HA induced HO-1 protein levels for up to 72 hours (Figure 3.1B).

A HO activity assay was performed to determine whether 15mg/kg of HA increased HO activity relative to PBS-treated mice. Hepatic HO activity was significantly increased 24 and 48 after HA administration, compared with that observed in PBS-treated mice (Figure 3.1C). Hence, twice weekly administration of 15mg/kg HA was chosen as the optimal treatment regime in db/db mice.

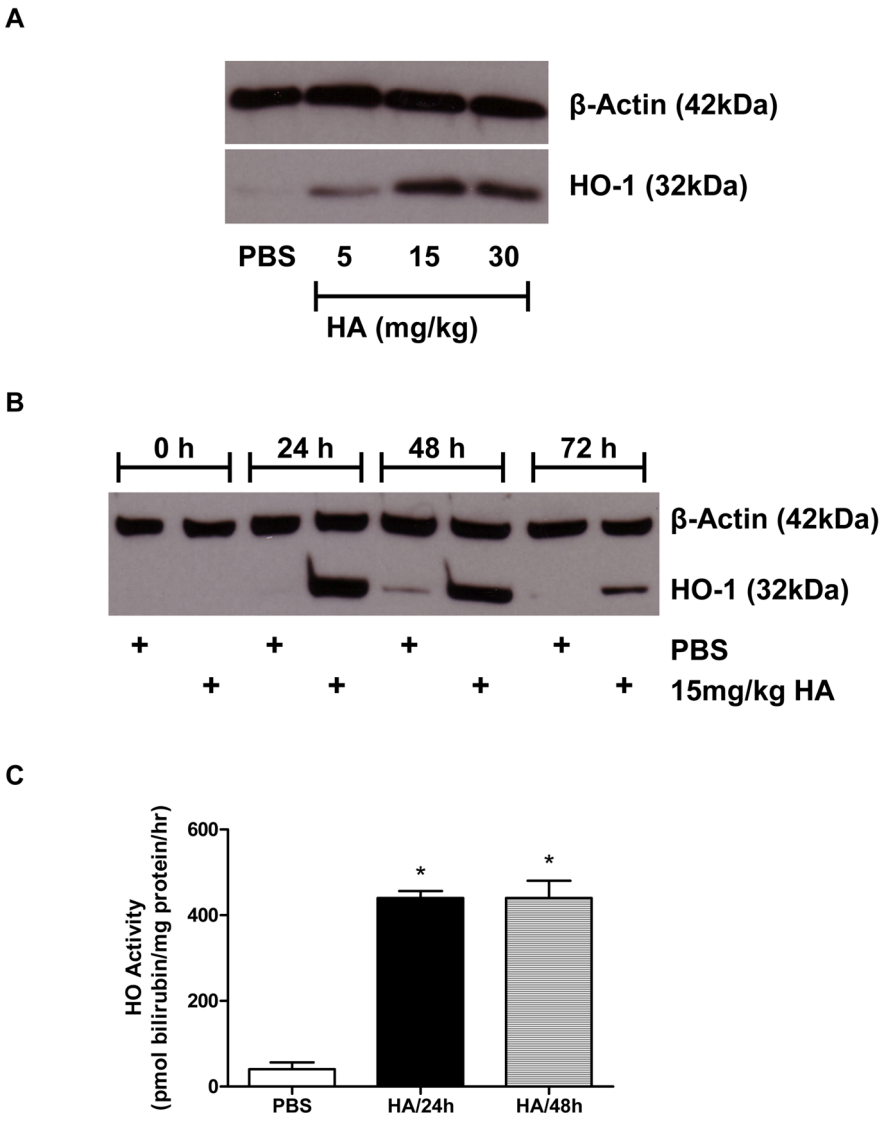


**Figure 3.1 Optimisation of dose and frequency of administration of HA in C57BL/KsJ mice.** Sustained induction of hepatic HO-1 protein and activity levels in C57BL/KsJ mice were the parameters used to select the optimal HA concentration and frequency of administration **A.** HA treatment at 5, 15 and 30mg/kg for 24 hours induced HO-1 protein levels, relative to PBS-treated mice. The western blot is a representative blot of n=1 mice/treatment. **B.** A single dose of 15mg/kg of HA induced HO-1 protein levels for up to 72 hours relative to PBS-treatment. The western blot is a representative blot of n=1 mice/treatment. **C.** A significant increase in HO activity relative to PBS-treated mice was observed 24 and 48 hours after a single intravenous administration of HA, * $P<0.05$, P-value derived from Dunn's multiple comparison post-test when $P<0.05$ with Kruskal-Wallis test. The data given are means ± s.e.m. from n=4/treatment group.

## 3.4. *IN VIVO* EXPERIMENT DESIGN

HA contains 25 mg/ml of hemin and 26.6 mg/ml of L-arginine in a glycerol solution. L-arginine has been reported to stimulate islet β-cells to secrete insulin (Henningsson and Lundquist, 1998). Hence, the *in vivo* experiment required an L-arginine control group in addition to PBS to reliably assess the specific effect of the 'heme' component of HA. L-arginine (LA) was administered at a concentration (16mg/kg) that replicated the LA concentration in 15mg/kg of HA (Levere et al., 1990). The experiment was conducted over a period of 8 weeks with twice weekly intravenous administration of PBS, LA and HA as outlined in Figure 3.2. Readouts included those shown in Figure 3.2.

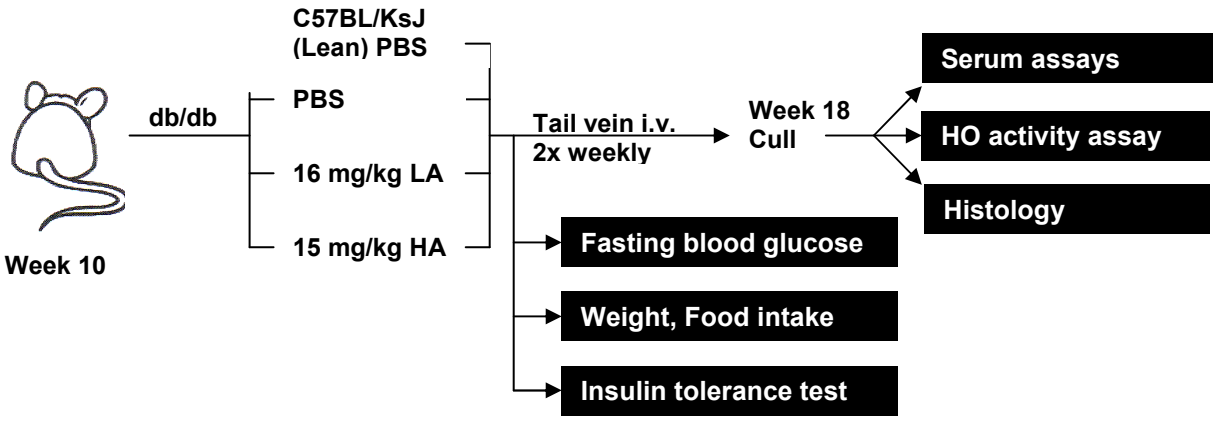


**Figure 3.2** ***In vivo*** **experiment design to determine HA efficacy in the db/db mouse model of type 2 diabetes.** Ten week old db/db diabetic mice and non-diabetic C57BL/KsJ (lean) mice were intravenously injected with PBS, LA, and HA at the stated doses twice weekly for 8 weeks. Weight and fasting (4 hour) blood glucose were monitored during the study and functional tests including food intake, ITT and urine collection in metabolic cage were performed. Mice were culled at 18 weeks of age and organs collected for HO activity assay and histological analysis.

## 3.5. DIABETIC PHENOTYPE OF db/db MICE AT THE BEGINNING OF THE STUDY

The treatment groups for db/db mice were determined by matching for the body weight (Table 3.1) at the beginning of the study. Ten week old db/db mice were significantly obese, hyperglycaemic and hyperinsulinaemic compared to lean C57BL/KsJ mice (Table 3.1).

| **Read-outs** | **Lean** | **db/db** | | |
|---|---|---|---|---|
| | **PBS** | **PBS** | **LA** | **HA** |
| **N number** | 3 | 4 | 4 | 3 |
| **Weight (gram)** | 27.4±0.3 | 44.8±1.3* | 43.7±1.3 | 44.8±1.2 |
| **Fasting glucose (mmol/l)** | 6.1±0.7 | 18.0±2.0* | 17.9±2.6 | 16.9±0.8 |
| **Fasting insulin (ng/ml)** | 0.8±0.1 | 5.1±0.6* | 4.9±0.6 | 3.9±0.3 |

**Table 3.1 Metabolic parameters at the beginning of the *in vivo* study.** Statistically significant differences in metabolic parameters, including weight, fasting blood glucose and insulin levels were observed between lean (C57BL/KsJ) and db/db mice at the beginning of the *in vivo* study. *P<0.05, P-values derived from two-tailed Mann Whitney test for comparison between Lean PBS and db/db PBS-treated mice. There were no significant differences in metabolic parameters, including weight, fasting blood glucose and insulin levels between the different treatment groups of db/db mice. P>0.05 by Kruskal-Wallis test for different treatment groups in db/db mice.

## 3.6. HA BUT NOT L-ARGININE REDUCED HYPERGLYCAEMIA

The mice were fasted for 4 hours prior to tail vein bleeding to measure fasting blood glucose concentration. A progressive increase in fasting blood glucose was observed in PBS-treated db/db mice. Non-parametric Friedman test along with Dunn's multiple comparison post-test demonstrated that HA treatment significantly reduced ($P<0.01$) fasting blood glucose levels relative to PBS-treated db/db mice (Figure 3.3.A). In contrast, twice weekly treatment of LA did not reduce hyperglycaemia. This strongly suggested that the anti-diabetic effect of HA was independent of the LA present in the HA solution.

Furthermore, area under the curve analysis suggested that hyperglycaemia was significantly reduced with HA treatment specifically between 6 and 8 weeks ($P<0.05$, Figure 3.3.B).

Additionally, the terminal glycosylated haemoglobin level ($HbA_{1C}$%), a measure of long-term blood glucose control, was significantly reduced with HA treatment ($P<0.05$, Figure 3.4.A). HA had no effect on haemoglobin levels (Figure 3.4.B).

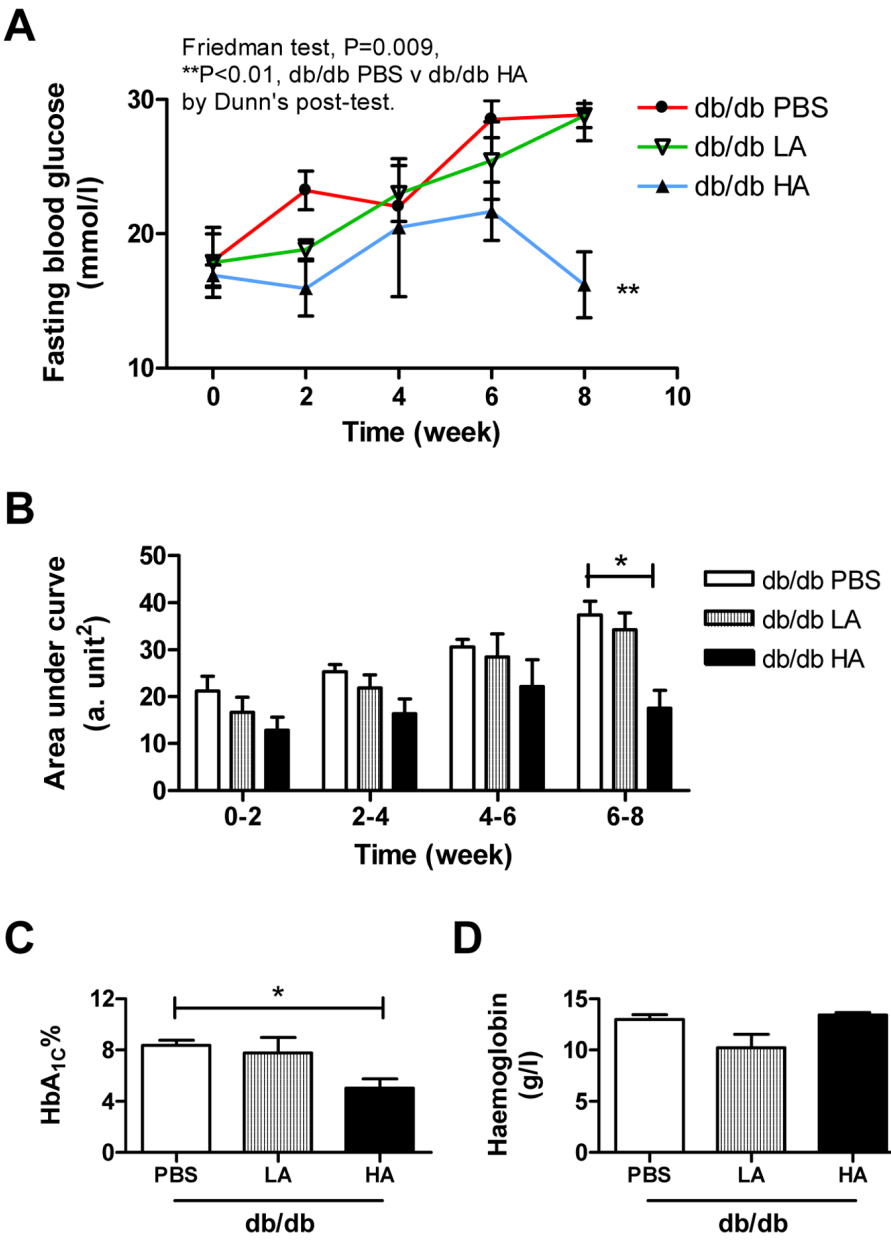


**Figure 3.3 Fasting blood glucose and $HbA_{1C}$%. A.** HA-treated db/db mice had significantly reduced levels of fasting blood glucose levels, relative to PBS-treated db/db mice. **P<0.01 (highlighted in figure), P-value derived from Dunn's multiple comparison post-test when P<0.05 with Friedman test. **B.** Area under curve (AUC) for fasting blood glucose levels between consecutive weeks (0-2, 2-4, 4-6, 6-8 week) showed that HA treatment significantly reduced fasting glucose levels between 6 and 8 weeks when compared to PBS-treated db/db mice. *P<0.05, P-value derived from Dunn's multiple comparison post-test when P<0.05 with Kruskal-Wallis test at the specified time-point. **C.** HA treatment led to a significant reduction in terminal $HbA_{1C}$% relative to PBS-treated db/db mice. *P<0.05, P-value derived from Dunn's multiple comparison post-test when P<0.05 with Kruskal-Wallis test. **D.** None of the treatments resulted in any significant change in terminal haemoglobin level. P>0.05 (non-significant) by Kruskal-Wallis test. **A, B, C, D:** The data are mean ± s.e.m. from n=3-4 mice/treatment group. a. unit$^2$: arbitrary unit$^2$.

## 3.7. HA BUT NOT LA PROMOTED BODY WEIGHT GAIN DESPITE NO DIFFERENCE IN FOOD INTAKE

There was a significant difference in body weight between treatment groups in db/db mice (Figure 3.4.A, P=0.009 by Friedman test). Body weight at each consecutive time-points were normalised to baseline (week 0) weight to assess weight gain (Figure 3.4.B). Significant increase in weight gain was noted for HA treatment ($P<0.05$) after 6 and 8 weeks of the *in vivo* study, relative to PBS-treated db/db mice (Figure 3.4.B). No significant differences in the weight of liver and fat pads, including subcutaneous (SFP), retroperitoneal (RFP) and epididymal (EFP) fat pads were observed between the different treatment groups (Figure 3.4.C).

Food intake was monitored over a period of 5 days during week 6 and 7 of the study. There was no significant difference in food intake between the treatment groups over the 5-day period (Figure 3.4.D).

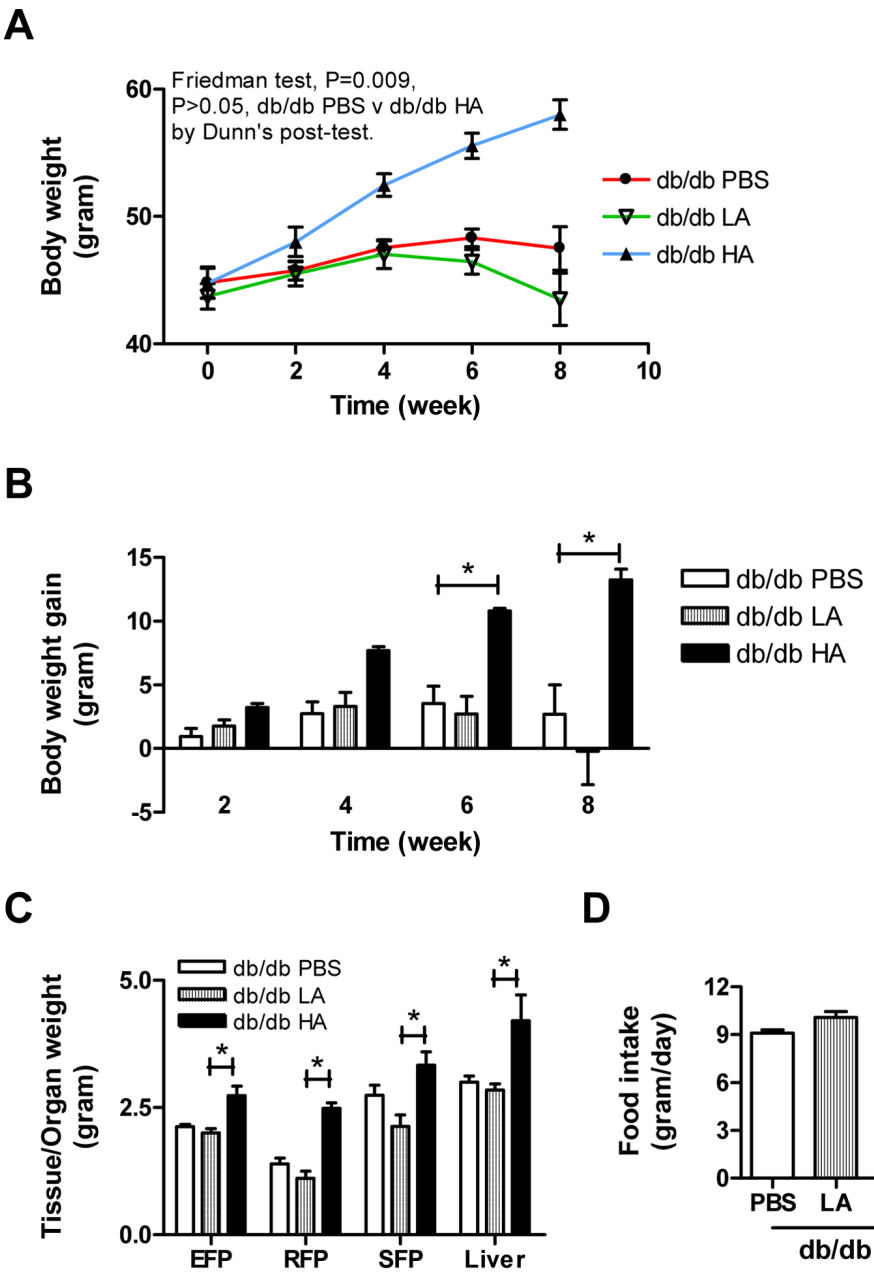


**Figure 3.4 Body weight, weight gain, tissue/organ weights and food intake. A.** Significant difference in body weight between treatment groups in db/db mice. P<0.05 (highlighted in figure) by Friedman test. **B.** Significant weight gain (body weight normalised to baseline weight) noted for HA treatment at 6 and 8 weeks, relative to PBS-treated db/db mice. *P<0.05, P-value derived from Dunn's multiple comparison post-test when P<0.05 with Kruskal-Wallis test at the specified time-point. **C.** No significant difference in either liver weight or fat pad weights, including epididymal fat pad (EFP), retroperitoneal fat pad (RFP) and sub-cutaneous fat pad (SFP), was observed between HA-treated and PBS-treated db/db mice (P>0.05). *P<0.05, P-value derived with Dunn's multiple comparison post-test when P<0.05 by Kruskal-Wallis test for specified tissue/organ type. **D.** None of the treatments had a significant impact on food intake in the db/db mice. P>0.05 (non-significant) by Kruskal-Wallis test. **A, B, C, D:** The data are mean ± s.e.m. from n=3-4 mice/treatment group.

## 3.8. HA AND LA HAD NO EFFECT ON INSULIN RESISTANCE

An insulin tolerance test (ITT) was performed during week 8 of the *in vivo* study. The db/db mice were fasted for 4 hours prior to intraperitoneal administration of insulin at a concentration of 1unit insulin/kg body weight of mouse. The blood glucose level was monitored at 0, 15, 30 and 60 minutes post insulin injection.

A significant difference in absolute blood glucose levels during the ITT was observed between different treatment groups in db/db mice ($P<0.05$ by Friedman test, Figure 3.5.A). However, an ITT is primarily performed to determine the rate of glucose disposal as an assessment of degree of insulin resistance. The baseline (0) glucose levels were different between the treatment groups in db/db mice (Figure 3.5.A). Hence, the glucose concentration at consequent time points (0, 15, 30 and 60 minutes) during ITT (Figure 3.5.A) were divided by baseline glucose concentration to express the ITT curve as fold change in glucose level relative to baseline (Figure 3.5.B).

No significant difference in the relative change in glucose levels was noted between treatment groups in db/db mice ($P>0.05$ by Friedman test, Figure 3.5.B). Area under the curve (AUC) for the relative change in glucose levels during the ITT demonstrated that none of the treatment regimes had a significant impact on the relative change in glucose level during the ITT (Figure 3.5.C).

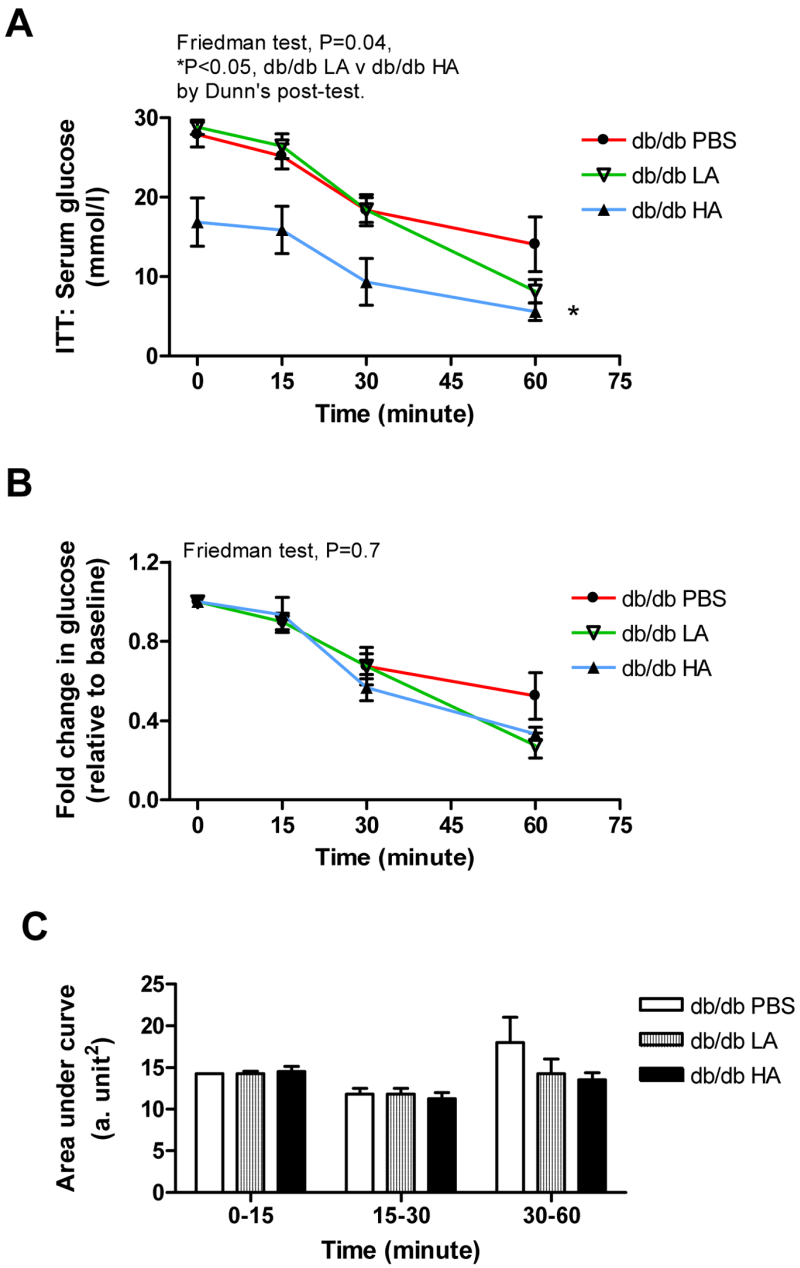


**<u>Figure 3.5</u> Insulin resistance as assessed by the insulin tolerance test (ITT). A.** Glucose concentration was determined at 0, 15, 30 and 60 minutes post exogenous insulin (1 unit/kg body weight) administration during the ITT in db/db mice. *P<0.05 (highlighted in figure) between db/db LA and db/db HA, P-value derived from Dunn's multiple comparison post-test when P<0.05 with Friedman test. **B.** ITT curve represented as fold change in blood glucose relative to baseline (0 minute) level. None of the treatment regimes significantly lowered the relative change in glucose level during ITT. P>0.05 (non-significant) by Friedman test. **C.** None of the treatment regimes significantly reduced relative change in glucose level between consecutive time-points (0-15, 15-30, 30-60 minutes) during the ITT, as assessed by area under the curve analysis (AUC). P>0.05 (non-significant) was noted for each time-point by Kruskal-Wallis test. **A, B, C:** The data are means ± s.e.m. from n=3-4 mice/treatment group. a unit$^2$: arbitrary unit$^2$.

## 3.9. HA INCREASED HEME OXYGENASE ACTIVITY AND EXPRESSION

Liver lysates from db/db mice were used to perform the heme oxygenase (HO) paired enzyme assay to determine the effect of HA on HO activity. HA treatment led to a significant increase ($P<0.01$) in HO activity compared to PBS-treated db/db mice (Figure 3.6.A). The increase in HO activity with HA treatment was concurrent with increase in HO-1 protein expression as detected by immuno-blotting (Figure 3.6.B). HO-1 protein levels in either PBS or LA-treated mice were undetectable.

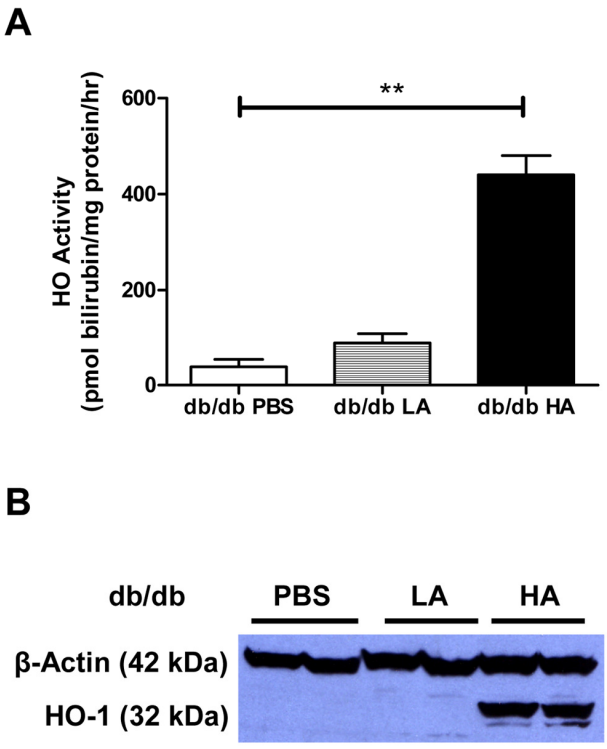


**Figure 3.6 Terminal HO activity and HO-1 protein levels in the liver of db/db mice.** **A.** HA treatment resulted in a significant increase in HO activity relative to PBS-treated db/db mice. **P<0.01, P-value derived from Dunn's multiple comparison post-test when P<0.05 with Kruskal-Wallis test. The data are mean ± s.e.m. from n=3-4 mice/treatment group. **B.** HO-1 protein was undetectable in PBS and LA-treated db/db mice. HA treatment increased HO-1 protein level. The western blot is a representative blot in which n=2 mice/treatment. β-actin was used as a control for loading equal concentration of protein.

## 3.10. HA TREATMENT HAD NO EFFECT ON ADIPONECTIN LEVELS

The end-point fasting serum high molecular weight (HMW) form of adiponectin was quantified to assess whether HA administration modulated the adiponectin concentration in the serum. No significant difference in serum adiponectin concentration was observed either between PBS-treated lean and db/db mice or between PBS and HA-treated db/db mice (Figure 3.7).

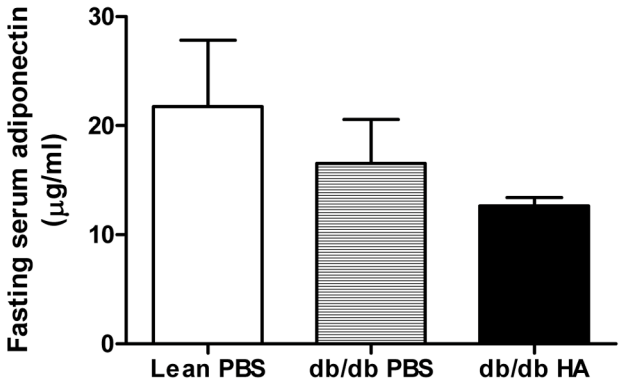


**Figure 3.7 Terminal fasting serum HMW adiponectin.** No significant difference in serum concentration of the high molecular weight (HMW) form of adiponectin was noted either between PBS-treated lean (C57BL/KsJ) and db/db mice or, between PBS and HA-treated db/db mice at the end of the 8-week study. P>0.05, P-value derived from Kruskal-Wallis test. The data are means ± s.e.m. from n=3-4/treatment group.

## 3.11. NO SIGNIFICANT DIFFERENCE IN INSULIN LEVELS BETWEEN PBS AND HA-TREATED db/db MICE

Over the full 8wk period, no significant difference in serial fasting serum insulin levels was observed between different treatment groups in db/db mice (Figure 3.8.A, P=0.3 by Friedman test). However, Area under the curve (AUC) for fasting insulin levels between consecutive weeks (0-2, 2-4, 4-6 and 6-8 weeks) showed that HA-treated db/db mice had significantly higher fasting insulin levels (P<0.05) specifically between 6 and 8 weeks compared with LA-treated mice (Figure 3.8.B).

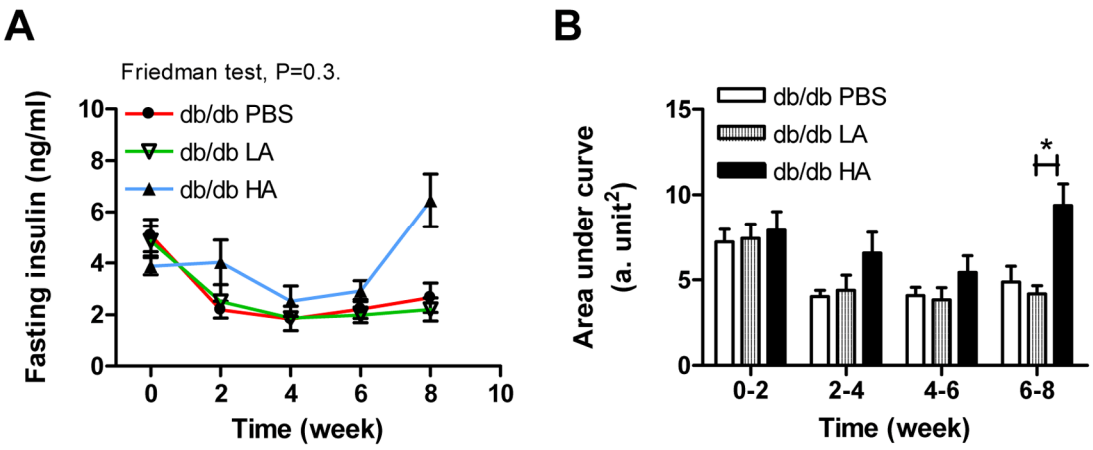


**Figure 3.8 Fasting serum Insulin levels. A.** No statistically significant difference in serial fasting insulin levels was observed between different treatment groups in db/db mice. P>0.05 (highlighted in figure) by Friedman test. **B.** Area under the curve (AUC) analysis for fasting insulin levels showed a significant increase in insulin levels with HA treatment between 6 and 8 weeks, relative to LA but not PBS-treated db/db mice. *P<0.05, P-values derived from Dunn's multiple comparison post-post when P<0.05 by Kruskal-Wallis test at the specified time-point. **A, B:** The data are means ± s.e.m. from n=3-4 mice/treatment group. a. unit$^2$: arbitrary unit$^2$.

### 3.12. HA TREATMENT REDUCED ISLET iNOS EXPRESSION

There was an increase in iNOS expression in PBS-treated but not HA-treated db/db mice relative to lean mice (Figure 3.9.A). Importantly, a proportion of the iNOS-stained cells, particularly the cells at the centre of the islet, showed co-localisation with insulin, suggesting that the iNOS-stained cells were in part β-cells (Figure 3.9.B). However, iNOS-stained cells at the periphery region of the islet did not exhibit insulin staining, suggesting that some iNOS-staining cells were not β-cells, but other cell types which may include macrophages and glucagon producing α-cells.

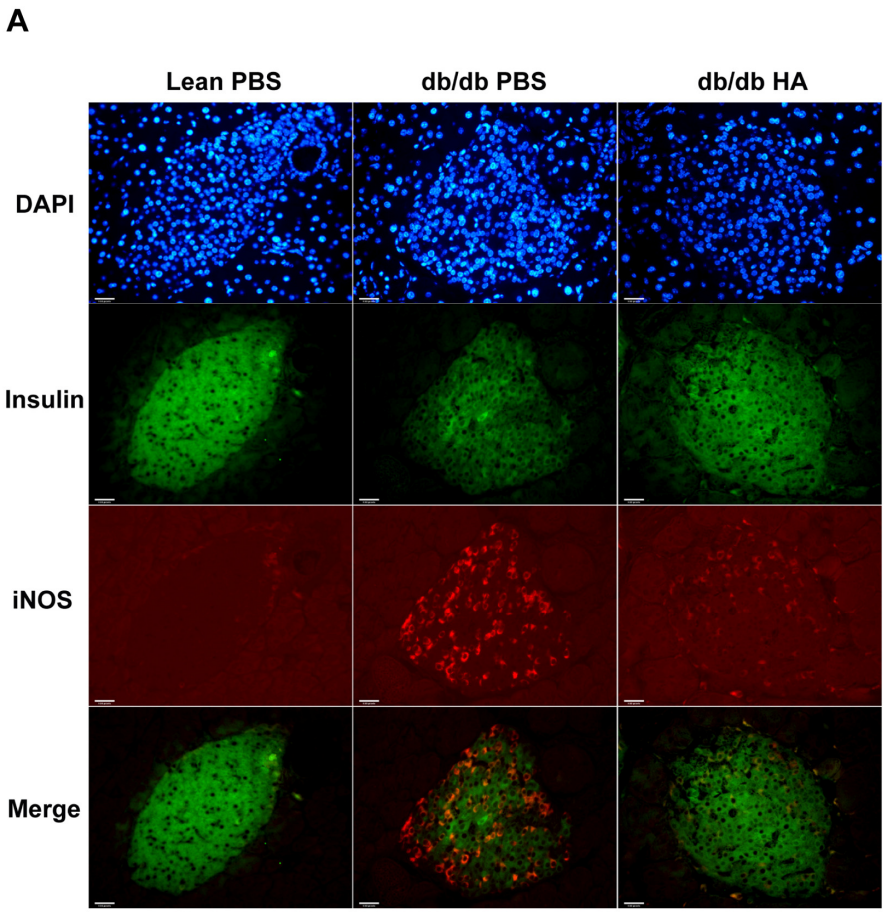

**B**

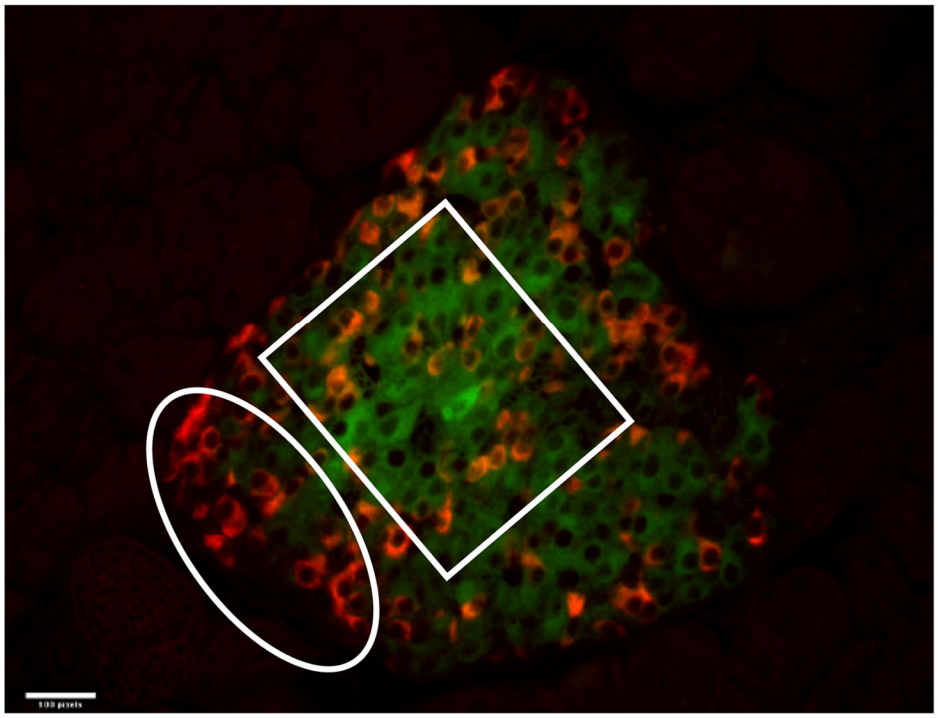

**Figure 3.9 Immuno-fluorescence staining for insulin and iNOS in islets.** Methacarn fixed tissues were stained with insulin/fluorophore 488 (green) and iNOS/fluorophore 594 (Red) whereas DAPI (4',6-diamidino-2-phenylindole, blue) was used for nuclear staining. **A.** An increase in iNOS staining was observed in pancreatic islets of PBS, but not HA-treated db/db mice, when compared to PBS-treated lean (C57BL/KsJ) mice. **B.** A proportion of iNOS-stained islet cells co-localised with insulin producing islet β-cells as highlighted by orange staining in the rectangular white box. Whereas, a cluster of iNOS-stained islet cells, particularly at the periphery of the islet as highlighted by oval box, did not co-localise with insulin-stained cells suggesting that other cell-types in the islet expressed iNOS. The scale bar indicates 100 pixels.

## 3.13. CHAPTER DISCUSSION

### 3.13.1. HA TREATMENT DISPLAYED ANTI-HYPERGLYCAEMIC EFFECT IN db/db MODEL OF TYPE 2 DIABETES

The preliminary 8-week *in vivo* study showed heme arginate (HA) treatment to be efficient at reducing the time-dependent increase in fasting hyperglycaemia, which was observed in db/db mice who were treated with PBS or L-arginine (LA) (Figure 3.3.A). The HA-mediated reduction in fasting hyperglycaemia was particularly significant towards the end of the *in vivo* study, between 6 and 8 weeks (Figure 3.3.B). Furthermore, the beneficial effect of HA treatment on hyperglycaemia was further confirmed by the significant reduction in glycosylated haemoglobin level ($HbA_{1C}$%, Figure 3.3.C). $HbA_{1C}$% reflects glycaemic status over a longer duration than fasting glucose because the half-life of erythrocytes in mice is believed to be 2-3 weeks (Magnani et al., 1988). Hence, two reliable and independent methods of quantifying the degree of hyperglycaemia demonstrated that intravenous administration of 15mg/kg of HA, twice weekly for 8 weeks, ameliorated hyperglycaemia in the db/db mice.

The reduction in hyperglycaemia by HA treatment coincided with a significant increase in HO activity and HO-1 protein levels in the liver of db/db mice (Figure 3.6). This is in agreement to previously published studies, where hemin therapy has been reported to induce HO activity and ameliorate hyperglycaemia in insulin-resistant Goto-Kakizaki (GK) and Zucker diabetic fatty (ZDF) rats (Ndisang et al.,

2009a, Ndisang et al., 2009b). Therefore, an additional *in vivo* study is required, where a pharmacological inhibitor of HO activity, such as stannous (IV) mesoporphyrin IX dichloride (SM) or chromium (III) mesoporphyrin IX chloride (CrMP), is employed to determine whether an increase in HO activity is responsible for anti-hyperglycaemic effect of HA in the db/db mouse model of type 2 diabetes.

### 3.13.2. HA TREATMENT PROMOTED WEIGHT GAIN

Previously, Li et al had reported that intraperitoneal administration of cobalt (III) protoporphyrin IX chloride (CoPP) induced HO activity, HO-1 protein and prevented weight gain by reducing visceral fat mass in the ob/ob mouse model of type 2 diabetes (Li et al., 2008). An identical phenotype has been reported by Kim et al in Zucker fatty rats (Kim et al., 2008). However, in the current study, an increase in HO activity and HO-1 protein with HA treatment coincided with a progressive increase in body weight in db/db mice (Figure 3.4.A), despite no significant increase in food intake (Figure 3.4.D). Consequently, a significant increase in weight gain was noted with HA treatment, when compared to PBS-treated db/db mice (Figure 3.4.B). Hence, the weight gain associated with HA treatment in db/db mice is in contrast to the prevention of weight gain observed with CoPP treatment in ob/ob mice.

The discrepancy in the body weights observed with HA and CoPP may be due to differences in the mouse models used for the studies. ob/ob mice are primarily used as a model of obesity and insulin resistance because compensatory islet hypertrophy and hyperinsulinaemia prevents profound increases in hyperglycaemia and promotes

weight gain (Genuth et al., 1971, Li et al., 2008). Whereas, the db/db mice are more often employed as a model of type 2 diabetes, where an initial increase in insulin resistance and hyperinsulinaemia is succeeded by loss of β-cell mass, an increase in hyperglycaemia and consequent weight loss in the later stage of life (Hummel et al., 1966, Coleman, 1978). Further support for this observation is provided by comparing the results from the current and Li et al studies. Vehicle (Tris-HCl pH 7.8 solution) treatment led to a progressive increase in body weight in ob/ob mice (Li et al., 2008). Whereas, PBS-treated db/db mice showed an initial rise in body weight followed by slight decrease during the latter half of the current *in vivo* study (Figure 3.4.A). An alternative explanation for the differing effects of HA- and CoPP-therapy on body weight is that the compounds themselves have different properties. For example, CoPP but not hemin may regulate the central nervous system to promote loss of appetite and body weight (Galbraith and Kappas, 1989) Although the reduction in food intake during CoPP treatment in the ob/ob mice (Li et al., 2008) did not reach statistical significance, the 10% reduction observed may still be biologically important.

A key question is: whether the weight gain promoted by HA treatment is key to its anti-diabetic properties or, a side effect. A simple experiment to answer this question is to test whether HA treatment can promote weight gain in non-diabetic mice. If so, then the weight gain with HA can be attributed to be a side effect rather than a key phenotypic change associated with anti-hyperglycaemic effect of HA.

### 3.13.3. THE ANTI-HYPERGLYCEMIC EFFECT OF HA IS INDEPENDENT OF INSULIN SENSITIVITY

An important approach to reduce hyperglycaemia is to reduce insulin resistance in peripheral organs to facilitate insulin-dependent regulation of hepatic glucose production and glucose disposal in muscles. The insulin tolerance test is a crude functional test of insulin sensitivity but not specific to a particular organ. Insulin has a suppressive effect on glycogenolysis and gluconeogenesis (Barthel and Schmoll, 2003) and mediates glucose uptake mainly in skeletal muscle by up-regulating GLUT4 (Dugani and Klip, 2005). Therefore, the ITT largely reflects the degree of insulin resistance in muscle and liver.

The similar relative reduction in glucose levels during the ITT observed in all three groups suggested that HA and LA treatment, both failed to significantly reduce insulin resistance, relative to PBS-treated db/db mice (Figure 3.5.B, C). This observation is in contrast to the increase in insulin sensitivity reported by hemin and CoPP in different murine models of obesity and type 2 diabetes (Li et al., 2008, Ndisang et al., 2009b, Ndisang and Jadhav, 2009). However, these studies used absolute glucose levels rather than relative reductions in glucose levels at specified time-points during the ITT, to measure insulin resistance. Therefore, the reduction in blood glucose levels observed throughout the course of the ITT may simply reflect lower baseline levels, rather than an increase in insulin sensitivity. Hence, the effect of HA, hemin or CoPP may be largely independent of improvements in insulin sensitivity in all three models.

Adiponectin is an adipose tissue derived adipokine that increases insulin sensitivity in the peripheral organs by promoting fatty acid oxidation in the liver and muscle and thereby reducing ectopic deposition of triglycerides in these organs (Yamauchi et al., 2001, Kadowaki et al., 2006). Induction of the HO activity-adiponectin axis has been reported to be a key mechanism for reducing insulin resistance with hemin and CoPP treatment in GK rats and ob/ob mice respectively. However, HA treatment for 8 weeks failed to significantly modulate serum adiponectin levels in db/db mice (Figure 3.7). Hence, the combined results of the ITT and the terminal adiponectin level demonstrate that the anti-hyperglycaemic effect of HA is independent of an effect on insulin-sensitivity either directly or via adiponectin.

### 3.13.4. NO SIGNIFICANT INCREASE IN INSULIN SECRETION WITH HA TREATMENT

In PBS-treated db/db mice there was a steady decrease in fasting insulin levels during the first 4 weeks of the *in vivo* study, indicating reduced capability of islet β-cells to secrete insulin as the diabetic state progressed (Figure 3.8.A). This may be due to the deleterious effects of hyperglycaemia, which include a decrease in the islet β-cell mass and secretory function (Donath et al., 2008) along with dedifferentiation of β-cells in the db/db mice (Kjorholt et al., 2005). Additionally, a proportion of β-cells in the islet of PBS-treated db/db mice expressed iNOS as determined by immuno-fluorescence (Figure 3.9). It has been reported that increased iNOS expression in pancreatic islet cells may contribute to the pathogenesis of islet β-cell dysfunction in an experimental model of type 2 diabetes (Salehi et al., 2008).

There was an increase in serum insulin levels in db/db mice after between 6 to 8 weeks of HA compared with LA-therapy (Figure 3.8.B). A similar difference was observed between HA and PBS-treated mice, however this did not meet statistical significance, possibly due to the small sample size (n=3-4 mice/group) in this pilot study. The reduction in iNOS, partly in β-cells, in the islets, suggests a possible mechanism for preserved insulin secretion (Figure 3.9.A, B) as iNOS may impair β-cell function. Furthermore, the increase in insulin secretion may be responsible for the weight gain observed with HA treatment. However, further experiments, employing larger numbers of mice, will be required to conclusively determine whether the anti-diabetic effect of HA was in part due to an increase in insulin secretion.

### 3.13.5. ANTI-HYPERGLYCEMIC EFFECT OF HA IS INDEPENDENT OF L-ARGININE COMPONENT OF HA

HA is soluble composition of human blood-derived hemin and L-arginine (LA) in a solution mixture containing propylene glycol, ethanol and water (Tenhunen et al., 1987). LA at millimolar concentration has been reported to stimulate islet β-cell insulin secretion in vitro (Henningsson and Lundquist, 1998). Hence, an LA control group at a concentration identical to that present in HA was used to reliably assess the specific effect of the 'heme' component of HA. No improvement in glycaemic control or serum insulin levels was observed in LA-treated db/db mice, demonstrating the effect of HA to be independent of the effect of LA. Hemin alone was not included in the study due to its relative poor solubility and the tendency to

form aggregates in the solution, which became apparent while performing in vitro studies to characterise the effect of hemin in primary macrophages.

### 3.13.6. CONCLUDING REMARK

To conclude, HA treatment led to a significant induction of HO activity and an increase in HO-1 protein in db/db mice. Eight weeks of HA but not LA treatment, significantly reduced the progressive increase in hyperglycaemia observed in PBS-treated db/db mice, demonstrating that the anti-hyperglycaemic effect of HA was mediated by its 'heme' rather than LA component. HA ameliorated hyperglycaemia despite no improvement in relative insulin sensitivity in peripheral organs. The anti-hyperglycaemic effect of HA may have been due to an increased adipogenic capacity to store excess lipids and divert them away from key metabolic tissues such as liver and muscles. Alternatively, HA did increase blood insulin levels compared with LA but not PBS in the latter stages of the model, but whether this was responsible for its anti-diabetic effect needs to be confirmed with studies that employ larger numbers of mice.

Finally, the phenotype observed with HA, in particular the increase in body weight, was different to that observed with other inducers of HO-1, such as CoPP and hemin. This raises the possibility that the anti-diabetic properties of HA may be independent of its ability to induce HO activity and additional experiments, which include inhibitors of HO activity, are require to address this important question.

# 4. CHAPTER 4: *IN VIVO* STUDY 2: ROLE OF HEME ARGINATE INDUCED HEME OXYGENASE (HO) ACTIVITY IN THE LEPTIN RECEPTOR DEFICIENT db/db MOUSE MODEL OF TYPE 2 DIABETES

## 4.1. INTRODUCTION

The preliminary *in vivo* study with heme arginate (HA) in the db/db mice model of type 2 diabetes demonstrated that HA therapy ameliorated hyperglycemia (chapter 3). Equivalent doses of L-arginine had no effect on blood glucose levels suggesting that the anti-diabetic effect of HA is dependent on the heme component. Heme is a potent inducer of heme oxygenase-1 (HO-1) and previous studies employing other inducers of HO-1, such as hemin or cobalt (III) protoporphyrin IX chloride (CoPP) have also demonstrated an anti-diabetic effect (Ndisang and Jadhav, 2009, Ndisang et al., 2009b, Ndisang et al., 2009a, Kim et al., 2008, Li et al., 2008).

Published studies have employed HO activity inhibitors such as chromium (III) mesoporphyrin IX chloride (CrMP) or stannous (IV) mesoporphyrin IX dichloride (SnPP/SM) (Ndisang and Jadhav, 2009, Li et al., 2008) to determine that the anti-diabetic effect of CoPP or hemin was mediated via increased HO activity.

An *in vivo* experiment was designed to include an inhibitor of HO activity SM to test the hypothesis that **the anti-hyperglycaemic effect of HA was dependent on its ability to induce HO activity**.

## 4.2. OPTIMISATION OF THE DOSE OF STANNOUS (IV) MESOPORPHYRIN IX DICHLORIDE (SM), AN INHIBITOR OF HO ACTIVITY

Li et al employed SM as an HO activity inhibitor to determine whether the anti-diabetic effect of CoPP was dependent on HO activity in the ob/ob mouse model of type 2 diabetes (Li et al., 2008). They administered 20mg/kg of SM intraperitoneally (i.p.) thrice weekly in the ob/ob mice (Li et al., 2008) and determined that this effectively inhibited HO activity. Hence, a concentration of 20mg/kg of SM was selected to determine if SM reduced HA-induced HO activity in non-diabetic C57BL/KsJ mice.

The SM solution was prepared in TRIS-HCl pH 7.8 buffer. 10-12 week old C57BL/KsJ mice were divided into three groups, including PBS, HA and HA+SM (n=3/group). The mice in the PBS and HA groups were administered i.p. with TRIS-HCl pH 7.8, whereas the HA+SM group was administered i.p. 20 mg/kg of SM. After 24 hours of TRIS-HCl pH 7.8 or SM administration, PBS was administered intravenously (i.v.) to the PBS group, whereas the HA and HA+SM group were administered i.v. 15 mg/kg of HA. The livers were harvested from all treatment groups after 24 hours of PBS or HA administration to determine HO activity.

A significant increase ($P<0.05$) in HO activity was noted following injection of 15 mg/kg HA when compared to PBS-treated mice (Figure 4.1). In contrast, a single i.p. administration of SM abrogated the HA-induced increase in HO activity (Figure 4.1).

Hence, 20 mg/kg of SM was selected as the concentration to be used for administration in the db/db mice. The treatment regime for SM (thrice i.p. administration of SM per week) was as employed previously in ob/ob mice (Li et al., 2008).

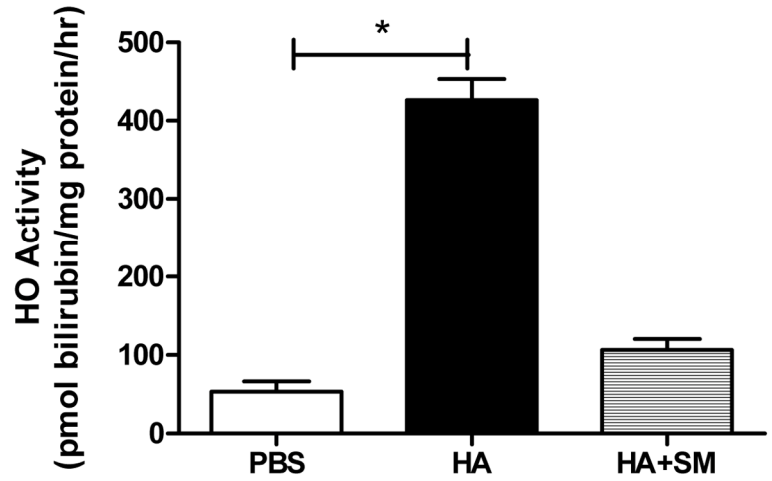


**Figure 4.1 Optimisation of the dose of SM required to inhibit HA-induced HO activity in C57BL/KsJ mice.** The significant increase in HO activity following a single intravenous administration of 15mg/kg of HA was abrogated by pre-treating with a single intraperitoneal administration of 20mg/kg SM in non-diabetic C57BL/KsJ mice. The data are means ± s.e.m. from n=3 mice/treatment group. * $P<0.05$, P-value derived from Dunn's multiple comparison post-test when $P<0.05$ with Kruskal-Wallis test.

## 4.3. *IN VIVO* EXPERIMENT DESIGN

The *in vivo* experiment was conducted over a period of 8 weeks and was comprised of four groups of db/db mice who received either PBS (n=4), HA (n=4), SM (n=5) or HA+SM (n=8) (Figure 4.2). PBS and 15mg/kg HA were administered intravenously (i.v.) twice weekly whereas 20mg/kg SM was administered intraperitoneally (i.p.) thrice weekly. The SM solution was prepared in TRIS-HCl buffer, hence db/db mice on PBS and HA single treatments were injected intraperitoneally with TRIS-HCl, pH 7.8 solution as a control. C57BL/KsJ non diabetic (lean) mice acted as controls and were given either PBS or 15mg/kg HA intravenously twice weekly. The *in vivo* study design and readouts are shown in Figure 4.2.

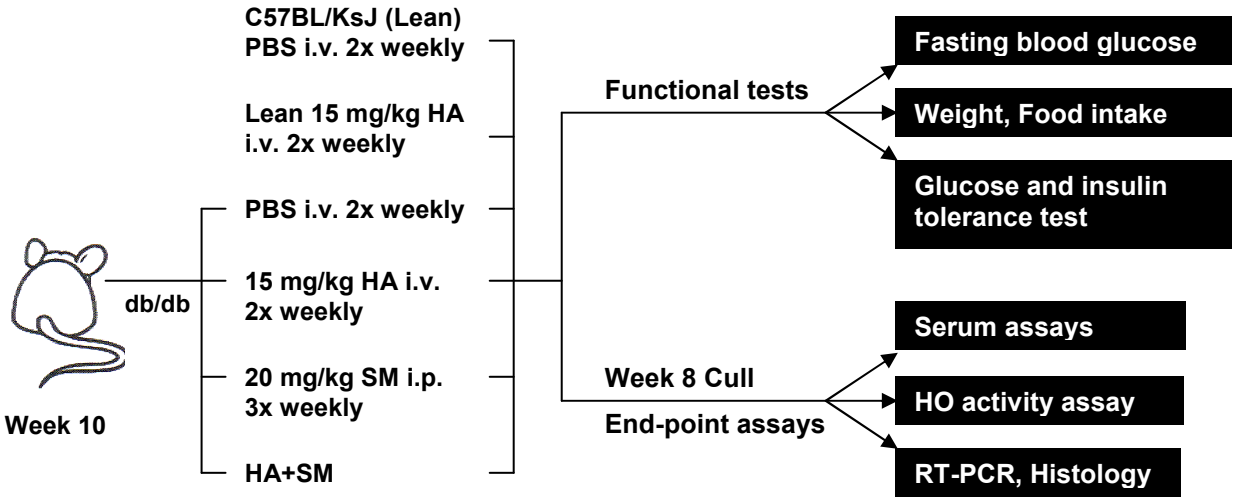


**Figure 4.2 *In vivo* experiment design to investigate whether the anti-diabetic effect of HA is dependent on HO activity.** Ten week old db/db diabetic mice along with non-diabetic C57BL/KsJ (lean) mice were injected with PBS, HA, SM or HA+SM for 8 weeks. Weight, fasting (4 hour) blood glucose, food intake, GTT and ITT were performed. Mice were culled at 18 weeks of age and organs collected for HO activity assay, quantification of gene expression and histological analysis.

## 4.4. DIABETIC PHENOTYPE OF db/db MICE AT THE BEGINNING OF THE STUDY

The treatment groups for db/db mice were formed by matching their body weight (Table 4.1) taken at the beginning of the study. Ten week old db/db mice were significantly obese, hyperglycaemic and hyperinsulinaemic in comparison to lean C57BL/KsJ mice (Table 4.1). There were no significant differences in any of the metabolic parameters between the db/db mice treatment groups.

| **Parameters** | **Lean** | **db/db** | | | |
|---|---|---|---|---|---|
| | **PBS** | **PBS** | **HA** | **SM** | **HA+SM** |
| **N number** | 4 | 4 | 4 | 5 | 8 |
| **Weight (gram)** | 25.4±1.0 | 42.3±1.2** | 42.9±1.1 | 41.6±0.8 | 41.2±0.7 |
| **Fasting glucose (mmol/l)** | 6.7±0.4 | 16.9±2.6** | 16.1±1.7 | 17.6±1.8 | 15.2±2.2 |
| **Fasting insulin (ng/ml)** | 0.8±0.1 | 8.6±1.4* | 7.1±0.8 | 8.0±2.1 | 8.7±0.9 |

**Table 4.1 Metabolic parameters at the beginning of the *in vivo* study.** Statistically significant differences in metabolic parameters, including weight, fasting glucose and insulin levels were observed between lean (C57BL/KsJ) and db/db mice at the beginning of the *in vivo* study. *P<0.05, **P<0.01, P-values derived from one-tailed Mann Whitney test for comparison between lean and db/db mice on PBS treatment. There were no significant differences in metabolic parameters, including weight, fasting blood glucose and insulin levels between different treatment groups in db/db mice (P>0.05 by Kruskal-Wallis test).

## 4.5. HA TREATMENT HAD NO SIGNIFICANT EFFECT ON BODY WEIGHT AND FASTING BLOOD GLUCOSE IN THE LEAN MICE

HA treatment produced a progressive increase in body weight in db/db mice in the previous *in vivo* study (chapter 3). Hence, it was important to determine whether HA induced weight gain per se, or whether this is a directly related to its anti-diabetic effects. Therefore, C57BL/KsJ (lean) mice were administered either PBS or HA over an 8 week period.

No significant differences were observed between the two treatment groups. (Table 4.2). Furthermore, the fasting blood glucose of PBS and HA-treated lean mice were comparable.

| Parameter | Week | Lean PBS | Lean HA | P-value |
|---|---|---|---|---|
| **N number** | | 4 | 5 | |
| **Body weight (gram)** | **0** | 25.4±1.0 | 24.7±0.9 | >0.05 |
| | **8** | 28.1±0.6 | 27.4±0.9 | >0.05 |
| **Fasting blood glucose (mmol/l)** | **0** | 6.7±0.4 | 6.7±0.5 | >0.05 |
| | **8** | 6.6±0.4 | 7.0±0.1 | >0.05 |

**Table 4.2 Effect of HA treatment on body weight and fasting blood glucose in non-diabetic C57BL/KsJ (lean) mice.** No significant changes in body weight and fasting glucose levels were observed with HA treatment in lean mice, when compared to PBS-treated lean mice. P>0.05 by two-tailed Mann Whitney test for comparison between PBS and HA-treated lean mice.

## 4.6. EFFICIENT INHIBITION OF HO ACTIVITY BUT NOT PROTEIN LEVEL WITH SM TREATMENT

At the end of the experiment, liver lysates from db/db mice were used to determine HO activity by the HO paired enzyme assay. HA treatment led to a significant increase ($P<0.05$) in hepatic HO activity compared to PBS treated db/db mice (Figure 4.3.A). No significant change in HO activity was observed with SM treatment alone, when compared to PBS-treated db/db mice. The concurrent treatment of SM with HA (will be referred as HA+SM from this point forward in the text) significantly reduced ($P<0.05$) the HA-mediated increase in HO activity (Figure 4.3.A). The HO activity with HA+SM treatment was comparable to the HO activity level observed with PBS treatment in db/db mice.

Quantification of heme was an alternative method to confirm inhibition of HO activity in the *in vivo* study. A significant suppression of HO activity with SM treatment would reduce heme degradation into carbon monoxide, bilirubin and ferritin and should increase the intracellular heme content when supplied with exogenous HA.

HA+SM treatment resulted in a significant increase in hepatic heme content ($P<0.01$) compared to PBS treatment (Figure 4.3.B) in db/db mice. The HO activity and heme concentration data together demonstrated that SM treatment efficiently blocked the HA mediated increase in HO activity and intracellular heme degradation.

Immuno-blotting in liver lysates detected no basal HO-1 protein expression in PBS-treated db/db mice. An increase in HO-1 protein expression was observed with HA but not SM single agent treatment. HA+SM treatment led to a profound and synergistic increase in HO-1 protein expression (Figure 4.3.C). A comparable level of protein expression of the constitutively expressed HO-2 isoform was observed between different the treatment regimes.

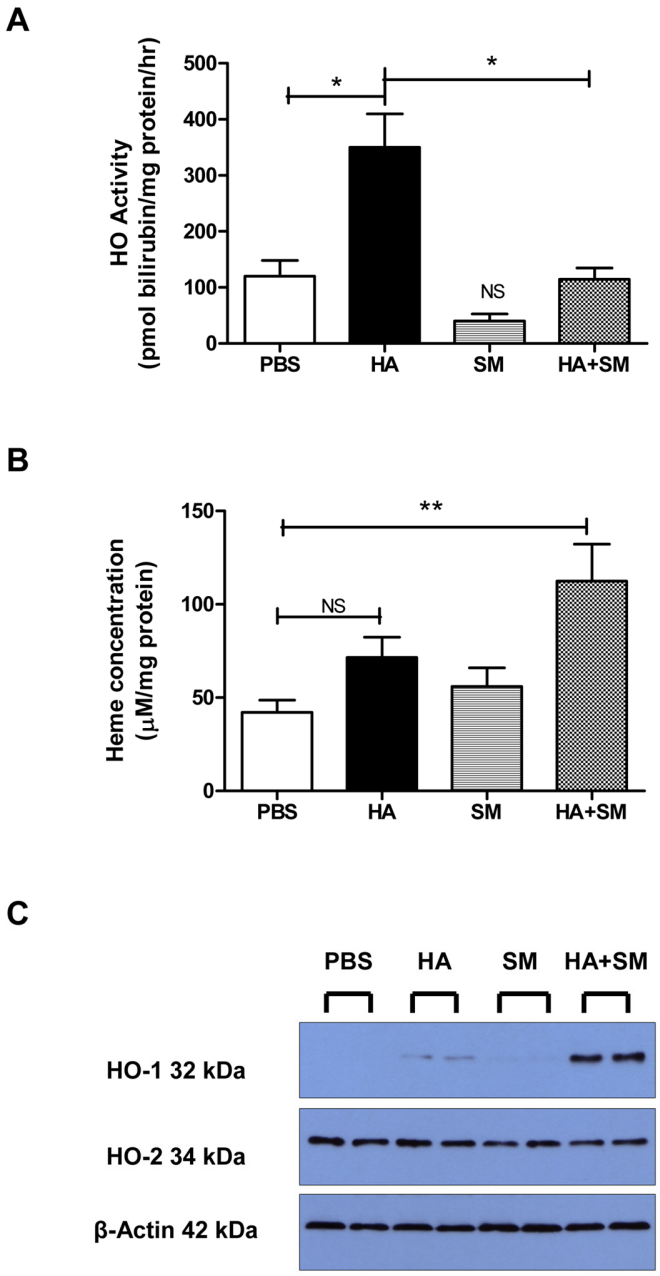


**Figure 4.3 Terminal HO activity, heme concentration and HO-1 protein expression in liver lysates of the db/db mice. A.** Concurrent SM treatment significantly suppressed the HA-mediated increase in HO activity. *P<0.05, P-value derived from Dunn's multiple comparison post-test when P<0.05 with Kruskal-Wallis test. NS: Non-significant (P>0.05) between PBS and SM by Dunn's post-test. **B.** HA+SM treatment led to an increase in the hepatic heme concentration. **P<0.01, P-value derived from Dunn's multiple comparison post-test when P<0.05 with Kruskal-Wallis test. **C.** A synergistic increase in HO-1 protein expression was observed with HA+SM treatment. No difference in HO-2 protein expression was observed between the different treatment groups. The western blot is a representative blot in which n=2 mice/treatment. β-actin was used as a control for loading equal concentrations of protein. **A, B:** The data are mean ± s.e.m. from n=4-8 mice/treatment group.

## 4.7. HA AND SM IN COMBINATION DRAMATICALLY AMELIORATED HYPERGLYCAEMIA IN db/db MICE

Ten week old db/db mice were hyperglycaemic comparative to age-matched non-diabetic lean mice (Table 4.1). PBS-treated db/db mice showed a progressive increase in the mean fasting blood glucose from 18mmol/l to 36mmol/l (Figure 4.4.A) during the 8-week study.

Area under the curve (AUC) for fasting glucose levels showed that HA treatment significantly reduced ($P<0.05$) hyperglycaemia between 6 and 8 weeks when compared to PBS-treated db/db mice (Figure 4.4.B). SM treatment did not lead to a significant reduction in fasting glucose concentration in db/db mice. HA+SM treatment markedly reduced fasting glucose levels (Figure 4.4.A, $P<0.01$ by Dunn's multiple post-test when $P<0.05$ by Friedman test) in db/db mice. HA+SM, unlike HA treatment, resulted in a significant reduction in fasting glucose levels at early time-points including 2-4 ($P<0.01$), 4-6 ($P<0.01$) and 6-8 ($P<0.001$) weeks (Figure 4.4.B).

Glycosylated haemoglobin ($HbA_{1C}$%) was used as an alternative marker of glycaemic control. PBS-treated db/db mice had significantly higher $HbA_{1C}$% than lean mice (Figure 4.4.C, $P<0.001$). HA+SM, but not single agent treatment with HA and SM, resulted in a significant reduction (Figure 4.4.C, $P<0.01$) in the level of glycosylated haemoglobin.

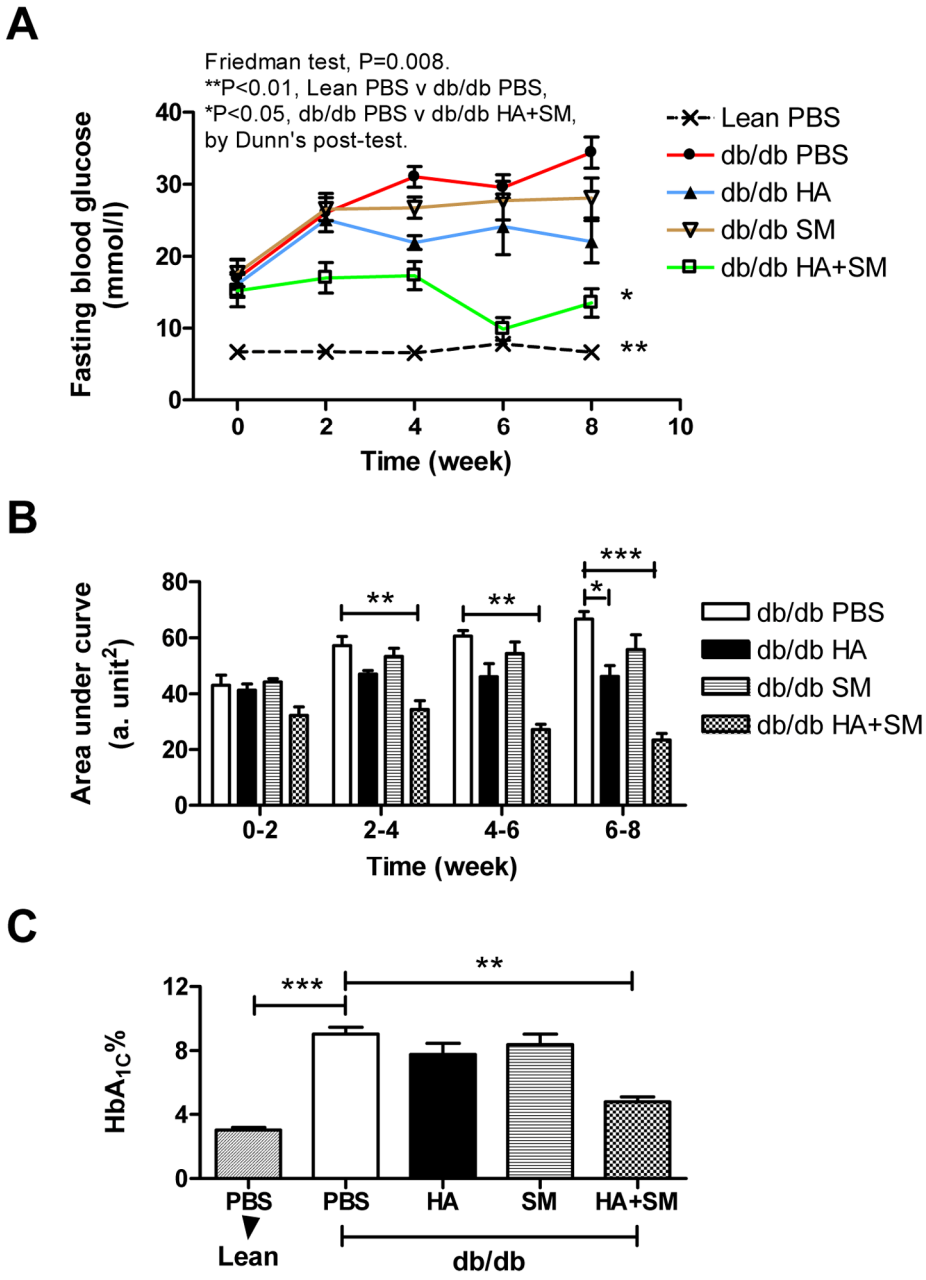


**Figure 4.4 Fasting blood glucose and $HbA_{1C}$%. A.** HA+SM-treated db/db mice had significantly reduced (P<0.05) levels of fasting glucose levels, relative to PBS-treated db/db mice. *P<0.05, **P<0.01 (highlighted in figure legends), P-value derived from Dunn's multiple comparison post-test when P<0.05 with Friedman test. **B.** Area under the curve (AUC) for fasting glucose levels between consecutive weeks (0-2, 2-4, 4-6, 6-8 week) demonstrated that HA+SM treatment significantly reduced fasting glucose levels at 2-4, 4-6 and 6-8 weeks, as opposed to only 6-8 weeks with HA treatment. *P<0.05, **P<0.01, ***P<0.001. P-value derived from Dunn's multiple comparison post-test when P<0.05 with Kruskal-Wallis test at the specified time-point. **C.** HA+SM but not HA treatment led to a significant reduction in terminal (week 8) $HbA_{1C}$% relative to PBS-treated db/db mice. **P<0.01, ***P<0.001. P-value derived from Dunn's multiple comparison post-test when P<0.05 with Kruskal-Wallis test. **A, B, C:** The data are mean ± s.e.m. from n=4-8 mice/treatment group. a. unit$^2$: arbitrary unit$^2$.

## 4.8. HA AND HA+SM TREATMENT LED TO COMPARABLE WEIGHT GAIN

The body weight of the PBS-treated db/db mice remained constant during the course of the 8-week *in vivo* study (Figure 4.5.A). Significant weight gain with HA treatment was particularly evident after 6 and 8 weeks of the *in vivo* study (Figure 4.5.B., $P<0.05$). However, the greatest increase in body weight was observed with HA+SM treatment as these mice gained an average of 16.5 grams during the 8 week study (Figure 4.5.A). Significant weight gain with HA+SM treatment was evident after 2 weeks, which progressively increased till 8 weeks of the *in vivo* study, when compared to PBS-treated db/db mice (Figure 4.5.B., $P<0.001$).

The increase in body weight with HA ($P<0.01$) and HA+SM ($P<0.001$) was in part due to a significant increase in the weights of the epididymal fat pads (EFD) but not liver (Figure 4.5.C). Food intake was monitored over a period of 6 days during week 5 and 6 of the study. The increase in weight gain with HA and HA+SM was despite no significant increase in food intake, when compared to PBS treated db/db mice (Figure 4.5.D).

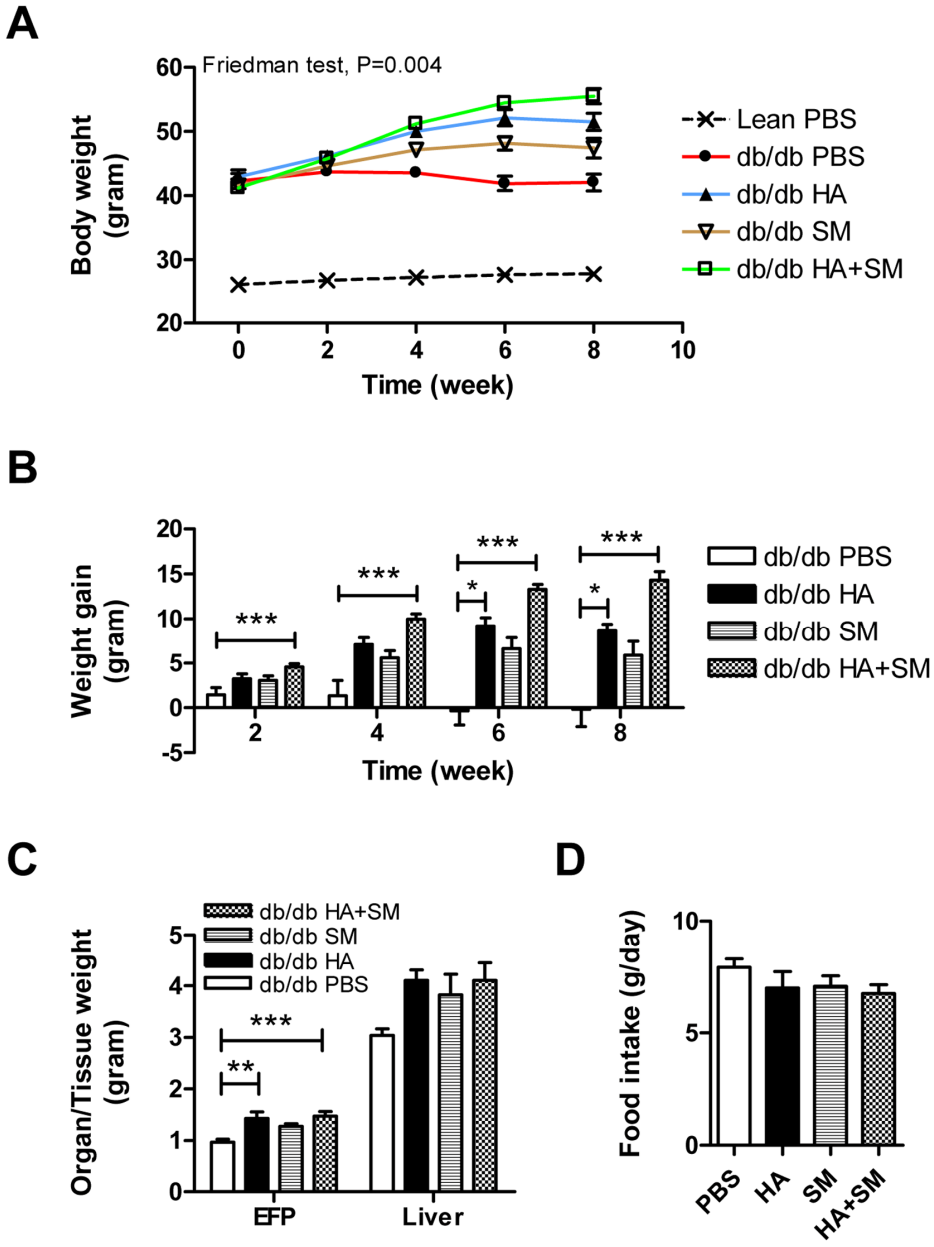


**Figure 4.5 Body weight, weight gain, organ/tissue weight and food intake. A.** A significant difference was noted for body weight between different treatment groups in db/db mice $P<0.05$ with Friedman test. **B.** Significant weight gain (body weight normalised to baseline weight) was observed after 6 and 8 weeks of HA treatment in db/db mice. Weight gain with HA+SM treatment was noted after 2 weeks, which significantly increased till 8 weeks of the *in vivo* study. *$P<0.05$, ***$P<0.001$. P-value derived from Dunn's multiple comparison post-test when $P<0.05$ with Kruskal-Wallis test at the specified time-point. **C.** HA and HA+SM significantly increased epididymal fat pad (EFP) but not liver weight in db/db mice. **$P<0.01$, ***$P<0.001$. P-value derived from Dunn's multiple comparison post-test when $P<0.05$ with Kruskal-Wallis test for EFP. $P>0.05$ (non-significant) by Kruskal-Wallis test for Liver. **D.** No significant difference in food intake was noted between different treatment groups in db/db mice. $P>0.05$ with Kruskal-Wallis test. **A, B, C, D:** The data are mean ± s.e.m. from n=4-8/treatment group.

## 4.9. HA±SM TREATMENT FAILED TO IMPROVE GLUCOSE TOLERANCE AS ASSESSED BY GLUCOSE TOLERANCE TEST

A glucose tolerance test (GTT) was performed to assess the rate of glucose disposal by endogenously produced insulin during week 7 of the *in vivo* study. The db/db mice were fasted for 4 hours before intraperitoneal administration of 2 grams of glucose per kilogram body weight and the serum glucose concentration at the indicated time points was determined by the hexokinase glucose assay.

HA+SM-treated db/db mice had significantly lower glucose levels ($P<0.05$) during the GTT when compared to PBS-treated db/db mice (Figure 4.6). However, baseline (0 minute) fasting glucose levels were different for various treatment groups in db/db mice (Figure 4.6.A).

The glucose levels increased steeply in the first 10-15 minutes after exogenous administration of a glucose bolus during the GTT. Hence, the glucose concentration at 15 minutes ($1^{st}$ read-out point after glucose administration) was used to normalise glucose levels at consequent time-points during GTT to compare the relative change in glucose levels during GTT (Figure 4.6.B).

Area under the curve (AUC) for relative change in glucose levels between 15 and 120 minutes during the GTT demonstrated no significant difference in serum glucose levels between different treatment regimes in db/db mice at 15-30, 30-60 and 60-120 minutes, relative to PBS-treated db/db mice (Figure 4.6.C).

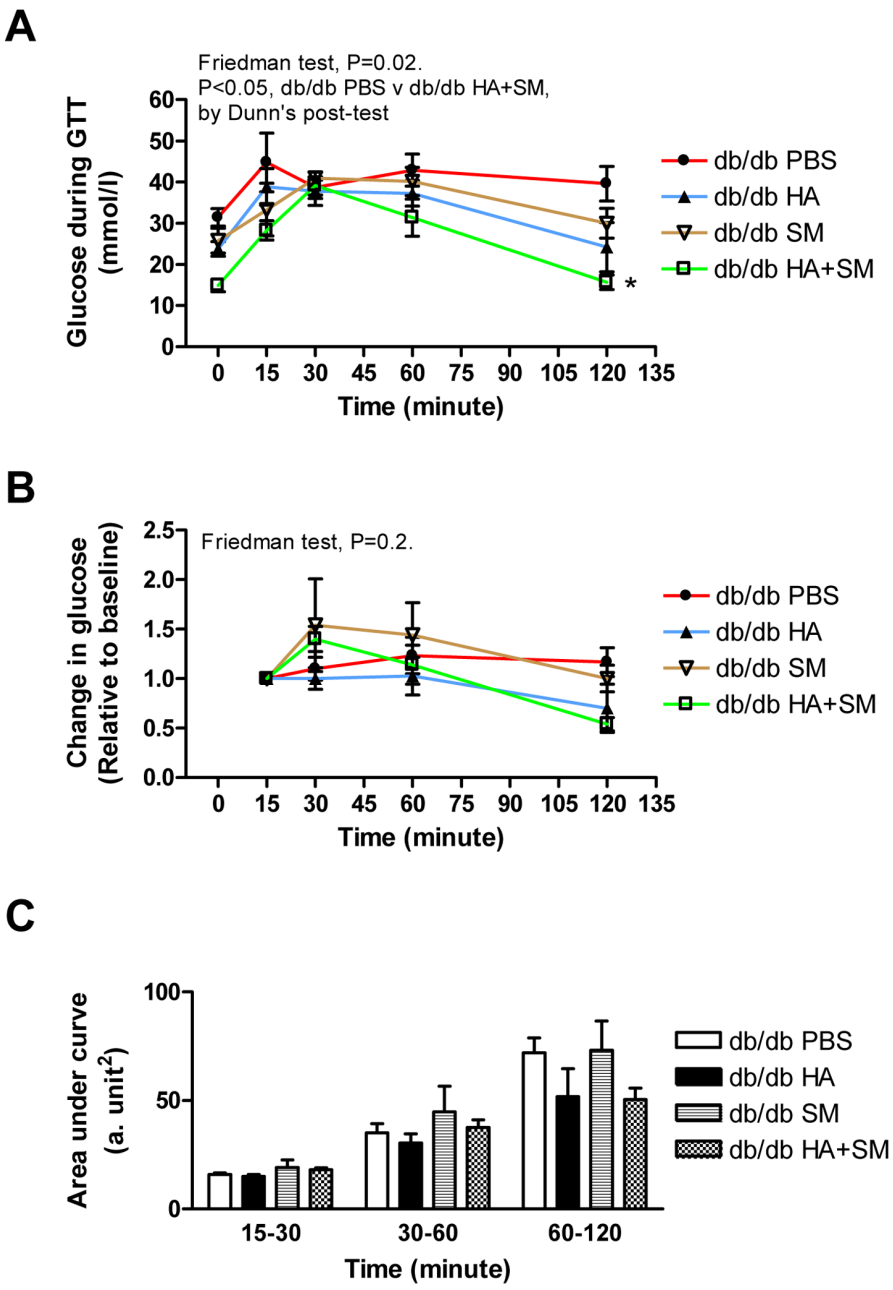


**Figure 4.6 Glucose tolerance as assessed by glucose tolerance test (GTT). A.** Serum glucose concentrations were determined at 0, 15, 30, 60 and 120 minutes after exogenous glucose (2g/kg body weight) was administration during the GTT in db/db mice. HA+SM-treated db/db mice had significantly lower levels of serum glucose during GTT. *P<0.05, (indicated in the figure). P-value derived by Dunn's multiple comparison post-test when P<0.05 by Friedman test. **B.** Relative change in glucose levels (glucose concentrations at consecutive time-points divided by glucose concentration at 15 minutes during GTT) during GTT was not significant between the various treatment regimes in db/db mice. P>0.05 (indicated in figure) by Friedman test. **C.** Area under the curve (AUC) for relative changes in glucose levels during GTT demonstrated no significant change in relative glucose levels between different treatment regimes in db/db mice. P>0.05 by Kruskal-Wallis test for specified time-points. **A, B, C:** The data are mean ± s.e.m. from n=4-8 mice/treatment group. a. unit$^2$: arbitrary unit$^2$.

## 4.10. HA±SM TREATMENT HAD NO EFFECT ON INSULIN RESISTANCE AS ASSESSED BY INSULIN TOLERATNCE TEST

An insulin tolerance test (ITT) was performed during week 8 of the *in vivo* study to assess whole body insulin sensitivity. The blood glucose level was monitored for an hour after intraperitoneal administration of insulin at a dose of 1 unit insulin per kilogram body weight.

HA+SM-treated db/db mice had significantly lower glucose levels ($P<0.01$) during ITT when compared to PBS-treated db/db mice (Figure 4.7.A). However, baseline (0 minute) fasting glucose levels were different for various treatment groups in db/db mice (Figure 4.7.A). Hence, glucose levels at consequent time-points during ITT were divided by baseline concentration of glucose to compare relative fold change in glucose levels (Figure 4.6.B).

Normalisation of glucose concentrations at consecutive time-points during the ITT demonstrated no significant difference in relative changes in glucose levels between different treatment groups in db/db mice (Figure 4.7.B). Area under the curve (AUC) for relative change in glucose levels during ITT demonstrated that no significant change in relative glucose level was evident between various different groups at consequent time-points (Figure 4.7.C).

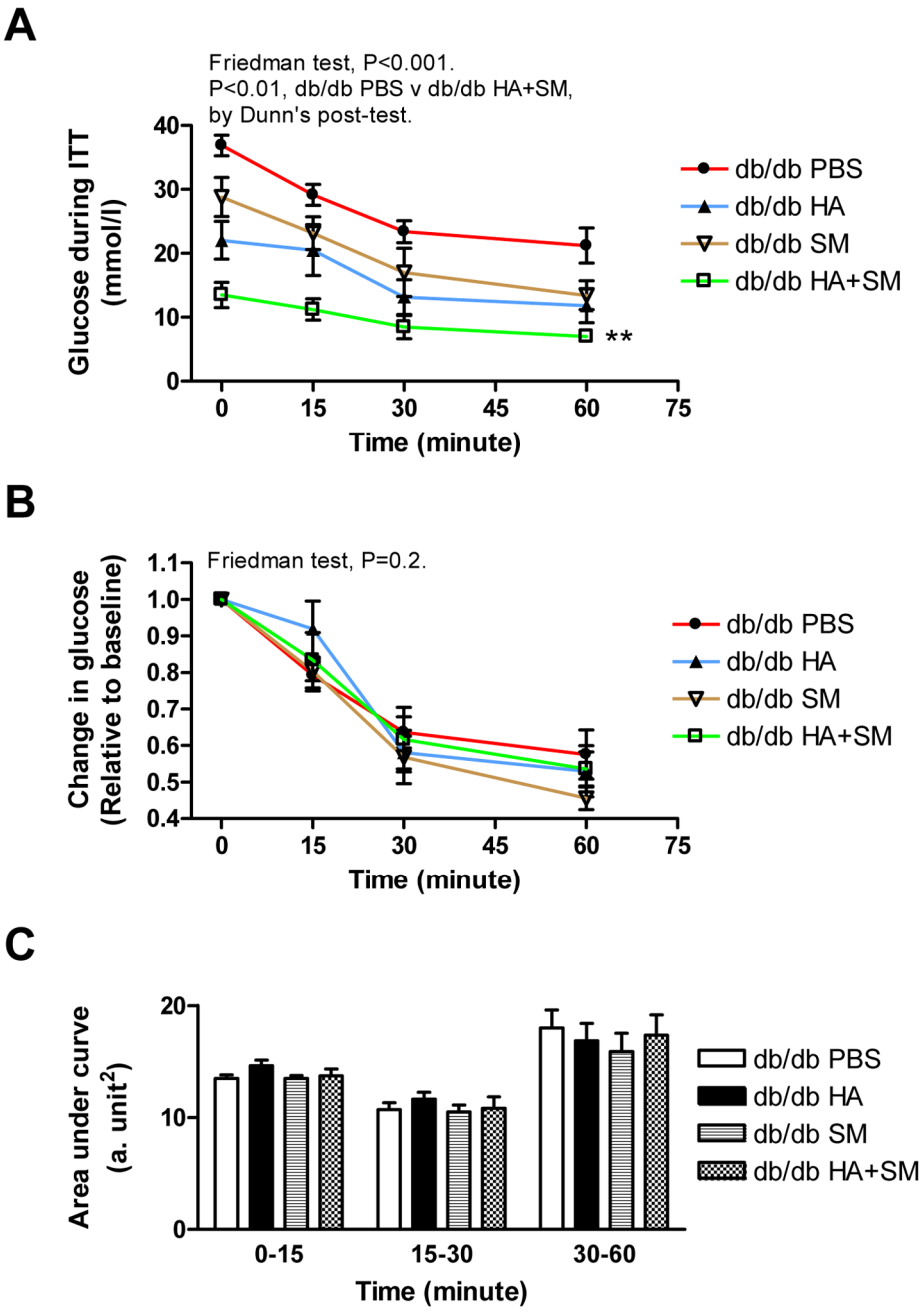


**Figure 4.7 Insulin resistance as assessed by insulin tolerance test (ITT). A.** Glucose concentrations were determined at 0, 15, 30 and 60 minutes, after exogenous insulin (1 unit/kg body weight) administration in db/db mice. HA+SM-treated db/db mice had significantly lower glucose levels, relative to PBS-treated db/db mice*P<0.05, (indicated in the figure). P-value derived by Dunn's multiple comparison post-test when P<0.05 by Friedman test. **B.** Relative change in glucose levels (normalised by dividing with baseline glucose concentration) during ITT was not significant between different treatment groups in db/db mice. P>0.05 (indicated in figure) by Friedman test. **C.** Area under the curve (AUC) for relative changes in glucose levels during ITT demonstrated no significant difference between treatment groups in db/db mice. P>0.05 by Kruskal-Wallis test for specified time-points. **A, B, C:** The data are mean ± s.e.m. from n=4-8 mice/treatment group. a. unit$^2$: arbitrary unit$^2$.

## 4.11. HA±SM TREATMENT MODULATED TERMINAL FASTING SERUM PARAMETERS

The 8-week fasting serum samples were used to determine insulin, non-esterified fatty acid (NEFA) and high molecular weight (HMW) adiponectin. PBS-treated db/db mice had significantly elevated level of circulatory insulin (Figure 4.8.A, $P<0.05$), NEFA (Figure 4.8.C, $P<0.05$) and reduced levels of HMW adiponectin (Figure 4.8.E, $P<0.05$), relative to PBS-treated lean (C57BL/KsJ) mice.

Treatment with HA ($P<0.05$) and HA+SM ($P<0.01$) for 8 weeks in db/db mice resulted in a significant increase in fasting insulin levels when compared to PBS-treated db/db mice (Figure 4.8.B). However, none of the treatment regimes in db/db mice significantly altered fasting NEFA levels (Figure 4.8.D). HA+SM-treated db/db mice had significantly improved serum adiponectin levels (Figure 4.8.F), relative to PBS-treated db/db mice.

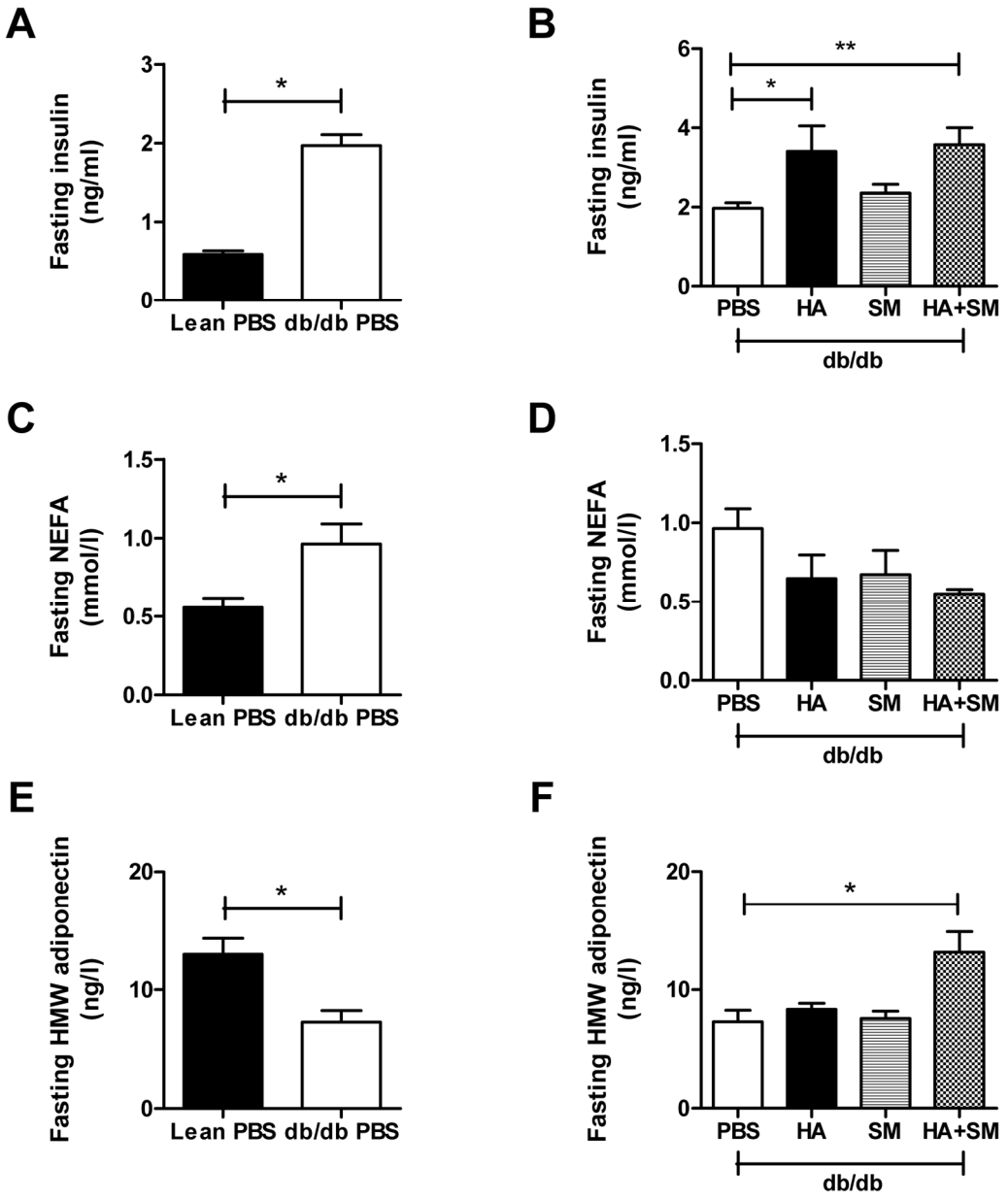


**Figure 4.8 Terminal fasting serum insulin, non-esterified fatty acid (NEFA) and HMW adiponectin levels.** PBS-treated db/db mice had significantly increased levels of **A.** Insulin, **C.** NEFA and reduced levels of **E.** High molecular weight (HMW) adiponectin, relative to PBS-treated lean (C57BL/KsJ) mice. *P<0.05, P-values derived from one-tailed Mann Whitney test for comparison between lean and db/db mice on PBS treatment. HA and HA+SM treatment for 8-weeks resulted in a significant increase in fasting levels of **B.** Insulin but had no statistically significant effect on **D.** NEFA. HA+SM treatment markedly increased HMW adiponectin levels in db/db mice. **B.** *P<0.05, **P<0.01. P-value derived from Dunn's multiple comparison post-test when P<0.05 with Kruskal-Wallis test. For **D,** P>0.05 (non-significant) by Kruskal-Wallis test. **A, C, E:** The data are means ± s.e.m. from n=4 mice/treatment group. **B, D, F:** The data are means ± s.e.m. from n=4-8 mice/treatment group.

## 4.12. HA+SM TREATMENT REDUCED ISLET iNOS EXPRESSION

In the preliminary *in vivo* study (chapter 3), prominent iNOS protein expression by immuno-fluorescence was observed in the islets of PBS-treated db/db mice (Figure 3.9.A, B in chapter 3). Hence, quantification of cells expressing iNOS protein was performed in the current study to determine whether HA, SM or HA+SM treatment had a significant impact on reducing iNOS protein expression within the islets of db/db mice.

The number of cells staining positively for iNOS within pancreatic islets was quantified by immuno-histochemistry (IHC). The islets were identified by co-staining with anti-mouse insulin antibody (Figure 4.9). The mean cross-sectional area of the islets of db/db mice was significantly larger ($P<0.05$) than lean mice (Figure 4.10.A). However, no significant difference in the mean cross-sectional area of the islets was observed between db/db mice on different treatment regimes (Figure 4.10.B). The mean number of iNOS positive cells was corrected for the mean surface area per islet.

The number of iNOS-protein expressing cells within the islets of PBS-treated db/db mice was significantly greater (Figure 4.10.C $P<0.05$) than in lean mice. Single agent treatment of HA and SM did not result in a significant decrease in number of iNOS stained cells in the islets (Fig 4.10.D). However, HA+SM treatment significantly reduced ($P<0.01$) the number of iNOS expressing cells within the islets (Figure 4.11.D) to comparable levels to those observed in lean mice (Figure 4.10.C).

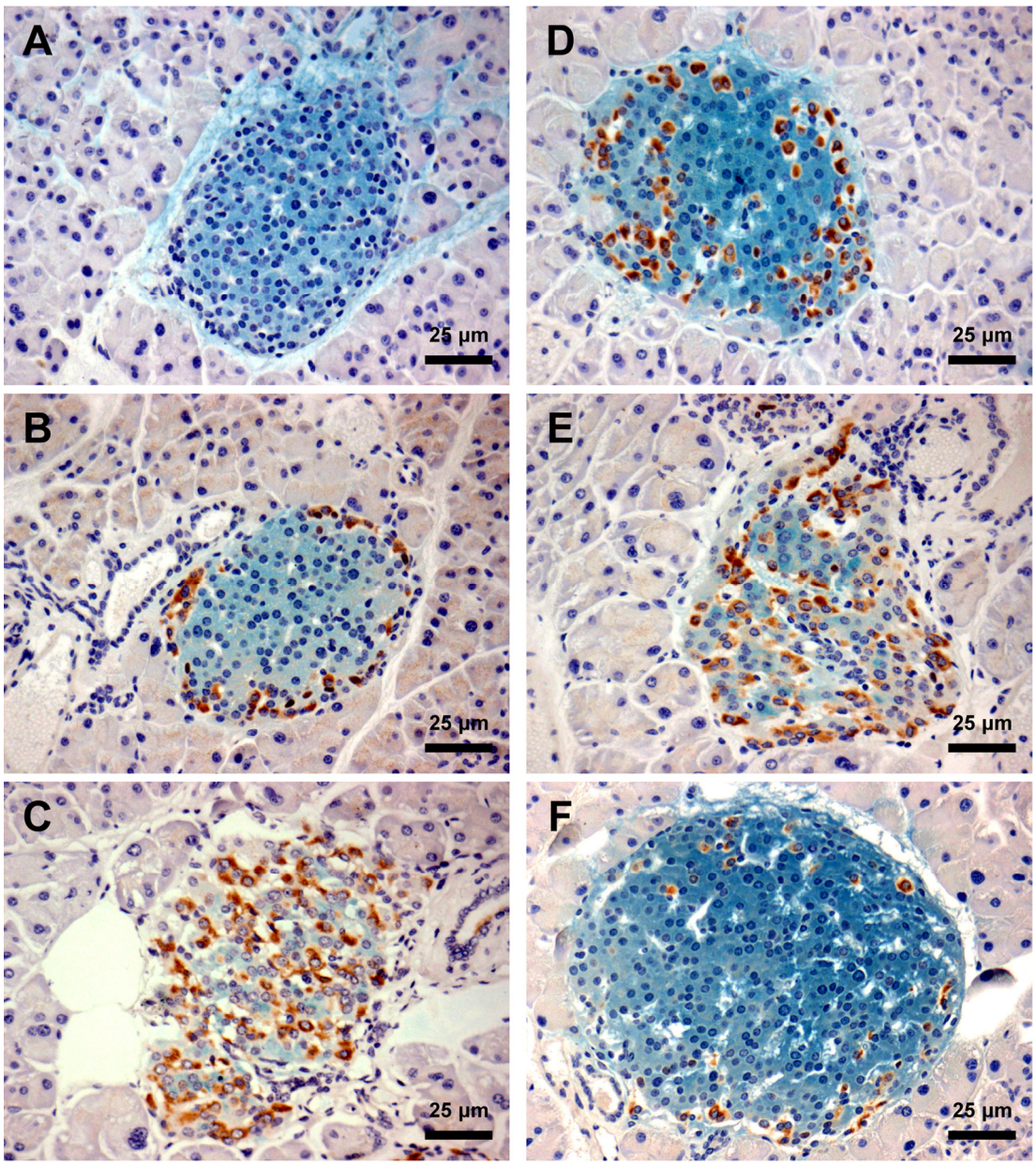


**Figure 4.9 Immuno-histochemical (IHC) staining for iNOS expression in pancreatic islets.** Co-staining for iNOS (brown) and insulin (green) was performed on methyl-carbonyl fixed sections of pancreas. **A.** Staining with insulin antibody only **B.** Lean mice PBS **C.** db/db PBS **D.** db/db HA **E.** db/db SM **F.** db/db HA+SM. Pictures taken at x 200 magnification. Scale bar represents 25 µm.

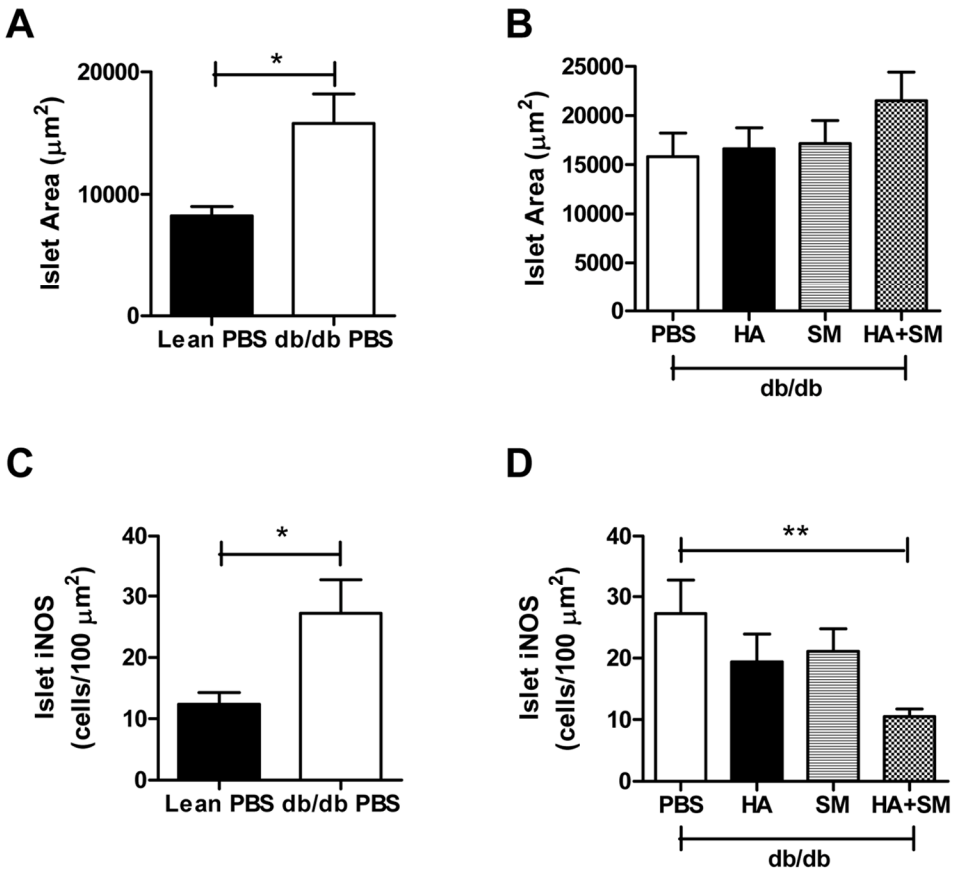


**Figure 4.10 Determination of iNOS-protein expression in pancreatic islets. A.** Mean cross-sectional area of islets of PBS-treated db/db mice was significantly greater than lean mice. *P<0.05, P-values derived from two-tailed Mann Whitney test for comparison between Lean and db/db mice on PBS treatment. **B.** No significant difference in mean cross-sectional area of islets was observed for various treatment regimes in db/db mice. P>0.05 (non-significant) by Kruskal-Wallis test. **C.** PBS-treated db/db mice had significantly higher numbers of iNOS-protein expressing cells compared to lean mice. *P<0.05, P-values derived from two-tailed Mann Whitney test for comparison between Lean and db/db mice on PBS treatment. **D.** HA+SM treatment resulted in a significant reduction in the number of iNOS-protein expressing cells in the db/db mice. **P<0.01, P-value derived from Dunn's multiple comparison post-test when P<0.05 with Kruskal-Wallis test. **A, C:** The data are means ± s.e.m. from n=4 mice/treatment group. **B, D:** The data are means ± s.e.m. from n=4-8 mice/treatment group. A minimum of 25 islets/mouse from cross-sections cut at a minimum difference of 75 micron (to avoid repeated counting of same islet) was used for quantification.

## 4.13. HA AND HA+SM TREATMENT REDUCED ISLET MACROPHAGE INFILTRATION

Macrophage infiltration into pancreatic islets has been observed in both patients with type 2 diabetes and in rodent models of type 2 diabetes (Ehses et al., 2007b). Hence, F4/80, a pan-macrophage marker was used to stain and quantify islet macrophage infiltration (Figure 4.11). Co-staining with insulin was performed to identify islet β-cells.

The mean cross-sectional area of the islets of PBS-treated db/db mice was significantly larger (Fig 4.12.A) than in PBS-treated lean mice. PBS treated db/db mice had a significantly greater number ($P<0.05$) of total (Figure 4.13.C), intra-islet (Figure 4.12.E) and peri-islet (Figure 4.12.G) $F4/80^+$ cells compared to PBS-treated lean mice.

HA alone led to a significant reduction in the number of intra-islet (Figure 4.12.F) $F4/80^+$ cells, relative to PBS-treated db/db mice. No significant reduction in islet macrophage infiltration was noted for SM treatment in db/db mice. Importantly, HA+SM treatment significantly reduced ($P<0.01$) macrophage numbers (Figure 4.12.D) in islets of db/db mice to levels observed in lean mice. This was due to a reduction in both intra-islet (Figure 4.12.F, $P<0.001$) and peri-islet $F4/80^+$ cells (Figure 4.12.H, $P<0.01$).

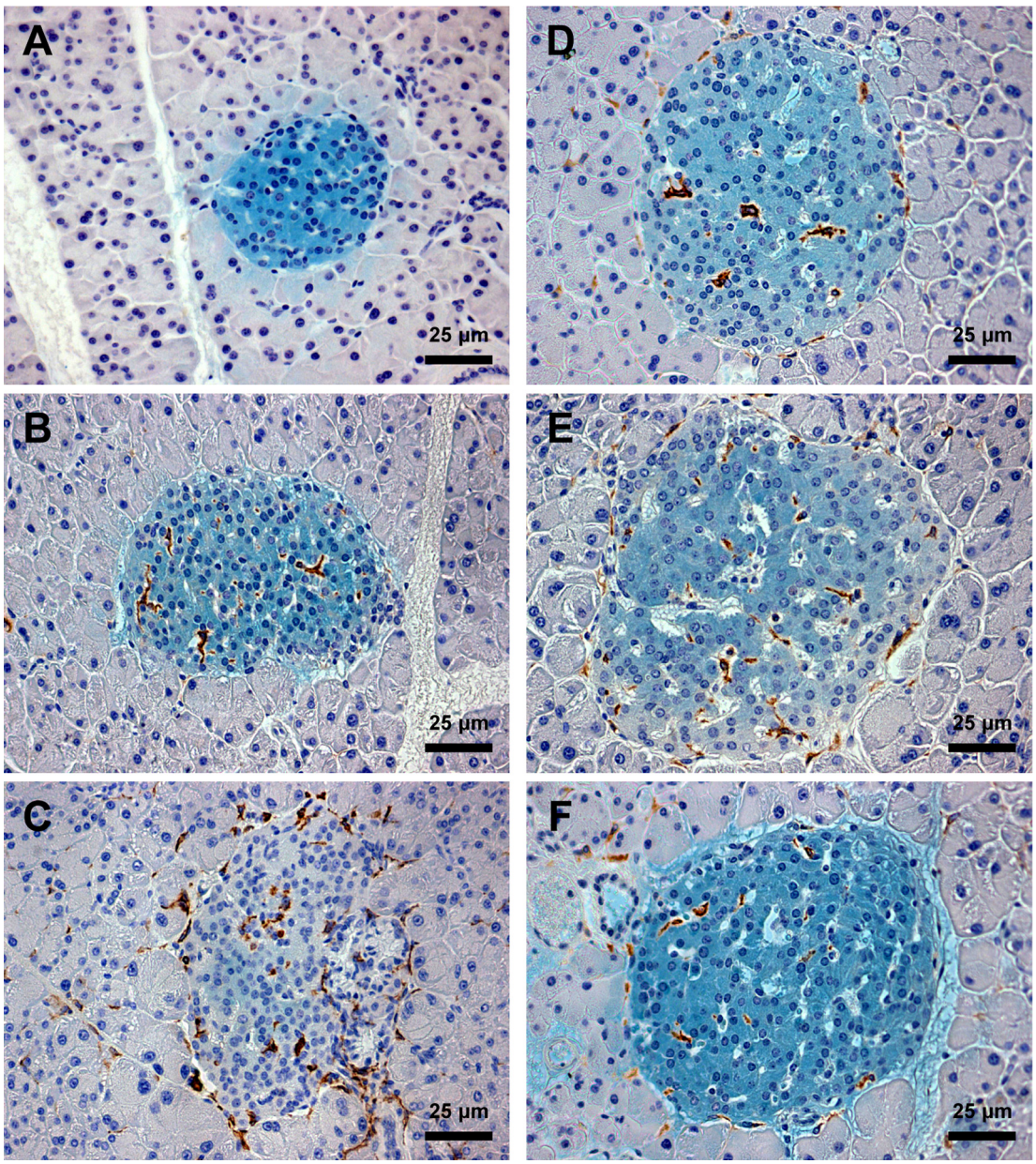


**Figure 4.11 Immuno-histochemical (IHC) staining for macrophage (F4/80) infiltration in pancreatic islets.** Co-staining for F4/80 (brown) and insulin (green) was performed on methyl-carbonyl fixed sections of pancreas. **A.** Staining with insulin antibody only **B.** Lean mice PBS **C.** db/db PBS **D.** db/db HA **E.** db/db SM **F.** db/db HA+SM. Pictures taken at x 200 magnification. Scale bar represents 25 µm.

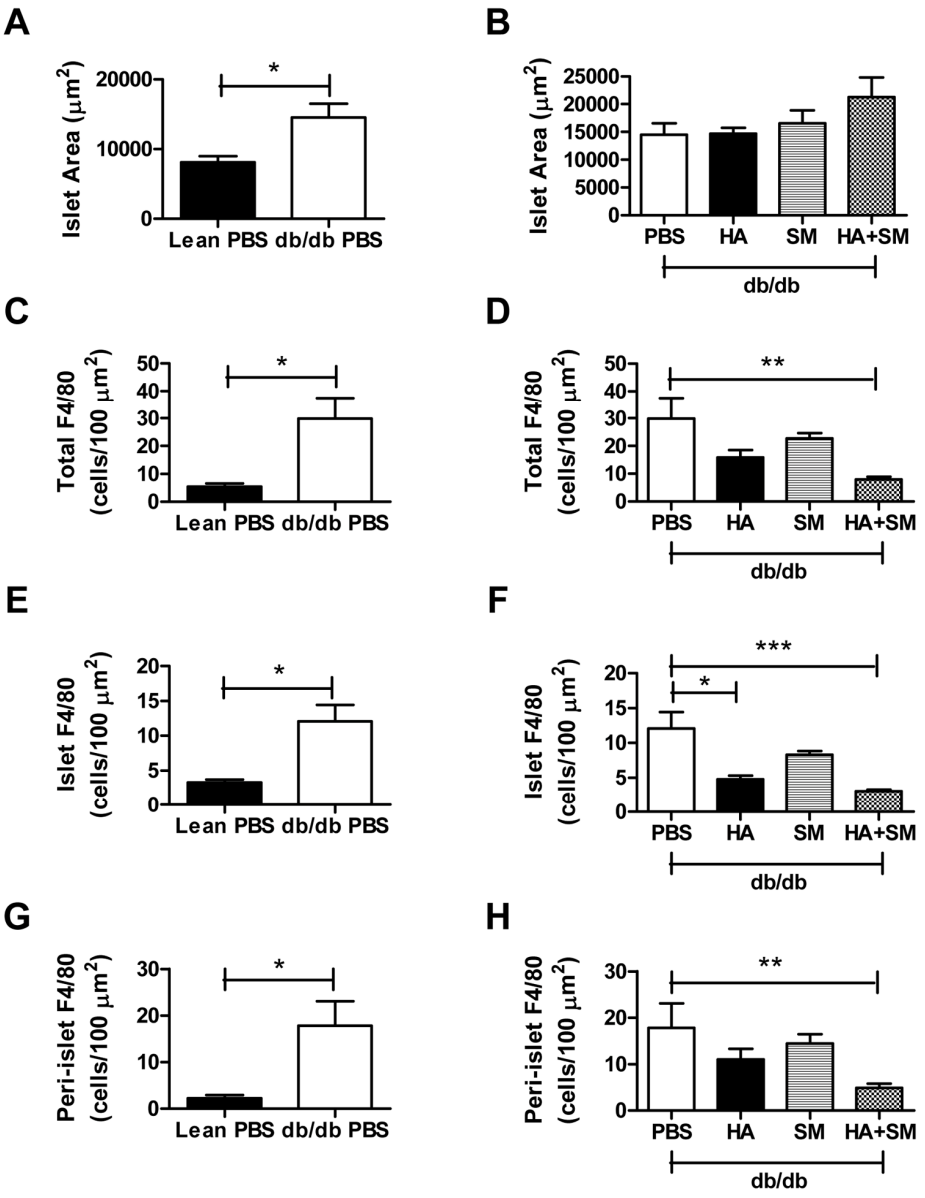


**Figure 4.12 Determination of macrophage infiltration in pancreatic islets.** A significant difference in the mean islet cross-sectional area was noted between **A.** lean and db/db mice on PBS-treatment ($P<0.05$, two-tailed Mann Whitney test) but not between **B.** various treatment groups in db/db mice ($P>0.05$, Kruskal-Wallis test). PBS-treated db/db mice had significantly increased number of **C.** Total (islet+peri-islet) F4/80, **E.** Islet F4/80 and **G.** Peri-islet F4/80 cells, relative to lean mice. *$P<0.05$, P-values derived from two-tailed Mann Whitney test for comparison between lean and db/db mice on PBS treatment. In HA-treated db/db mice, there was a significant reduction in the number of **F.** Islet F4/80 cells, relative to PBS-treated db/db mice. In HA+SM-treated db/db mice, there was a significant reduction in the number of **D.** Total F4/80, **F.** Islet F4/80 and **H.** Peri-islet F4/80 cells, relative to PBS-treated db/db mice. **D, F, H:** *$P<0.05$, **$P<0.01$, ***$P<0.001$ by Dunn's multiple comparison post-test when $P<0.05$ with Kruskal-Wallis test. **A, C, E, G:** The data are means ± s.e.m. from n=4 mice/treatment group. **B, D, F, H:** The data are means ± s.e.m. from n=4-8 mice/treatment group. A minimum of 25 islets/mouse from cross-sections cut at a minimum difference of 75 micron (to avoid repeated counting of same islet) was used for quantification.

## 4.14. THE MODULATORY EFFECT OF TREATMENT REGIMES ON mRNA TRANSCRIPT LEVELS IN EPIDIDYMAL FAT

The mRNA levels of the pro-inflammatory mediators including cytokines (TNF-α and IL-6) and chemokines (MCP-1α and Cxcl-2) along with Pref-1 (an inhibitor of adipogenesis), PPAR-γ (marker of adipocyte differentiation) and fatty acid synthase (FASN, mediator of lipogenesis) were determined in epididymal fat using RT-PCR.

HA treatment resulted in a significant increase in mRNA level of HO-1 (Figure 4.13.A, $P<0.05$) but failed to significantly change the mRNA levels of other listed genes in figure 4.13. SM treatment alone failed to significantly increase mRNA level of HO-1 but significantly reduced mRNA levels of CD68 (Figure 4.13.B, $P<0.01$) and MCP-1α (Figure 4.13.E, $P<0.001$). There was a significant increase in the mRNA level of HO-1 (Figure 4.13.A, $P<0.001$) which coincided with a significant decrease in mRNA levels of CD68 (Figure 4.13.B, $P<0.05$) and MCP-1α (Figure 4.13.E, $P<0.05$) and a marked increase in Cxcl-2 (Figure 4.13.F, $P<0.001$) with HA+SM treatment in db/db mice. None of the treatment regimes, including HA, SM and HA+SM, significantly modulated mRNA levels of pro-inflammatory mediators, such as TNF-α and IL-6 (Figure 4.13.C, D). Furthermore, with HA+SM treatment, there was a significant reduction in mRNA levels of Pref-1 ($P<0.05$, Figure 4.13.G) and significant increase in mRNA levels of PPAR-γ and FASN ($P<0.05$, Figure 4.13.H, I).

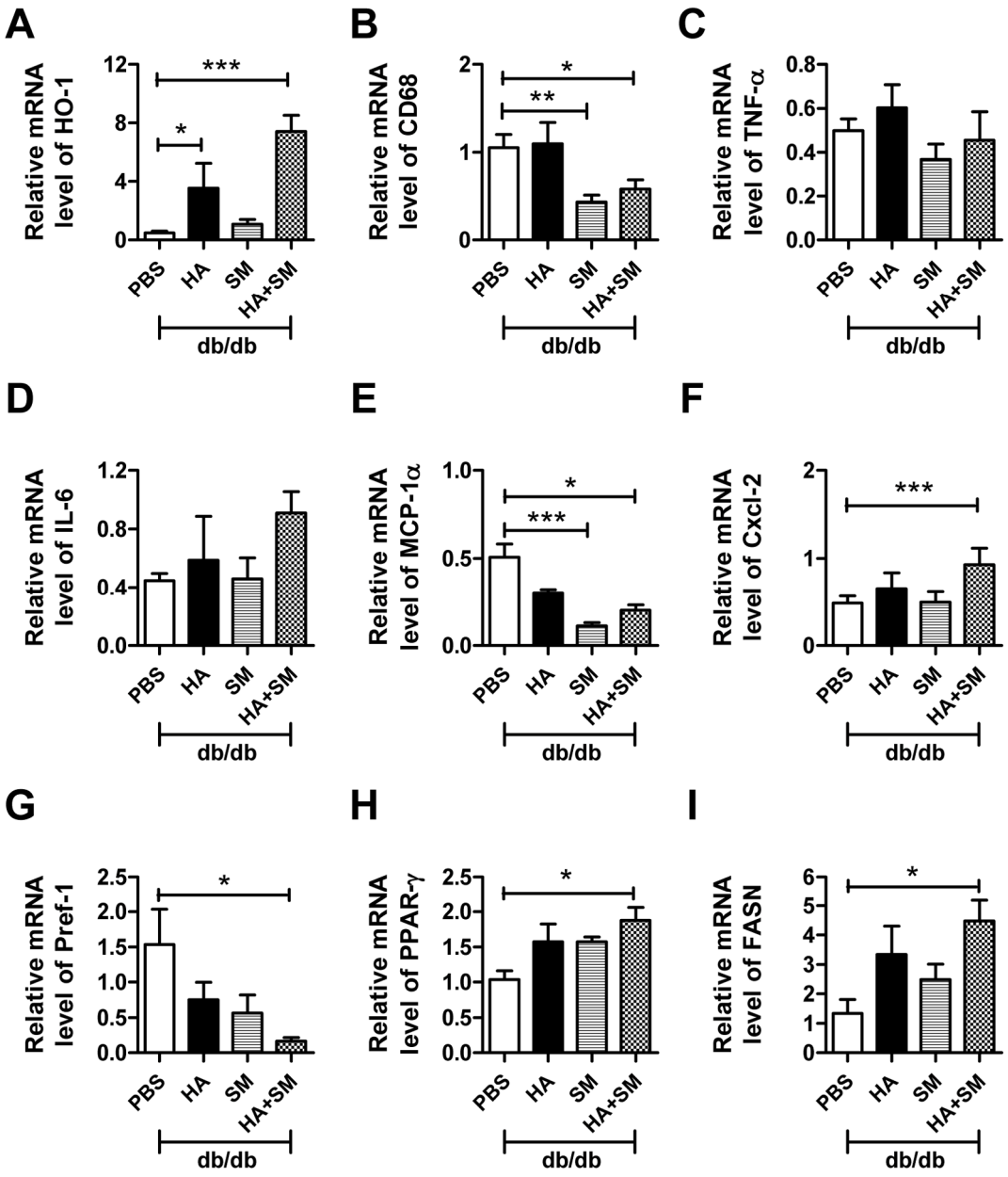


**Figure 4.13 Gene expressions in the epididymal fat of db/db mice on different treatment regimes.** Relative mRNA levels of **A.** HO-1, **B.** CD68, **C.** TNF-α, **D.** IL-6, **E.** MCP-1α, **F.** Cxcl-1, **G.** Pref-1, **H.** PPAR-γ and **I.** FASN, in the epididymal fat of db/db mice receiving PBS, HA, SM and HA+SM treatment. *P<0.05, **P<0.01, ***P<0.001 by Dunn's multiple comparison post-test when P<0.05 with Kruskal-Wallis test. The data are mean ± s.e.m. from n=4-8 mice/treatment group. **A-F:** 18S gene was used as endogenous control gene. **G-I:** TBP gene was used as endogenous control gene.

## 4.15. NO SIGNIFICANT INCREASE IN LIVER FAT DEPOSITION BY ALL TREATMENTS

No significant change in either hepatic triglyceride content per unit mass or, hepatic total triglyceride (triglyceride/unit mass x liver weight) was observed with any of the treatment regimes in db/db mice (Figure 4.14).

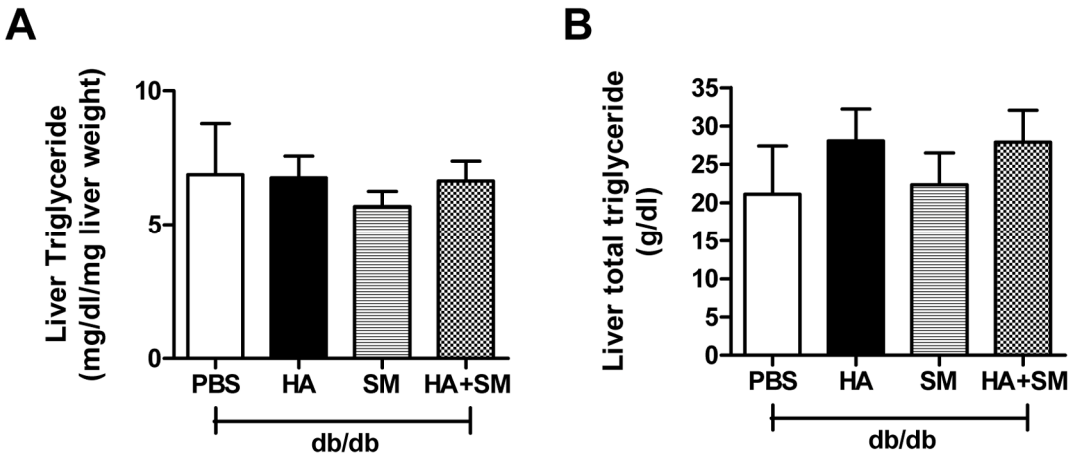


**Figure 4.14 Hepatic triglyceride deposition in db/db mice on different treatment regimes.** None of the treatment regimes significantly modulated the levels of either **A.** Hepatic triglyceride content per unit mass (mg) or, **B.** Total hepatic triglyceride content, relative to PBS-treated db/db mice. P>0.05 (non-significant) by Kruskal-Wallis test. The data are mean ± s.e.m. from n=4-8 mice/treatment group.

## 4.16. NONE OF THE TREATMENT REGIMES RESULTED IN A REDUCTION IN GLUCONEOGENIC GENE EXPRESSION

Previously, a study examining the role of the nuclear receptor hormone, Rev-erbα in hepatocyte cell culture (HepG2) established heme as a Rev-erbα ligand that suppresses expression of key gluconeogenic genes, such as phosphoenol pyruvate carboxy kinase (PEPCK) and glucose-6-phosphatase (G-6-P) by recruiting the nuclear co-repressor-histone deacetylase 3 (NCoR-HDAC-3) gene repressor complex (Yin et al., 2007).

To determine whether the anti-hyperglycaemic effect of HA or HA+SM was mediated by suppression of gluconeogenic enzymes, the relative gene expression of PEPCK and G-6-P in the liver was determined. Treatment regimes including HA, SM and HA+SM did not result in significant modulation of the mRNA levels of PEPCK and G-6-P (Figure 4.15).

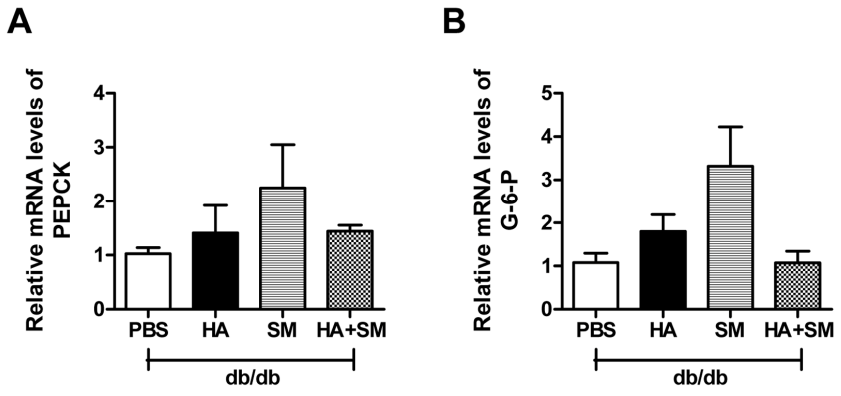


**Figure 4.15 Gene expression of gluconeogenic genes in the liver of db/db mice on different treatment regimes.** Treatment regimes including HA, SM and HA+SM failed to significantly modulate mRNA levels of **A.** PEPCK **B.** G-6-P (glucose-6-phosphatase) in the liver of db/db mice. P>0.05 (non-significant) by Kruskal-Wallis test. The data are mean ± s.e.m. from n=4-8 mice/treatment group. 18S gene was used as endogenous control gene.

## 4.17. CHAPTER DISCUSSION

### 4.17.1. HO ACTIVITY INDEPENDENT ANTI-HYPERGLYCAEMIC EFFECT OF HA

The current *in vivo* study was performed to test the hypothesis that anti-hyperglycaemia effect of heme arginate (HA) is dependent on HA's ability to induce heme oxygenase (HO) activity. Consistent with the preliminary *in vivo* study, a HA-mediated increase in hepatic HO-activity (Figure 4.3.A) was associated with reduced fasting hyperglycaemia between 6 to 8 weeks (Figure 4.4.B) of the *in vivo* study. However, no significant decrease in $HbA_{1C}$% (glycosylated haemoglobin, Figure 4.4.C), a marker of sustained hyperglycaemia, was noted for HA treatment. Therefore, the two independent measures of hyperglycaemia demonstrated that HA was effective at reducing hyperglycaemia during the latter stages of *in vivo* study, only for short period of time, specifically between 6 to 8 weeks.

Stannous (IV) mesoporphyrin IX dichloride (SM) was employed in the current *in vivo* study to inhibit the HA-mediated increase in HO activity. SM treatment alone did not significantly modulate the fasting hyperglycaemia and $HbA_{1C}$% (Figure 4.4.A-C). However, the most intriguing result of the current *in vivo* study was the further improvement in glycaemic control (Figure 4.4.A), that was observed when SM was co-administered with HA (HA+SM). This occurred despite complete abrogation of the HA mediated increase in HO activity (Figure 4.3.A). The anti-hyperglycaemic effect of HA+SM treatment was confirmed by a significant

reduction in the level of glycosylated haemoglobin (Figure 4.4. C). Furthermore, the profound improvement in glycaemic control with HA+SM treatment was highlighted by the significant reduction in fasting glucose levels from an earlier time-point, between 2 and 4 weeks (Figure 4.4.B). The anti-hyperglycemic effect of HA+SM treatment is in contrast to a previous study, where chromium (III) mesoporphyrin IX chloride (CrMP), an inhibitor of HO activity, reversed the anti-hyperglycaemic effect of hemin in non-obese insulin-resistant Goto-Kakizaki (GK) rats (Ndisang and Jadhav, 2009). Hence, the current *in vivo* study demonstrated a novel anti-hyperglycaemic phenotype, where inhibition of HO activity accentuated the ameliorative potential of HA. This observation was in contrast to the hypothesis of the present study that the anti-hyperglycaemic effect of HA is dependent on HA's ability to induce HO activity.

### 4.17.2. INCREASED OBESITY MAY BE RESPONSIBLE FOR ANTI-HYPERGLYCAEMIC EFFECT OF HA±SM

Remarkably, improvement in glycaemic control with HA±SM treatment occurred despite a significant gain in weight (Figure 4.5.B). The increase in body weight with HA±SM treatment compared to PBS-treated db/db mice was in part due to a significant increase in adiposity as reflected by an increase in the weight of the epididymal fat pad (Figure 4.5.C). The increase in body weight with HA±SM treatment was not due to an increase in food intake (Figure 4.5.D).

Both the HA±SM-mediated reduction in fasting hyperglycaemia and increase in adiposity in db/db mice occurred from an early point in the study (Figure 4.4.B, 4.5B). The inverse relationship between weight gain and reduction in fasting glucose levels suggests that the two events are related to each other. This is important as the elevated adipocyte storage capacity of db/db mice when compared to obesity-resistant (over-expressing leptin receptor-b) db/db mice, has been reported to be critical for delaying the onset and severity of type 2 diabetes (Wang et al., 2008).

HA+SM treatment increased circulatory levels of adiponectin (Figure 4.8.F), an insulin-sensitising adipokine (Kadowaki et al., 2006), indicating an improvement in the endocrine function of adipose tissue despite profound adiposity. Furthermore, HA+SM treatment increased gene expression of PPAR-γ (Figure 4.13.H), a key mediator of adipocyte differentiation (Lazar, 1999). The increase in gene expression of PPAR-γ and circulatory levels of adiponectin are similar to the effect of PPAR-γ agonists, such as thiazolidinedione (TZD) group of compounds, which bind to and activate PPAR-γ to promote adipocyte differentiation (Okuno et al., 1998). An increase in adipocyte differentiation with HA+SM treatment was further supported by the significant decrease in gene expression of Pref-1 (Figure 4.13.G), an inhibitor of adipocyte differentiation (Wang et al., 2006). Additionally, HA+SM treatment increased the gene expression of FASN (Figure 4.13.I), which facilitates *de novo* lipogenesis, where excess carbohydrate is converted into lipids for storage (Wang et al., 2004). Hence, these observations indicate that HA+SM treatment led to a metabolically favourable remodelling of visceral fat to improve adipocyte storage

capacity, which may have prevented ectopic lipid deposition in the liver of db/db mice.

To determine whether the increase in body weight was a generic side-effect of HA treatment or a specific phenotype in db/db mice Lean (C57BL/KsJ) mice were administered 15mg/kg of HA, twice weekly for 8 weeks. No significant difference in fasting glucose and body weight was noted with HA treatment in lean mice (Table 4.2), indicating weight gain with HA treatment to be a specific phenotype of HA in db/db mice.

### 4.17.3. THE ANTI-HYPERGLYCAEMIC EFFECT OF HA±SM IS INDEPENDENT OF INSULIN SENSITIVITY

Amelioration of peripheral insulin resistance is a key mechanism for reducing hyperglycaemia by promoting insulin mediated glucose disposal (Dugani and Klip, 2005) and reducing hepatic gluconeogenesis (Barthel and Schmoll, 2003).

In the current *in vivo* study, significant reduction in fasting hyperglycaemia with HA±SM treatment was noted despite no improvement in insulin resistance compared to PBS-treated db/db mice (Figure 4.7.B, C). HA+SM-treated db/db mice had significantly lower glucose levels during insulin tolerance test (ITT), however this was due to the difference in baseline (0 minute) glucose levels (Figure 4.7.A). When the glucose levels during the ITT were normalised to determine relative changes in glucose levels, there was no significant change in the rate of glucose disappearance

between the different treatment groups in db/db mice (Figure 4.7.B, C). The HA+SM treatment may have been ineffective in improving insulin sensitivity as it had limited efficacy in altering the following key pathogenic pathways that are responsible for insulin resistance in type 2 diabetes:

- **Ectopic lipid deposition paradigm:** Lipid deposition in peripheral organs, such as liver reduces the control of insulin on gluconeogenesis (Matsumoto et al., 2006). In the current *in vivo* study, HA±SM treatment failed to reduce hepatic triglyceride content (Figure 4.14.B) or gene expression of gluconeogenic genes, including PEPCK and glucose-6-phosphatase (Figure 4.15), suggesting that the glucose output from the liver HA±SM-treated db/db mice was likely to not be different to diabetic PBS-treated db/db mice.

- **Endocrine function of adipose tissue paradigm:** Pro-inflammatory adipokines, such as TNF-α and IL-6, has been reported to promote insulin resistance (Fontana et al., 2007, Hotamisligil et al., 1995). HA±SM treatment failed to significantly reduce mRNA levels of key pro-inflammatory mediators, such as TNF-α, IL-6, Cxcl-2 (Figure 4.13.C, D, F). HA+SM treatment selectively reduced mRNA levels of CD68 (Figure 4.13.B), a marker for macrophages, and MCP-1α, (Figure 4.13.E) monocyte chemo-attractant. However, these changes in mRNA levels with HA+SM treatment did not seem to have an impact on peripheral insulin sensitivity.

It is possible that HA+SM therapy improved insulin sensitivity in the earlier stages of the model as the ITT was performed in week 8. However, it seems likely that the HA+SM was exerting its anti-diabetic effect primarily via an alternative mechanism to actions on insulin sensitivity.

### 4.17.4. PRESERVATION OF ISLET β-CELL FUNCTION BY HA±SM

One mechanism by which HA±SM may ameliorate hyperglycaemia is by improving islet function as indicated by the increase in fasting terminal insulin levels (Figure 4.9.B). Several mechanisms by which HA±SM therapy could preserve islet function are listed below,

- Firstly, it may simply be a secondary effect of reduced glucotoxicity (Maedler et al., 2002) with HA±SM treatment in db/db mice.

- Secondly, HA+SM but not HA treatment resulted in inhibition β-cell iNOS expression (Figure 4.10.D) which is important as nitric oxide, the product of iNOS has been reported to inhibit glucose-stimulated insulin secretion from islets *in vitro* (Mosen et al., 2006) and iNOS inhibitors have been shown to ameliorate hyperglycaemia in rodent models of type 2 diabetes (Shimabukuro et al., 1997).

- Finally, HA±SM may reduce islet inflammation as there was a striking reduction in intra-islet macrophage infiltration (Figure 4.12.F), which is pertinent given that

strategies that target pro-inflammatory cytokines are efficacious in rodents and humans with type 2 diabetes (Ehses et al., 2009).

A separate *in vivo* study is required to conclusively determine whether preservation of islet β-cell function primarily is responsible for anti-hyperglycaemic effect of HA+SM treatment in db/db mice or whether it is simply a secondary response to reduced β-cell glucotoxicity. The *in vivo* study should be terminated after 2 to 3 weeks, the time-point when HA+SM begins to improve glycaemic control, relative to PBS treatment in db/db mice. Examining islet histology along with glucose stimulated insulin secretion (assessed by the serum insulin level during GTT) at this point may shed light whether improved insulin release from β-cells is indeed primarily responsible for the anti-hyperglycaemic effect of HA+SM in db/db mice.

### 4.17.5. THE MODE OF ACTION OF HA IS DIFFERENT TO ANTI-DIABETIC EFFECT OF PUBLISHED HO ACTIVITY INDUCERS

The mode of action of HA and heme *per se* may be different to that reported previously. The efficacious phenotype of hemin in GK and Zucker diabetic fatty (ZDF) rats and cobalt (III) protoporphyrin IX chloride (CoPP) in ob/ob mice was reversed with the HO activity inhibitors CrMP and SM, respectively (Li et al., 2008, Ndisang and Jadhav, 2009, Ndisang et al., 2009a). In contrast to published results, the current *in vivo* study demonstrates that pharmacological inhibition of HO activity enhances the anti-hyperglycaemic effect of HA. Importantly, the anti-hyperglycaemic effect of HA±SM coincided with weight gain and preservation of

islet function rather than an increase in peripheral insulin sensitivity and weight loss as reported with either CoPP or hemin treatment in murine models of type 2 diabetes (Li et al., 2008, Ndisang and Jadhav, 2009, Ndisang et al., 2009a).

The discrepancy between the findings of the current and previous studies may due to following reasons

- The different models of type 2 diabetes employed (db/db mouse v ob/ob mouse (Li et al., 2008) or obese rats (Ndisang and Jadhav, 2009, Ndisang et al., 2009b, Ndisang et al., 2009a)

- The different combinations of HO-1 inducers and inhibitors (HA+SM v CoPP+SM or (Li et al., 2008) or hemin+CrMP (Ndisang and Jadhav, 2009, Ndisang et al., 2009a, Ndisang et al., 2009b).

- The different concentration, treatment regime and administration route of HO activity inducers and inhibitors employed in the various studies (Table 1.3, 1.4).

### 4.17.6. POSSIBLE MECHANISM FOR THE ANTI-DIABETIC EFFICACY OF HA±SM

The most intriguing question is how concurrent HA and SM interact to dramatically improve glycaemic control. It may be that they act via different mechanisms, however an alternative possibility is that the effect of HA+SM may be due to an

additive dose-dependent effect of either the porphyrin structure *per se* or HO-1 protein levels or intracellular heme concentration.

- **Additive effect of porphyrin structure *per se*:** HA and SM contain a porphyrin ring and it may be that this structure *per se* that is efficacious. However, earlier published studies have also employed different porphyrin based pharmacological inducers and inhibitors of HO activity but have not observed an additive to synergistic interaction between HO activity modulators (Ndisang and Jadhav, 2009, Li et al., 2008) suggesting that the porphyrin structure *per se* is unlikely to be the mechanism by which HA and SM interact to ameliorate hyperglycaemia. However, to test the hypothesis that porphyrin ring *per se* has an anti-hyperglycaemic effect; protoporphyrin IX (without a metal ion and therefore unable to modulate HO-1 protein or activity, P8293 from Sigma Aldrich or, P562-9 from Frontier scientific) could be employed at different concentrations to determine whether protoporphyrin IX has a dose-dependent modulatory effect on hyperglycaemia in db/db mice.

- **Additive effect of HO-1 protein:** HO-1 protein has been reported to translocate to the nucleus independently of HO activity and induce expression of anti-oxidants and protect against oxidative stress (Hori et al., 2002, Lin et al., 2007). HA+SM treatment resulted in a synergistic increase in HO-1 protein in the liver of db/db mice (Figure 4.3.C). Hence, future work may focus on testing the hypothesis that HO-1 protein expression is vital for anti-hyperglycaemic effect of HA+SM treatment. To test this hypothesis, either global knock-out or tissue

specific homozygous HO-1 knock-out db/db mice will be required. Tissue-specific knock-out would be the most incisive method as it would provide information on the importance of HO-1 in individual organs. It would also help overcome the challenges posed by the poor survival rate of homozygous HO-1 knock-out in mice (Poss and Tonegawa, 1997), which is likely to be further reduced in diabetic (db/db) mice.

- **Additive effect of heme *per se*:** HA+SM treatment was shown to significantly increase the intracellular heme concentration in the liver of db/db mice (Figure 4.3.B). This was due to administration of a heme-based compound and simultaneous inhibition of the major heme degradation pathway with SM treatment. Heme is a ligand for the nuclear receptor Rev-erbα and heme promotes recruitment and stabilisation of the nuclear receptor corepressor–histone deacetylase 3 (NCoR-HDAC3) complex to the promoter regions of key gluconeogenic enzymes resulting in inhibition of gene expression in hepatocytes *in vitro* (Yin et al., 2007). Furthermore, heme has been reported to promote adipocyte differentiation by acting as a ligand for Rev-erbα in the 3T3-L1 cell line (Kumar et al., 2010). The majority of the modulatory effects facilitated by heme and Rev-erbα interaction are limited to *in vitro* studies. However, recently the focus has shifted to determine the physiological effect of either synthetic agonists of Rev-erbα or, organ and tissue specific Rev-erbα knockout in murine models of type 2 diabetes (Cho et al., 2012a, Solt et al., 2012a). Hence, HA+SM treatment in db/db mice with organ and tissue specific Rev-erb knock-out may

help to establish whether the increase in intracellular heme concentration is responsible for anti-hyperglycaemic effect of HA+SM in db/db mice.

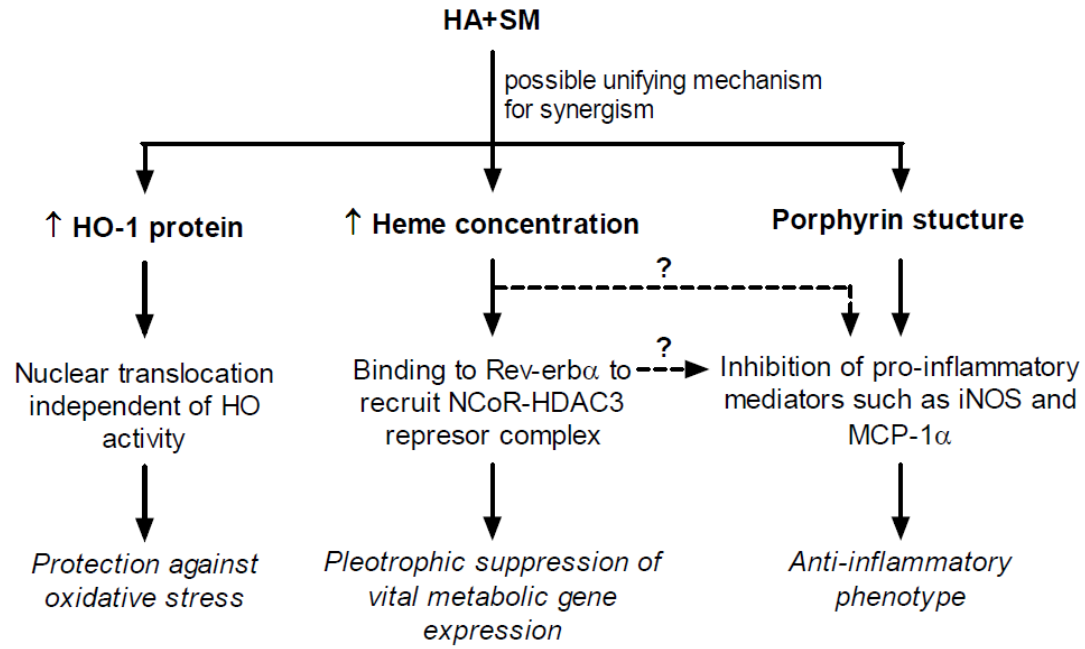


**Figure 4.16 Possible mode of actions for the synergism between HA and SM.** HA+SM which are porphyrin based compounds resulted in a synergistic increase in HO-1 protein and intracellular heme concentration. Published studies based on *in vitro* studies report that HO-1 protein translocation to the nucleus protects from oxidative stress (Lin et al., 2007), increased intracellular heme can repress metabolic genes via Rev-erbα (Yin et al., 2010) and porphyrin based pharmacological inhibitors of HO activity such as zinc protoporphyrin have the ability to inhibit iNOS activity and expression (Grundemar and Ny, 1997). The synergism between HA and SM may be due to one or all of these properties. Black arrows represent observations made in either the present study or reported earlier in the literature and the dotted arrows represent possible interactions that have not been established yet but are of interest for future research.

### 4.17.7. CONCLUDING REMARK

In conclusion, HA treatment in db/db mouse model of type 2 diabetes was found to reduce fasting hyperglycaemia during the end of 8-week study. Paradoxical to the hypothesis of current *in vivo* study, concurrent treatment of HA and the HO inhibitor,

SM, resulted in a profound improvement in glycaemic control indicating that a HA mediated increase in HO activity is not the primary mechanism for the anti-hyperglycaemic effect of HA±SM. The relatively delayed and an early improvement in glycaemic control with HA+SM treatment occurred despite an increase in obesity. The anti-hyperglycaemic effect of HA±SM was possibly due to an increase in adipocyte storage capacity, preservation of islet β-cell function and reduced islet inflammation. It would be of great interest in future to determine the primary metabolic event responsible for ameliorative potential of HA±SM in the db/db mouse model of type 2 diabetes. Further *in vivo* studies are also needed to investigate whether the anti-hyperglycaemic effect of HA+SM is due to additive increase in HO-1 protein or heme *per se*.

Concurrent to the present *in vivo* study, the anti-inflammatory effects of HA±SM were characterized in cell culture models of inflammation including cytokine administration to a MIN6 β-cell line (chapter 5) and lipopolysaccharide activation of primary macrophages (chapter 6).

# 5. CHAPTER 5: CHARACTERISATION OF THE EFFECT OF HEME OXYGENASE ACTIVITY MODULATORS IN CYTOKINE MIX-STIMULATED MIN6 β-CELL LINE

## 5.1. INTRODUCTION

*In vivo* studies have demonstrated that increased expression of pro-inflammatory cytokines and chemokines in the islets of rodents or humans with type 2 diabetes can promote macrophage infiltration and impair islet β-cell function (Ehses et al., 2007, Donath et al., 2009). In keeping with this, the *in vivo* study to determine the anti-diabetic efficacy of heme arginate (HA) in the db/db model of type 2 diabetes (chapter 4) demonstrated increased islet macrophage infiltration and islet iNOS protein expression in the db/db mice when compared with non-diabetic C57BL/KsJ (lean) mice. There was a marked reduction in islet inflammation with HA and HA+SM (SM - Stannous (IV) mesoporphyrin IX dichloride, an inhibitor of heme oxygenase activity) treatment in the db/db mice. However, the preservation of islet β-cells with HA+SM treatment in the db/db mice may be due to either a direct anti-inflammatory effect of HA and SM on islets or reduced glucotoxicity. Therefore, it was important to determine whether HA and SM alone or in combination had a direct anti-inflammatory effect on the insulin producing β-cells.

Chronic exposure of pancreatic islet β-cells to pro-inflammatory cytokines (Corbett and McDaniel, 1995) and elevated levels of lipids (Shimabukuro et al., 1997) promotes islet β-cell destruction (insulitis) mediated in part via increased iNOS expression and production of nitric oxide (Thomas et al., 2002). *Ex vivo* culture of rodent islets with the pro-inflammatory cytokine interleukin-1β (IL-1β) in combination with tumor necrosis factor-α (TNF-α) or interferon-γ (IFN-γ) is routinely used to mimic the effects of insulitis that occur in rodent models of type 1

diabetes (Corbett and McDaniel, 1995). The *ex vivo* culture of mouse and rat islets in the presence of IL-1β inhibits islet insulin release (Southern et al., 1990) and coincides with increased iNOS gene and protein expression and production of nitrite (Corbett and McDaniel, 1995). Inhibitors of iNOS including NG-monomethyl-L-arginine (NMMA), aminoguanidine, nitro-L-arginine methylester (L-NAME) and ONO-1714 have been reported to reverse the detrimental effects of IL-1β (Southern et al*.,* 1990, Corbett et al*.,* 1992, Welsh and Sandler, 1992, Corbett and McDaniel, 1995, Kato et al*.,* 2003).

In the current *in vitro* study, MIN6 β-cells were employed to test the hypothesis that **HA exerts anti-inflammatory effects in β-cells via induction of heme oxygenase (HO) activity.**

## 5.2. *IN VITRO* β-CELL INFLAMMATION MODEL

The MIN6 β-cell is a cell line derived from *in vivo* immortalized mouse insulin-secreting pancreatic β-cells. MIN6 β-cells were stimulated with a combination of recombinant cytokine proteins including IL-1β, TNF-α and IFN-γ to mimic the pro-inflammatory stress on β-cells *in vivo*. The final concentration of HA, SM and recombinant pro-inflammatory cytokine proteins applied to the MIN6 β-cells are listed in table 5.1. MIN6 β-cells were pre-treated for 2 hours with PBS or SM prior to addition of HA for another 4 hours. Post 4 hours incubation with HA±SM, a cytokine mix (CM) comprising of IL-1β, IFN-γ and TNF-α at concentrations listed in table 5.1 was added to MIN6 β-cells and incubated for a further 20 hours (Fig 5.1).

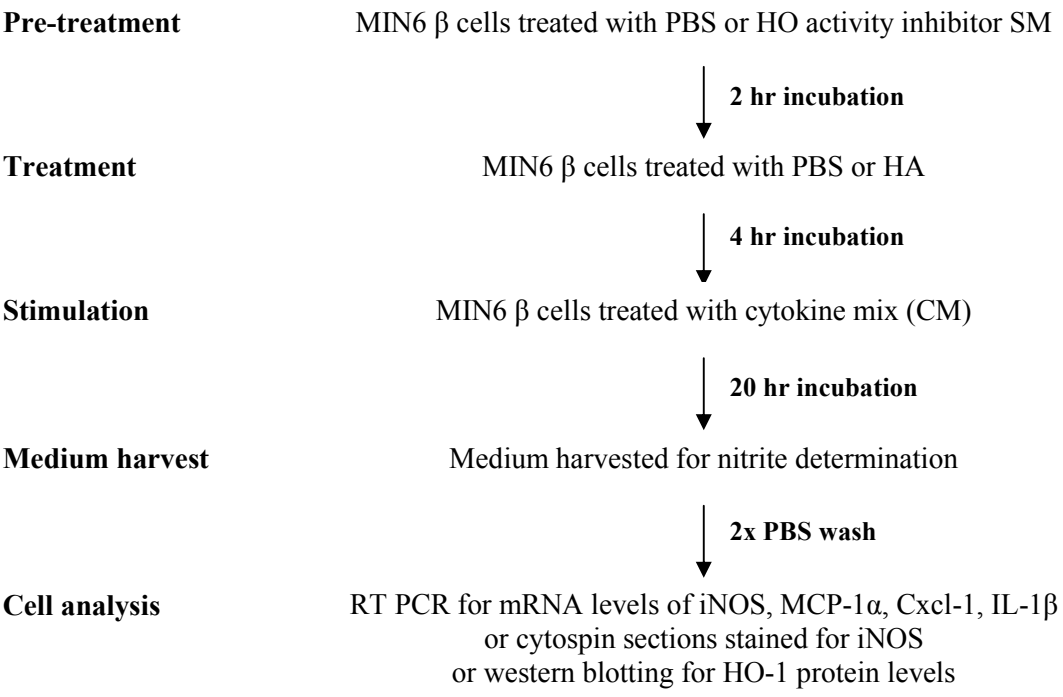


**Figure 5.1** ***In vitro*** **experimental protocol in the MIN6 β-cell line.** The aim of the study was to determine whether HA and SM had anti-inflammatory properties in an *in vitro* model of pro-inflammatory stress on β-cells that are observed *in vivo*.

| Stimulants | LA | HA | SM | IL-1β | IFN-γ | TNF-α |
|---|---|---|---|---|---|---|
| | | | | | | |
| **Concentration** | 100μM | 20μM | 20μM | 5ng/ml | 100ng/ml | 10ng/ml |

**Table 5.1 Final concentrations of the heme oxygenase inducer and inhibitor and the pro-inflammatory stimulants applied to MIN6 β-cells.** LA: L-arginine, HA: Heme arginate, SM: Stannous mesoporphyrin, IL-1β: Interleukin-1β, IFN-γ: Interferon-γ, TNF-α: Tumor necrosis factor-α.

## 5.3. CO-TREATMENT WITH SM ABROGATED THE HA MEDIATED INCREASE IN HO ACTIVITY BUT NOT HO-1 PROTEIN EXPRESSION

Treatment with 20μM of HA induced HO-1 protein expression in MIN6 β-cells (Figure 5.2.A). Co-treatment with HA and SM, a HO activity inhibitor, synergistically increased HO-1 protein levels when employed at the two different (10μM and 20μM) concentrations (Figure 5.2.A). A 20μM concentration of HA and SM was selected to determine their effect on HO activity as single and concomitant treatments. Treatment of MIN6 β-cells with 20μM of HA resulted in a significant increase ($P<0.05$) in HO activity, which was abrogated on co-treatment with 20μM of SM (Figure 5.2.B). Based on the HO activity result, HA and SM at 20μM concentration was selected for further experiments in MIN6 β-cells.

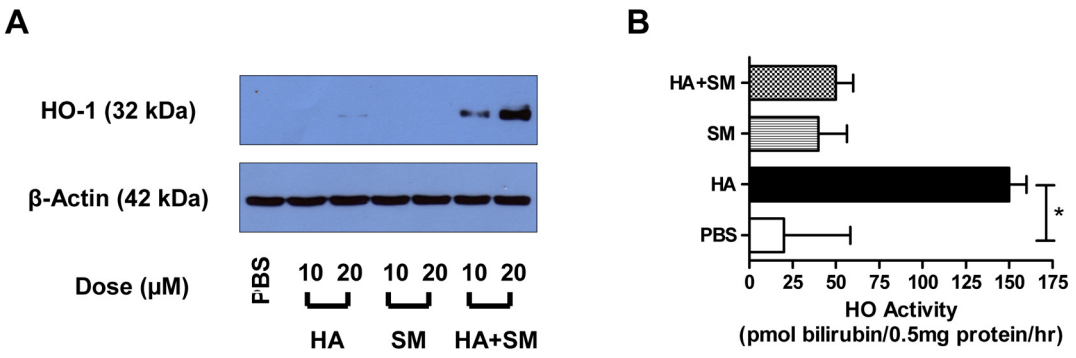


**Figure 5.2 HO-1 protein levels and HO activity in MIN6 β-cells. A.** 20μM of HA-induced HO-1 protein levels whereas co-treatment of HA and SM (HA+SM) synergistically increased HO-1 protein level when compared to single agent treatment. This was evident for the two concentrations (10μM and 20μM) of SM employed in the study. Representative western-blot from n=2, separate experiments. B. The significant increase in HO activity with 20μM of HA treatment was abrogated in MIN6 β-cells when co-treated with 24 hour treatment of SM. *$P<0.05$, P-value derived by Dunn's multiple comparison post-test when $P<0.05$ by Kruskal-Wallis test. The data given are mean ± s.e.m. from n=3 independent cell culture experiments where each 'n' was performed in duplicates.

## 5.4. THE MIN6 β-CELL LINE IS NOT A GOOD MODEL OF GLUCOSE-INDUCED INSULIN SECRETION

L-arginine (LA) and hemin, both constituents of HA, are reported to induce insulin secretion in ex vivo culture of islets from mice (Henningsson and Lundquist, 1998). Therefore, the effect of HA and LA on insulin release by MIN6 β-cells was determined.

MIN6 β-cells plated in DMEM medium containing either 5mM or 30mM D-glucose, were treated with either PBS (vehicle) or 100μM of LA or 20μM of HA (HA), and incubated for 24 hours at 37$^{o}$C. Post incubation, MIN6 β-cells were washed twice with warm PBS. MIN6 β-cells were again incubated with DMEM medium containing either 5mM or 30mM D-glucose for 30 minutes at 37$^{o}$C, before collecting medium from different treatment wells to determine the insulin concentration.

The incubation of MIN6 β-cells at different concentration of glucose did not result in any significant difference in insulin release (Figure 5.3.B). Additionally, LA or HA treatment for 24 hours in presence of 5mM (Figure 5.3.C) or 30mM (Figure 5.3.D) D-glucose failed to markedly increase insulin release when MIN6 β-cells were re-incubated with different concentration of glucose for 30 minutes.

The DMEM medium employed in the experiment contained fetal calf serum (FCS), a potential source of exogenous insulin, which may have masked the insulin secretion induced by glucose in the MIN6 β-cell line., Hence the insulin concentration in FCS

was also measured and found to be much lower than that obtained from the MIN6 cell supernatants (Figure 5.3.A). This demonstrated that the insulin concentrations determined for test samples were not due to the presence of exogenous insulin contained in the FCS present in the DMEM medium. Fasting serum sample of HA-treated db/db mice was employed as a positive control in the test.

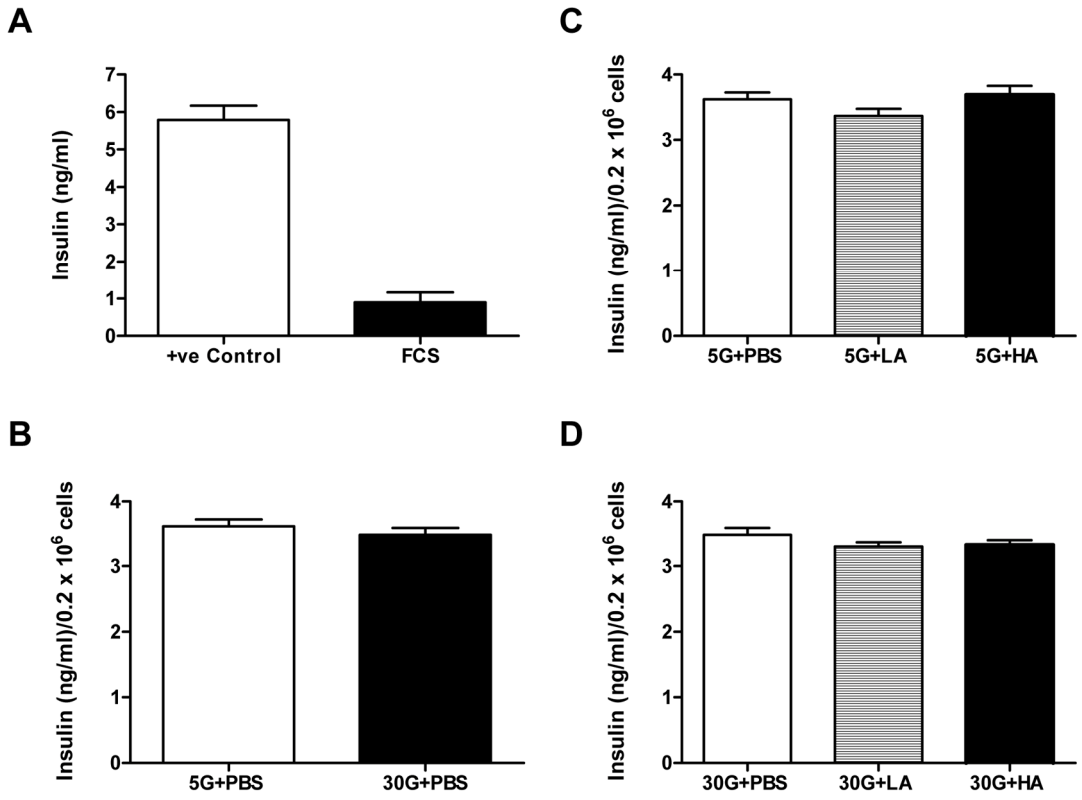


**Figure 5.3 Insulin released by MIN6 β-cells in response to a low or high concentration of glucose. A.** No detectable insulin content was measured in FCS. Week 8 fasting serum sample from HA-treated mice was used as positive (+ve) control. **B.** No significant difference in insulin release was observed in PBS-treated MIN6 β-cells incubated with 5mM (5G) and 30mM (30G) of D-glucose. P>0.05 by two-tailed Mann Whitney test. **C.** No significant difference in insulin release by MIN6 β-cells incubated in 5G, in presence of PBS (vehicle), 100μM L-arginine (LA) or 20μM heme arginate (HA). P>0.05 by Kruskal-Wallis test. **D.** No significant difference in insulin release by MIN6 β-cells incubated in 30G, in presence of PBS (vehicle), LA or HA. P>0.05 by Kruskal-Wallis test. The data given are mean ± s.e.m. from n=3 independent cell culture experiments where each 'n' was performed in duplicates.

## 5.5. CYTOKINES INDUCED AN INCREASE IN NITRITE PRODUCTION IN MIN6 β-CELLS

A pilot experiment was performed to determine the optimal combination of IL-1β, TNF-α and IFN-γ required to stimulate nitrite production in MIN6 β-cells. The combination of IL-1β and TNF-α, in the absence or presence of IFN-γ was found to significantly increase nitrite release (Figure 5.4) when compared to PBS-treated MIN6 cells after 48 hours of treatment. A combination of IL-1β, IFN-γ and TNF-α (cytokine mix) was selected to stimulate a pro-inflammatory response in MIN6 β-cells in further experiments.

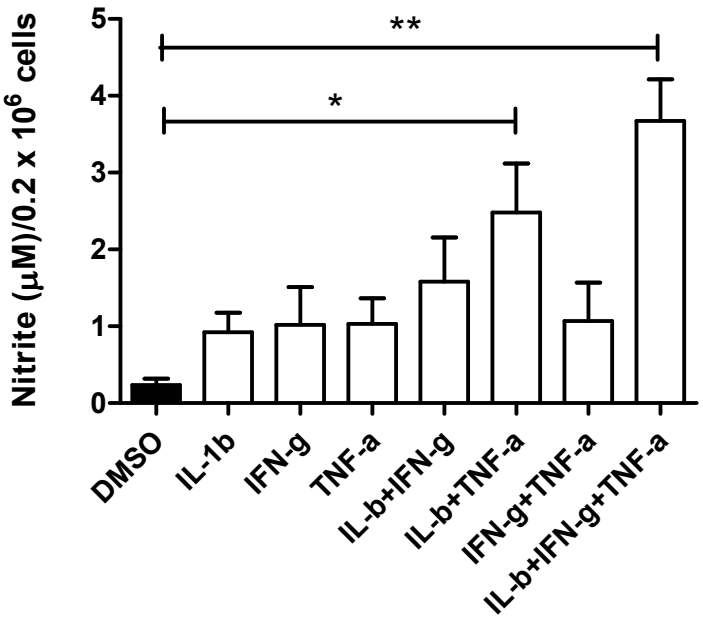


**Figure 5.4 Nitrite produced by MIN6 β-cells following treatment with IL-1β, TNF-α and IFN-γ either alone or in different combination for 48 hours.** The combination of IL-1β and TNF-α, in the absence or presence of IFN-γ resulted in a significant release of nitrite after 48 hours. *P<0.05, **P<0.01, P-values derived from Dunn's multiple comparison post-test when P<0.05 by Kruskal-Wallis test. The data given are mean ± s.e.m. from n=3 independent cell culture experiments where each 'n' was performed in duplicates.

## 5.6. CO-TREATMENT OF MIN6 β-CELLS WITH HA REDUCED CYTOKINE MIX-INDUCED INCREASE IN iNOS EXPRESSION

Treatment of MIN6 β-cells for 24 hours with the cytokine mix led to a substantial increase in iNOS protein expression when compared to PBS-treated MIN6 β-cells (Figure 5.5). However, co-treatment of MIN6 β-cells with HA and the cytokine mix reduced the levels of iNOS protein expression (Figure 5.5) in comparison to cytokine mix treated MIN6 β-cells.

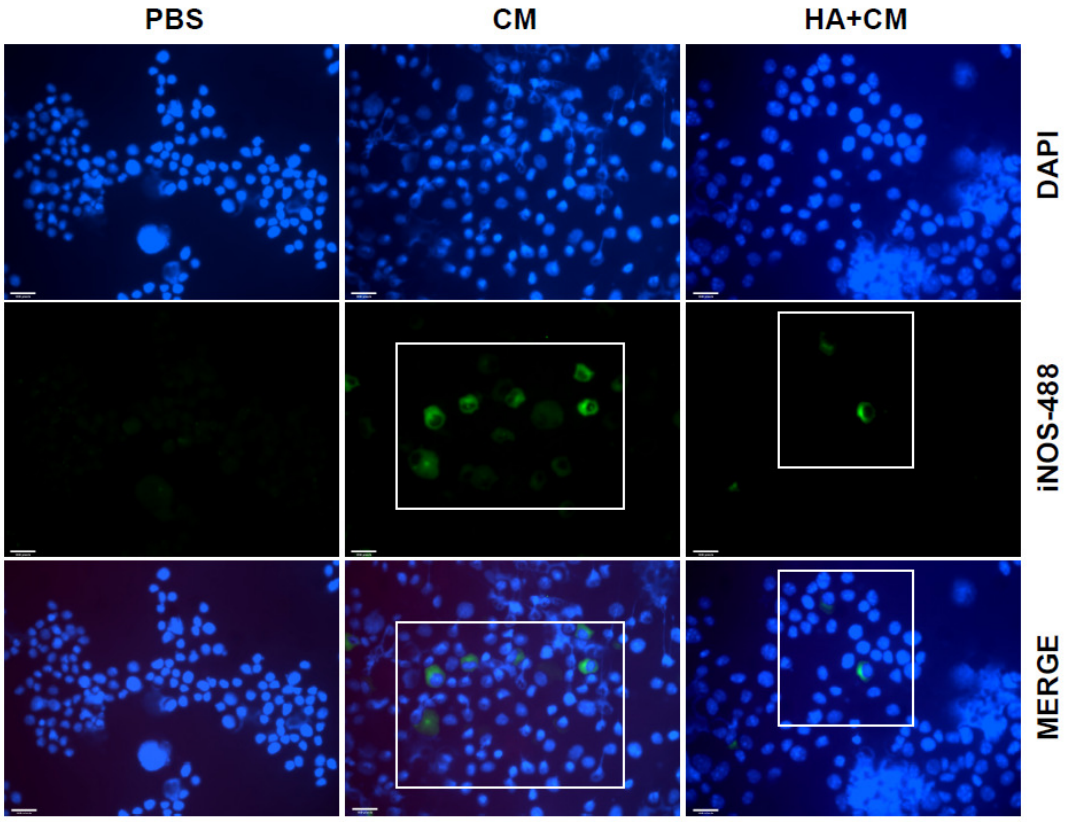


**Figure 5.5 Immuno-fluorescence staining for iNOS in MIN6 β-cells stimulated with a cytokine mix for 24 hours.** Incubation of MIN6 β-cells with a cytokine mix for 24 hours resulted in increased iNOS protein expression. Concurrent treatment with HA reduced the cytokine mix induced iNOS protein expression. The figure is representative of n=2 separate experiments. Scale bar represents 100 pixels.

## 5.7. HA±SM REDUCED THE PRO-INFLAMMATORY RESPONSE TO CYTOKINE MIX IN MIN6 β-CELLS

Treatment of MIN6 β-cells (non-stimulated) for 24 hours with either single or co-treatment of HA and SM did not result in a significant modulation of mRNA levels of iNOS, IL-1β, and monocyte chemo-attractants MCP-1α and Cxcl-1 (also known as chemokine KC) (Figure 5.7.A, C, E, G). Cytokine mix (CM) stimulation of MIN6 β-cells resulted in a significant increase in the relative mRNA levels of iNOS, IL-1β and MCP-1α (Figure 5.6, $P<0.05$).

Co-treatment of CM-stimulated MIN6 β-cells with HA but not SM resulted in a significant reduction in mRNA levels of iNOS, IL-1β, MCP-1α and Cxcl-1 (Figure 5.7.B, D, F, H, $P<0.05$).

Pre-treatment of MIN6 β-cells with SM prior to co-treatment with HA and CM partially inhibited the HA-mediated reduction in mRNA levels of iNOS (Figure 5.6.B). However, SM pre-treatment of MIN6 β-cells failed to reverse HA-mediated reduction in mRNA levels of IL-1β, MCP-1α and Cxcl-1 (Figure 5.7.D, F, H).

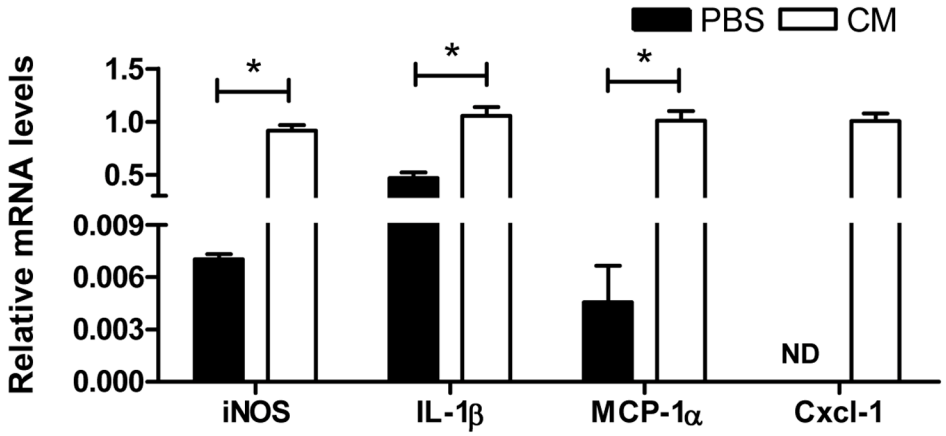


**Figure 5.6 mRNA levels of pro-inflammatory mediators stimulated by cytokine mix in MIN6 β-cells.** Cytokine mix stimulation of MIN6 β-cells for 24 hours significantly increased relative mRNA levels of iNOS, IL-1β and MCP-1α. The mRNA level of Cxcl-1 with PBS treatment could not be determined; hence statistical significance could not be calculated when compared to the mRNA level induced by cytokine mix. *P<0.05, P-values derived by two-tailed Mann Whitney test for each specified gene. 18S gene was used as endogenous control gene. The data given are mean ± s.e.m. from n=3 independent cell culture experiments where each 'n' was performed in duplicates. ND: Not determined.

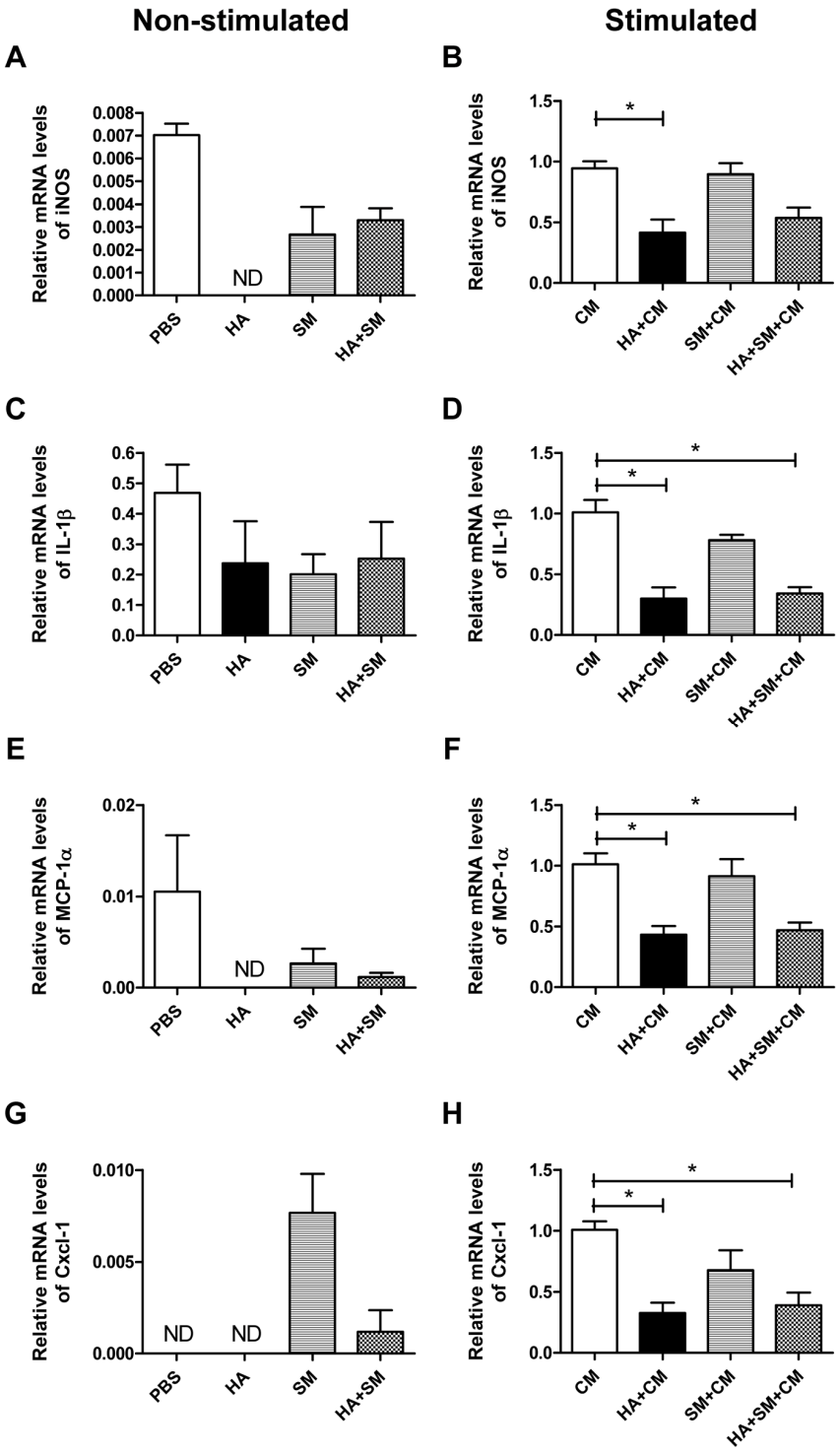


**Figure 5.7 Effect of HA and SM on mRNA levels of pro-inflammatory mediators stimulated by a cytokine mix in MIN6 β-cells.** Relative mRNA levels of **A.** iNOS, **C.** IL-1β, **E.** MCP-1α, **G.** Cxcl-1 observed in non-stimulated MIN6 β-cells. P>0.05 by Kruskal-Wallis test. Relative mRNA levels of **B.** iNOS, **D.** IL-1β, **F.** MCP-1α, **H.** Cxcl-1 in cytokine mix stimulated MIN6 β-cells. *P<0.05, P-values derived by Dunn's multiple comparison post-test when P<0.05 by Kruskal-Wallis test. 18S gene was used as endogenous control gene. The data given are mean ± s.e.m. from n=3 independent cell culture experiments where each 'n' was performed in duplicates. ND: Not determined.

## 5.8. CHAPTER DISCUSSION

### 5.8.1. THE ANTI-INFLAMMATORY EFFECTS OF HA ARE INDEPENDENT OF HO ACTIVITY AND HO-1 PROTEIN EXPRESSION

Heme arginate (HA) was observed to reduce iNOS expression and markedly reduce islet infiltration in the pancreatic islet of db/db mouse model of type 2 diabetes, and this was independent of induction of HO activity (chapter 4). However, it could not be determined whether this was simply due to a decrease in gluco/lipotoxicity as HA reduced hyperglycaemia or a direct effect of HA±SM on β-cells. Therefore, the anti-inflammatory effect of HA was investigated in cytokine mix (CM; 5ng/ml IL-1β + 10ng/ml TNF-α + 100ng/ml IFN-γ) stimulated MIN6 β-cells. CM stimulation of MIN6 β-cells for 24 hours resulted in a substantial induction in iNOS protein expression and a significant increase in expression (mRNA levels) of pro-inflammatory mediators, such as iNOS, IL-1β, and chemo-attractants, including MCP-1α and Cxcl-1 genes (Figure 5.5, 5.6).

I had initially hypothesised that HA may exert an anti-inflammatory effect in MIN6 cells via it's ability to induce HO activity. HA treatment did indeed reduce CM-stimulated iNOS protein expression and significantly reduce mRNA levels of iNOS in MIN6 β-cells. Pre-treatment with SM partially reversed the HA-mediated reduction in mRNA levels of iNOS, demonstrating that the effect of HA may be partly dependent on its ability to induce HO activity. However, pre-treatment of

MIN6 β-cells with SM, prior to co-treatment with HA and CM failed to reverse the significant reduction in relative mRNA levels of IL-1β, MCP-1α and Cxcl-1 genes despite abrogating the HA-mediated increase in HO activity. Hence, while HA treatment did indeed have anti-inflammatory effects in CM-stimulated MIN6 β-cells, contrary to the initial hypothesis, this was largely independent of its ability to induce HO activity (Figure 5.2.B).

The anti-inflammatory effect of HA in MIN6 β-cells is also unlikely to be due to the increase in HO-1 protein levels as HA+SM resulted in a synergistic increase in HO-1 protein in comparison to HA treatment alone, however, this did not result in a significantly greater decrease in mRNA levels of iNOS, IL-1β, MCP-1α and Cxcl-1.

The current study in MIN6 β-cells demonstrates that HA treatment may protect islet β-cells from the deleterious effects of islet inflammation, which recently has been postulated to be responsible for the loss of β-cell mass and function in type 2 diabetes (Donath et al., 2009, Ehses et al., 2007b). Furthermore, published *ex vivo* studies have reported that reductions in β-cell iNOS expression *per se* may restore islet insulin release (Kato et al., 2003).

### 5.8.2. POSSIBLE EXPLANATION FOR THE MECHANISM OF THE ANTI-INFLAMMATORY EFFECTS OF HA±SM IN MIN6 CELLS

A possible explanation for HO activity independent anti-inflammatory effects of HA and HA+SM treatment may be the ability of heme to interact with the nuclear

hormone receptor Rev-erb (Yin et al., 2010). In a recent study, Vieira et al has demonstrated that siRNA knock-down of Rev-erbα in MIN6 β-cells decreased the expression of genes which facilitate lipogenesis, insulin exocytosis and β-cell proliferation (Vieira et al., 2012). Additionally, Rev-erbα has been demonstrated to facilitate repression of pro-inflammatory genes, such as iNOS and MCP-1α in murine macrophages (Huang et al., 2011, Pascual et al., 2005). However, the effect of the interaction between heme and Rev-erbα on pro-inflammatory genes in pancreatic β-cells has not been explored. On the basis of the results from the current study and emerging evidence on the role of Rev-erbα in pancreatic β-cells, it will be of interest in future to test the hypothesis that the increase in intracellular heme concentration with HA±SM treatment exerts anti-inflammatory effects via Rev-erb in islet β-cells.

### 5.8.3. THE MIN6 β-CELL LINE IS A POOR MODEL TO STUDY THE DETRIMENTAL EFFECT OF INFLAMMATION ON INSULIN SECRETION

Although a significant reduction in the CM stimulated pro-inflammatory response in MIN6 β-cells was observed with HA±SM pre-treatment, it could not be determined whether these anti-inflammatory changes could potentially improve β-cell function as the insulin secretion in response to low and high concentration of D-glucose was found to be indistinguishable. This is a major limitation of using the MIN6 β-cell line as a model of β-cells.

Collagenase digestion of the pancreas to isolate pancreatic islets is the physiological option for β-cell studies. This could not be carried out during the PhD due to time constraints. Hence pre-treatment of isolated islets with HA±SM prior to stimulation with pro-inflammatory cytokines would be a useful experiment to determine whether HA±SM could preserve glucose-stimulated insulin secretion in β-cells. However the heterogeneity of cell-types in the pancreatic islets would make it difficult to determine whether the anti-inflammatory effect of HA±SM are due to a direct effect on β-cells within the islet or to the effect on other cell types including macrophages.

### 5.8.4. CONCLUDING REMARK

In conclusion, HA was demonstrated to have a direct anti-inflammatory effects in cytokine mix stimulated MIN6 β-cells with a reduction in gene expression of pro-inflammatory mediators, including iNOS and IL-1β. The anti-inflammatory effect of HA on insulin secretion could not be demonstrated due to the lack of glucose-responsive insulin production by MIN6 β-cells. Also, HA significantly reduced the mRNA levels of the immune cell chemo-attractants MCP-1α and Cxcl-1 (also known as Chemokine KC, a homologue of human IL-8), two chemokines that may promote islet macrophage infiltration in rodent models of type 2 diabetes (Ehses et al., 2007b). This may in part explain the reduction in macrophage infiltration in the islets of HA±SM treated db/db mice (chapter 4). The anti-inflammatory effects of HA in the MIN6 β-cells were demonstrated to be broadly independent of HO activity, and the mechanism by which HA exerts its anti-inflammatory effects remains elusive. In addition it is possible that HA may have a role not only in reducing macrophage

infiltration, but also in changing the macrophage activation status both in islets and adipose tissue. Hence, the effect of HA on macrophage phenotype will be investigated in chapter 6.

# 6. CHAPTER 6: CHARACTERISATION OF THE EFFECT OF HEME OXYGENASE ACTIVITY MODULATORS IN LIPOPOLYSACCHARIDE ACTIVATED PRIMARY MACROPHAGES

## 6.1. INTRODUCTION

Induction of heme oxygenase (HO)-1 has been shown to have anti-inflammatory effects on macrophages (Lee and Chau, 2002, Weis et al., 2009) and classical activation of macrophages is important in the pathogenesis of type 2 diabetes (Lumeng et al., 2007). Therefore, the current study was performed to test the hypothesis that **the anti-inflammatory effects of HA are due to induction of HO activity in primary macrophages.**

In the present study, cobalt (III) protoporphyrin IX chloride (CoPP), which like HA, is a protoporphyrin based inducer of HO activity, was included to determine whether any anti-inflammatory effects of HA are specific to HA or shared by other metallo-porphyrins, either due to their ability to induce HO activity or due to the protoporphyrin ring structure *per se*.

The anti-inflammatory effects of HA in the db/db mice and pancreatic β-cell line, MIN6, were not reversed by treatment with stannous (IV) mesoporphyrin IX dichloride (SM), despite SM efficiently inhibiting the HA mediated increase in HO activity. To exclude off-target effects of SM, chromium (III) mesoporphyrin IX chloride (CrMP) was included in the present study, as it is reported to be a more selective inhibitor of HO activity. CrMP has been reported not to inhibit nitric oxide synthase activity (Appleton et al., 1999) and it does not induce HO-1 protein (Ndisang and Jadhav, 2009).

## 6.2. *IN VITRO* MODEL OF CLASSICALLY ACTIVATED MACROPHAGES

Classically activated macrophages are used routinely to screen for anti-inflammatory effects of various cytokine proteins, compounds and cell types including IL-10 (Lee and Chau, 2002), immune complexes (Gerber and Mosser, 2001) and apoptotic cells (Fadok et al., 1998), respectively.

LPS is a cell-wall component of gram-negative bacteria which activates macrophages by binding to the cell-surface receptors present on macrophages, including TLR-4 (Poltorak et al., 1998) and CD14 (Meng and Lowell, 1997). LPS activation of macrophages evokes a pro-inflammatory response that include release of nitrite, TNF-α, IL-12 p40 and IL-6 (Gerber and Mosser, 2001, Meng and Lowell, 1997). Hence, the *in vitro* model of LPS-activated macrophage was used to characterize the anti-inflammatory phenotype of metallo-porphyrins.

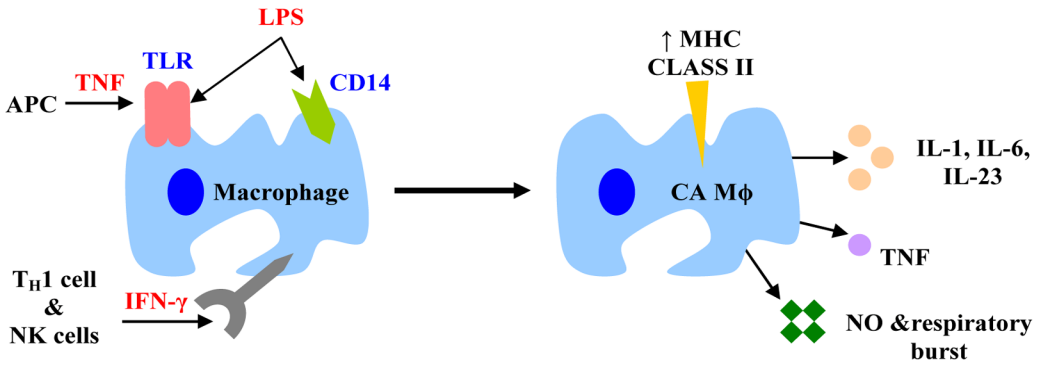


**Figure 6.1 Diagrammatic representation of IFN-γ, LPS or TNF-α mediated classical activation (CA) of macrophages (Mϕ).** The cell surface receptors such as TLRs, CD14 and IFN-receptor 1 present on macrophages facilitate classical activation of macrophages by stimulants including TNF-α, LPS and IFN-γ to evoke a pro-inflammatory response which is characterised by release of IL-1, IL-6, TNF-α and nitric oxide. Text in red font and blue font represent stimulants and cell-surface macrophage receptors respectively.

In the current study, bone marrow derived macrophages (BMDM) from C57BL/KsJ mice were pre-treated with either PBS, HO activity inhibitors or trichostatin (TSA; an inhibitor of histone deacetylases (HDACs)) for 2-4 hours prior to treatment with HO activity inducers for a further 20 hours. BMDM were then washed with PBS before being stimulated with LPS for 24 hours (Figure 6.2).

The supernatants harvested were used to determine the concentration of nitrite and cytokines released, while cells were then washed with PBS before lysing in TRIZOL reagent in order to determine the levels of expression of pro-inflammatory genes by real time polymerase chain reaction (RT PCR). The compounds, their action and the final concentrations used are listed in table 6.1 below.

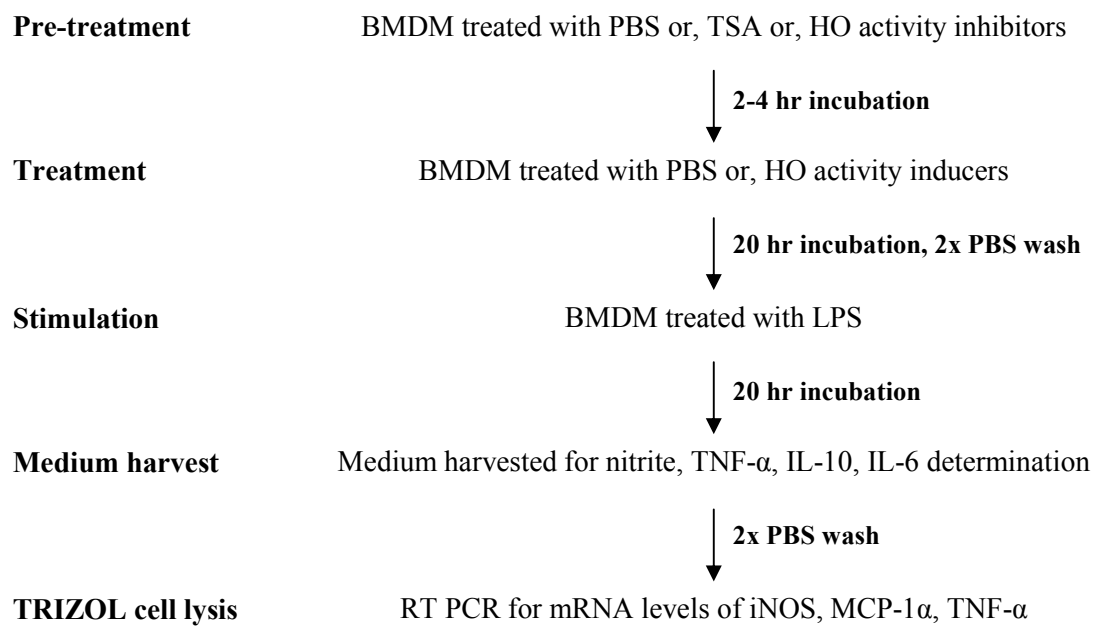


**Figure 6.2** ***In vitro*** **experiment protocol in bone marrow derived macrophages (BMDMs).** The primary objective was to determine the effect of HO activity inducers and inhibitors and their combination on the pro-inflammatory response of LPS-stimulated BMDMs.

| S.N. | Compounds | Abr. | Function | Final concentration |
|---|---|---|---|---|
| | | | | |
| **01** | Heme arginate | HA | HO activity inducer | 10 μM |
| **02** | L-arginine | LA | Component of HA | 50 μM |
| **03** | Cobalt (III) protoporphyrin IX chloride | CoPP | HO activity inducer | 10 μM |
| **04** | Stannous (IV) mesoporphyrin IX dichloride | SM | HO activity inhibitor | 10 μM |
| **05** | Chromium (III) mesoporphyrin IX chloride | CrMP | HO activity inhibitor | 5 μM |
| **06** | Trichostatin | TSA | Inhibitor of HDACs | 10 nM |
| **07** | Lipopolysaccharide | LPS | BMDM activator | 100 ng/ml |

**Table 6.1 List of compounds, their function/purpose and final concentration used to treat BMDM.**

## 6.3. LPS STIMULATION RESULTED IN A PRO-INFLAMMATORY RESPONSE IN ACTIVATED BMDM

A time-course experiment was performed to determine the duration of LPS stimulation that evoked a substantial pro-inflammatory response. The BMDMs were stimulated with either PBS or LPS for 1, 6 and 24 hours. The supernatant was used to determine the concentration of nitrite, TNF-α and IL-6 released at the stated time points.

LPS stimulation of BMDM led to a time-dependent increase in nitrite, TNF-α and IL-6. LPS stimulation of BMDM significantly increased the release of nitrite, TNF-α and IL-6 ($P<0.05$, Figure 6.3.A-C) after 24 hours of LPS stimulation.

A significant increase in mRNA levels of iNOS and TNF-α ($P<0.05$, Figure 6.3.D) was observed after 24 hour of LPS stimulation. Hence, 24 hours of LPS stimulation of BMDMs was selected for future experiments to generate a robust pro-inflammatory response.

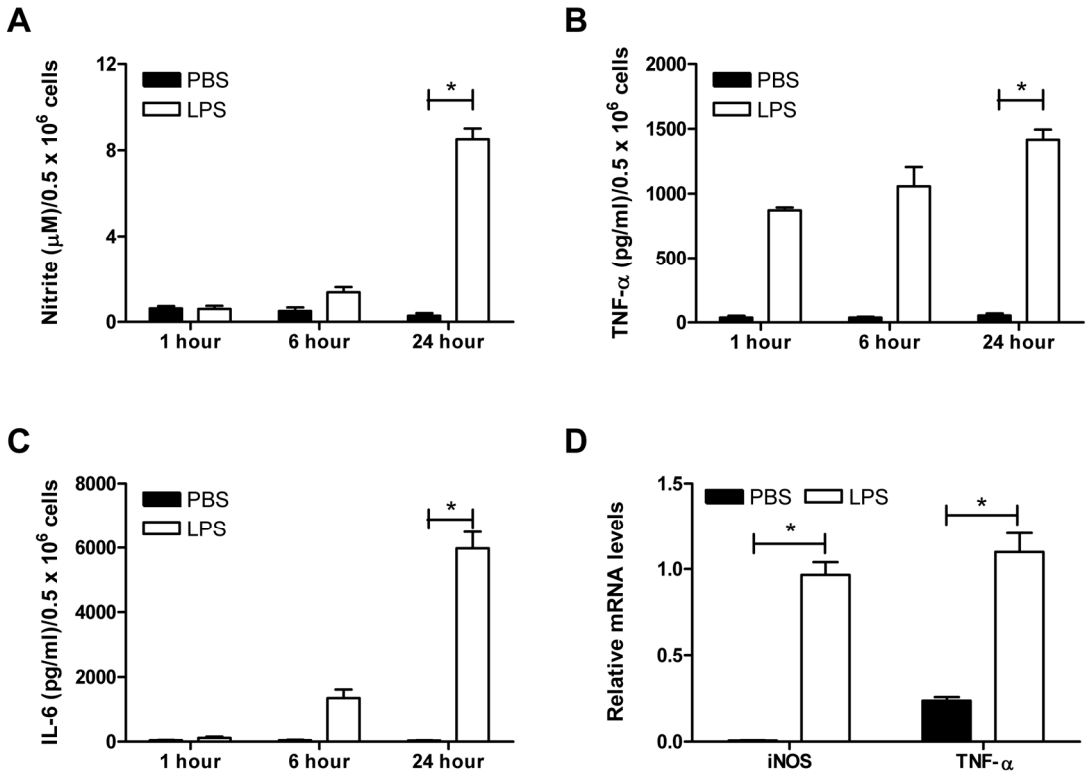


**Figure 6.3 Time-course of the LPS-stimulated pro-inflammatory response in BMDM.** LPS stimulation of BMDM for 24 hours resulted in a significant increase in release of **A.** nitrite, **B.** TNF-α, **C.** IL-6 protein and in mRNA levels of **D.** iNOS and TNF-α. **A-C:** *P<0.05, P-values derived by two-tailed Mann Whitney test between PBS and LPS-treated BMDM for each specified time-points. **D.** *P<0.05, P-values derived by two-tailed Mann Whitney test between PBS and LPS-treated BMDM for each specified gene. The data given are mean ± s.e.m. from n=3 independent cell culture experiments where each 'n' was performed in triplicates.

## 6.4. EFFECT OF HA AND METALLO-PORPHYRIN COMPOUNDS ON HO ACTIVITY AND HO-1 PROTEIN LEVELS

The BMDM were pre-treated with either PBS or SM or CrMP for 4 hours prior to treatment with the HO activity inducers HA or CoPP for 20 hours. HO activity and HO-1 protein levels were determined by the paired enzyme assay and by western blotting respectively.

A dose-dependent increase in HO-1 protein level was noted in BMDMs-treated with 2, 10, 20, 50 and 100μM of HA for 24 hours (Figure 6.4.A). 10μM of HA was further tested for its effect on HO activity. HA treatment of BMDMs resulted in a significant increase ($P<0.05$, Figure 6.4.B) in HO activity which was partially reduced by pre-treatment with either SM or CrMP (Figure 6.4.B). CoPP treatment increased HO activity by approximately 3 fold when compared with PBS-treated BMDM however; this increase was not statistically significant (Figure 6.4.C). SM pre-treatment reduced CoPP induced HO activity from 3 fold to <2 fold however, large variations in the CoPP+CrMP group made it difficult to confidently state that CrMP also reduced the CoPP-mediated increase in HO activity (Figure 6.4.C).

HA and CoPP treatment resulted in a substantial induction of HO-1 protein (Figure 6.4.D). SM and CrMP, the two HO activity inhibitors used in the current study, induced HO-1 protein levels. CrMP was more potent at increasing HO-1 protein levels when compared to SM. Co-treatment of SM with either CoPP or HA increased HO-1 protein levels compared with either CoPP or HA alone (Figure 6.4.D).

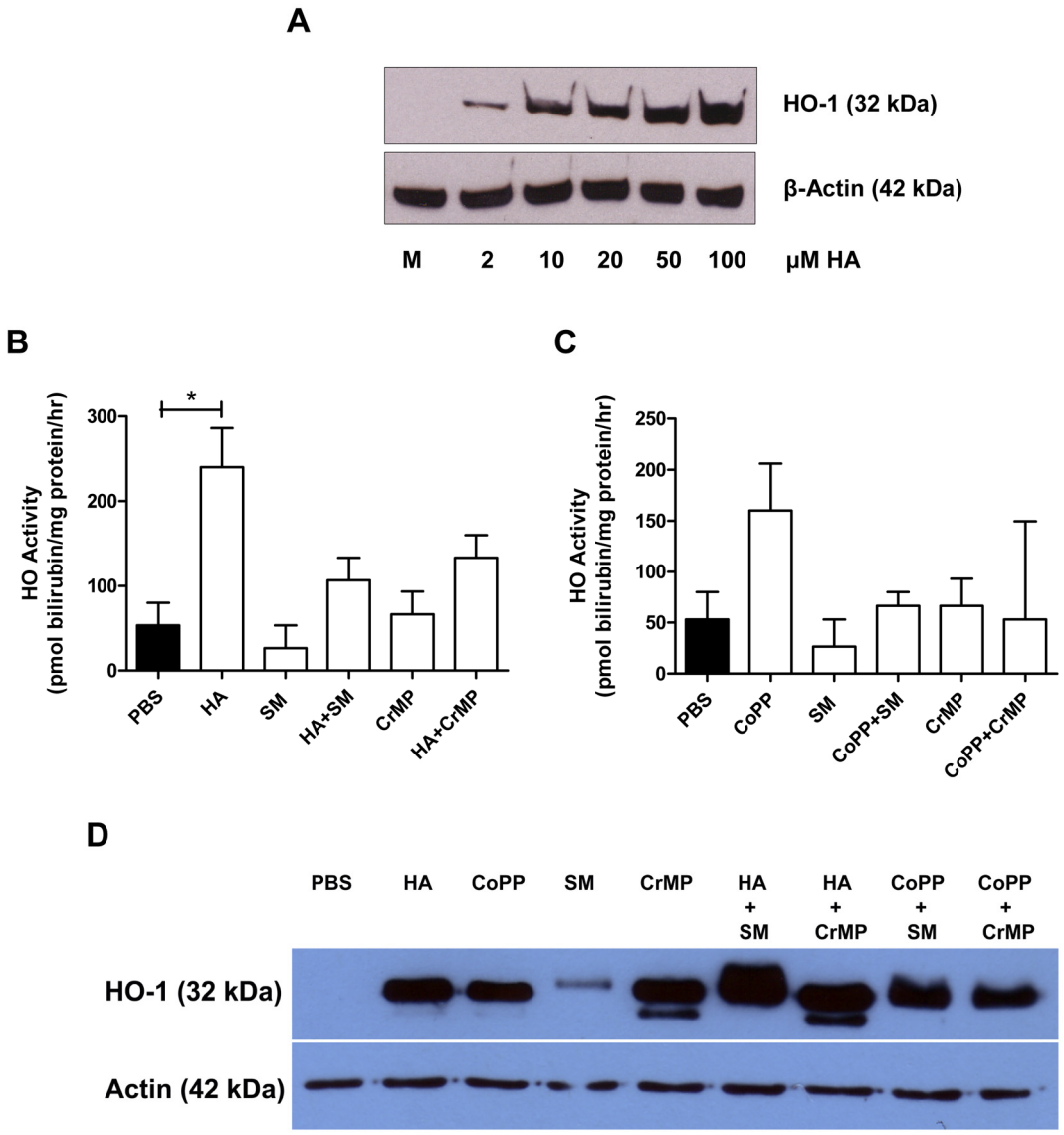


**Figure 6.4 Determination of HO activity and HO-1 protein level with HA and metallo-porphyrin compounds in BMDM. A.** HA treatment for 24 hours resulted in a dose-dependent increase in HO-1 protein level in BMDMs. The western blot is a representative figure of n=2 separate experiments. **B.** 10μM of HA treatment for 20 hours significantly increased the HO activity in BMDMs which was partially inhibited by pre-treatment with the HO activity inhibitors, 10μM SM and 5μM CrMP. *P<0.05, P-value derived by Dunn's multiple comparison post-test when P<0.05 by Kruskal-Wallis test. **C.** 10μM of CoPP for 20 hours failed to significantly increase HO activity relative to PBS-treated BMDMs. 10μM of SM reduced the CoPP-mediated 3 fold increase in HO activity however, the large variation within the CrMP (5μM) group precluded a definitive analysis. P>0.05 (non-significant) by Kruskal-Wallis test. **B, C:** The data given are mean ± s.e.m. from n=3 independent cell culture experiments where each 'n' was performed in duplicates. **D.** HA, CoPP, SM and CrMP treatment for 24 hours resulted in an increase in HO-1 protein level. The increase in HO-1 protein with SM was comparatively lower than that with CrMP. The addition of SM to either CoPP or HA resulted in an additive increase in HO-1 protein level. The western blot is a representative figure of n=2 separate experiments.

## 6.5. HA AND METALLO-PORPHYRIN COMPOUNDS WERE NOT CYTOTOXIC

The effect of HA and other metallo-porphyrins on the viability of BMDMs was assessed by the Alamar blue cell viability assay. HA and CoPP in the presence or, absence of PBS, SM or CrMP did not result in any significant change in cell viability (Figure 6.5) at the concentrations listed in table 6.1. Hence these compounds are not cytotoxic at the concentrations and combinations employed in the next series of experiments.

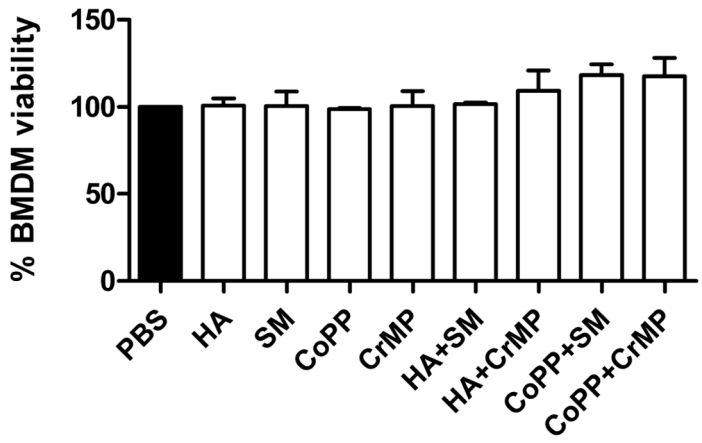


**Figure 6.5 Cell viability of BMDMs following treatment with various metallo-porphyrin compounds.** BMDMs were treated with HA or CoPP in the presence or absence of PBS, SM or CrMP for 24 hours prior to Alamar blue treatment for 4 hours. No significant change in % cell viability was noted for different treatments when compared to PBS (vehicle)-treated BMDMs. $P>0.05$ (non-significant) by Kruskal-Wallis test. The data given are mean ± s.e.m. from n=4 independent cell culture experiments where each 'n' was performed in triplicates.

## 6.6. THE ANTI-INFLAMMATORY EFFECT OF HA IS INDEPENDENT OF THE L-ARGININE COMPONENT PRESENT IN HA

The nitric oxide synthase (NOS) enzyme catalyses the reaction between L-arginine (LA) and oxygen to produce nitric oxide and citrulline (Alderton et al., 2001). As nitrite release was a vital read-out for determining the effect of HA on the pro-inflammatory response of LPS activated macrophages and since HA contains both heme and LA; an iNOS substrate, the *in vitro* experiment required an LA control group to reliably assess the contribution of LA to the effect of HA. LA was used at a concentration (50μM) identical to that present in 10μM HA.

BMDMs were pre-treated with PBS, HA or LA for 24 hours prior to stimulation with LPS. LA but not HA pre-treatment, markedly increased the release of TNF-α in non-stimulated BMDMs ($P<0.05$, Figure 6.6.E).

In LPS-stimulated BMDMs, HA pre-treatment significantly reduced mRNA levels of iNOS ($P<0.05$, Figure 6.6.G), relative to LA pre-treatment. HA pre-treatment markedly reduced mRNA levels of MCP-1α ($P<0.05$, Figure 6.6.I) but not TNF-α (Figure 6.6.H), relative to PBS pre-treatment, in LPS-stimulated BMDMs. HA pre-treatment resulted in a significant reduction in nitrite release ($P<0.05$, Figure 6.6.J) but had no significant impact on the release of the pro-inflammatory cytokine TNF-α (Figure 6.6.K) or the immuno-suppressive cytokine IL-10 (Figure 6.6.L), in LPS-stimulated BMDMs. LA pre-treatment significantly reduced TNF-α secretion when compared to HA pre-treatment, in LPS-stimulated BMDMs ($P<0.05$, Figure 6.6.K).

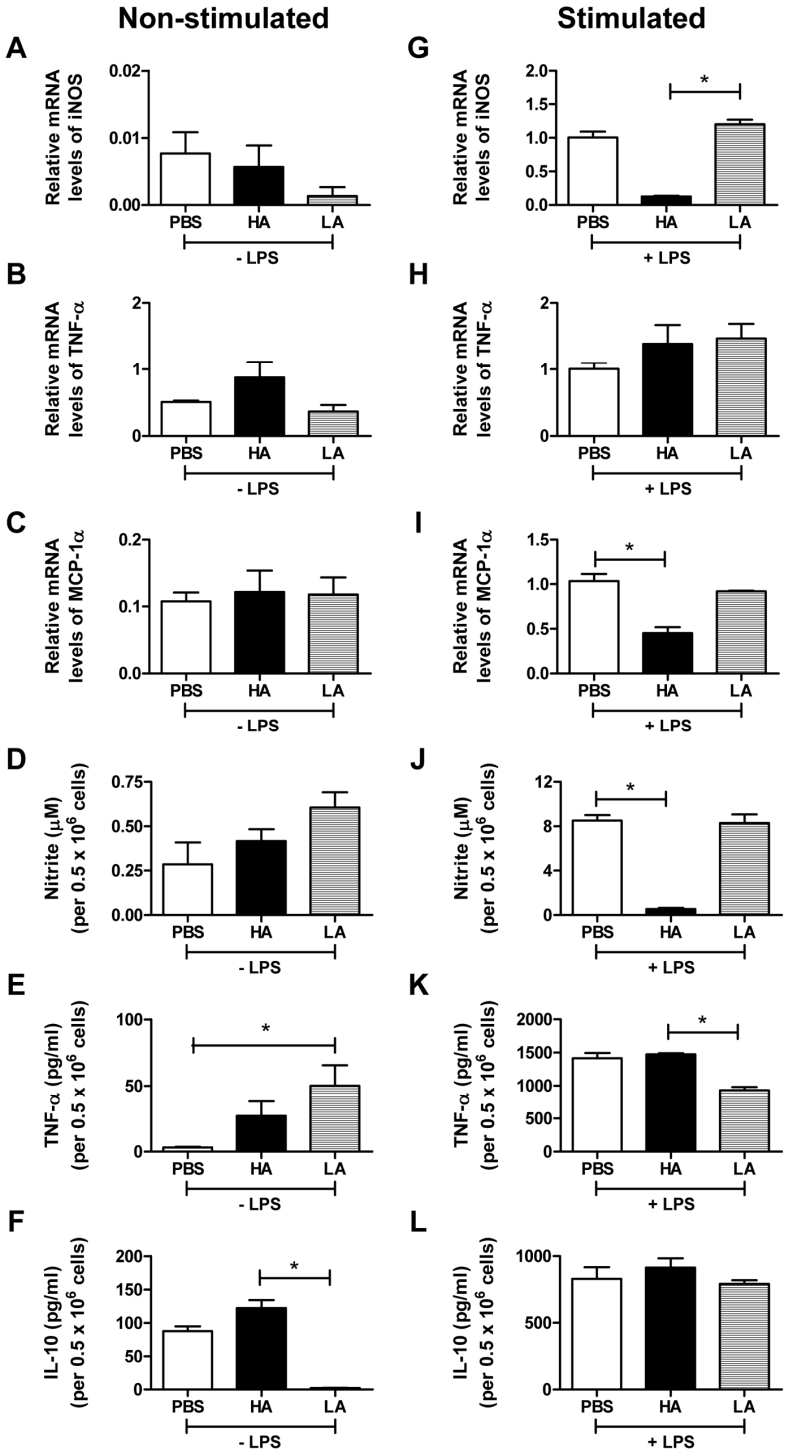


**Figure 6.6 Effect of heme arginate (HA) and L-arginine (LA) pre-treatment on the LPS-stimulated pro-inflammatory response in BMDMs.** The effect of HA and LA pre-treatment on mRNA levels of **A.** iNOS, **B.** TNF-α, **C.** MCP-1α and release of **D.** Nitrite, **E.** TNF-α, **F.** IL-10, in non-stimulated BMDMs. Effect of HA and LA pre-treatment on mRNA levels of **G.** iNOS, **H.** TNF-α, **I.** MCP-1α and release of **J.** Nitrite, **K.** TNF-α, **L.** IL-10, in LPS-stimulated BMDMs. *P<0.05, P-value derived by Dunn's multiple comparison post-test when P<0.05 by Kruskal-Wallis test. The data given are mean ± s.e.m. from n=4 independent cell culture experiments where each 'n' was performed in duplicates. 18S gene was used as endogenous control gene.

## 6.7. THE ANTI-INFLAMMATORY EFFECT OF HA AND CoPP WERE INDEPENDENT OF HO ACTIVITY

Two pharmacological inhibitors of HO activity, SM and CrMP were used to determine whether the anti-inflammatory effects of HA were dependent on HO activity. Another protoporphyrin based inducer of HO activity; CoPP was used to determine whether the anti-inflammatory effects of HA was mimicked by another protoporphyrin based inducer of HO activity.

None of the compounds had any effect on inflammatory cytokines in quiescent BMDMs (Figure 6.7.A, D, G and 6.8.A, D) except for a significant increase in release of IL-10 with CrMP pre-treatment ($P<0.001$, Figure 6.8.G). HA pre-treatment significantly reduced nitrite release ($P<0.01$, Figure 6.8.B) and mRNA levels of iNOS ($P<0.001$, Figure 6.7.B) and MCP-1α ($P<0.05$, Figure 6.7.H) in LPS-stimulated BMDMs. However, it had no effect on either the mRNA levels or secretion of TNF-α (Figure 6.7.E, 6.8.E). CoPP like HA pre-treatment reduced nitrite release ($P<0.001$, Fig 6.8.C) and mRNA levels of iNOS ($P<0.001$, Fig 6.7.C) and MCP-1α ($P<0.001$; Fig 6.7.I) in LPS-stimulated BMDMs.

Pre-treatment with SM and CrMP, the two inhibitors of HO activity, did not result in significant modulation of the LPS-stimulated pro-inflammatory response. Pre-treatment of BMDM with HO activity inhibitors i.e. SM or, CrMP, failed to reverse the significant reduction in nitrite release (Figure 6.8.B, C) and mRNA levels of iNOS (Figure 6.7.B, C) and MCP-1α (Figure 6.7.H, I), noted with HA and CoPP

treatment in LPS-stimulated BMDMS. Additionally, CoPP+SM pre-treatment significantly reduced the release of TNF-α in LPS-stimulated BMDMs (P<0.05, Figure 6.8.F).

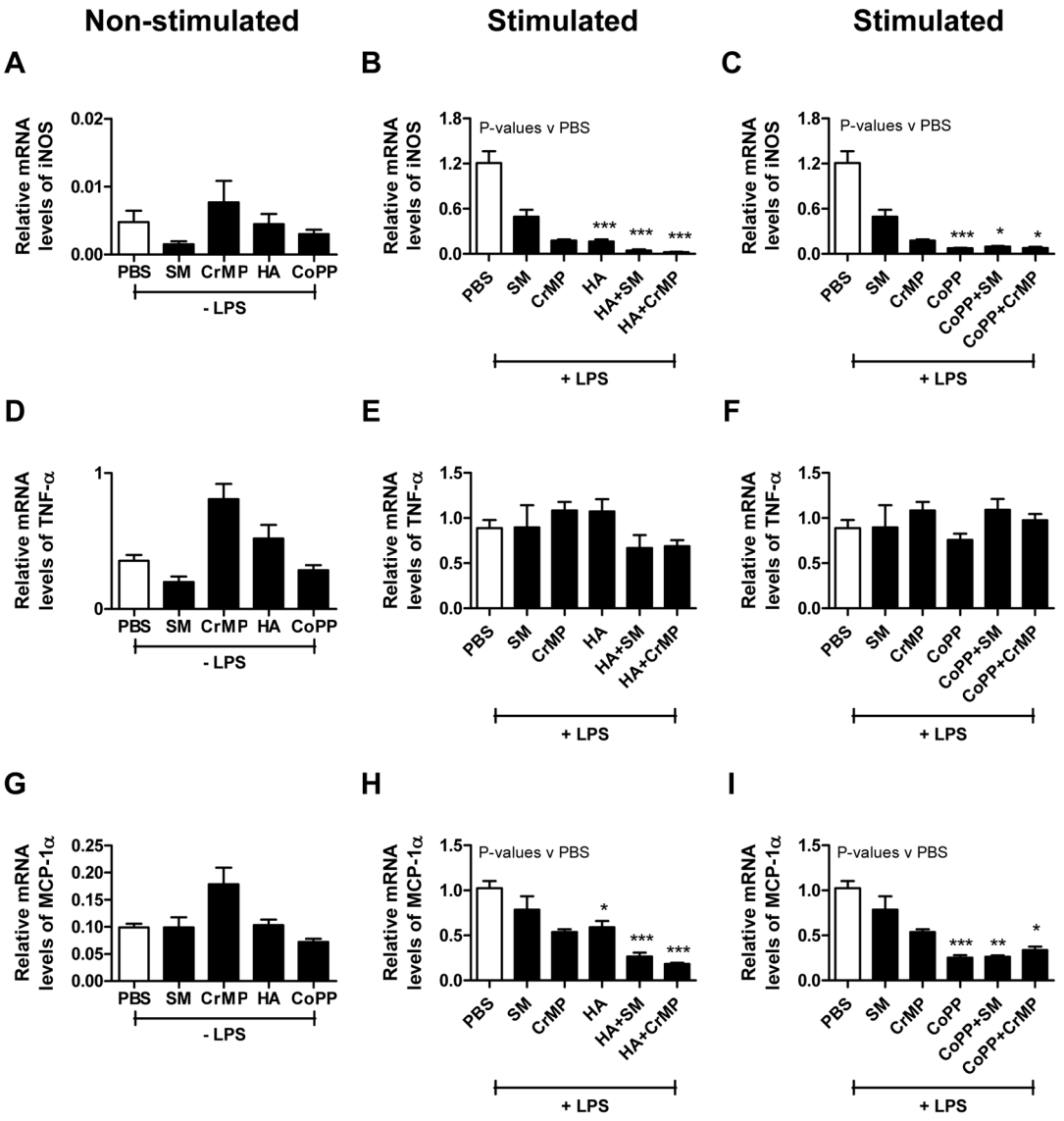


**Figure 6.7 Effect of HA and other metallo-porphyrin compounds on expression of pro-inflammatory genes in LPS-activated BMDMs.** Effect of the modulators of HO activity on mRNA levels of **A.** iNOS, **D.** TNF-α, **G.** MCP-1α in non-stimulated BMDMs. The modulatory effects of HA **(B, E, H)** and CoPP **(C, F, I)** pre-treatment in the presence or absence of HO activity inhibitors, SM and CrMP, on mRNA levels of **B, C.** iNOS, **E, F.** TNF-α, **H, I.** MCP-1α in LPS-stimulated BMDMs. *P<0.05, ***P<0.001. P-values derived with Dunn's multiple comparison post-test when P<0.05 by Kruskal-Wallis test. **A-I.** The data given are mean ± s.e.m. from n=4-8 independent cell culture experiments where each 'n' was performed in duplicates. 18S gene was used as endogenous control gene.

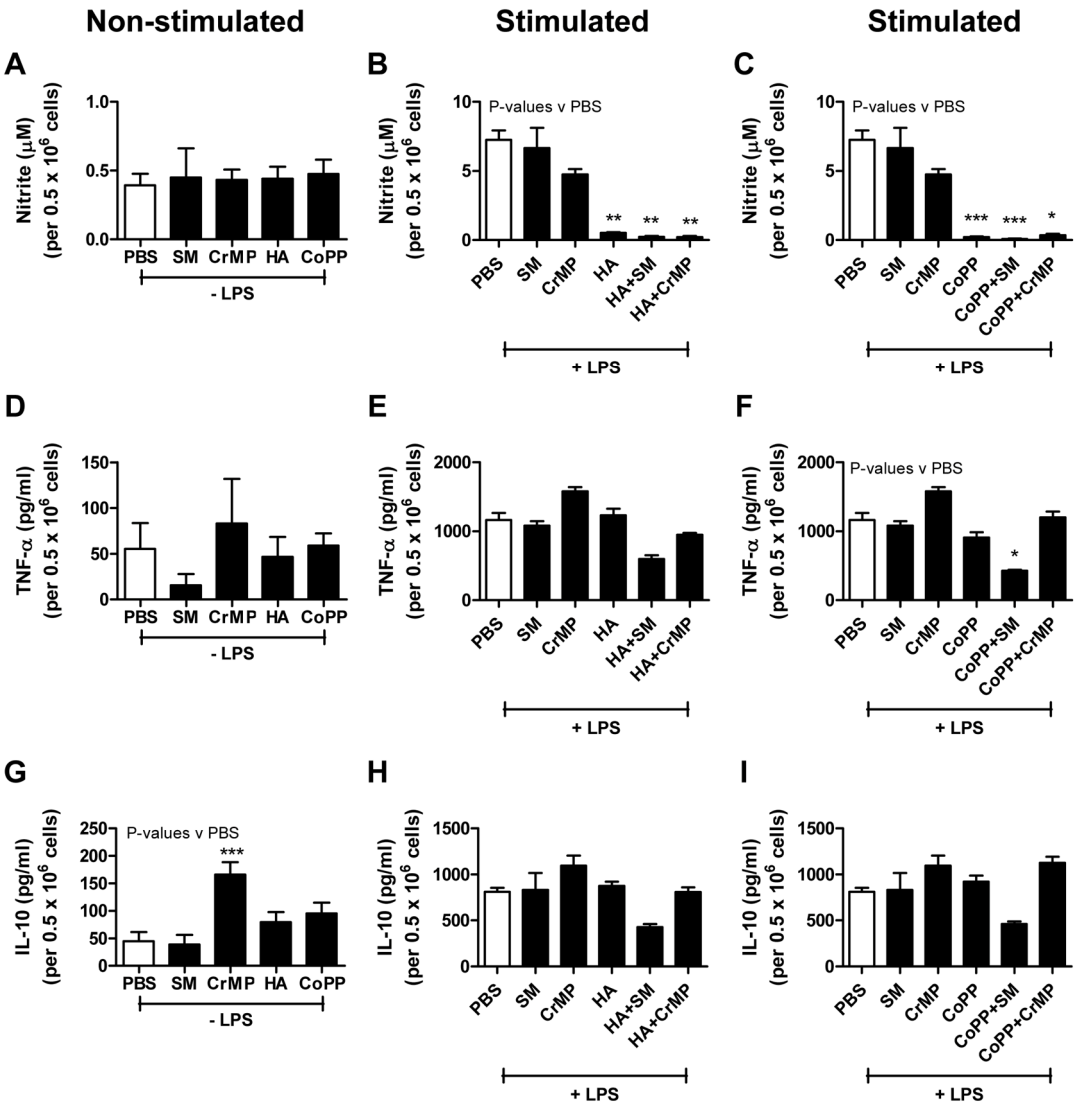


**Figure 6.8 Effect of HA and other metallo-porphyrin compounds on the release of inflammatory mediators by LPS-activated BMDMs.** Effect of the modulators of HO activity on release of **A.** Nitrite, **D.** TNF-α, **G.** IL-10 in non-stimulated BMDMs. The modulatory effects of HA **(B, E, H)** and CoPP **(C, F, I)** pre-treatment in the presence or absence of HO activity inhibitors, SM and CrMP, on release of **B, C.** Nitrite, **E, F.** TNF-α, **H, I.** IL-10 in LPS-stimulated BMDMs. *P<0.05, **P<0.01, ***P<0.001. P-values derived with Dunn's multiple comparison post-test when P<0.05 by Kruskal-Wallis test. **A-I.** The data given are mean ± s.e.m. from n=4-8 independent cell culture experiments where each 'n' was performed in duplicates.

## 6.8. REDUCTION IN NITRITE RELEASE BY HA IN LPS ACTIVATED BMDM IS INDEPENDENT OF HO-1 PROTEIN

BMDMs isolated from C57BL/6J mice with a targeted deletion of the Hmox-1 (Hmox KO) gene (Poss and Tonegawa, 1997) [a kind gift from A. Agarwal, Birmingham, Alabama to University of Edinburgh] were pre-treated with either PBS or HA for 24 hours prior to LPS stimulation for another 24 hours. Treatment with HA for 24 hours substantially increased HO-1 protein in BMDMs isolated from C57BL/6J (Hmox WT, HO WT) mice but failed to do so in HO KO BMDM (Figure 6.9.I).

BMDMs from HO WT and HO KO treated with PBS for 24 hours showed relatively comparable levels of release of nitrite (Figure 6.9.A) and TNF-α (Figure 6.9.E). LPS-stimulation for 24 hours resulted in significantly higher levels of nitrite ($P<0.05$, Figure 6.9.B) and TNF-α ($P<0.05$, Figure 6.9.F), in the supernatant of BMDMs from HO KO mice compared with WT mice.

HA pre-treatment efficiently abrogated the LPS-mediated increase in the release of nitrite by BMDMs from both HO WT (Figure 6.9.C) and HO KO (Figure 6.9.D) mice. Additionally, HA pre-treatment failed to significantly modulate the release of TNF-α in BMDMs from either HO WT orHO KO mice (Figure 6.9.G, H).

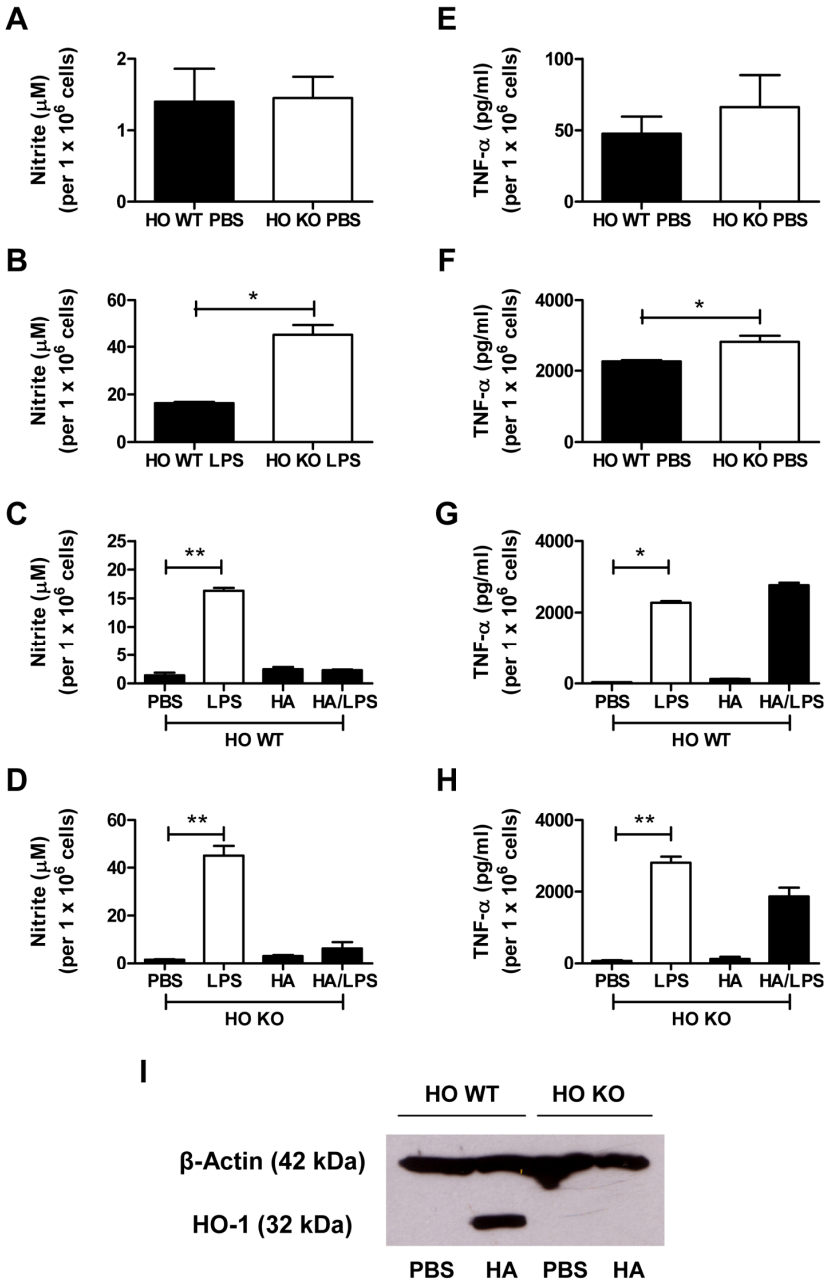


**Figure 6.9 Effect of HA in LPS-activated BMDM from Hmox1 knock-out (KO) and wild-type (WT) C57BL/6J mice.** Release of **A.** Nitrite, **E.** TNF-α by non-stimulated BMDMs isolated from Hmox wild type (HO WT) and knockout (HO KO) mice. P>0.05 (non-significant) by two-tailed Mann Whitney test. Release of **B.** Nitrite, **F.** TNF-α in LPS-stimulated BMDMs isolated from HO WT and HO KO mice. P<0.05 by two-tailed Mann Whitney test. Effect of HA pre-treatment on release of **C.** Nitrite, **G.** TNF-α in LPS-stimulated BMDMs isolated from HO WT mice. Effect of HA pre-treatment on release of **D.** Nitrite, **H.** TNF-α in LPS-stimulated BMDMs isolated from HO KO mice. **C, D, G, H.** *P<0.05, **P<0.01. P-values derived with Dunn's multiple comparison post-test when P<0.05 by Kruskal-Wallis test. **I.** The effect of HA on induction of HO-1 protein in BMDMs isolated from HO WT and HO KO mice. The western blot is a representative figure of n=2 separate experiments. **A-H.** The data given are mean ± s.e.m. from n=3 independent cell culture experiments.

## 6.9. INHIBITION OF HISTONE DEACETYLASES REVERSED THE ANTI-INFLAMMATORY EFFECTS OF HA AND CoPP

To determine whether the anti-inflammatory effects of HA involved histone deacetylase (HDAC), BMDMs were pre-treated for 2 hours with trichostatin (TSA), a pharmacological inhibitor of histone deacetylases. TSA pre-treated BMDMs were treated with either PBS, HA or CoPP for 20 hours. BMDMs were then washed with PBS prior to stimulation with LPS in the presence of TSA for 24 hours. CoPP was included to determine whether any effect observed was specific to heme or shared by other compounds with a protoporphyrin ring structure.

Pre-treatment with TSA did not led to a significant modulation of mRNA levels of iNOS, TNF-α and MCP-1α in non-stimulated (Figure 6.10.A, E, I) and LPS-stimulated BMDMs (Figure 6.10.B, F, J).

Pre-treatment with HA and CoPP significantly reduced mRNA levels of iNOS and MCP-1α ($P<0.05$, Figure 6.10.C, K) but not TNF-α (Figure 6.10.G) in LPS-stimulated BMDMs. However, pre-treatment of BMDMs with TSA completely abrogated the HA and CoPP mediated reduction in mRNA levels of iNOS (Figure 6.10.D) and MCP-1α (Figure 6.10.L) in LPS activated BMDMs.

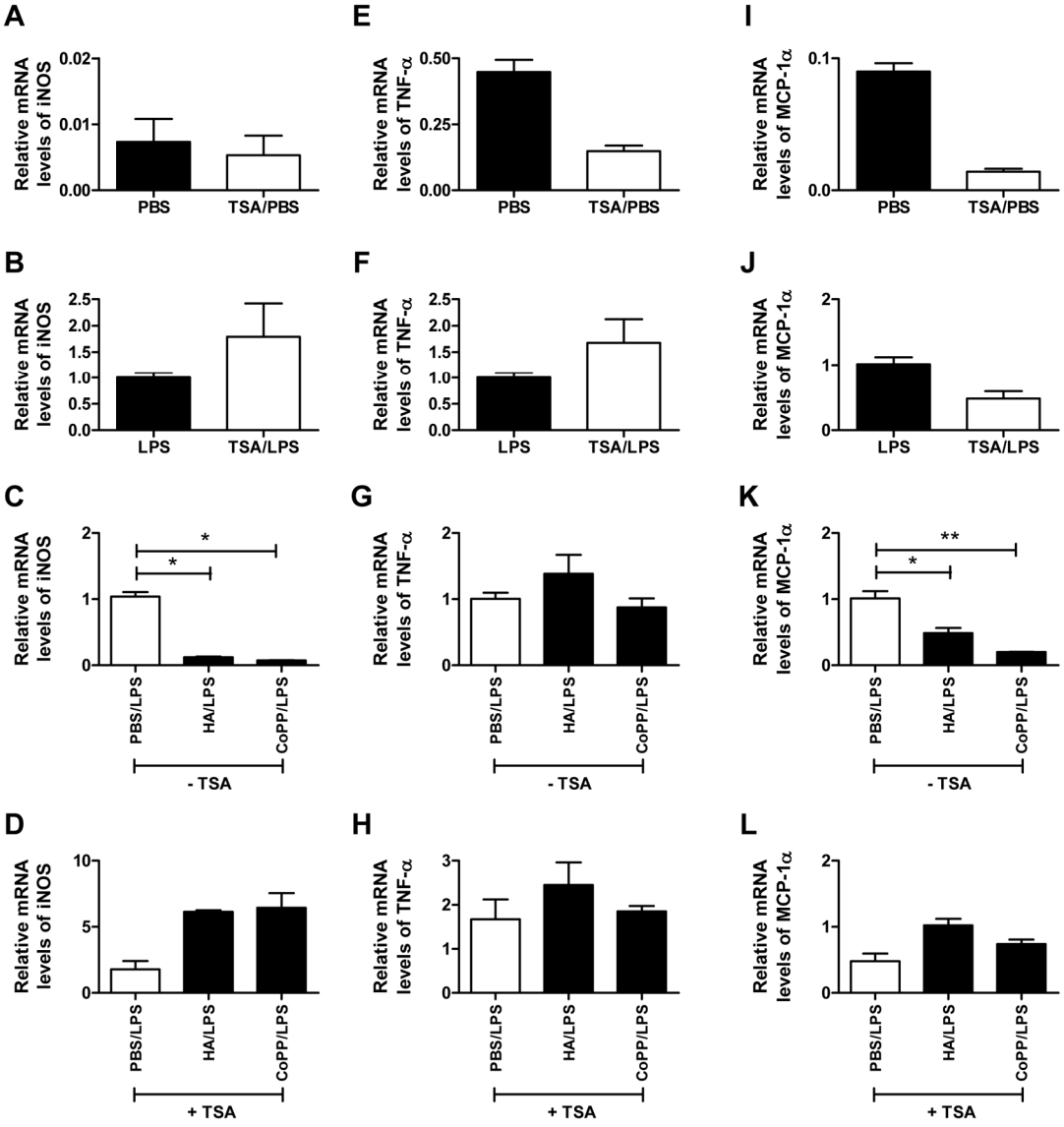


**Figure 6.10 Effect of histone deacetylases (HDAC) inhibition on anti-inflammatory effects of HA and CoPP in LPS-activated BMDMs.** Effect of TSA pre-treatment on mRNA levels of **A.** iNOS, **E.** TNF-α, **I.** MCP-1α in non-stimulated BMDMs. P>0.05 (non-significant) by two-tailed Mann Whitney test. Effect of TSA pre-treatment on mRNA levels of **B.** iNOS, **F.** TNF-α, **J.** MCP-1α in LPS-stimulated BMDMs. P>0.05 (non-significant) by two-tailed Mann Whitney test. Effect of treatment with HA and CoPP on mRNA levels of **C.** iNOS, **J.** TNF-α, **K.** MCP-1α in LPS-stimulated BMDMs. *P<0.05, **P<0.01, P-values derived with Dunn's multiple comparison post-test when P<0.05 by Kruskal-Wallis test. Effect of pre-treatment with TSA prior to treatment with HA and CoPP on mRNA levels of **D.** iNOS, **H.** TNF-α, **L.** MCP-1α in LPS-stimulated BMDMs. P>0.05 (non-significant) by Kruskal-Wallis test. **A-L.** The data given are mean ± s.e.m. from n=4 independent cell culture experiments where each 'n' was performed in duplicates. 18S gene was used as endogenous control gene.

## 6.10. CHAPTER DISCUSSION

### 6.10.1. THE ANTI-INFLAMMATORY EFFECT OF HA IS INDEPENDENT OF THE L-ARGININE COMPONENT OF HA

A significant induction of iNOS gene and protein expression and an increase in iNOS activity and nitric oxide generation are some of the key pro-inflammatory effects observed with LPS activation of murine macrophages (Tsang et al., 2000, Pascual et al., 2005). As the heme arginate (HA) solution contains L-arginine (LA), which is a substrate for nitric oxide production by enzyme nitric oxide synthase (NOS) (Alderton et al., 2001), it was important to ensure that the LA component of HA did not influence the results.

The initial screening showed that HA pre-treatment had a selective anti-inflammatory effect in LPS-stimulated BMDMs. HA pre-treatment significantly reduced the mRNA levels of iNOS and MCP-1α and the release of nitrite in LPS-stimulated BMDMs (Figure 6.6.G, I, J). However, HA pre-treatment failed to reduce LPS mediated increase in TNF-α gene expression and release in BMDMs (Figure 6.6.H, K). Also, HA pre-treatment did not affect the production of IL-10 (Figure 6.6.L), a potent anti-inflammatory cytokine that has been reported to mediate the anti-inflammatory effects of HO activity in several studies (Lee and Chau, 2002, Ma et al., 2007).

None of the changes associated with HA pre-treatment in LPS activated BMDM were mimicked by pre-treatment with L-arginine (LA) alone suggesting that heme rather than the LA component was responsible for the anti-inflammatory effects of HA. Initially, hemin dissolved in 10mM Tris-HCl pH 7.4 solution was included in the study. However, the hemin precipitated and formed aggregates on a BMDM monolayer, and hence was excluded from further studies.

### 6.10.2. ANTI-INFLAMMATORY EFFECTS OF HA IS INDEPENDENT OF HO ACTIVITY AND HO-1 PROTEIN

The anti-inflammatory properties of HA were observed at a concentration at which it induces HO-1 protein and HO activity. Previous studies have reported that induction of HO activity confers anti-inflammatory effects on murine macrophages (Otterbein et al*.,* 2000, Lee and Chau, 2002, Weis et al*.,* 2009, Ma et al*.,* 2007), therefore the critical question was whether the anti-inflammatory effects of HA were due to its ability to induce HO activity.

The anti-inflammatory effects of pre-treatment with HA included a significant reduction in mRNA levels of iNOS, MCP-1α and in the release of nitrite in LPS-stimulated BMDMs (Figure 6.6, 6.7, 6.8). However, the anti-inflammatory effect of HA pre-treatment was selective as no significant change in gene expression and release of TNF-α was noted in LPS-stimulated BMDMs. Co-treatment of HA with either SM or CrMP, two HO activity inhibitors, failed to reverse the anti-inflammatory effects of HA (Figure 6.7.B, H, Figure 6.8.B) despite a reduction in

HO activity (Figure 6.4.B). Similarly addition of SM to CoPP pre-treatment reduced the extent of increase in HO activity (Figure 6.4.C) but failed to significantly reverse the anti-inflammatory effects of CoPP (Figure 6.7.C, I, Figure 6.8.C) which were similar to those of HA. Hence, the body of evidence indicates that the anti-inflammatory effect of HA are independent of its ability to induce HO activity.

SM and CrMP were effective at partially reversing the increase in HO activity but they increased HO-1 protein levels (Figure 6.4.D). This was of interest as it has recently been reported that HO-1 protein may translocate to the nucleus and activate gene expression to facilitate an anti-oxidative effect (Lin et al., 2007). To determine whether an increase in HO-1 protein could explain the anti-inflammatory effect of HA, BMDMs from Hmox knock-out mice were employed. Interestingly in the absence of HA treatment, HO deficiency did increase the production of nitrite and TNF-α in response to LPS stimulation in BMDMs (Figure 6.9.B, F), demonstrating that HO *per se* also has some anti-inflammatory effects. However, HA pre-treatment remained efficient at significantly reducing the release of nitrite by BMDMs isolated from Hmox knock-out C57BL/6J mice on stimulation with LPS (Figure 6.9.C, D), demonstrating that up-regulation of HO-1 protein was unlikely to be responsible for the anti-inflammatory effects of HA.

### 6.10.3. POSSIBLE ROLE OF HDAC MEDIATED REPRESSION FOR ANTI-INFLAMMATORY EFFECTS OF HA

Having concluded that the anti-inflammatory effect of HA was dependent on the heme component, but independent of HO-1 protein or HO activity. Hence, it was important to determine the mechanism by which heme was acting.

In a recent study, Gibbs et al has demonstrated Rev-erbα to be a vital for circadian clock-dependent variation in gene expression of inflammatory mediators, including IL-6, Cxcl-1, CCL2/MCP-1α, but not TNF-α (Gibbs et al., 2012). The recognition of heme as a ligand of the nuclear hormone receptor Rev-erb (Yin et al., 2007) and its ability to recruit and stabilise the interaction between the components of the NCoR-HDAC3 co-repressor complex (Yin et al., 2010) has generated interest in exploring the role of heme in the regulation of the circadian clock and inflammatory processes. The NCoR-HDAC3 co-repressor complex has been shown to be bound to the iNOS promoter region in non-stimulated murine macrophages (Pascual et al., 2005). LPS stimulation promotes release of the NCoR-HDAC3 co-repressor complex facilitating iNOS gene expression (Pascual et al., 2005). Ligand binding to PPAR-γ stabilises the NCoR-HDAC3 co-repressor complex in macrophages *in vitro*, thereby preventing LPS-induced release of NCoR-HDAC3. Interestingly this is observed at the promoters of the iNOS and MCP-1 but not TNF-α genes (Pascual et al., 2005, Huang et al., 2011). As this pattern of gene repression is very similar to that observed with heme it was important to test if the anti-inflammatory effect of HA could be reversed

by inhibiting the NCoR-HDAC3 co-repressor complex. To do this, BMDMs were pre-treated with the histone deacetylase inhibitor trichostatin (TSA).

Pre-treatment of BMDM with the HDAC inhibitor TSA completely abrogated the HA mediated reduction in mRNA levels of iNOS and MCP-1α (Figure 6.10.C, D, K, L), suggesting HDAC activity to be an integral component of the mechanism by which HA facilitates its anti-inflammatory effects. TSA non-specifically inhibits several members of HDAC family. Furthermore it may have anti-inflammatory effects *per se* (Han and Lee, 2009). Although in the current study, TSA pre-treatment failed to markedly modulate the mRNA levels of iNOS, TNF-α and MCP-1α in non-stimulated and LPS-stimulated BMDMs (Figure 6.10.A, B, E, F, I, J ). However, the validity of the hypothesis that anti-inflammatory effects of HA are mediated via Rev-erb interaction with NCoR-HDAC-3 co-repressor complex needs further incisive studies. The incisive studies should include either deleting or silencing important determinants of the mechanism including Rev-erb, NCoR and HDAC-3 to convincingly demonstrate that HA's anti-inflammatory effects are mediated through the interaction between heme and Rev-erb leading to stabilisation of the NCoR-HDAC-3 complex on the promoter of specific pro-inflammatory genes.

### 6.10.4. THE PROTOPORPHYRIN STRUCTURE OF HEME MAY BE RESPONSIBLE FOR THE ANTI-INFLAMMATORY EFFECT OF HA

The anti-inflammatory effects of HA including a marked reduction in nitrite release and mRNA levels of iNOS and MCP-1α in LPS activated BMDMs were mimicked by administration of CoPP (Figure 6.8, 6.9) which is another protoporphyrin based inducer of HO activity like HA. Indeed co-treatment of CoPP with HO activity inhibitors failed to reverse the above cited anti-inflammatory effects of CoPP in LPS-stimulated BMDMs. Pre-treatment of BMDMs with trichostatin reversed the anti-inflammatory effects of CoPP and HA in LPS-stimulated BMDMs (Figure 6.10). Hence, HA and CoPP displayed similar phenotypic effects in LPS-activated BMDMs in the absence or presence of the HDAC inhibitor trichostatin suggesting that they may share a similar mode of action for their anti-inflammatory effects. As HA and CoPP, both have a protoporphyrin ring in their structure, it is possible that their anti-inflammatory effects in LPS activated BMDMs are imparted by the protoporphyrin structure *per se*. To incisively determine whether the anti-inflammatory effect of HA and CoPP in LPS activated BMDMs is due to protoporphyrin structure *per se*, the future experiments should include two definite control groups including

- **i.** Protoporphyrin compound with-out a metal ion attached to it, and hence which would not affect the level of HO-1 protein or activity
- **ii.** A heterocyclic compound such as corrin which is similar but not identical to the porphyrin structure of protoporphyrin as a negative control.

### 6.10.5. CONCLUDING REMARK

The characterisation of the anti-inflammatory effects of HA and other metallo-porphyrin compounds in LPS-activated murine macrophages demonstrated that all the compounds exhibited anti-inflammatory properties. This was independent of their ability to either induce or inhibit HO activity and increase HO-1 protein. Interestingly, TSA pre-treatment completely abrogated the inhibitory effect of HA on mRNA levels of iNOS and MCP-1α in LPS activated BMDMs. Further work is required to pursue the hypothesis that the heme component of HA facilitates the repression of inflammatory genes via recruitment and stabilising the interaction between NCoR-HDAC3 co-repressor complex and Rev-erb.

# 7. CHAPTER 7: GENERAL DISCUSSION, LIMITATIONS AND FUTURE WORK

## 7.1. INTRODUCTION

Heme oxygenase (HO) is a rate-limiting enzyme, and consists of two isoforms, inducible (HO-1) and constitutive (HO-2), which play an integral role in maintaining heme homeostasis (Maines and Gibbs, 2005). Induction of HO activity facilitates oxidative breakdown of free heme into equi-molar concentrations of carbon monoxide (CO), the bile pigment biliverdin IX and free iron. Consequently biliverdin reductase converts biliverdin IX into bilirubin IX and free iron is stored as ferritin (Maines, 2005, Abraham and Kappas, 2008). The products of heme catabolism have immuno-modulatory and anti-oxidative properties (Wagener et al., 2003). Hence, induction of HO enzyme activity is an attractive approach for treatment of diseases characterised by low-grade inflammation and oxidative stress, including obesity-associated insulin resistance and type 2 diabetes.

HO-1 protein levels and carbon monoxide generation are reported to be down-regulated in murine models of obesity and type 2 diabetes, including obese (ob/ob) mice and Zucker diabetic fatty (ZDF) rats (Li et al., 2008, Nicolai et al., 2009). Indeed, pharmacological induction of HO activity is reported to reduce obesity, adipogenesis and insulin resistance in different murine model of type 2 diabetes (Ndisang, 2010, Nicolai et al., 2009, Li et al., 2008). The anti-diabetic effect of hemin, a natural substrate for HO enzyme, has been reported to be observed for up to 3-months after termination of treatment in Goto-kakizaki (GK) and ZDF rat models of type 2 diabetes (Ndisang et al., 2009a, Ndisang et al., 2009b). An increase in peripheral insulin sensitivity with hemin treatment has been attributed to the HO

activity-dependent increase in circulatory levels of adiponectin, restoration of AMPK protein level and reduced inflammatory and oxidative mediators in the soleus muscle of GK rats (Ndisang and Jadhav, 2009). Cobalt (III) protoporphyrin IX dichloride (CoPP), a non-heme protoporphyrin inducer of HO activity, induces the HO activity-adiponectin axis to reduce peripheral insulin resistance along with a reduction in body weight gain, adipogenesis and systemic inflammation in the ob/ob mouse model of obesity and type 2 diabetes (Li et al., 2008). The published studies in experimental models of obesity and type 2 diabetes demonstrate that pharmacological induction of HO activity is effective for the treatment of systemic inflammation and insulin resistance. However, the relative insolubility and instability of hemin in solution (Goetsch and Bissell, 1986) and the multiple side-effects of CoPP, including weight loss (Galbraith and Kappas, 1989), preclude their use for treatment of patients in clinic.

Heme arginate (HA) is a stable and soluble composition of hemin, isolated from human blood, and L-arginine in a solution containing propylene glycol, ethanol and water (Tenhunen et al., 1987). The induction of HO-1 with HA treatment is reported to confer protection against acute kidney injury *in vivo* (Ferenbach et al., 2011). Furthermore, HA is licensed for the treatment of acute porphyria in several European countries. Hence, HA has translational potential to be used in clinical trials.

The *in vivo* studies during my PhD were sought to test the hypothesis that the heme component of HA ameliorates hyperglycaemia via induction of HO activity in the db/db mouse model of type 2 diabetes. Concurrently, *in vitro* studies in MIN6 β-cells

and primary macrophages from C57BL/KsJ mice were performed to test the hypothesis that the anti-inflammatory effects of HA are dependent on the induction of HO activity. The LPS-stimulated model of pro-inflammatory response in primary macrophages was used to test consequent hypotheses, including that the anti-inflammatory effects of HA are dependent on induction of HO-1 protein level or on gene repression mediated by inhibition of histone deacetylases. The key findings of the project are discussed below.

## 7.2. INHIBITION OF HO ACTIVITY ACCENTUATES THE ANTI-DIABETIC EFFECT OF HA IN THE LEPTIN RECEPTOR DEFICIENT db/db MODEL OF TYPE 2 DIABETES

### 7.2.1. DISCUSSION OF THE RESULTS OF THE *IN VIVO* STUDIES IN db/db MICE AND THE *IN VITRO STUDY* IN MIN6 β-CELL LINE

The preliminary *in vivo* study demonstrated that the intravenous (i.v.) administration of HA (15mg/kg, twice weekly) for 8 weeks resulted in a significant reduction in hyperglycaemia. The anti-hyperglycaemic effect of HA coincided with weight gain, an increase in fasting serum insulin levels between 6 and 8 weeks and induction of HO activity. These phenotypic changes were not reciprocated by i.v. administration of L-arginine (LA, 16mg/kg, twice weekly for 8 weeks), at a concentration equivalent to that present in 15mg/kg of HA (Table 7.1). The failure of LA but not HA treatment to increase fasting insulin levels is of significance because LA, at millimolar concentration has been reported to stimulate islet β-cell insulin secretion in mouse islets cultured *ex vivo* (Henningsson and Lundquist, 1998). Therefore, it can be stated that the anti-hyperglycaemic effect of HA is not due to an increase in insulin release stimulated by the LA component of HA. Additionally, none of the HA-mediated phenotypic changes were mimicked by treatment with LA, suggesting that the hemin/heme component of HA is responsible for the anti-diabetic effect of HA. Ideally, a hemin treatment group should have been included in the preliminary *in vivo* study as a comparison with the phenotypic changes achieved with HA treatment. However, hemin in solution showed a propensity to precipitate and form

aggregates in initial *in vitro* studies in BMDM. Hence, hemin was excluded from the *in vivo* and *in vitro* studies.

| **Parameters** | **Changes relative to PBS-treated db/db mice** | |
|---|---|---|
| | **HA** | **LA** |
| Terminal HO activity in liver | ↑ | - |
| Terminal HO-1 protein levels in liver | ↑ | - |
| Fasting hyperglycaemia (AUC) | ↓ (6-8 wk) | - |
| Terminal $HbA_{IC}$% | ↓ | - |
| Weight gain | ↑ (6 and 8 wk) | - |
| Serum insulin level (AUC) | ↑ (6-8 wk) | - |
| Relative glucose level during ITT (AUC) | - | - |
| Terminal serum adiponectin level | - | - |
| Terminal haemoglobin level | - | - |
| Food intake | - | - |

**Table 7.1 The effects of HA and LA treatment on the listed parameters in the db/db mouse model of type 2 diabetes.** ↑ indicates increase, ↓ indicates decrease, **-** indicates no change. Changes listed in the table are relative to PBS-treated db/db mice. Relative changes for the listed parameters (except for HO-1 protein levels) are based on statistical significance achieved with the appropriate non-parametric test.

Stannous (IV) mesoporphyrin IX dichloride (SM), an inhibitor of HO activity, was employed in the next *in vivo* study to test the hypothesis that the anti-diabetic effect of HA is dependent on the HA-mediated increase in HO activity. Paradoxical to this hypothesis, concomitant treatment of HA and SM resulted in further improvement in glycaemic control despite complete abrogation of the HA-mediated increase in HO activity. Hence, this result demonstrates that the HA-mediated increase in HO activity is not the primary mechanism for the anti-diabetic effect of HA. This observation is in contrast to a published study where chromium (III) mesoporphyrin IX chloride (CrMP), an inhibitor of HO activity, reversed the anti-hyperglycaemic effect of hemin in non-obese insulin-resistant GK rats (Ndisang and Jadhav, 2009).

| Parameters | Changes relative to PBS-treated db/db mice | | |
|---|---|---|---|
| | HA | SM | HA+SM |
| Terminal HO activity in liver | ↑ | - | - |
| Terminal HO-1 protein levels in liver | ↑ | - | ↑ |
| Fasting hyperglycaemia (AUC) | ↓ (6-8 wk) | - | ↓ (2-8 wk) |
| Weight gain | ↑ (6 and 8 wk) | - | ↑ (2 to 8 wk) |
| Epididymal fat pad weight | ↑ | - | ↑ |
| Terminal serum insulin level | ↑ | - | ↑ |
| Relative mRNA level of HO-1 in EFP | ↑ | - | ↑ |
| Terminal heme levels in liver | - | - | ↑ |
| Terminal $HbA_{IC}$% | - | - | ↓ |
| Terminal serum adiponectin level | - | - | ↑ |
| Number of islet iNOS expressing cells | - | - | ↓ |
| Total number of islet macrophages | - | - | ↓ |
| Relative mRNA level of Pref-1 in EFP | - | - | ↓ |
| Relative mRNA level of PPAR-γ in EFP | - | - | ↑ |
| Relative mRNA level of FASN in EFP | - | - | ↑ |
| Relative mRNA level of CD68 in EFP | - | ↓ | ↓ |
| Relative mRNA level of MCP-1α in EFP | - | ↓ | ↓ |
| Relative glucose levels during GTT (AUC) | - | - | - |
| Relative glucose levels during ITT (AUC) | - | - | - |
| Terminal serum NEFA levels | - | - | - |
| Relative mRNA level of TNF-α, IL-6 in EFP | - | - | - |
| Food intake | - | - | - |
| Liver weight and triglyceride content | - | - | - |
| Relative mRNA level of PEPCK, G-6-P in liver | - | - | - |

**Table 7.2 The effects of HA, SM and HA+SM treatment on the listed parameters in db/db mouse model of type 2 diabetes.** ↑ indicates increase, ↓ indicates decrease, **-** indicates no change. Changes listed in the table are relative to PBS-treated db/db mice. Relative changes for listed parameters except for HO-1 protein levels, are based on statistical significance achieved with non-parametric tests. Modulatory changes in listed parameters were not dependent on HO activity. Changes in listed parameters highlighted in red may likely be dependent on HO-1 protein level. Changes in listed parameters highlighted in blue may likely be dependent on intracellular heme concentration. Abbreviations. G-6-P: Glucose-6-phosphatase, FASN: Fatty acid synthase.

The improvement in glycaemic control with HA±SM treatment in db/db mice was unlikely to be due to an improvement in insulin sensitivity. The relative glucose levels between different treatment regimes were not significantly different during insulin tolerance test, performed in week 8 of the *in vivo* study. This is in contrast to previously reported studies where pharmacological induction of HO activity with CoPP and hemin treatment reduced peripheral insulin resistance in murine models of type 2 diabetes (Li et al., 2008, Ndisang et al., 2009b, Ndisang and Jadhav, 2009). However, these studies used absolute glucose levels, rather than relative reductions in glucose levels at specified time-points during the ITT, to measure insulin resistance. Normalisation of the absolute glucose levels during ITT from these studies may indicate that the effect of HA, hemin or CoPP treatment is largely independent of improvements in insulin sensitivity in all three models.

The improvement in glycemic control with HA±SM treatment in db/db mice is likely to be due to a change in adipose tissue phenotype and to preservation of islet β-cell function. Wang et al has demonstrated that an increase in adipocyte storage capacity is responsible for preserving islet mass and delaying the onset and severity of type 2 diabetes in normal db/db mice when compared to transgenic obesity resistant db/db mice (Wang et al., 2008). Indeed, HA±SM treatment resulted in a progressive body weight gain and increase in epididymal fat weight despite no significant difference in food intake. Furthermore, HA+SM but not HA alone treatment resulted in a significant increase in circulatory adiponectin levels, decrease in mRNA levels of Pref-1, a marker of pre-adipocytes (Wang et al., 2006), and an increase in mRNA levels of PPAR-γ, a marker of adipocyte differentiation (Lazar, 1999), and fatty acid

synthase (FASN), a marker of lipogenesis (Wang et al., 2004). These observations suggest that HA+SM treatment promotes a metabolically favourable expansion of adipose tissue to accommodate safe storage of excess lipid.

HA±SM-treated db/db mice were hyperinsulinaemic at the end of 8 week study, indicating preservation of islet β-cell function. Immuno-histology studies demonstrated that the HA±SM treatment markedly reduced islet macrophage infiltration which is known to play a key pathogenic role in β-cell dysfunction in type 2 diabetes (Ehses et al., 2007a). In addition, HA+SM therapy reduced islet iNOS staining to the levels observed in lean mice. This is likely to have improved β-cell function, given the suppressive effect of nitric oxide on glucose-stimulated insulin secretion *in vitro* (Henningsson et al., 2002) and that NOS inhibitors prevent β-cell dysfunction *in vivo* (Kato et al., 2003). Additionally, HA±SM treatment markedly reduced expression of pro-inflammatory genes, such as IL-1β, MCP-1α and Cxcl-1, in cytokine mix-stimulated MIN6 β-cells which suggests that the HA±SM treatment can directly impart a broader range of anti-inflammatory effects on β-cells.

The most intriguing question remains how concurrent treatment with HA and SM (HA+SM) interact to dramatically improve glycaemic control. It may be that they act via different mechanisms, however an alternative possibility is that the effect of HA+SM may be due to an additive increase in either HO-1 protein level or intracellular heme concentration. The parameters affected by HA, SM and HA+SM treatment in db/db mice (Table 7.2) and in cytokine mix-stimulated MIN6 β-cells

(Table 7.3) are grouped on the basis of the changes that mimic hepatic HO-1 protein expression (highlighted in red) and hepatic heme concentration (highlighted in blue).

| **Parameters** | **Changes relative to PBS or cytokine mix-treated MIN6 β-cells** | | |
|---|---|---|---|
| | **HA** | **SM** | **HA+SM** |
| HO activity | ↑ | - | - |
| Relative mRNA level of iNOS | ↓ | - | - |
| HO-1 protein level | ↑ | - | ↑ |
| Relative mRNA level of IL-1β | ↓ | - | ↓ |
| Relative mRNA level of MCP-1α | ↓ | - | ↓ |
| Relative mRNA level of Cxcl-1 | ↓ | - | ↓ |

**Table 7.3 The effects of HA, SM and HA+SM treatment on the listed parameters in cytokine mix-stimulated MIN6 β-cells.** ↑ indicates increase, ↓ indicates decrease, - indicates no change. Changes listed in the table for HO activity and HO-1 protein are relative to PBS (vehicle)-treated MIN6 β-cells. Changes listed in the table for mRNA levels of pro-inflammatory genes are relative to cytokine mix-stimulated MIN6 β-cells. Relative changes for listed parameters (except for HO-1 protein levels), are based on statistical significance achieved with the appropriate non-parametric test. Changes in listed parameters highlighted in red follow a similar pattern to the HO-1 protein level. Changes in listed parameters highlighted in green are associated with the level of HO activity.

The groupings of the affected parameters suggest that an increase in HO-1 protein level is associated with a reduction in fasting hyperglycaemia, weight gain and terminal hyperinsulinaemia during HA±SM treatment. Whereas, the HA+SM-mediated modulation of glycosylated haemoglobin levels, mRNA levels of adipogenic and lipogenic genes in visceral fat, total macrophage number and iNOS positive cells in the islets is associated with an increase in heme concentration in db/db mice. The additive increase in HO-1 protein level is less likely to account for the ameliorative effect of HA+SM treatment because Li et al in their study have demonstrated that an additive increase in HO-1 protein during concomitant treatment with CoPP and SM does not lead to an increase in insulin sensitivity in the ob/ob

mouse model of obesity and type 2 diabetes (Li et al., 2008). An additive increase in the intracellular heme concentration may be a more likely explanation for all the phenotypic changes associated with HA±SM treatment in db/db mice. It can be debated that all the changes in the listed parameters are not shared by HA and HA+SM treatment and that they therefore may be acting via different mechanisms (Table 7.2). However, an alternative explanation is that the addition of SM accentuated the effect of HA, as similar trends in many phenotypic markers were common to both HA and HA+SM treatments. It may be that administration of HA resulted in a transient increase in the intracellular heme concentration before it was degraded by a subsequent increase in HO activity, thereby limiting the effects of HA administration Whereas, concurrent inhibition of HO activity with HA+SM treatment resulted in a prolonged increase in the intracellular heme concentration which allowed heme to exert its protective effect for a longer duration in db/db mice. This may explain why inhibition of HO activity accentuates the anti-diabetic phenotype of HA.

A key question is to understand the mechanism by which heme may be responsible for the anti-diabetic effects of HA±SM. Heme is a ligand for the nuclear receptor Rev-erbα (Yin et al., 2010) and published studies demonstrate that Rev-erbα to regulates several metabolic pathways, such as adipocyte differentiation (Kumar et al., 2010), repression of gluconeogenic genes (Yin et al., 2007), and lipogenesis and exocytosis in pancreatic β-cells (Vieira et al., 2012). Recently, two independent studies have been published which demonstrate that Rev-erb is vital for the maintenance of energy homeostasis (Cho et al., 2012b, Solt et al., 2012b). Rev-erb

agonists have been reported to modulate the expression of key metabolic genes in the liver, skeletal muscle and adipose tissue, resulting in enhanced energy expenditure, a reduction in body weight and an improvement in glycaemic control in the high fat diet model of type 2 diabetes (Solt et al., 2012b). In tamoxifen-induced Rev-erb double knockout (Rev-erb $\alpha^{-/-}$ and $\beta^{-/-}$) in C57BL/6 mice, there was an increase in circulatory glucose and triglyceride levels when compared to wild-type mice (Cho et al., 2012b). Therefore, refinement of the hypothesis and the experiment design is required to deconstruct the mode of action of HA±SM treatment in db/db mice, as will be discussed later in the 'future work' section.

In conclusion, concurrent administration of HA+SM markedly ameliorates hyperglycaemia in the db/db model of type 2 diabetes via metabolically favourable expansion of visceral fat and preservation of islet β-cell mass and function. The improvement in glycaemic control by HA+SM is not due to an increase in HO activity, but may be due to an additive increase in HO-1 protein level or intracellular concentration of heme or both.

### 7.2.2. LIMITATIONS OF THE STUDIES

The key limitations of the *in vivo* studies, which should be considered while designing future *in vivo* experiments, are listed below,

- **Low number of mice employed in the *in vivo* studies:** The *in vivo* study was split into two separate experiments to test the hypothesis that **a.** the heme component of HA has an anti-diabetic effect and **b.** that this effect is dependent on an increase in HO activity. Initially, the plan was to merge the results of the PBS and HA treatment groups from the *in vivo* studies described in chapter 3 and chapter 4. However, there was a significant difference in the rate of progression and the severity of hyperglycaemia in the db/db mice on PBS-treatment between the two cohorts (Figure 7.1), therefore it was inappropriate to merge the results of the two studies. This resulted in there being less than 5 db/db mice in each of the PBS and HA treatment groups in the *in vivo* study described in chapter 4. Given the small sample size, it could not readily be ascertained as to whether a particular variable was normally distributed and therefore non-parametric statistical tests were employed. Non-parametric tests with small sample size have limited power to reject null hypothesis. This is best illustrated by the results of the terminal fasting NEFA levels in the *in vivo* study described in chapter 4. HA+SM treatment reduced the fasting NEFA concentration to levels comparable with lean mice, however this reduction was not found to be statistically significant. Given the small sample size, it is possible that this result represents a type 2 error, that is, declaring that HA+SM therapy had no effect on the fasting

NEFA concentration, when in reality it had a major impact on the NEFA concentration. If true, this size of effect may have biological significance as reduced lipid levels are known to have protective effect in type 2 diabetes. Hence, power calculations should be performed during the design of future experiments, to ensure that the sample size is adequate to reduce the risk of type 2 errors.

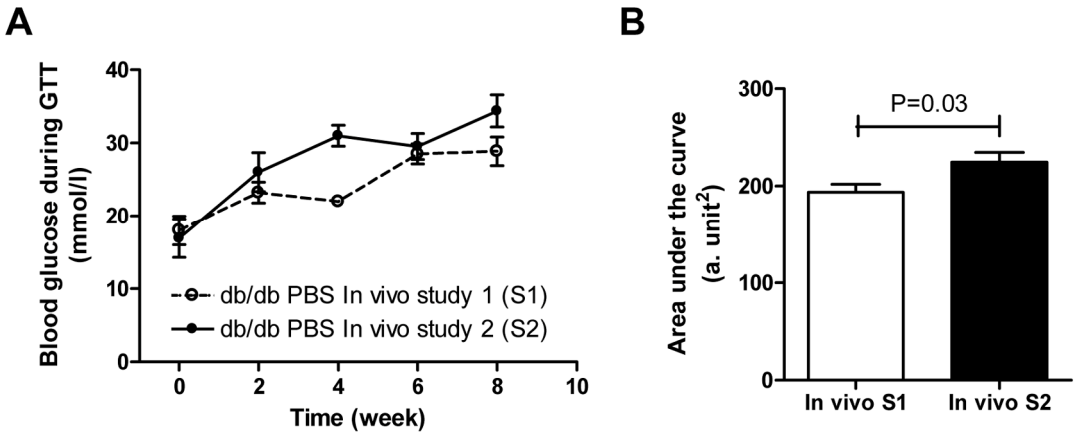


**Figure 7.1 Comparison of the progression and severity of hyperglycaemia in PBS-treated db/db mice from the two separate *in vivo* studies. A.** Fasting glucose levels for PBS-treated db/db mice from the two separate *in vivo* studies. **B.** Area under the curve for fasting glucose levels demonstrated a significant increase in the severity of hyperglycaemia in PBS-treated db/db mice in study 2 as compared to study 1. P=0.03 (significant) by two-tailed Mann Whitney test. The data given are mean ± s.e.m. from n=4/group. a. unit: arbitrary unit.

- **Single concentration of HA employed in the *in vivo* studies:** The use of dose/response curve for HA therapy would have helped to determine the pharmacokinetics, pharmacodynamics and toxicological effects, which may have proved vital to strengthen the case for it to be tested in humans. However, this was beyond the scope of my PhD project as the interest was to determine the efficacy and mechanism of action of HA in a mouse model of type 2 diabetes.

- **Single mouse model of type 2 diabetes employed to study the effects of HA and SM:** Leptin deficiency is a rare cause of obesity in humans, and therefore determining whether HA and SM ameliorated hyperglycaemia in a more physiological model of human obesity, such as the high fat diet model, would be prudent prior to performing clinical trials in humans. One potential mechanism by which HA+SM was acting was by preserving β-cell mass and function. C57BL/KsJ mice have approximately 50% less β-cell proliferative capacity along with increased β-cell susceptibility to glucotoxicity than C57BL/6J mice (Clee and Attie, 2007). Hence, a high fat diet induced model of glucose intolerance was performed in C57BL/KsJ mice to test whether HA treatment reduced glucose intolerance by preserving islet β-cell function. However, 16 weeks of feeding with high fat diet (constituting of 60% fat diet) failed to render the C57BL/KsJ mice intolerant to glucose as assessed by glucose tolerance test. Hence, the experiment was terminated without further testing of the effect of HA treatment.

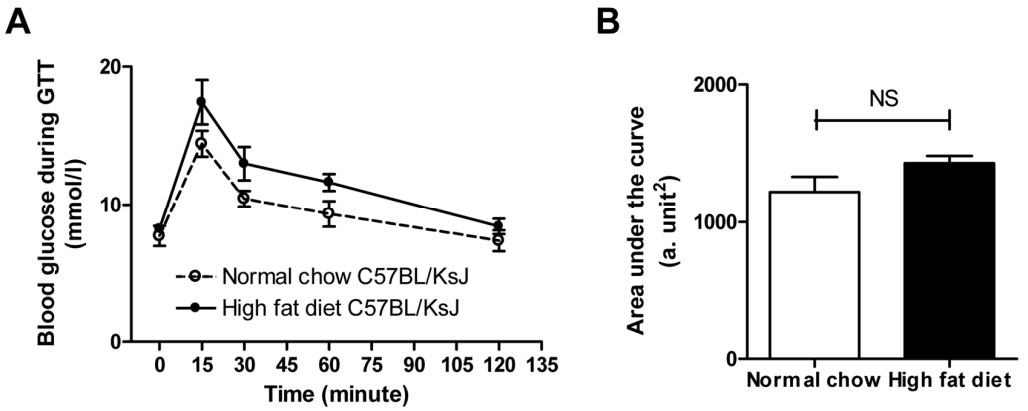


**Figure 7.2 Glucose tolerance test (GTT) in C57BL/KsJ mice on normal chow or high fat diet for 16 weeks. A.** The glucose levels after intraperitoneal administration of a 2g/kg glucose bolus in 4 hour fasted C57BL/KsJ mice which were either on normal chow or high fat diet for 16 weeks. **B.** Area under the curve for glucose concentration during the GTT demonstrated no significant difference in glucose levels between C57BL/KsJ mice on normal chow and high fat diet chow for 16 weeks. P>0.5 (NS: non-significant) by two-tailed Mann Whitney test. The data given are mean ± s.e.m. from n=5/group. a. unit: arbitrary unit.

### 7.2.3. FUTURE WORK

The current PhD project has suggested that HA may ameliorate hyperglycaemia by a novel HO activity independent mechanism and has helped to raise new questions. Therefore, the hypotheses tested in the current project need refinement to plan future work as they are listed below.

- **Hypothesis 1- The HA+SM-mediated anti-diabetic phenotype is dependent on prolonged interaction between heme and Rev-erb in the db/db mouse model of type 2 diabetes:** This hypothesis can be tested by using either pharmacological antagonists of Rev-erb or by employing organ-specific Rev-erb knock-out on C57BL/KsJ mice with the leptin receptor mutation (db/db) mice. A preliminary *in vivo* experiment should be designed to test whether the pharmacological antagonist of Rev-erb is able to reverse the anti-diabetic effect of HA+SM treatment in db/db mice. The HA+SM treatment regime should be for only 2 to 4 weeks, the time when phenotypic changes such as reduction in fasting glucose levels and weight gain begins to occur. An evaluation of insulin release during the glucose tolerance test at this time-point along with terminal fasting insulin levels and islet histology may help to determine whether the preservation of islet β-cell function is primarily responsible for the phenotypic changes associated with HA+SM treatment in db/db mice. This study can be followed by comparing the effects of HA+SM treatment in db/db mice with or without organ-specific knock-out of Rev-erb as this would be the most incisive method to

provide information on the importance of the interaction between heme and Rev-erb in individual organs.

- **Hypothesis 2- The increase in intracellular heme concentration with HA±SM treatment exerts anti-inflammatory effects via interacting with Rev-erb in cytokine mix-stimulated MIN6 β-cells:** The anti-inflammatory effects of HA±SM treatment, including a reduction in the mRNA levels of IL-1β, MCP-1α and Cxcl-1 in cytokine mix-stimulated MIN6 β-cells were demonstrated to be independent of HO activity. Therefore, pharmacological antagonist of Rev-erb should be employed to determine whether Rev-erb antagonist can reverse the anti-inflammatory effects of HA±SM treatment in MIN6 β-cells.

- **Hypothesis 3- The increase in intracellular heme concentration with HA±SM treatment promotes adipogenesis via interaction with Rev-erb in differentiated pre-adipocyte cell line 3T3-L1:** 3T3-LI is a widely used pre-adipocyte cell line to study adipocyte differentiation (Green and Meuth, 1974). The 3T3-LI cell line can be used to test the hypothesis that HA±SM treatment promotes adipogenesis. The read-out can include Oil red staining to determine the degree of lipid accumulation and in addition, the level of expression of genes which facilitate adipogenesis and lipogenesis may be quantified. Furthermore, a modified 3T3-LI cell line with knock-down of Rev-erb by administration of a lenti-virus containing shRNA against Rev-erb can be generated to test whether the increase in the intracellular heme concentration with HA±SM treatment promotes adipogenesis via interaction with Rev-erb.

- **Hypothesis 4- The anti-diabetic effect of HA is dose-dependent and has limited toxicity in mouse models of type 2 diabetes:** A dose-response study of HA would help to determine the ADME (**A**bsorption, **D**istribution, **M**etabolism, and **E**xcretion) characteristics for HA. Additionally, a dose-response study would help to determine whether the anti-hyperglycaemic effect of HA is observed across a wider dose-response curve with minimal toxicity. Elucidation of the pharmacokinetic and pharmacodynamic properties of HA across a dose-curve would both inform and strengthen the case for a clinical trial in patients with type 2 diabetes. It would be ideal to perform the dose-response study of HA in different genetic and diet-induced model of type 2 diabetes, to enable identification of *'global'* and model-specific factors responsible for the anti-diabetic efficacy.

### 7.2.4. PLACE OF HA AS A LINE OF TREATMENT FOR TYPE 2 DIABETES IN THE CLINIC

At present, the first line of treatment of patients with type 2 diabetes is recommended to be physical exercise, eating a healthy diet and weight loss if obese (Kimmel and Inzucchi, 2005). However, if these methods fail to control blood sugar levels anti-diabetic medications will be required. There are different classes of clinically approved drugs (Table 7.4) which either promote insulin sensitivity or stimulate insulin secretion (Kimmel and Inzucchi, 2005). These drugs are prescribed either as mono-therapy or in combination, based on the severity and duration of type 2 diabetes (Chitre and Burke, 2006).

| Line of treatment | Class of drugs | Drugs in clinic | Mode of action |
|---|---|---|---|
| | | | |
| Second | Biguanide | Metformin | Suppress hepatic glucose production, Improves insulin sensitivity. |
| | Thiazolidinedione | Pioglitazone | Improves insulin sensitivity, Promotes glucose utilisation by adipocytes and skeletal muscle. |
| Third | Sulphonylurea | Gliclazide, Glipizide | Stimulate insulin secretion by β-cells. |
| | Meglitinides (Non sulphonylurea) | Nateglinide, Repaglinide | Stimulate insulin secretion by β-cells for a shorter duration of time. |
| Fourth | Dipeptidyl peptidase (DPP) 4 inhibitors | Sitagliptin, Vildagliptin | Enhances the effect of incretins by blocking the action of incretin inhibitor DPP4. |
| Fifth | Insulin | | Pleotropic effect on glucose utilisation by peripheral organs. |
| | Glucagon-like peptide-1 (GLP-1) mimetic | Exenatide | Stimulate insulin secretion by β-cells in response to glucose, prevents glucagon release after meals. |

**Table 7.4 Line of treatment of type 2 diabetes with medication in clinic.** (Chitre and Burke, 2006, Kimmel and Inzucchi, 2005, Zhou et al., 2001, Cheng and Fantus, 2005).

The results of the *in vivo* studies in db/db mice demonstrated that HA treatment failed to improve peripheral insulin sensitivity but was able to preserve islet β-cell function. Hence, if HA were found to be effective in clinical trials, it may be best employed from an early point in the natural history of type 2 diabetes as its effect may prolong islet β-cell function and reduce the need for the sulphonylureas, which stimulate insulin secretion and may promote an effect known as 'β-cell burnout' (Robertson et al., 2003). Metformin is the preferred second line of treatment for type 2 diabetes as it restricts hepatic glucose production and promotes insulin sensitivity in peripheral organs (Zhou et al., 2001). It may be that dual therapy with metformin and HA may be a particularly potent combination as the act via different mechanisms.

At present, enrolment is open for the Radboud University Nijmegen Medical Centre sponsored clinical trial to test **'the effect of heme arginate treatment on insulin resistance and vascular dysfunction related to obesity' (**http://www.trialregister.nl/trialreg/admin/rctview.asp?TC=2472 last accessed on 21-06-2012). Hence, there is already an interest with regards to testing the efficacy of HA in patients with metabolic dysfunction. Currently, HA is marketed by the Orphan Europe pharmaceutical company and is available as a solution rather than tablets. It would be desirable that an oral formulation of HA were to be made available as prolonged intravenous infusion is unlikely to be palatable for patients. Furthermore, there may be problems with iron overload in chronic use. For this reason it is unlikely that chronic administration of HA will ever be used long-term as a treatment for type 2 diabetes, but that it will be useful in pilot studies such as the one

mentioned above. Hence it is important that the mechanisms by which HA ameliorate hyperglycaemia be determined so that more rationale therapies may be designed.

## 7.3. HISTONE DEACETYLASES MAY BE RESPONSIBLE FOR THE HO ACTIVITY INDEPENDENT ANTI-INFLAMMATORY EFFECTS OF HA IN BMDMs

### 7.3.1. DISCUSSION OF THE RESULTS OF *IN VITRO* STUDIES IN PRIMARY MACROPHAGES (BMDM)

Lipopolysaccharide (LPS) activation of bone marrow derived macrophages (BMDMs) was used as an *in vitro* model of inflammation to develop an understanding of the mode of action of HA as an anti-inflammatory agent.

The anti-inflammatory repertoire of HA included a significant reduction in mRNA levels of iNOS, MCP-1α and in the release of nitrite in LPS-stimulated BMDMs. HA pre-treatment of BMDMs failed to reduce mRNA levels of TNF-α or release of TNF-α protein. Additionally, HA pre-treatment did not result in an increase in release of the anti-inflammatory cytokine IL-10 which has been reported in previous studies to be the effector molecule responsible for the heme oxygenase dependent anti-inflammatory effect of hemin, carbon monoxide and biliverdin reductase in LPS stimulated macrophages (Ma et al., 2007, Otterbein et al., 2000, Wegiel et al., 2009). Hence, HA pre-treatment of BMDMs resulted in a selective anti-inflammatory effect in LPS-activated BMDMs. L-arginine (LA) when used at a concentration that was identical to the LA concentration in HA, did not mimic the anti-inflammatory phenotype of HA (Table 7.5) demonstrating that the heme component of HA was responsible for the anti-inflammatory effect in BMDMs.

A similar anti-inflammatory phenotype was observed with cobalt (III) protoporphyrin IX chloride (CoPP), a non-heme based modulator of HO activity (Table 7.5). This suggests that the anti-inflammatory properties may not be specific to heme but also apply to other protoporphyrins.

Two HO activity inhibitors, stannous (IV) mesoporphyrin IX dichloride (SM) and chromium (III) mesoporphyrin IX chloride (CrMP), were employed in the *in vitro* studies to investigate whether abrogation of the increase in HO activity reversed the anti-inflammatory effect of HA and CoPP. Concurrent treatment with the HO activity inhibitors failed to reverse the reduction in nitrite release and mRNA levels of iNOS and MCP-1α achieved with HA or CoPP pre-treatment in LPS-activated BMDMs (Table 7.5). Hence, the anti-inflammatory effects of HA and CoPP were not due to an increase in HO activity.

SM and CrMP are effective inhibitors of HO activity however they increase HO-1 protein expression in BMDMs. Nuclear localization of HO-1 protein has been reported to promote anti-oxidative gene expression *in vitro* (Lin et al., 2007). Therefore to determine whether the anti-inflammatory phenotype of HA was dependent on HO-1 protein, BMDMs from Hmox1 knock-out mice were employed. The lack of a functional HO-protein accentuated the LPS mediated pro-inflammatory response as a significant increase in nitrite and TNF-α release was observed in LPS-activated BMDMs from Hmox1 knock-out mice compared with wild type mice. However HA pre-treatment significantly reduced nitrite release in LPS- activated BMDMs from Hmox1 knock-out mice demonstrating that the anti-inflammatory effect of HA was independent of HO-1 protein and HO activity (Table 7.5).

The anti-inflammatory phenotype of HA and CoPP including a reduction in LPS-induced expression of iNOS and MCP-1α but not TNF-α closely resembles the anti-inflammatory effects of the peroxisome proliferator-activated receptor-γ (PPAR-γ) agonist *'rosiglitazone'*. Glass and co-workers have demonstrated that PPAR-γ agonists mediate transrepression of pro-inflammatory genes such as iNOS and MCP-1α by targeting PPAR-γ to nuclear receptor co-repressor (NCoR) - histone deacetylase-3 (HDAC3) complexes on pro-inflammatory gene promoters (Huang et al., 2011, Pascual et al., 2005). Heme is a ligand of the nuclear receptor Rev-erb and has been reported to stabilize the interaction between Rev-erb and NCoR-HDAC3 complexes at the promoter region of gluconeogenic genes including PEPCK and glucose-6-phosphatase to repress their expression (Yin et al., 2010, Yin et al., 2007).

A role for heme, Rev-erb and NCoR-HDAC3 in regulating inflammatory response has not previously been investigated. In the current PhD project, this area was briefly examined by employing trichostatin A (TSA), an inhibitor for the class I and II mammalian HDAC family which includes HDAC3. The anti-inflammatory effects of HA and CoPP, including a reduction in mRNA levels of iNOS and MCP-1α in LPS-activated BMDMs, was completely reversed by pre-treatment of BMDMs with TSA suggesting that the anti-inflammatory effect of HA and CoPP may be due to Rev-erb-NCoR-HDAC3 mediated gene repression (Table 7.5). A recently published study has demonstrated that the Rev-erbα is vital for the circadian clock-dependent variation in gene expression of inflammatory mediators, including IL-6, Cxcl-1, CCL2/MCP-1α, but not TNF-α (Gibbs et al., 2012). Furthermore, treatment of the THP-1 human macrophage-like cell line with either hemin (natural ligand of Rev-erb) or GSK4112,

a synthetic agonist of Rev-erbα, significantly lowered the mRNA levels of IL-6 and MCP-1α (Gibbs et al., 2012). Therefore, the evaluation of the anti-inflammatory effects of HA and CoPP in Rev-erb knock-out macrophages would be an incisive approach to determine the role of interaction between protoporphyrins and Rev-erb to mediate anti-inflammatory effects. It's worthwhile noting that the concept that it is the protoporphyrin structure rather than heme per se that acts as a ligand of Rev-erb has not been explored previously.

| Parameters | Changes relative to PBS or LPS-treated BMDMs | | | | | | | | |
|---|---|---|---|---|---|---|---|---|---|
| | LA | SM | CrMP | HA | HA+SM | HA+CrMP | CoPP | CoPP+SM | CoPP+CrMP |
| HO activity | ND | - | - | ↑ | - | - | - | - | - |
| HO-1 protein level | ND | ↑ | ↑ | ↑ | ↑ | ↑ | ↑ | ↑ | ↑ |
| Relative mRNA level of iNOS | - | - | - | ↓ | ↓ | ↓ | ↓ | ↓ | ↓ |
| Relative mRNA level of iNOS (+ TSA) | ND | ND | ND | - | ND | ND | - | ND | ND |
| Relative mRNA level of MCP-1α | - | - | - | ↓ | ↓ | ↓ | ↓ | ↓ | ↓ |
| Relative mRNA level of MCP-1α (+ TSA) | ND | ND | ND | - | ND | ND | - | ND | ND |
| Relative mRNA level of TNF-α | - | - | - | - | - | - | - | - | - |
| Relative mRNA level of TNF-α (+ TSA) | ND | ND | ND | - | ND | ND | - | ND | ND |
| Release of nitrite | - | - | - | ↓ | ↓ | ↓ | ↓ | ↓ | ↓ |
| Release of nitrite in HO KO | ND | ND | ND | ↓ | ND | ND | ND | ND | ND |
| Release of TNF-α | - | - | - | - | - | - | - | ↓ | - |
| Release of TNF-α in HO KO | ND | ND | ND | - | ND | ND | ND | ND | ND |
| Release of IL-10 | - | - | - | - | - | - | - | - | - |

**Table 7.5 The effects of HA, SM and HA+SM treatment on the listed parameters in LPS-stimulated BMDMs.** ↑ indicates increase, ↓ indicates decrease, **-** indicates no change. Changes listed in the table for HO activity and HO-1 proteins are relative to PBS (vehicle)-treated BMDMs. Other changes listed in the table are relative to LPS-stimulated BMDMs. Relative changes for listed parameters except for HO-1 protein levels, are based on statistical significance achieved with non-parametric tests. Changes in listed parameters highlighted in blue suggest the anti-inflammatory effects of HA to be independent of HO activity and HO-1 protein level. Changes in listed parameters highlighted in red suggest the anti-inflammatory effects of HA and CoPP to involve histone deacetylases (HDACs). **Abbreviations.** TSA: Trichostatin (HDACs inhibitor), HO KO: Heme oxygenase knock out mice.

### 7.3.2. LIMITATIONS OF THE STUDIES

The key limitations of the *in vitro* studies in primary macrophages from C57BL/KsJ mice are mentioned below and should be addressed in future *in vitro* experiments.

- **Low sample size:** The terminally differentiated primary macrophages, such as BMDMs and peritoneal macrophages are considered a better representation of the macrophage phenotype *in vivo* than macrophage-like cell lines. However, extensive studies with large sample sizes require the sacrifice of a large number of mice, which is best avoided if possible. The caveat of such an approach is to interpret the results based on non-parametric statistical tests which tend to be less powerful to rejection a null hypothesis. Therefore, it will be useful to generate a pro-inflammatory model using a murine macrophage-like cell line which mimics the classical activation of primary macrophages.

- **Exclusion of nitrate read-out:** In the current PhD project, nitrite ($NO_2^-$) (a stable metabolite of nitric oxide, NO) was used as a lone read-out to determine the effect of the modulators of HO activity on nitric oxide production in LPS-stimulated BMDMs, while the release of nitrate ($NO_3^-$) in LPS-stimulated BMDMs was not determined. This error resulted in the loss of a key read-out as the determination of peroxynitrite ($ONOO^-$), an unstable structural isomer of nitrate (Pacher et al., 2007), would have helped to indicate whether HA and CoPP had anti-oxidative effects in LPS-stimulated BMDMs. The formation of peroxynitrite is largely responsible for mediating the cytotoxic effects of NO

(Boccini and Herold, 2004). Hence, the release of nitrite as well as nitrate should be determined in future experiments.

### 7.3.3. FUTURE WORK

The *in vitro* studies with modulators of HO activity in LPS-activated BMDMs have demonstrated a novel HO activity independent anti-inflammatory phenotype of protoporphyrin-based compounds, including HA and CoPP. Therefore, the re-defined hypotheses to determine the mode of action of HA and CoPP in LPS-stimulated BMDMs are listed below.

- **Hypothesis 1- Rev-erb-mediated recruitment of NCoR-HDAC co-repressor complex is responsible for the anti-inflammatory effects of HA and CoPP in LPS-activated BMDMs:** The preliminary test with TSA has demonstrated that inhibition of histone deacetylase activity reverses the selective anti-inflammatory effects of HA and CoPP in LPS-activated BMDMs. In the light of the knowledge that LPS activation of macrophages releases the NCoR-HDAC co-repressor complex from the promoter region of the iNOS and MCP-1α genes, it is possible that HA and CoPP may exert their anti-inflammatory effects by stabilising the NCoR-HDAC co-repressor complex on the promoter region of iNOS (Pascual et al., 2005). Furthermore, interaction of Rev-erbα with it's natural ligand, heme, has been reported to reduce expression of gluconeogenic genes in the hepatic (HepG2) cell line via stabilisation of the NCoR-HDAC co-repressor complex at the promoter region of PEPCK and glucose-6-phosphatase (Yin et al., 2007). Therefore, to test whether heme interaction with Rev-erb also facilitates recruitment of the NCoR-HDAC co-repressor complex at the promoter region of iNOS and MCP-1α to mediate anti-inflammatory effects of HA, isoforms of Rev-

erb (α and β), NCoR and HDAC should be knocked down independently in primary macrophages to incisively determine the role of Rev-erb along with the NCoR-HDAC co-repressor complex in exerting the inflammatory effects of HA (Figure 7.3). To explore whether the protoporphyrin structure *per se,* shared by HA and CoPP, interacts with Rev-erb to facilitate repression of iNOS and MCP-1α genes, the future experiments should include a protoporphyrin compound without a metal ion as a positive control, along with a heterocyclic compound such as corrin, which is similar but not identical to the porphyrin structure of protoporphyrin, as a negative control.

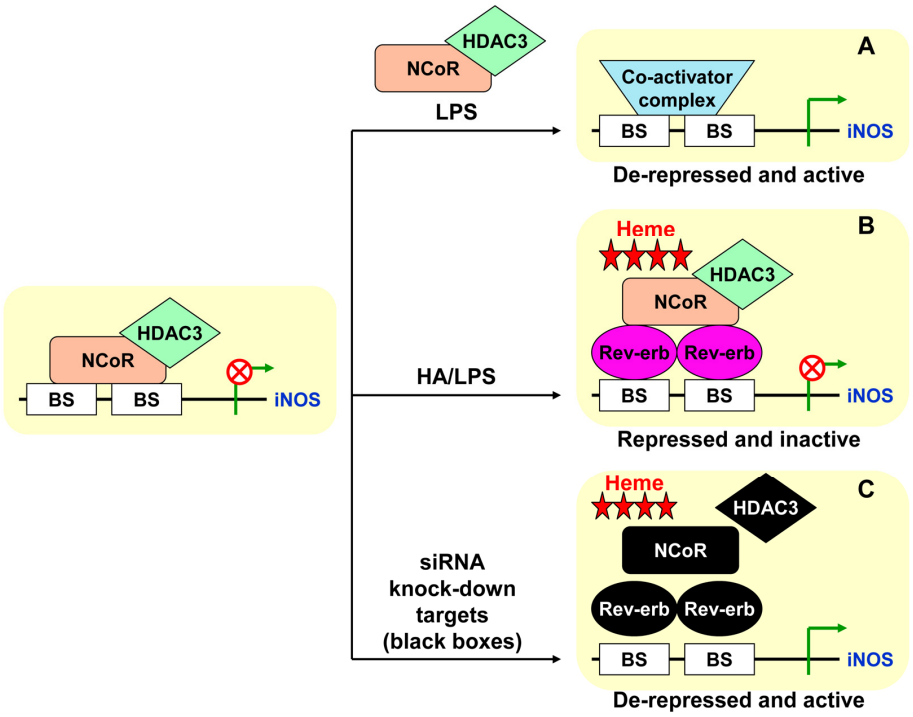


**Figure 7.3 Working hypothesis for HA facilitating Rev-erb-NCoR-HDAC3 mediated repression of the iNOS gene in BMDMs. A.** It is known that LPS stimulation of macrophages releases the NCoR-HDAC3 complex from the promoter region of the iNOS gene (Pascual et al., 2005). **B. *Working hypothesis:*** HA represses iNOS gene expression by stabilising Rev-erb-NCoR-HDAC3 binding on the promoter region of iNOS gene thereby preventing its degradation in response to LPS. **C.** An incisive way to test the working hypothesis is to perform si-RNA knockdown of either Rev-erb or NCoR or HDAC3 to avoid the formation of co-repressor complexes. **Abbreviation.** BS: Binding site.

## REFERENCE LIST


ABRAHAM, N. G. & KAPPAS, A. (2008) Pharmacological and Clinical Aspects of Heme Oxygenase. *Pharmacol Rev,* 60**,** 79-127.

AGUIRRE, V., WERNER, E. D., GIRAUD, J., LEE, Y. H., SHOELSON, S. E. & WHITE, M. F. (2002) Phosphorylation of Ser307 in Insulin Receptor Substrate-1 Blocks Interactions with the Insulin Receptor and Inhibits Insulin Action. *Journal of Biological Chemistry,* 277**,** 1531-1537.

AJIOKA, R. S., PHILLIPS, J. D. & KUSHNER, J. P. (2006) Biosynthesis of heme in mammals. *Biochimica et Biophysica Acta (BBA) - Molecular Cell Research,* 1763**,** 723-736.

AKTAN, F. (2004) iNOS-mediated nitric oxide production and its regulation. *Life Sciences,* 75.

ALBERTI, K., ASCHNER, P., ASSAL, J. P., BENNETT, P., GROOP, L., JERVELL, J., KANAZAWA, Y., KEEN, H., KLEIN, R., MBANYA, J. C., MCCARTY, D., MOTALA, A., X–R, P., RAMACHANDRAN, A., SAMAD, N., UNWIN, N., VARDI, P. & ZIMMET, P. (1999) Definition, diagnosis and classification of Diabetes Mellitus and its complications. Part 1: Diagnosis and classification of Diabetes Mellitus *Report of a WHO Consultation,* WHO/NCD/NCS/99.2**,** 59.

ALDERTON, W. K., COOPER, C. E. & KNOWLES, R. G. (2001) Nitric oxide synthases: structure, function and inhibition. *Biochem. J.,* 357**,** 593-615.

ANDREW, P. J. & MAYER, B. (1999) Enzymatic function of nitric oxide synthases. *Cardiovascular Research,* 43**,** 521-531.

APPLETON, S. D., CHRETIEN, M. L., MCLAUGHLIN, B. E., VREMAN, H. J., STEVENSON, D. K., BRIEN, J. F., NAKATSU, K., MAURICE, D. H. & MARKS, G. S. (1999) Selective Inhibition of Heme Oxygenase, without Inhibition of Nitric Oxide Synthase or Soluble Guanylyl Cyclase, by Metalloporphyrins at Low Concentrations. *Drug Metabolism and Disposition,* 27**,** 1214-1219.

ASHCROFT, F. M. & RORSMAN, P. (1989) Electrophysiology of the pancreatic beta cell. *Progress in Biophysics and Molecular Biology,* 54**,** 87-143.

BAEK, K. J., THIEL, B. A., LUCAS, S. & STUEHR, D. J. (1993) Macrophage nitric oxide synthase subunits. Purification, characterization, and role of prosthetic groups and substrate in regulating their association into a dimeric enzyme. *Journal of Biological Chemistry,* 268**,** 21120-9.

BANSAL, P. & WANG, Q. (2008) Insulin as a physiological modulator of glucagon secretion. *American Journal of Physiology - Endocrinology And Metabolism,* 295**,** E751-E761.

BANTING, F. G., BEST, C. H., COLLIP, J. B., CAMPBELL, W. R. & FLETCHER, A. A. (1922) Pancreatic extracts in the treatment of diabetes mellitus: preliminary report. *Canadian Medical Association Journal,* 12**,** 6.

BARINAGA, M. (1995) "Obese" protein slims mice. *Science,* 269**,** 475-476.

BARTHEL, A. & SCHMOLL, D. (2003) Novel concepts in insulin regulation of hepatic gluconeogenesis. *American Journal of Physiology - Endocrinology And Metabolism,* 285**,** E685-E692.

BEUTLER, B. (2004) Innate immunity: an overview. *Molecular Immunology,* 40**,** 15.

BLUMENTHAL, S. B., KIEMER, A. K., TIEGS, G., SEYFRIED, S., HÃ¶LTJE, M., BRANDT, B., HÃ¶LTJE, H.-D., ZAHLER, S. & VOLLMAR, A. M. (2005) Metalloporphyrins inactivate caspase-3 and -8. *The FASEB Journal,* 19**,** 1272-1279.

BOCCINI, F. & HEROLD, S. (2004) Mechanistic Studies of the Oxidation of Oxyhemoglobin by Peroxynitriteâ€ *Biochemistry,* 43**,** 16393-16404.

BODEN, G. & SHULMAN, G. I. (2002) Free fatty acids in obesity and type 2 diabetes: defining their role in the development of insulin resistance and β-cell dysfunction. *European Journal of Clinical Investigation,* 32**,** 14-23.

BONI-SCHNETZLER, M., BOLLER, S., DEBRAY, S., BOUZAKRI, K., MEIER, D. T., PRAZAK, R., KERR-CONTE, J., PATTOU, F., EHSES, J. A., SCHUIT, F. C. & DONATH, M. Y. (2009) Free Fatty Acids Induce a Proinflammatory Response in

Islets via the Abundantly Expressed Interleukin-1 Receptor I. *Endocrinology,* 150**,** 5218-5229.
BREDT, D. S., HWANG, P. M., GLATT, C. E., LOWENSTEIN, C., REED, R. R. & SNYDER, S. H. (1991) Cloned and expressed nitric oxide synthase structurally resembles cytochrome P-450 reductase. *Nature,* 351**,** 714-718.
BREDT, D. S. & SNYDER, S. H. (1990) Isolation of nitric oxide synthetase, a calmodulin-requiring enzyme. *Proceedings of the National Academy of Sciences,* 87**,** 682-685.
BROWN, M. S. & GOLDSTEIN, J. L. (2008) Selective versus Total Insulin Resistance: A Pathogenic Paradox. *Cell Metabolism,* 7**,** 95-96.
BRYAN, N. S., FERNANDEZ, B. O., BAUER, S. M., GARCIA-SAURA, M. F., MILSOM, A. B., RASSAF, T., MALONEY, R. E., BHARTI, A., RODRIGUEZ, J. & FEELISCH, M. (2005) Nitrite is a signaling molecule and regulator of gene expression in mammalian tissues. *Nat Chem Biol,* 1**,** 290-297.
BURNEY, S., CAULFIELD, J. L., NILES, J. C., WISHNOK, J. S. & TANNENBAUM, S. R. (1999) The chemistry of DNA damage from nitric oxide and peroxynitrite. *Mutation Research/Fundamental and Molecular Mechanisms of Mutagenesis,* 424**,** 37-49.
CHENG, A. Y. Y. & FANTUS, I. G. (2005) Oral antihyperglycemic therapy for type 2 diabetes mellitus. *Canadian Medical Association Journal,* 172**,** 213-226.
CHITRE, M. M. & BURKE, S. (2006) Treatment Algorithms and the Pharmacological Management of Type 2 Diabetes. *Diabetes Spectrum,* 19**,** 249-255.
CHO, H., ZHAO, X., HATORI, M., YU, R. T., BARISH, G. D., LAM, M. T., CHONG, L.-W., DITACCHIO, L., ATKINS, A. R., GLASS, C. K., LIDDLE, C., AUWERX, J., DOWNES, M., PANDA, S. & EVANS, R. M. (2012a) Regulation of circadian behaviour and metabolism by REV-ERB-[agr] and REV-ERB-[bgr]. *Nature,* advance online publication.
CHO, H., ZHAO, X., HATORI, M., YU, R. T., BARISH, G. D., LAM, M. T., CHONG, L.-W., DITACCHIO, L., ATKINS, A. R., GLASS, C. K., LIDDLE, C., AUWERX, J., DOWNES, M., PANDA, S. & EVANS, R. M. (2012b) Regulation of circadian behaviour and metabolism by REV-ERB-α and REV-ERB-β. *Nature,* 485**,** 123-127.
CHO, H. J., XIE, Q. W., CALAYCAY, J., MUMFORD, R. A., SWIDEREK, K. M., LEE, T. D. & NATHAN, C. (1992) Calmodulin is a subunit of nitric oxide synthase from macrophages. *The Journal of Experimental Medicine,* 176**,** 599-604.
CHOW, F., OZOLS, E., NIKOLIC-PATERSON, D. J., ATKINS, R. C. & TESCH, G. H. (2004) Macrophages in mouse type 2 diabetic nephropathy: Correlation with diabetic state and progressive renal injury. *Kidney Int,* 65**,** 116-128.
CINTI, S., MITCHELL, G., BARBATELLI, G., MURANO, I., CERESI, E., FALOIA, E., WANG, S., FORTIER, M., GREENBERG, A. S. & OBIN, M. S. (2005) Adipocyte death defines macrophage localization and function in adipose tissue of obese mice and humans. *Journal of Lipid Research,* 46**,** 2347-2355.
CLEE, S. M. & ATTIE, A. D. (2007) The Genetic Landscape of Type 2 Diabetes in Mice. *Endocrine Reviews,* 28**,** 48-83.
COLEMAN, D. (1978) Obese and diabetes: Two mutant genes causing diabetes-obesity syndromes in mice. *Diabetologia,* 14**,** 141-148.
COLEMAN, D. & HUMMEL, K. (1967) Studies with the mutation, diabetes, in the mouse. *Diabetologia,* 3**,** 238-248.
CORBETT, J. A. & MCDANIEL, M. L. (1995) Intraislet release of interleukin 1 inhibits beta cell function by inducing beta cell expression of inducible nitric oxide synthase. *The Journal of Experimental Medicine,* 181**,** 559-568.
CRANE, B. R., ARVAI, A. S., GHOSH, D. K., WU, C., GETZOFF, E. D., STUEHR, D. J. & TAINER, J. A. (1998) Structure of Nitric Oxide Synthase Oxygenase Dimer with Pterin and Substrate. *Science,* 279**,** 2121-2126.
DALTON, J., MCAULIFFE, C. A. & SLATER, D. H. (1972) Reaction between Molecular Oxygen and Photo-excited Protoporphyrin IX. *Nature,* 235**,** 388-388.
DAVIS, R. C., VAN NAS, A., CASTELLANI, L. W., ZHAO, Y., ZHOU, Z., WEN, P., YU, S., QI, H., ROSALES, M., SCHADT, E. E., BROMAN, K. W., PÃ©TERFY, M. S. & LUSIS, A. J. (2012) Systems genetics of susceptibility to obesity-induced diabetes in mice. *Physiological Genomics,* 44**,** 1-13.

DAVIS, R. J. (2000) Signal Transduction by the JNK Group of MAP Kinases. *Cell,* 103**,** 239-252.
DAY, C. (1999) Thiazolidinediones: a new class of antidiabetic drugs. *Diabetic Medicine,* 16**,** 179-192.
DONATH, M. Y., BONI-SCHNETZLER, M., ELLINGSGAARD, H. & EHSES, J. A. (2009) Islet Inflammation Impairs the Pancreatic b-Cell in Type 2 Diabetes. *Physiology,* 24**,** 325-331.
DONATH, M. Y., EHSES, J. A., MAEDLER, K., SCHUMANN, D. M., ELLINGSGAARD, H., EPPLER, E. & REINECKE, M. (2005) Mechanisms of b-Cell Death in Type 2 Diabetes. *Diabetes,* 54**,** S108-S113.
DONATH, M. Y., SCHUMANN, D. M., FAULENBACH, M., ELLINGSGAARD, H., PERREN, A. & EHSES, J. A. (2008) Islet Inflammation in Type 2 Diabetes. *Diabetes Care,* 31**,** S161-S164.
DONATH, M. Y. & SHOELSON, S. E. (2011) Type 2 diabetes as an inflammatory disease. *Nat Rev Immunol,* 11**,** 98-107.
DONNELLY, R., REED, M. J., AZHAR, S. & REAVEN, G. M. (1994) Expression of the major isoenzyme of protein kinase-C in skeletal muscle, nPKC theta, varies with muscle type and in response to fructose-induced insulin resistance. *Endocrinology,* 135**,** 2369-74.
DRONAVALLI, S., DUKA, I. & BAKRIS, G. L. (2008) The pathogenesis of diabetic nephropathy. *Nat Clin Pract End Met,* 4**,** 444-452.
DUGANI, C. B. & KLIP, A. (2005) Glucose transporter 4: cycling, compartments and controversies. *EMBO Rep,* 6**,** 1137-1142.
EFANOVA, I. B., ZAITSEV, S. V., ZHIVOTOVSKY, B., KÃ¶HLER, M., EFENDIÄ‡, S., ORRENIUS, S. & BERGGREN, P.-O. (1998) Glucose and Tolbutamide Induce Apoptosis in Pancreatic b-Cells. *Journal of Biological Chemistry,* 273**,** 33501-33507.
EHSES, J., MEIER, D., WUEEST, S., RYTKA, J., BOLLER, S., WIELINGA, P., SCHRAENEN, A., LEMAIRE, K., DEBRAY, S., VAN LOMMEL, L., POSPISILIK, J., TSCHOPP, O., SCHULTZE, S., MALIPIERO, U., ESTERBAUER, H., ELLINGSGAARD, H., RUTTI, S., SCHUIT, F., LUTZ, T., BONI-SCHNETZLER, M., KONRAD, D. & DONATH, M. (2010) Toll-like receptor 2-deficient mice are protected from insulin resistance and beta cell dysfunction induced by a high-fat diet. *Diabetologia,* 53**,** 1795-1806.
EHSES, J. A., LACRAZ, G., GIROIX, M. H., SCHMIDLIN, F., COULAUD, J., KASSIS, N., IRMINGER, J. C., KERGOAT, M., PORTHA, B., HOMO-DELARCHE, F. & DONATH, M. Y. (2009) IL-1 antagonism reduces hyperglycemia and tissue inflammation in the type 2 diabetic GK rat. *Proceedings of the National Academy of Sciences,* 106**,** 13998-14003.
EHSES, J. A., PERREN, A., EPPLER, E., RIBAUX, P., POSPISILIK, J. A., MAOR-CAHN, R., GUERIPEL, X., ELLINGSGAARD, H., SCHNEIDER, M. K., BIOLLAZ, G., FONTANA, A., REINECKE, M., HOMO-DELARCHE, F. & DONATH, M. Y. (2007a) Increased number of islet-associated macrophages in type 2 diabetes. *Diabetes,* 56**,** 2356-70.
EHSES, J. A., PERREN, A., EPPLER, E., RIBAUX, P., POSPISILIK, J. A., MAOR-CAHN, R., GUERIPEL, X., ELLINGSGAARD, H., SCHNEIDER, M. K. J., BIOLLAZ, G., FONTANA, A., REINECKE, M., HOMO-DELARCHE, F. & DONATH, M. Y. (2007b) Increased Number of Islet-Associated Macrophages in Type 2 Diabetes. *Diabetes,* 56**,** 2356-2370.
EMING, S. A., KRIEG, T. & DAVIDSON, J. M. (2007) Inflammation in Wound Repair: Molecular and Cellular Mechanisms. *J Invest Dermatol,* 127**,** 514-525.
ERICKSON, J. C., HOLLOPETER, G. & PALMITER, R. D. (1996) Attenuation of the Obesity Syndrome of ob/ob Mice by the Loss of Neuropeptide Y. *Science,* 274**,** 1704-1707.
FADOK, V. A., BRATTON, D. L., KONOWAL, A., FREED, P. W., WESTCOTT, J. Y. & HENSON, P. M. (1998) Macrophages that have ingested apoptotic cells in vitro inhibit proinflammatory cytokine production through autocrine/paracrine mechanisms involving TGF-beta, PGE2, and PAF. *The Journal of Clinical Investigation,* 101**,** 890-898.

FEBBRAIO, M. A. (2007) gp130 receptor ligands as potential therapeutic targets for obesity. *The Journal of Clinical Investigation,* 117**,** 841-849.
FENG, C. (2012) Mechanism of nitric oxide synthase regulation: Electron transfer and interdomain interactions. *Coordination Chemistry Reviews,* 256**,** 393-411.
FERENBACH, D. A., NKEJABEGA, N. C. J., MCKAY, J., CHOUDHARY, A. K., VERNON, M. A., BEESLEY, M. F., CLAY, S., CONWAY, B. C., MARSON, L. P., KLUTH, D. C. & HUGHES, J. (2011) The induction of macrophage hemeoxygenase-1 is protective during acute kidney injury in aging mice. *Kidney Int,* 79**,** 966-976.
FERRANNINI, E. (1998) Insulin Resistance versus Insulin Deficiency in Non-Insulin-Dependent Diabetes Mellitus: Problems and Prospects. *Endocrine Reviews,* 19**,** 477-490.
FONTANA, L., EAGON, J. C., TRUJILLO, M. E., SCHERER, P. E. & KLEIN, S. (2007) Visceral Fat Adipokine Secretion Is Associated With Systemic Inflammation in Obese Humans. *Diabetes,* 56**,** 1010-1013.
FORAN, S. E. & ÃBEL, G. (2003) Guide to Porphyrias. *American Journal of Clinical Pathology. Pathology Patterns Reviews.,* 119**,** S86-S93.
FORSTERMANN, U. (2008) Oxidative stress in vascular disease: causes, defense mechanisms and potential therapies. *Nat Clin Pract Cardiovasc Med,* 5**,** 338-349.
FORSTERMANN, U. & MUNZEL, T. (2006) Endothelial Nitric Oxide Synthase in Vascular Disease. *Circulation,* 113**,** 1708-1714.
FOWLER, M. J. (2008) Microvascular and Macrovascular Complications of Diabetes. *Clinical Diabetes,* 26**,** 77-82.
FRIEDMAN, J. M. (1997) The alphabet of weight control. *Nature,* 385**,** 119-120.
FRIEDMAN, J. M. & HALAAS, J. L. (1998) Leptin and the regulation of body weight in mammals. *Nature,* 395**,** 763-770.
FURUYAMA, K., KANEKO, K. & VARGAS V, P. D. (2007) Heme as a Magnificent Molecule with Multiple Missions: Heme Determines Its Own Fate and Governs Cellular Homeostasis. *The Tohoku Journal of Experimental Medicine,* 213**,** 16.
GALBRAITH, R. A. & KAPPAS, A. (1989) Regulation of food intake and body weight by cobalt porphyrins in animals. *Proceedings of the National Academy of Sciences,* 86**,** 7653-7657.
GALLEN, I. (2004) Review: The evolution of insulin treatment in type 1 diabetes: the advent of analogues. *The British Journal of Diabetes & Vascular Disease,* 4**,** 378-381.
GAVIN, J. R., ALBERTI, K. G. M. M., DAVIDSON, M. B., DEFRONZO, R. A., DRASH, A., GABBE, S. G., GENUTH, S., HARRIS, M. I., KAHN, R., KEEN, H., KNOWLER, W. C., LEBOVITZ, H., MACLAREN, N. K., PALMER, J. P., RASKIN, P., RIZZA, R. A. & STERN, M. P. (2002) Report of the Expert Committee on the Diagnosis and Classification of Diabetes Mellitus. *Diabetes Care,* 25**,** s5-s20.
GENUTH, S. M., PRZYBYLSKI, R. J. & ROSENBERG, D. M. (1971) Insulin Resistance in Genetically Obese, Hyperglycemic Mice. *Endocrinology,* 88**,** 1230-1238.
GERBER, J. S. & MOSSER, D. M. (2001) Reversing Lipopolysaccharide Toxicity by Ligating the Macrophage Fc{{gamma}} Receptors. *J Immunol,* 166**,** 6861-6868.
GIBBS, J. E., BLAIKLEY, J., BEESLEY, S., MATTHEWS, L., SIMPSON, K. D., BOYCE, S. H., FARROW, S. N., ELSE, K. J., SINGH, D., RAY, D. W. & LOUDON, A. S. I. (2012) The nuclear receptor REV-ERBα mediates circadian regulation of innate immunity through selective regulation of inflammatory cytokines. *Proceedings of the National Academy of Sciences,* 109**,** 6.
GIRARD, J. (2006) The Inhibitory Effects of Insulin on Hepatic Glucose Production Are Both Direct and Indirect. *Diabetes,* 55**,** S65-S69.
GOETSCH, C. A. & BISSELL, D. M. (1986) Instability of Hematin Used in the Treatment of Acute Hepatic Porphyria. *New England Journal of Medicine,* 315**,** 235-238.
GOODPASTER, B. H., THAETE, F. L., SIMONEAU, J. A. & KELLEY, D. E. (1997) Subcutaneous abdominal fat and thigh muscle composition predict insulin sensitivity independently of visceral fat. *Diabetes,* 46**,** 1579-1585.
GREEN, H. & MEUTH, M. (1974) An established pre-adipose cell line and its differentiation in culture. *Cell,* 3**,** 127-133.
GRUNDEMAR, L. & NY, L. (1997) Pitfalls using metalloporphyrins in carbon monoxide research. *Trends in Pharmacological Sciences,* 18**,** 193-195.

HAMILTON, J. W., BEMENT, W. J., SINCLAIR, P. R., SINCLAIR, J. F., ALCEDO, J. A. & WETTERHAHN, K. E. (1991) Heme regulates hepatic 5-aminolevulinate synthase mRNA expression by decreasing mRNA half-life and not by altering its rate of transcription. *Archives of Biochemistry and Biophysics,* 289**,** 387-392.

HAN, S.-B. & LEE, J. (2009) Anti-inflammatory effect of Trichostatin-A on murine bone marrow-derived macrophages. *Archives of Pharmacal Research,* 32**,** 613-624.

HANDSCHIN, C., LIN, J., RHEE, J., PEYER, A.-K., CHIN, S., WU, P.-H., MEYER, U. A. & SPIEGELMAN, B. M. (2005) Nutritional Regulation of Hepatic Heme Biosynthesis and Porphyria through PGC-1alpha. *Cell,* 122**,** 505-515.

HANSSON, G. R. K. (2005) Inflammation, Atherosclerosis, and Coronary Artery Disease. *New England Journal of Medicine,* 352**,** 1685-1695.

HARDING, H. P. & RON, D. (2002) Endoplasmic Reticulum Stress and the Development of Diabetes. *Diabetes,* 51**,** S455-S461.

HAVERSEN, L., DANIELSSON, K. N. N., FOGELSTRAND, L. & WIKLUND, O. (2009) Induction of proinflammatory cytokines by long-chain saturated fatty acids in human macrophages. *Atherosclerosis,* 202**,** 382-393.

HAWLEY, S. A., GADALLA, A. E., OLSEN, G. S. & HARDIE, D. G. (2002) The Antidiabetic Drug Metformin Activates the AMP-Activated Protein Kinase Cascade via an Adenine Nucleotide-Independent Mechanism. *Diabetes,* 51**,** 2420-2425.

HEILBRONN, L., SMITH, S. R. & RAVUSSIN, E. (2004) Failure of fat cell proliferation, mitochondrial function and fat oxidation results in ectopic fat storage, insulin resistance and type II diabetes mellitus. *Int J Obes Relat Metab Disord,* 28**,** S12-S21.

HENNINGSSON, R. & LUNDQUIST, I. (1998) Arginine-induced insulin release is decreased and glucagon increased in parallel with islet NO production. *American Journal of Physiology - Endocrinology And Metabolism,* 275**,** E500-E506.

HENNINGSSON, R., SALEHI, A. & LUNDQUIST, I. (2002) Role of nitric oxide synthase isoforms in glucose-stimulated insulin release. *Am J Physiol Cell Physiol,* 283**,** C296-304.

HERMAN, M. A. & KAHN, B. B. (2006) Glucose transport and sensing in the maintenance of glucose homeostasis and metabolic harmony. *The Journal of Clinical Investigation,* 116**,** 1767-1775.

HIBBS, J. B., TAINTOR, R. R. & VAVRIN, Z. (1987) Macrophage cytotoxicity: role for L-arginine deiminase and imino nitrogen oxidation to nitrite. *Science,* 235**,** 473-476.

HIMSWORTH, H. P. (1936) DIABETES MELLITUS : ITS DIFFERENTIATION INTO INSULIN-SENSITIVE AND INSULIN-INSENSITIVE TYPES. *The Lancet,* 227**,** 127-130.

HOMO-DELARCHE, F. O., CALDERARI, S., IRMINGER, J.-C., GANGNERAU, M.-N. L., COULAUD, J., RICKENBACH, K., DOLZ, M., HALBAN, P., PORTHA, B. & SERRADAS, P. (2006) Islet Inflammation and Fibrosis in a Spontaneous Model of Type 2 Diabetes, the GK Rat. *Diabetes,* 55**,** 1625-1633.

HORI, R., KASHIBA, M., TOMA, T., YACHIE, A., GODA, N., MAKINO, N., SOEJIMA, A., NAGASAWA, T., NAKABAYASHI, K. & SUEMATSU, M. (2002) Gene transfection of H25A mutant heme oxygenase-1 protects cells against hydroperoxide-induced cytotoxicity. *J Biol Chem,* 277**,** 10712-8.

HORTON, J. D., GOLDSTEIN, J. L. & BROWN, M. S. (2002) SREBPs: activators of the complete program of cholesterol and fatty acid synthesis in the liver. *The Journal of Clinical Investigation,* 109**,** 1125-1131.

HOSOGAI, N., FUKUHARA, A., OSHIMA, K., MIYATA, Y., TANAKA, S., SEGAWA, K., FURUKAWA, S., TOCHINO, Y., KOMURO, R., MATSUDA, M. & SHIMOMURA, I. (2007) Adipose Tissue Hypoxia in Obesity and Its Impact on Adipocytokine Dysregulation. *Diabetes,* 56**,** 901-911.

HOTAMISLIGIL, G. S. (2006) Inflammation and metabolic disorders. *Nature,* 444**,** 860-867.

HOTAMISLIGIL, G. S., ARNER, P., CARO, J. F., ATKINSON, R. L. & SPIEGELMAN, B. M. (1995) Increased adipose tissue expression of tumor necrosis factor-alpha in human obesity and insulin resistance. *The Journal of Clinical Investigation,* 95**,** 2409-2415.

HOTAMISLIGIL, G. S., SHARGILL, N. S. & SPIEGELMAN, B. M. (1993) Adipose expression of tumor necrosis factor-alpha: direct role in obesity-linked insulin resistance. *Science,* 259**,** 87-91.

HUANG, W., GHISLETTI, S., SAIJO, K., GANDHI, M., AOUADI, M., TESZ, G. J., ZHANG, D. X., YAO, J., CZECH, M. P., GOODE, B. L., ROSENFELD, M. G. & GLASS, C. K. (2011) Coronin 2A mediates actin-dependent de-repression of inflammatory response genes. *Nature,* 470**,** 414-418.

HUMMEL, K. P., DICKIE, M. M. & COLEMAN, D. L. (1966) Diabetes, a New Mutafton in the Mouse. *Science,* 153**,** 1127-1128.

INADA, S., KANEKO, S., SUZUKI, K., MIYAZAKI, J.-I., ASAKURA, H. & FUJIWARA, M. (1996) Rectification of diabetic state in C57BL/KsJ-db/db mice by the implantation of pancreatic beta cell line MIN6. *Diabetes Research and Clinical Practice,* 32**,** 125-133.

JAGER, J., GRÃ©MEAUX, T., CORMONT, M., LE MARCHAND-BRUSTEL, Y. & TANTI, J.-F. O. (2007) Interleukin-1b-Induced Insulin Resistance in Adipocytes through Down-Regulation of Insulin Receptor Substrate-1 Expression. *Endocrinology,* 148**,** 241-251.

JONES, P. M. & PERSAUD, S. J. (1998) Protein Kinases, Protein Phosphorylation, and the Regulation of Insulin Secretion from Pancreatic Beta Cells. *Endocrine Reviews,* 19**,** 429-461.

JONES, R. L. (1986) Hematin-derived anticoagulant. Generation in vitro and in vivo. *The Journal of Experimental Medicine,* 163**,** 724-739.

JORDAN, W. J., WALKER, J. M. & RAPLEY, R. (2005) Enzyme-Linked Immunosorbent Assay Medical Biomethods Handbook. Humana Press.

KADOWAKI, T., YAMAUCHI, T., KUBOTA, N., HARA, K., UEKI, K. & TOBE, K. (2006) Adiponectin and adiponectin receptors in insulin resistance, diabetes, and the metabolic syndrome. *The Journal of Clinical Investigation,* 116**,** 1784-1792.

KAHN, B. B. & FLIER, J. S. (2000) Obesity and insulin resistance. *The Journal of Clinical Investigation,* 106**,** 473-481.

KAHN, S. E., HULL, R. L. & UTZSCHNEIDER, K. M. (2006) Mechanisms linking obesity to insulin resistance and type 2 diabetes. *Nature,* 444**,** 840-846.

KASUGA, M., OGAWA, W. & OHARA, T. (2003) Tissue glycogen content and glucose intolerance. *The Journal of Clinical Investigation,* 111**,** 1282-1284.

KATO, Y., MIURA, Y., YAMAMOTO, N., OZAKI, N. & OISO, Y. (2003) Suppressive effects of a selective inducible nitric oxide synthase (iNOS) inhibitor on pancreatic beta-cell dysfunction. *Diabetologia,* 46**,** 1228-1233.

KAUPPINEN, R. & VON UND ZU FRAUNBERG, M. (2002) Molecular and Biochemical Studies of Acute Intermittent Porphyria in 196 Patients and Their Families. *Clinical Chemistry,* 48**,** 1891-1900.

KELM, M. (1999) Nitric oxide metabolism and breakdown. *Biochimica et Biophysica Acta (BBA) - Bioenergetics,* 1411**,** 273-289.

KIDO, Y., NAKAE, J. & ACCILI, D. (2001) The Insulin Receptor and Its Cellular Targets. *Journal of Clinical Endocrinology & Metabolism,* 86**,** 972-979.

KIM, D. H., BURGESS, A. P., LI, M., TSENOVOY, P. L., ADDABBO, F., MCCLUNG, J. A., PURI, N. & ABRAHAM, N. G. (2008) Heme Oxygenase-Mediated Increases in Adiponectin Decrease Fat Content and Inflammatory Cytokines Tumor Necrosis Factor-α and Interleukin-6 in Zucker Rats and Reduce Adipogenesis in Human Mesenchymal Stem Cells. *Journal of Pharmacology and Experimental Therapeutics,* 325**,** 833-840.

KIM, M.-K., KIM, H.-S., LEE, I.-K. & PARK, K.-G. (2012) Endoplasmic Reticulum Stress and Insulin Biosynthesis: A Review. *Experimental Diabetes Research,* 2012.

KIMMEL, B. & INZUCCHI, S. E. (2005) Oral Agents for Type 2 Diabetes: An Update. *Clinical Diabetes,* 23**,** 64-76.

KJORHOLT, C., AKERFELDT, M. C., BIDEN, T. J. & LAYBUTT, D. R. (2005) Chronic Hyperglycemia, Independent of Plasma Lipid Levels, Is Sufficient for the Loss of b-Cell Differentiation and Secretory Function in the db/db Mouse Model of Diabetes. *Diabetes,* 54**,** 2755-2763.

KOLLURI, S., SADLON, T. J., MAY, B. K. & BONKOVSKY, H. L. (2005) Haem repression of the housekeeping 5-aminolaevulinic acid synthase gene in the hepatoma cell line LMH. *Biochem J.,* 392**,** 7.

KUMAR, N., SOLT, L. A., WANG, Y., ROGERS, P. M., BHATTACHARYYA, G., KAMENECKA, T. M., STAYROOK, K. R., CRUMBLEY, C., FLOYD, Z. E., GIMBLE, J. M., GRIFFIN, P. R. & BURRIS, T. P. (2010) Regulation of Adipogenesis by Natural and Synthetic REV-ERB Ligands. *Endocrinology,* 151**,** 3015-3025.

KWON, N. S., NATHAN, C. F., GILKER, C., GRIFFITH, O. W., MATTHEWS, D. E. & STUEHR, D. J. (1990) L-citrulline production from L-arginine by macrophage nitric oxide synthase. The ureido oxygen derives from dioxygen. *Journal of Biological Chemistry,* 265**,** 13442-13445.

LARSEN, C. M., FAULENBACH, M., VAAG, A., VÃ¸LUND, A., EHSES, J. A., SEIFERT, B., MANDRUP-POULSEN, T. & DONATH, M. Y. (2007) Interleukin-1-Receptor Antagonist in Type 2 Diabetes Mellitus. *New England Journal of Medicine,* 356**,** 1517-1526.

LAYBUTT, D. R., KANETO, H., HASENKAMP, W., GREY, S., JONAS, J.-C., SGROI, D. C., GROFF, A., FERRAN, C., BONNER-WEIR, S., SHARMA, A. & WEIR, G. C. (2002) Increased Expression of Antioxidant and Antiapoptotic Genes in Islets That May Contribute to Î²-Cell Survival During Chronic Hyperglycemia. *Diabetes,* 51**,** 413-423.

LAZAR, M. A. (1999) PPARγ in Adipocyte Differentiation. *Journal of Animal Science,* 77**,** 16-22.

LEBOVITZ, H. E. (2002) Review: Type 2 diabetes: how far have we come? *The British Journal of Diabetes & Vascular Disease,* 2**,** 446-449.

LEDRU, F., DUCIMETIÈRE, P., BATTAGLIA, S., COURBON, D., BEVERELLI, F., GUIZE, L., GUERMONPREZ, J.-L. & DIÉBOLD, B. (2001) New diagnostic criteria for diabetes and coronary artery disease: insights from an angiographic study. *Journal of the American College of Cardiology,* 37**,** 1543-1550.

LEE, J. Y., SOHN, K. H., RHEE, S. H. & HWANG, D. (2001) Saturated Fatty Acids, but Not Unsaturated Fatty Acids, Induce the Expression of Cyclooxygenase-2 Mediated through Toll-like Receptor 4. *Journal of Biological Chemistry,* 276**,** 16683-16689.

LEE, T.-S. & CHAU, L.-Y. (2002) Heme oxygenase-1 mediates the anti-inflammatory effect of interleukin-10 in mice. *Nat Med,* 8**,** 240-246.

LEE, T.-S., TSAI, H.-L. & CHAU, L.-Y. (2003) Induction of Heme Oxygenase-1 Expression in Murine Macrophages Is Essential for the Anti-inflammatory Effect of Low Dose 15-Deoxy-{Delta}12,14-prostaglandin J2. *J. Biol. Chem.,* 278**,** 19325-19330.

LEVERE, R. D., MARTASEK, P., ESCALANTE, B., SCHWARTZMAN, M. L. & ABRAHAM, N. G. (1990) Effect of heme arginate administration on blood pressure in spontaneously hypertensive rats. *The Journal of Clinical Investigation,* 86**,** 213-219.

LI, M., HYUN KIM, D., TSENOVOY, P. L., PETERSON, S. J., REZZANI, R., RODELLA, L. F., ARONOW, W. S., IKEHARA, S. & ABRAHAM, N. G. (2008) Treatment of Obese Diabetic Mice with an Heme Oxygenase Inducer Reduces Visceral and Subcutaneous Adiposity, Increases Adiponectin Levels and Improves Insulin Sensitivity and Glucose Tolerance. *Diabetes*.

LIN, Q., WEIS, S., YANG, G., WENG, Y.-H., HELSTON, R., RISH, K., SMITH, A., BORDNER, J., POLTE, T., GAUNITZ, F. & DENNERY, P. A. (2007) Heme Oxygenase-1 Protein Localizes to the Nucleus and Activates Transcription Factors Important in Oxidative Stress. *Journal of Biological Chemistry,* 282**,** 20621-20633.

LIST, B. M., KLÖSCH, B., VÖLKER, C., GORREN, A. C., SESSA, W. C., WERNER, E. R., KUKOVETZ, W. R., SCHMIDT, K. & MAYER, B. (1997) Characterization of bovine endothelial nitric oxide synthase as a homodimer with down-regulated uncoupled NADPH oxidase activity: tetrahydrobiopterin binding kinetics and role of haem in dimerization. *Biochem J.,* 323**,** 7.

LOWENSTEIN, C. J. & PADALKO, E. (2004) iNOS (NOS2) at a glance. *Journal of Cell Science,* 117**,** 2865-2867.

LUFT, R. (1989) Oskar Minkowski: Discovery of the pancreatic origin of diabetes, 1889. *Diabetologia,* 32**,** 399-401.

LUMENG, C. N., BODZIN, J. L. & SALTIEL, A. R. (2007) Obesity induces a phenotypic switch in adipose tissue macrophage polarization. *The Journal of Clinical Investigation,* 117**,** 175-184.

MA, J. L., YANG, P. Y., RUI, Y. C., LU, L., KANG, H. & ZHANG, J. (2007) Hemin modulates cytokine expressions in macrophage-derived foam cells via heme oxygenase-1 induction. *Journal of Pharmacological Sciences,* 103**,** 6.

MACDONALD, P. E. & RORSMAN, P. (2006) Oscillations, Intercellular Coupling, and Insulin Secretion in Pancreatic Beta-Cells. *PLoS Biol,* 4**,** e49.

MAEDA, N., TAKAHASHI, M., FUNAHASHI, T., KIHARA, S., NISHIZAWA, H., KISHIDA, K., NAGARETANI, H., MATSUDA, M., KOMURO, R., OUCHI, N., KURIYAMA, H., HOTTA, K., NAKAMURA, T., SHIMOMURA, I. & MATSUZAWA, Y. (2001) PPARg Ligands Increase Expression and Plasma Concentrations of Adiponectin, an Adipose-Derived Protein. *Diabetes,* 50**,** 2094-2099.

MAEDLER, K., SERGEEV, P., RIS, F. D. R., OBERHOLZER, J., JOLLER-JEMELKA, H. I., SPINAS, G. A., KAISER, N., HALBAN, P. A. & DONATH, M. Y. (2002) Glucose-induced b cell production of IL-1b contributes to glucotoxicity in human pancreatic islets. *The Journal of Clinical Investigation,* 110**,** 851-860.

MAGNANI, M., ROSSI, L., STOCCHI, V., CUCCHIARINI, L., PIACENTINI, G. & FORNAINI, G. (1988) Effect of age on some properties of mice erythrocytes. *Mechanisms of Ageing and Development,* 42**,** 37-47.

MAINES, M. D. (2005) The Heme Oxygenase System: Update 2005. *ANTIOXIDANTS & REDOX SIGNALING,* 7.

MAINES, M. D. & GIBBS, P. E. M. (2005) 30 some years of heme oxygenase: From a "molecular wrecking ball" to a "mesmerizing" trigger of cellular events. *Biochemical and Biophysical Research Communications,* 338**,** 568-577.

MAINES, M. D. & KAPPAS, A. (1975) Cobalt stimulation of heme degradation in the liver. Dissociation of microsomal oxidation of heme from cytochrome P-450. *Journal of Biological Chemistry,* 250**,** 4171-7.

MARTINON, F., BURNS, K. & TSCHOPP, J. (2002) The Inflammasome: A Molecular Platform Triggering Activation of Inflammatory Caspases and Processing of proIL-². *Molecular cell,* 10**,** 417-426.

MATSUMOTO, M., HAN, S., KITAMURA, T. & ACCILI, D. (2006) Dual role of transcription factor FoxO1 in controlling hepatic insulin sensitivity and lipid metabolism. *The Journal of Clinical Investigation,* 116**,** 2464-2472.

MCNALLY, S. J., HARRISON, E. M., ROSS, J. A., GARDEN, O. J. & WIGMORE, S. J. (2007) Curcumin induces heme oxygenase 1 through generation of reactive oxygen species, p38 activation and phosphatase inhibition. *International Journal of Molecular Medicine,* 19**,** 8.

MCNALLY, S. J., ROSS, J. A., JAMES GARDEN, O. & WIGMORE, S. J. (2004) Optimization of the paired enzyme assay for heme oxygenase activity. *Analytical Biochemistry,* 332**,** 398-400.

MENG, F. & LOWELL, C. A. (1997) Lipopolysaccharide (LPS)-induced Macrophage Activation and Signal Transduction in the Absence of Src-Family Kinases Hck, Fgr, and Lyn. *The Journal of Experimental Medicine,* 185**,** 1661-1670.

MOLNAR, Z. (2004) Thomas Willis (1621-1675), the founder of clinical neuroscience. *Nat Rev Neurosci,* 5**,** 329-335.

MORIMOTO, C., TSUJITA, T. & OKUDA, H. (1998) Antilipolytic actions of insulin on basal and hormone-induced lipolysis in rat adipocytes. *Journal of Lipid Research,* 39**,** 957-962.

MORITA, T. & KOUREMBANAS, S. (1995) Endothelial cell expression of vasoconstrictors and growth factors is regulated by smooth muscle cell-derived carbon monoxide. *The Journal of Clinical Investigation,* 96**,** 2676-2682.

MORITA, T., PERRELLA, M. A., LEE, M. E. & KOUREMBANAS, S. (1995) Smooth muscle cell-derived carbon monoxide is a regulator of vascular cGMP. *Proceedings of the National Academy of Sciences,* 92**,** 1475-1479.

MORRIS, S. M. & BILLIAR, T. R. (1994) New insights into the regulation of inducible nitric oxide synthesis. *American Journal of Physiology - Endocrinology And Metabolism,* 266**,** E829-E839.

MORSE, D. & CHOI, A. M. K. (2002) Heme Oxygenase-1 . The "Emerging Molecule" Has Arrived. *Am. J. Respir. Cell Mol. Biol.,* 27**,** 8-16.
MOSEN, H., SALEHI, A., HENNINGSSON, R. & LUNDQUIST, I. (2006) Nitric oxide inhibits, and carbon monoxide activates, islet acid a-glucoside hydrolase activities in parallel with glucose-stimulated insulin secretion. *Journal of Endocrinology,* 190**,** 681-693.
MUSTAJOKI, P. & NORDMANN, Y. (1993) Early Administration of Heme Arginate for Acute Porphyric Attacks. *Arch Intern Med,* 153**,** 2004-2008.
MYERS, M. G., COWLEY, M. A. & MUNZBERG, H. (2008) Mechanisms of Leptin Action and Leptin Resistance. *Annal Review of Physiology,* 70**,** 19.
NATH, K. A. (2006) Heme oxygenase-1: A provenance for cytoprotective pathways in the kidney and other tissues. *Kidney Int,* 70**,** 432-443.
NDISANG, J. F. (2010) Role of Heme Oxygenase in Inflammation, Insulin-Signalling, Diabetes and Obesity. *Mediators of Inflammation,* 2010.
NDISANG, J. F. & JADHAV, A. (2009) Up-Regulating the Hemeoxygenase System Enhances Insulin Sensitivity and Improves Glucose Metabolism in Insulin-Resistant Diabetes in Goto-Kakizaki Rats. *Endocrinology,* 150**,** 2627-2636.
NDISANG, J. F., LANE, N. & JADHAV, A. (2009a) The Heme Oxygenase System Abates Hyperglycemia in Zucker Diabetic Fatty Rats by Potentiating Insulin-Sensitizing Pathways. *Endocrinology,* 150**,** 2098-2108.
NDISANG, J. F., LANE, N. & JADHAV, A. (2009b) Upregulation of the heme oxygenase system ameliorates postprandial and fasting hyperglycemia in type 2 diabetes. *American Journal of Physiology - Endocrinology And Metabolism,* 296**,** E1029-E1041.
NICOLAI, A., LI, M., KIM, D. H., PETERSON, S. J., VANELLA, L., POSITANO, V., GASTALDELLI, A., REZZANI, R., RODELLA, L. F., DRUMMOND, G., KUSMIC, C., L'ABBATE, A., KAPPAS, A. & ABRAHAM, N. G. (2009) Heme Oxygenase-1 Induction Remodels Adipose Tissue and Improves Insulin Sensitivity in Obesity-Induced Diabetic Rats. *Hypertension,* 53**,** 508-515.
NOLAN, C., LEAHY, J., DELGHINGARO-AUGUSTO, V., MOIBI, J., SONI, K., PEYOT, M. L., FORTIER, M., GUAY, C., LAMONTAGNE, J., BARBEAU, A., PRZYBYTKOWSKI, E., JOLY, E., MASIELLO, P., WANG, S., MITCHELL, G. & PRENTKI, M. (2006) Beta cell compensation for insulin resistance in Zucker fatty rats: increased lipolysis and fatty acid signalling. *Diabetologia,* 49**,** 2120-2130.
OKUNO, A., TAMEMOTO, H., TOBE, K., UEKI, K., MORI, Y., IWAMOTO, K., UMESONO, K., AKANUMA, Y., FUJIWARA, T., HORIKOSHI, H., YAZAKI, Y. & KADOWAKI, T. (1998) Troglitazone increases the number of small adipocytes without the change of white adipose tissue mass in obese Zucker rats. *The Journal of Clinical Investigation,* 101**,** 1354-1361.
ORCI, L., RAVAZZOLA, M., AMHERDT, M., YANAIHARA, C., YANAIHARA, N., HALBAN, P., RENOLD, A. E. & PERRELET, A. (1984) Insulin, not C-peptide (proinsulin), is present in crinophagic bodies of the pancreatic B-cell. *The Journal of Cell Biology,* 98**,** 222-228.
ORCI, L., RAVAZZOLA, M., STORCH, M. J., ANDERSON, R. G. W., VASSALLI, J. D. & PERRELET, A. (1987) Proteolytic maturation of insulin is a post-Golgi event which occurs in acidifying clathrin-coated secretory vesicles. *Cell,* 49**,** 865-868.
OTTERBEIN, L. E., BACH, F. H., ALAM, J., SOARES, M., TAO LU, H., WYSK, M., DAVIS, R. J., FLAVELL, R. A. & CHOI, A. M. K. (2000) Carbon monoxide has anti-inflammatory effects involving the mitogen-activated protein kinase pathway. *Nat Med,* 6**,** 422-428.
OTTERBEIN, L. E., OTTERBEIN, S. L., IFEDIGBO, E., LIU, F., MORSE, D. E., FEARNS, C., ULEVITCH, R. J., KNICKELBEIN, R., FLAVELL, R. A. & CHOI, A. M. (2003) MKK3 Mitogen-Activated Protein Kinase Pathway Mediates Carbon Monoxide-Induced Protection Against Oxidant-Induced Lung Injury. *The American Journal of Pathology,* 163**,** 2555-2563.
OWENS, D. R., ZINMAN, B. & BOLLI, G. B. (2001) Insulins today and beyond. *The Lancet,* 358**,** 739-746.
PACHER, P., BECKMAN, J. S. & LIAUDET, L. (2007) Nitric Oxide and Peroxynitrite in Health and Disease. *Physiological Reviews,* 87**,** 315-424.

PAE, H., KIM, E, AND CHUNG, H (2008) Integrative Survival Response Evoked by Heme Oxygenase-1 and Heme Metabolites. *J. Clin. Biochem. Nutr,* 42**,** 7.

PALMER, R. M. J., FERRIGE, A. G. & MONCADA, S. (1987) Nitric oxide release accounts for the biological activity of endothelium-derived relaxing factor. *Nature,* 327**,** 524-526.

PANCHAL, S. K. & BROWN, L. (2010) Rodent Models forMetabolic Syndrome Research. *Journal of Biomedicine and Biotechnology,* 2011**,** 14.

PASCUAL, G., FONG, A. L., OGAWA, S., GAMLIEL, A., LI, A. C., PERISSI, V., ROSE, D. W., WILLSON, T. M., ROSENFELD, M. G. & GLASS, C. K. (2005) A SUMOylation-dependent pathway mediates transrepression of inflammatory response genes by PPAR-[gamma]. *Nature,* 437**,** 759-763.

PATEL, M. & DAY, B. J. (1999) Metalloporphyrin class of therapeutic catalytic antioxidants. *Trends in Pharmacological Sciences,* 20**,** 359-364.

PELUFFO, G. & RADI, R. (2007) Biochemistry of protein tyrosine nitration in cardiovascular pathology. *Cardiovascular Research,* 75**,** 291-302.

PIROLA, L., JOHNSTON, A. & VAN OBBERGHEN, E. (2004) Modulation of insulin action. *Diabetologia,* 47**,** 170-184.

POBLETE-GUTIÉRREZ, P., WIEDERHOLT, T., MERK, H. F. & FRANK, J. (2006) The porphyrias: clinical presentation, diagnosis and treatment. *European journal of dermatology EJD* 16**,** 10.

POH-FITZPATRICK, M. B. (1985) Porphyrin-sensitized cutaneous photosensitivity: Pathogenesis and treatment. *Clinics in Dermatology,* 3**,** 41-82.

POITOUT, V., HAGMAN, D., STEIN, R., ARTNER, I., ROBERTSON, R. P. & HARMON, J. S. (2006) Regulation of the Insulin Gene by Glucose and Fatty Acids. *The Journal of Nutrition,* 136**,** 873-876.

POLTORAK, A., HE, X., SMIRNOVA, I., LIU, M.-Y., HUFFEL, C. V., DU, X., BIRDWELL, D., ALEJOS, E., SILVA, M., GALANOS, C., FREUDENBERG, M., RICCIARDI-CASTAGNOLI, P., LAYTON, B. & BEUTLER, B. (1998) Defective LPS Signaling in C3H/HeJ and C57BL/10ScCr Mice: Mutations in Tlr4 Gene. *Science,* 282**,** 2085-2088.

POSS, K. D. & TONEGAWA, S. (1997) Heme oxygenase 1 is required for mammalian iron reutilization. *Proceedings of the National Academy of Sciences,* 94**,** 10919-10924.

PRENTKI, M. & NOLAN, C. J. (2006) Islet b-cell failure in type 2 diabetes. *The Journal of Clinical Investigation,* 116**,** 1802-1812.

PUIGSERVER, P., RHEE, J., DONOVAN, J., WALKEY, C. J., YOON, J. C., ORIENTE, F., KITAMURA, Y., ALTOMONTE, J., DONG, H., ACCILI, D. & SPIEGELMAN, B. M. (2003) Insulin-regulated hepatic gluconeogenesis through FOXO1-PGC-1[alpha] interaction. *Nature,* 423**,** 550-555.

PUIGSERVER, P. & SPIEGELMAN, B. M. (2003) Peroxisome Proliferator-Activated Receptor-y Coactivator 1alpha (PGC-1alpha): Transcriptional Coactivator and Metabolic Regulator. *Endocrine Reviews,* 24**,** 78-90.

QIU, Y., GUO, M., HUANG, S. & STEIN, R. (2002) Insulin Gene Transcription Is Mediated by Interactions between the p300 Coactivator and PDX-1, BETA2, and E47. *Molecular and Cellular Biology,* 22**,** 412-420.

RADI, R., BECKMAN, J. S., BUSH, K. M. & FREEMAN, B. A. (1991a) Peroxynitrite-induced membrane lipid peroxidation: the cytotoxic potential of superoxide and nitric oxide. *Arch Biochem Biophys.,* 288**,** 7.

RADI, R., BECKMAN, J. S., BUSH, K. M. & FREEMAN, B. A. (1991b) Peroxynitrite oxidation of sulfhydryls. The cytotoxic potential of superoxide and nitric oxide. *J Biol Chem.,* 266**,** 7.

RENSTRÖM, E., RORSMAN, P., SEINO, S. & BELL, G. I. (2008) Regulation of Insulin Granule Exocytosis Pancreatic Beta Cell in Health and Disease. Springer Japan.

REUSCH, J. E. B. (2003) Diabetes, microvascular complications, and cardiovascular complications: what is it about glucose? *The Journal of Clinical Investigation,* 112**,** 986-988.

ROBERTSON, C., DREXLER, A. J. & VERNILLO, A. T. (2003) Update on diabetes diagnosis and management. *The Journal of the American Dental Association,* 134**,** 16S-23S.

ROGLIC, G., UNWIN, N., BENNETT, P. H., MATHERS, C., TUOMILEHTO, J., NAG, S., CONNOLLY, V. & KING, H. (2005) The Burden of Mortality Attributable to Diabetes. *Diabetes Care,* 28**,** 2130-2135.

RONTI, T., LUPATTELLI, G. & MANNARINO, E. (2006) The endocrine function of adipose tissue: an update. *Clinical Endocrinology,* 64**,** 355-365.

ROSENFELD, L. (2002) Insulin: Discovery and Controversy. *Clin Chem,* 48**,** 2270-2288.

RUI, L., AGUIRRE, V., KIM, J. K., SHULMAN, G. I., LEE, A., CORBOULD, A., DUNAIF, A. & WHITE, M. F. (2001) Insulin/IGF-1 and TNF-alpha stimulate phosphorylation of IRS-1 at inhibitory Ser307 via distinct pathways. *The Journal of Clinical Investigation,* 107**,** 181-189.

RYTER, S. W., OTTERBEIN, L. E., MORSE, D. & CHOI, A. M. K. (2002) Heme oxygenase/carbon monoxide signaling pathways: Regulation and functional significance. *Molecular and Cellular Biochemistry,* 234-235**,** 249-263.

SALEHI, A., MEIDUTE ABARAVICIENE, S., JIMENEZ-FELTSTROM, J., Ã–STENSON, C.-G. R., EFENDIC, S. & LUNDQUIST, I. (2008) Excessive Islet NO Generation in Type 2 Diabetic GK Rats Coincides with Abnormal Hormone Secretion and Is Counteracted by GLP-1. *PLoS ONE,* 3**,** e2165.

SALTIEL, A. R. & KAHN, C. R. (2001) Insulin signalling and the regulation of glucose and lipid metabolism. *Nature,* 414**,** 799-806.

SANDERS, L. J. (2002) From Thebes to Toronto and the 21st Century: An Incredible Journey. *Diabetes Spectrum,* 15**,** 56-60.

SAWLE, P., FORESTI, R., MANN, B. E., JOHNSON, T. R., GREEN, C. J. & MOTTERLINI, R. (2005) Carbon monoxide-releasing molecules (CO-RMs) attenuate the inflammatory response elicited by lipopolysaccharide in RAW264.7 murine macrophages. *British Journal of Pharmacology,* 145**,** 800-810.

SCHENK, S., SABERI, M. & OLEFSKY, J. M. (2008) Insulin sensitivity: modulation by nutrients and inflammation. *The Journal of Clinical Investigation,* 118**,** 2992-3002.

SEINO, S., SHIBASAKI, T. & MINAMI, K. (2011) Dynamics of insulin secretion and the clinical implications for obesity and diabetes. *The Journal of Clinical Investigation,* 121**,** 2118-2125.

SEO, K., SOOK CHOI, M., JUNG, U. J., JIN KIM, H., YEO, J., MIN JEON, S. & KYUNG LEE, M. (2008) Effect of curcumin supplementation on blood glucose, plasma insulin, and glucose homeostasis related enzyme activities in diabetic db/db mice. *Mol. Nutr. Food Res.,* 52**,** 10.

SHAFRIR, E., ZIV, E. & MOSTHAF, L. (1999) Nutritionally Induced Insulin Resistance and Receptor Defect Leading to β-Cell Failure in Animal Models. *Annals of the New York Academy of Sciences,* 892**,** 223-246.

SHEEHAN, M. T. (2003) Current Therapeutic Options in Type 2 Diabetes Mellitus: A Practical Approach. *CLINICAL MEDICINE & RESEARCH,* 1**,** 189-200.

SHIMABUKURO, M., OHNEDA, M., LEE, Y. & UNGER, R. H. (1997) Role of nitric oxide in obesity-induced beta cell disease. *The Journal of Clinical Investigation,* 100**,** 290-295.

SHIMOMURA, I., MATSUDA, M., HAMMER, R. E., BASHMAKOV, Y., BROWN, M. S. & GOLDSTEIN, J. L. (2000) Decreased IRS-2 and Increased SREBP-1c Lead to Mixed Insulin Resistance and Sensitivity in Livers of Lipodystrophic and ob/ob Mice. *Molecular cell,* 6**,** 77-86.

SHOELSON, S. E., LEE, J. & GOLDFINE, A. B. (2006) Inflammation and insulin resistance. *The Journal of Clinical Investigation,* 116**,** 1793-1801.

SMIRNOV, I., LEVINA, A., KUZNETSOV, I., TSIBUL'SKAYA, M., GLADUN, V., MININA, L., BOVENKO, V. & PIVNIK, A. (2000) Hemin arginate as a porphyrin metabolism corrector. *Pharmaceutical Chemistry Journal,* 34**,** 223-225.

SOLT, L. A., WANG, Y., BANERJEE, S., HUGHES, T., KOJETIN, D. J., LUNDASEN, T., SHIN, Y., LIU, J., CAMERON, M. D., NOEL, R., YOO, S.-H., TAKAHASHI, J. S., BUTLER, A. A., KAMENECKA, T. M. & BURRIS, T. P. (2012a) Regulation of circadian behaviour and metabolism by synthetic REV-ERB agonists. *Nature,* advance online publication.

SOLT, L. A., WANG, Y., BANERJEE, S., HUGHES, T., KOJETIN, D. J., LUNDASEN, T., SHIN, Y., LIU, J., CAMERON, M. D., NOEL, R., YOO, S.-H., TAKAHASHI, J. S.,

BUTLER, A. A., KAMENECKA, T. M. & BURRIS, T. P. (2012b) Regulation of circadian behaviour and metabolism by synthetic REV-ERB agonists. *Nature,* 485**,** 62-68.
SØNDERGAARD, L. (1993) Homology between the mammalian liver and the Drosophila fat body. *Trends in Genetics,* 9**,** 193-193.
SOUTHERN, C., SCHULSTER, D. & GREEN, I. C. (1990) Inhibition of insulin secretion by interleukin-1[beta] and tumour necrosis factor-[alpha] via an L-arginine-dependent nitric oxide generating mechanism. *FEBS Letters,* 276**,** 42-44.
SPIKES, J. D. (1975) PORPHYRINS AND RELATED COMPOUNDS AS PHOTODYNAMIC SENSITIZERS*. *Annals of the New York Academy of Sciences,* 244**,** 496-508.
SPINAS, G. A. (1999) The Dual Role of Nitric Oxide in Islet b-Cells. *Physiology,* 14**,** 49-54.
SRIVASTAVA, G., BORTHWICK, I. A., BROOKER, J. D., WALLACE, J. C., MAY, B. K. & ELLIOTT, W. H. (1983) Hemin inhibits transfer of pre-delta-aminolevulinate synthase into chick embryo liver mitochondria. *Biochemical and Biophysical Research Communications,* 117**,** 5.
STANDL, E., SCHNELL, O. & CERIELLO, A. (2011) Postprandial Hyperglycemia and Glycemic Variability. *Diabetes Care,* 34**,** S120-S127.
STEVENS-TRUSS, R., BECKINGHAM, K. & MARLETTA, M. A. (1997) Calcium Binding Sites of Calmodulin and Electron Transfer by Neuronal Nitric Oxide Synthaseâ€ *Biochemistry,* 36**,** 12337-12345.
STUEHR, D. J. (1999) Mammalian nitric oxide synthases. *Biochimica et Biophysica Acta (BBA) - Bioenergetics,* 1411**,** 217-230.
STUEHR, D. J., KWON, N. S., NATHAN, C. F., GRIFFITH, O. W., FELDMAN, P. L. & WISEMAN, J. (1991) N omega-hydroxy-L-arginine is an intermediate in the biosynthesis of nitric oxide from L-arginine. *Journal of Biological Chemistry,* 266**,** 6259-6263.
SZENDROEDI, J. & RODEN, M. (2009) Ectopic lipids and organ function. *Current Opinion in Lipidology,* 20**,** 50-56 10.1097/MOL.0b013e328321b3a8.
TANIOKA, T., TAMURA, Y., FUKAYA, M., SHINOZAKI, S., MAO, J., KIM, M., SHIMIZU, N., KITAMURA, T. & KANEKI, M. (2011) Inducible Nitric-oxide Synthase and Nitric Oxide Donor Decrease Insulin Receptor Substrate-2 Protein Expression by Promoting Proteasome-dependent Degradation in Pancreatic Beta-Cells. *Journal of Biological Chemistry,* 286**,** 29388-29396.
TENHUNEN, R., TOKOLA, O. & LINDÉN, I. B. (1987) Haem arginate: a new stable haem compound. *Journal of Pharmacy and Pharmacology,* 39**,** 780-786.
THOMAS, H. E., DARWICHE, R., CORBETT, J. A. & KAY, T. W. H. (2002) Interleukin-1 Plus g-Interferon-Induced Pancreatic b-Cell Dysfunction Is Mediated by b-Cell Nitric Oxide Production. *Diabetes,* 51**,** 311-316.
TILG, H. & MOSCHEN, A. R. (2008) Inflammatory Mechanisms in the Regulation of Insulin Resistance. *Molecular Medicine,* 14**,** 9.
TOKOLA, O., TENHUNEN, R., VOLIN, L. & MUSTAJOKI, P. (1986) Pharmacokinetics of intravenously administered haem arginate. *British journal of clinical pharmacology,* 22**,** 331-5.
TSANG, A. W., OESTERGAARD, K., MYERS, J. T. & SWANSON, J. A. (2000) Altered membrane trafficking in activated bone marrow-derived macrophages. *Journal of Leukocyte Biology,* 68**,** 487-494.
TSIFTSOGLOU, A. S., TSAMADOU, A. I. & PAPADOPOULOU, L. C. (2006) Heme as key regulator of major mammalian cellular functions: Molecular, cellular, and pharmacological aspects. *Pharmacology & Therapeutics,* 111**,** 327-345.
TURNER, R. C., HOLMAN, R. R., CULL, C. A., STRATTON, I. M., MATTHEWS, D. R., FRIGHI, V., MANLEY, S. E., NEIL, A., MCELROY, H., WRIGHT, D., KOHNER, E., FOX, C. & HADDEN, D. (1998) Intensive blood-glucose control with sulphonylureas or insulin compared with conventional treatment and risk of complications in patients with type 2 diabetes (UKPDS 33). *The Lancet,* 352**,** 837-853.
UKPDS, G. (1995) U.K. prospective diabetes study 16. Overview of 6 years' therapy of type II diabetes: a progressive disease. U.K. Prospective Diabetes Study Group. *Diabetes,* 44**,** 1249-1258.

UNGER, R. H. (2003) Lipid overload and overflow: metabolic trauma and the metabolic syndrome. *Trends in Endocrinology and Metabolism,* 14**,** 398-403.
VANGUILDER, H. D., VRANA, K. E. & FREEMAN, W. M. (2008) Twenty-five years of quantitative PCR for gene expression analysis. *BioTechniques,* 44**,** 7.
VASAVADA, N. & AGARWAL, R. (2005) Role of oxidative stress in diabetic nephropathy. *Advances in chronic kidney disease,* 12**,** 146-154.
VIEIRA, E., MARROQUÃ, L., BATISTA, T. M., CABALLERO-GARRIDO, E., CARNEIRO, E. M., BOSCHERO, A. C., NADAL, A. & QUESADA, I. (2012) The Clock Gene Rev-erbα Regulates Pancreatic Beta-Cell Function: Modulation by Leptin and High-Fat Diet. *Endocrinology,* 153**,** 10.
VOLIN, L., RASI, V., VAHTERA, E. & TENHUNEN, R. (1988) Heme arginate: effects on hemostasis. *Blood,* 71**,** 625-628.
WAGENER, F. A. D. T. G., VOLK, H.-D., WILLIS, D., ABRAHAM, N. G., SOARES, M. P., ADEMA, G. J. & FIGDOR, C. G. (2003) Different Faces of the Heme-Heme Oxygenase System in Inflammation. *Pharmacological Reviews,* 55**,** 551-571.
WANG, M.-Y., GRAYBURN, P., CHEN, S., RAVAZZOLA, M., ORCI, L. & UNGER, R. H. (2008) Adipogenic capacity and the susceptibility to type 2 diabetes and metabolic syndrome. *Proceedings of the National Academy of Sciences,* 105**,** 6139-6144.
WANG, Y., JONES VOY, B., URS, S., KIM, S., SOLTANI-BEJNOOD, M., QUIGLEY, N., HEO, Y.-R., STANDRIDGE, M., ANDERSEN, B., DHAR, M., JOSHI, R., WORTMAN, P., TAYLOR, J. W., CHUN, J., LEUZE, M., CLAYCOMBE, K., SAXTON, A. M. & MOUSTAID-MOUSSA, N. (2004) The Human Fatty Acid Synthase Gene and De Novo Lipogenesis Are Coordinately Regulated in Human Adipose Tissue. *The Journal of Nutrition,* 134**,** 1032-1038.
WANG, Y., KIM, K.-A., KIM, J.-H. & SUL, H. S. (2006) Pref-1, a Preadipocyte Secreted Factor That Inhibits Adipogenesis. *The Journal of Nutrition,* 136**,** 2953-2956.
WEGIEL, B., BATY, C. J., GALLO, D., CSIZMADIA, E., SCOTT, J. R., AKHAVAN, A., CHIN, B. Y., KACZMAREK, E., ALAM, J., BACH, F. H., ZUCKERBRAUN, B. S. & OTTERBEIN, L. E. (2009) Cell Surface Biliverdin Reductase Mediates Biliverdin-induced Anti-inflammatory Effects via Phosphatidylinositol 3-Kinase and Akt. *Journal of Biological Chemistry,* 284**,** 21369-21378.
WEIS, N., WEIGERT, A., VON KNETHEN, A. & BRUNE, B. (2009) Heme Oxygenase-1 Contributes to an Alternative Macrophage Activation Profile Induced by Apoptotic Cell Supernatants. *Molecular Biology of the Cell,* 20**,** 1280-1288.
WEISBERG, S. P., LEIBEL, R. & TORTORIELLO, D. V. (2008) Dietary Curcumin Significantly Improves Obesity-Associated Inflammation and Diabetes in Mouse Models of Diabesity. *Endocrinology,* 149**,** 3549-3558.
WEISS, M. A. (2009) Proinsulin and the Genetics of Diabetes Mellitus. *Journal of Biological Chemistry,* 284**,** 19159-19163.
WELLEN, K. E. & HOTAMISLIGIL, G. K. S. (2005) Inflammation, stress, and diabetes. *The Journal of Clinical Investigation,* 115**,** 1111-1119.
XU, H., BARNES, G. T., YANG, Q., TAN, G., YANG, D., CHOU, C. J., SOLE, J., NICHOLS, A., ROSS, J. S., TARTAGLIA, L. A. & CHEN, H. (2003) Chronic inflammation in fat plays a crucial role in the development of obesity-related insulin resistance. *The Journal of Clinical Investigation,* 112**,** 1821-1830.
YACHIE, A., NIIDA, Y, WADA, T, IGARASHI, N, KANEDA, H & TOMA, T., OHTA, K, KASAHARA, Y, AND KOIZUMI, S (1999) Oxidative stress causes enhanced endothelial cell injury in human heme oxygenase-1 deficiency. *The Journal of Clinical Investigation,* 103**,** 7.
YAMAMOTO, M., KURE, S., ENGEL, J. D. & HIRAGA, K. (1988) Structure, turnover, and heme-mediated suppression of the level of mRNA encoding rat liver delta-aminolevulinate synthase. *Journal of Biological Chemistry,* 263**,** 15973-9.
YAMAUCHI, T., KAMON, J., WAKI, H., TERAUCHI, Y., KUBOTA, N., HARA, K., MORI, Y., IDE, T., MURAKAMI, K., TSUBOYAMA-KASAOKA, N., EZAKI, O., AKANUMA, Y., GAVRILOVA, O., VINSON, C., REITMAN, M. L., KAGECHIKA, H., SHUDO, K., YODA, M., NAKANO, Y., TOBE, K., NAGAI, R., KIMURA, S., TOMITA, M., FROGUEL, P. & KADOWAKI, T. (2001) The fat-derived hormone adiponectin

reverses insulin resistance associated with both lipoatrophy and obesity. *Nat Med,* 7**,** 941-946.
YE, J., GAO, Z., YIN, J. & HE, Q. (2007) Hypoxia is a potential risk factor for chronic inflammation and adiponectin reduction in adipose tissue of ob/ob and dietary obese mice. *American Journal of Physiology - Endocrinology And Metabolism,* 293**,** E1118-E1128.
YIN, L., WU, N., CURTIN, J. C., QATANANI, M., SZWERGOLD, N. R., REID, R. A., WAITT, G. M., PARKS, D. J., PEARCE, K. H., WISELY, G. B. & LAZAR, M. A. (2007) Rev-erb alpha, a Heme Sensor That Coordinates Metabolic and Circadian Pathways. *Science,* 318**,** 1786-1789.
YIN, L., WU, N. & LAZAR, M. A. (2010) Nuclear receptor Rev-erbα: a heme receptor that coordinates circadian rhythm and metabolism. *Nuclear Receptor Signaling,* 8**,** 6.
YIN, M.-J., YAMAMOTO, Y. & GAYNOR, R. B. (1998) The anti-inflammatory agents aspirin and salicylate inhibit the activity of I[kappa]B kinase-[beta]. *Nature,* 396**,** 77-80.
YU, C., CHEN, Y., CLINE, G. W., ZHANG, D., ZONG, H., WANG, Y., BERGERON, R., KIM, J. K., CUSHMAN, S. W., COONEY, G. J., ATCHESON, B., WHITE, M. F., KRAEGEN, E. W. & SHULMAN, G. I. (2002) Mechanism by Which Fatty Acids Inhibit Insulin Activation of Insulin Receptor Substrate-1 (IRS-1)-associated Phosphatidylinositol 3-Kinase Activity in Muscle. *Journal of Biological Chemistry,* 277**,** 50230-50236.
YUAN, M., KONSTANTOPOULOS, N., LEE, J., HANSEN, L., LI, Z.-W., KARIN, M. & SHOELSON, S. E. (2001) Reversal of Obesity- and Diet-Induced Insulin Resistance with Salicylates or Targeted Disruption of IkkÎ². *Science,* 293**,** 1673-1677.
ZHOU, G., MYERS, R., LI, Y., CHEN, Y., SHEN, X., FENYK-MELODY, J., WU, M., VENTRE, J., DOEBBER, T., FUJII, N., MUSI, N., HIRSHMAN, M. F., GOODYEAR, L. J. & MOLLER, D. E. (2001) Role of AMP-activated protein kinase in mechanism of metformin action. *The Journal of Clinical Investigation,* 108**,** 1167-1174.

## WEBSITES

Diabetes in UK, 2011. *Scottish Diabetes Survey 2010 (Publication).* Available at: http://www.diabetesinscotland.org.uk/Publications.aspx. [Accessed date: 27 June 2012].
Nederland Trial Register. *The effect of heme arginate treatment on insulin resistance and vascular dysfunction related to obesity (Trial Info).* Available at: http://www.trialregister.nl/trialreg/admin/rctview.asp?TC=2472. [Accessed date: 27 June 2012].